



Tesis de Doctorado

Opción Biología Celular y Molecular

PEDECIBA



El complejo SIRT1/DBC1: su regulación por vías de
señalización y papel en el metabolismo glucídico.

Presentada por MSc Verónica Nin

Tutor: Dr Eduardo N. Chini, Mayo Clinic

Co-tutor: Dra Silvia Chifflet, Universidad de la Republica

Julio 2014

Agradecimientos.

Quiero agradecer a mis compañeros del laboratorio del Dr. Eduardo Chini en la Mayo Clinic, que colaboraron con experimentos, ideas, discusiones y sobre todo hicieron que los días difíciles fueran mejores. Ellos son: Juliana Camacho, Thereza Barbosa, Anatilde González-Guerrico, Jonathan Matalonga, Verena Capellini, Thomas White, Mikkel Vandelbo y Berthil Classen. Un lugar especial ocupa Claudia Chini, quien me enseñó todas las técnicas de biología molecular que aprendí durante mis años de tesista y fue mi guía principal en el trabajo de mesada. Sin ellos esta tesis no hubiese sido posible.

También quisiera agradecer a Tamar Tchkonía, Tamar Pirtskhalava y Nino Giorgadze por hacer más cálido mi tiempo en el Kogod Center for Aging de Mayo Clinic.

Asimismo agradezco a Silvia Chifflet, quien aceptó ser mi cotutora, acompañó diligentemente el desarrollo de esta tesis desde Uruguay y por lo tanto hizo posible el desarrollo de esta tesis vía PEDECIBA.

Estaré por siempre agradecida a Eduardo Chini, quien me abrió las puertas de su laboratorio cuando apenas me conocía. El me enseñó mucho sobre ciencia y mucho de la vida. Fue un gran tutor, exigente, honesto y accesible, e intentó mantenerme motivada aun cuando los experimentos se negaban a funcionar.

Finalmente, no hay un agradecimiento lo suficientemente grande para mis hijos Manuel y Mateo, que soportaron que su mamá se fuera a trabajar, a veces, durante las noches y los fines de semana siendo ellos muy chiquitos. Y muy especialmente a mi esposo y compañero de laboratorio Carlos Escande, que me enseñó muchísimo, soportó, apoyó y trabajó conmigo hasta el hartazgo (literalmente hasta unas horas antes de tomarnos el avión para regresar a Uruguay) para que algunos de los experimentos de esta tesis salieran adelante. A ellos tres dedico esta tesis.

Verónica Nin

Mayo de 2014

ÍNDICE	3
RESUMEN	5
INTRODUCCIÓN	7
METABOLISMO Y ENFERMEDADES METABÓLICAS EN LA ACTUALIDAD	7
EL AUGE DE LA RESTRICCIÓN CALÓRICA.....	12
EL ACALORADO DEBATE SOBRE SIR2, RESTRICCIÓN CALÓRICA Y LONGEVIDAD	14
LA BÚSQUDA DE ACTIVADORES DE SIRT1	15
OBESIDAD, RESTRICCIÓN CALÓRICA Y AMPK.....	17
PROTEÍNAS QUE SENSAN LA DISPONIBILIDAD DE ENERGÍA: AMPK Y SIRTUINAS.....	18
AMPK.....	19
SIRT1	20
Estructura de SIRT1	22
Procesos metabólicos regulados por SIRT1	24
En el tejido adiposo	24
En el páncreas.....	25
En el hígado	25
Procesos inflamatorios	26
Regulación transcripcional de SIRT1.....	27
Regulación por cambios en los niveles de NAD	29
DBC1	30
HIPÓTESIS DE TRABAJO	35
RESULTADOS	36
CONTRIBUCIONES, PERSPECTIVAS Y CONTROVERSIAS	62
REGULACIÓN DE LA INTERACCIÓN ENTRE SIRT1 Y DBC1: PREGUNTAS Y CONTROVERSIAS.....	62
REGULACIÓN DE LOS NIVELES DE DBC1: INTERROGANTES	66
DBC1 Y FÁRMACOS ACTIVADORES DE SIRT1.....	67

DBC1, EPIGENÉTICA Y EL ACETILOMA.....	68
<u>ANEXO 1.....</u>	<u>70</u>
<u>ANEXO 2.....</u>	<u>85</u>
<u>REFERENCIAS.....</u>	<u>105</u>

SIRT1 es una enzima desacetilasa NAD-dependiente que juega un papel central en la adaptación del metabolismo a los cambios en la disponibilidad energética. SIRT1 regula la acetilación de numerosos sustratos, entre ellos factores de transcripción clave en la regulación del metabolismo como FOXO, CREB y PPAR γ . Es además una proteína candidata a mediar parte de los efectos beneficiosos de la restricción calórica, y se ha debatido apasionadamente si es blanco del resveratrol y otras pequeñas moléculas que tienen efectos favorables en un contexto de obesidad. DBC1 es una proteína nuclear que une e inhibe a SIRT1. En el hígado, el complejo SIRT1-DBC1 es dinámico y su asociación es regulada por el estado metabólico del individuo, aunque las claves moleculares que impactan en la interacción entre ambas proteínas era una pregunta totalmente abierta al comienzo de esta tesis. De la misma manera, el papel de DBC1 en la activación farmacológica de SIRT1 era una interrogante. El papel de SIRT1 en la gluconeogénesis hepática también ha sido terreno de gran debate, con datos que apuntan tanto a que SIRT1 promueve e inhibe este proceso. Mas aun, la posibilidad que DBC1 participe en la regulación de dicho proceso no había sido explorado. Durante el desarrollo de la tesis, abordamos varias problemáticas vinculadas al complejo SIRT1-DBC1: la regulación de la interacción entre ambas proteínas, su participación como blanco farmacológico del resveratrol y otras drogas, y su papel en la regulación del metabolismo glucídico en el hígado. Los resultados obtenidos durante el desarrollo de la tesis se publicaron en dos artículos en la revista Journal of Biological Chemistry.

El primer trabajo versa sobre el papel de la vía del AMP cíclico (AMPc) y la kinasa dependiente de AMPc (PKA) en la regulación de la interacción entre SIRT1 y DBC1. Esta vía es típicamente activada por glucagón y glucocorticoides durante periodos de ayuno. Nuestra publicación muestra que un aumento en los niveles intracelulares de AMPc generan un incremento transitorio en la actividad de PKA y la kinasa activada por AMP (AMPK), que a su vez promueve la disociación de SIRT1 y DBC1. Estos eventos resultan en el aumento de la actividad desacetilasa de SIRT1. Este es el primer trabajo que muestra que una vía de señalización endógena, relevante en el metabolismo, regula la interacción entre ambas proteínas. Mas aun, en ese trabajo mostramos que el resveratrol y otros moléculas que provocan un aumento en la actividad de SIRT1 lo hacen a

través de la activación intermediaria de AMPK, que resulta en la disociación de SIRT1 y DBC1. Esta última parte del trabajo tiene implicaciones importantes en el debate sobre la activación farmacológica de SIRT1, y pone a la interacción entre SIRT1 y DBC1 en un lugar central como blanco de activadores de SIRT1.

En el segundo trabajo publicado nos centramos en el papel de DBC1 en la regulación del metabolismo hepático, en particular en la gluconeogénesis. Para esto utilizamos principalmente un modelo de ratón en el que se incorporó un cassette de neomicina en el gen de DBC1, generando un knock out para DBC1. Este modelo presenta la actividad de SIRT1 elevada. En los ratones knock out para DBC1, la gluconeogénesis hepática es mayor y es mediada por un aumento en la transcripción del gen para la enzima fosfoenolpiruvatocarboxikinasa (PEPCK), que cataliza un paso irreversible en vía de la síntesis de glucosa. También mostramos que la regulación de PEPCK en ausencia de DBC1 es mediada por SIRT1 y por el receptor nuclear Rev-erb α . Este último es parte de un complejo represor que regula la transcripción de algunos genes del metabolismo y del ciclo circadiano. En ausencia de DBC1, los niveles de Rev-erb α disminuyen, fenómeno que es mediado por SIRT1 y eventos de acetilación/desacetilación.

En conjunto, nuestros trabajos confirman un rol central del complejo SIRT1-DBC1 en el entramado de proteínas que regulan procesos metabólicos, y lo pone en un lugar central de regulación tanto por vías de señalización intracelulares como farmacológicas.

Metabolismo y enfermedades metabólicas en la actualidad

Las últimas décadas del siglo pasado y las primeras de este se han caracterizado por un aumento continuo en el número de personas que sufren enfermedades metabólicas [1-3]. Según la organización mundial para la salud, cerca de mil millones y medio de personas en el mundo sufren de sobrepeso, y 500 millones de personas en el mundo son obesas [4-6] (ver figura 1 por la distribución mundial), más de 300 millones sufren de diabetes tipo II (figura 2), y se estima que el número llegaría a cerca de los 600 millones en unos treinta años [7].

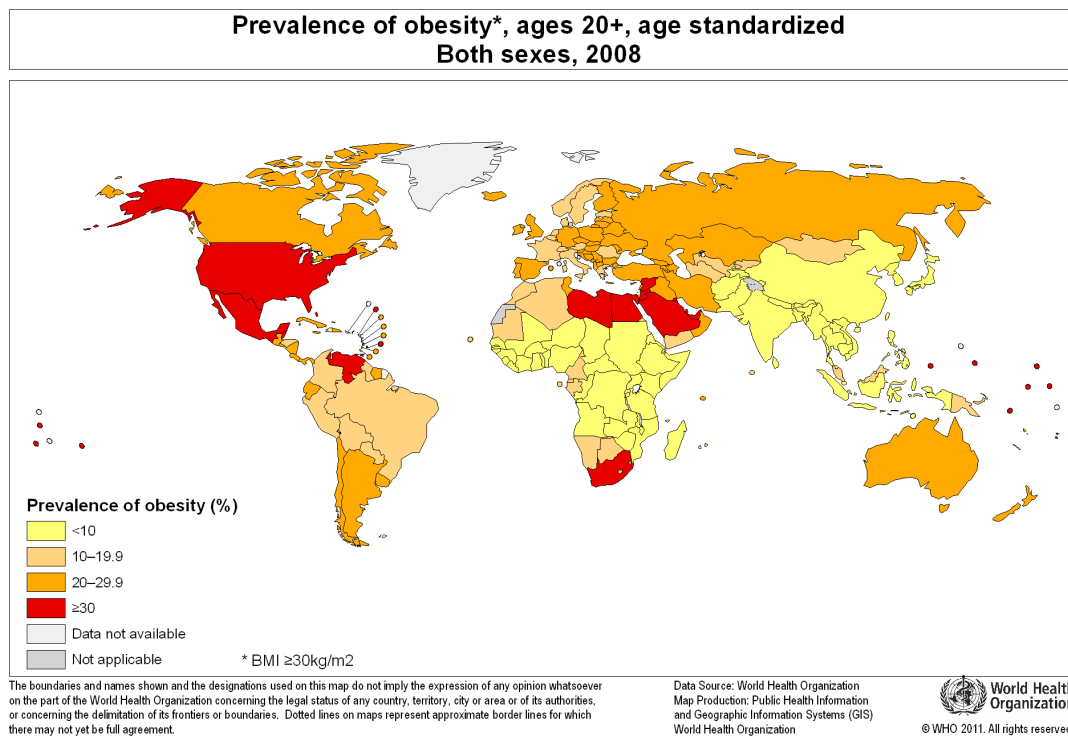


Figura 1. Prevalencia mundial en el año 2008 de obesidad ($BMI > 30 \text{ kg/m}^2$) en adultos mayores a 20 años. Fuente: World Health Organization [6].

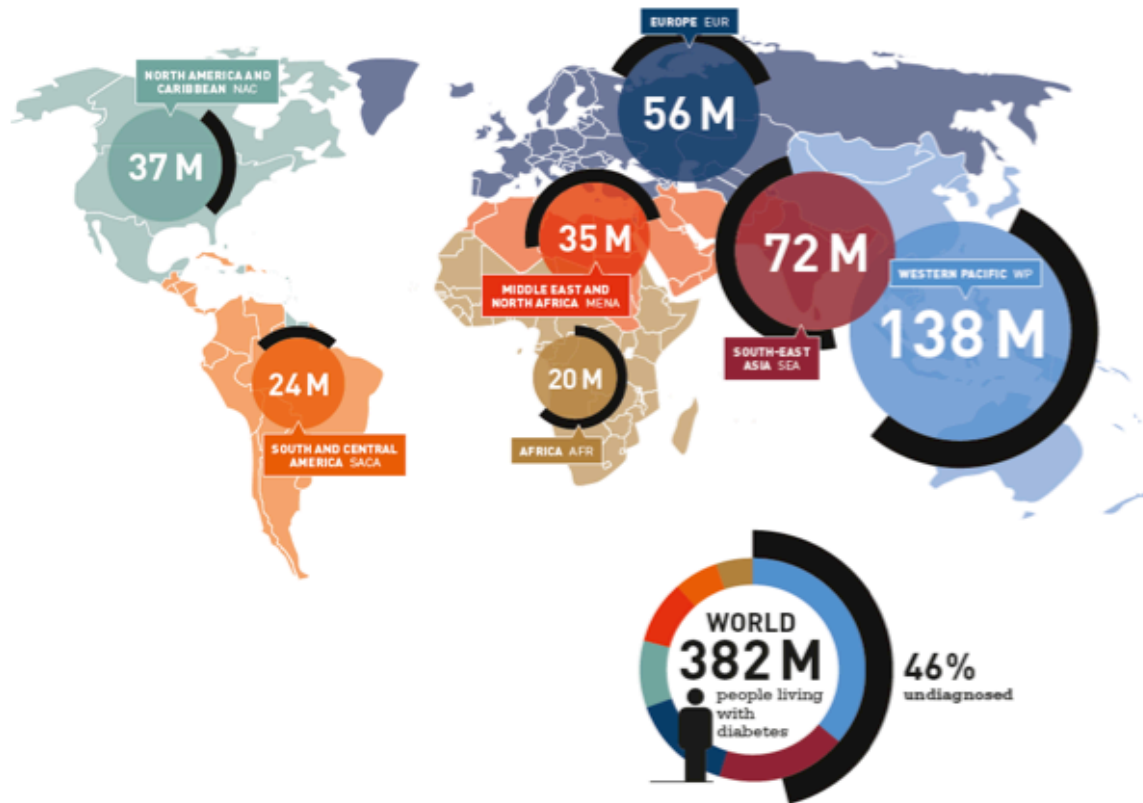


Figura 2. Número de personas que sufren diabetes por región, según la International Diabetes Federation. Tomado de [7].

La obesidad está directamente vinculada al desarrollo de desregulaciones metabólicas, como dislipidemia, glicemia elevada y resistencia a la insulina, una constelación de factores de riesgo que se denominan síndrome metabólico [8]. Además de ser considerada una enfermedad *per se*, la obesidad predispone a los individuos a padecer diabetes tipo II, problemas cardiacos y cáncer, entre otros. Esta situación determinó que la Organización Mundial de la Salud definiera que la obesidad es una epidemia global [9]. Las enfermedades metabólicas suponen un enorme costo económico y social. Desde el punto de vista clínico, la intolerancia a la glucosa, la hiperinsulinemia, la resistencia a la insulina y la obesidad central están estrechamente conectadas. ¿Que son estas patologías y como se explican desde el punto de vista molecular?

La resistencia a la insulina se considera un elemento central en la patogénesis del síndrome metabólico [10-12]. El término resistencia a la insulina hace referencia a que esta hormona genera una menor respuesta de captación, metabolización y almacenamiento de glucosa en sus órganos

blanco [13]. Estos órganos, tanto en humanos como modelos murinos son el hígado, el músculo y el tejido adiposo [12]. En un contexto de obesidad y diabetes tipo II, la resistencia a la insulina se manifiesta como una menor captación y metabolización de glucosa por parte del tejido adiposo y muscular y la incapacidad de disminuir la neosíntesis de glucosa por parte del hígado [12]. De manera adicional, la insulina también afecta el metabolismo de triglicéridos en todos sus órganos blanco y la síntesis de proteínas, en particular en el músculo [13].

Varios estudios han mostrado que la obesidad (ya sea en modelos genéticos o inducida a través de dietas ricas en grasas), provoca un estado inflamatorio en el tejido adiposo, mediado por la secreción de TNF α [14-17] y MCP-1 [18], lo que deriva en una infiltración de macrófagos [19, 20]. Las dietas ricas en grasa potencian el anclaje de los macrófagos al tejido adiposo, debido a que el ácido graso saturado palmitato promueve el incremento en la expresión de la proteína de anclaje netrin-1 [21]. Sorprendentemente, MCP-1 no solo promueve la infiltración de macrófagos, sino la división de este tipo celular *in situ* [22]. La relación causativa entre la inflamación crónica del tejido adiposo y el desarrollo de resistencia a la insulina está bien documentada. La neutralización de TNF α disminuye la resistencia a la insulina en ratones obesos [16]. Además, ratones que carecen de TNF α o sus receptores [23-25], o MCP-1 o su receptor [18], desarrollan resistencia a la insulina en un contexto de obesidad en un grado mucho menor. Sin embargo, los mecanismos precisos que vinculan estos dos fenómenos aun no han sido completamente clarificados.

Uno de los primeros fenómenos que desencadena una dieta rica en grasas es un aumento en la acumulación de triglicéridos en el hígado, incluso antes de que aumente el peso del individuo o incremente el contenido de grasas en el músculo y tejido graso [26]. Este fenómeno temprano resulta en que toda la vía de señalización de la insulina responda menos a la hormona, generando resistencia a la insulina en el hígado [26]. De hecho, el hígado graso se correlaciona con resistencia a la insulina en pacientes sin sobrepeso u obesidad [27]. La importancia de la resistencia a la insulina en el hígado en el desarrollo de diabetes tipo 2 fue demostrada a través de la generación de un ratón knock out para el receptor de insulina en el hígado. Este modelo presenta hiperinsulinemia, intolerancia a la glucosa y resistencia a la insulina a nivel sistémico [28, 29]. En condiciones normales, la insulina provoca una disminución en la producción y liberación de glucosa a la sangre (gluconeogénesis hepática) [13]. Sin embargo, en ratones con resistencia hepática a la insulina, la hormona no logra disminuir la expresión de los genes para

fosfoenolpiruvatocarboxikinasa (PEPCK) y glucosa-6-fosfatasa (G6-P), dos enzimas clave en la vía gluconeogénica [28]. El factor de transcripción PPAR γ , un factor de transcripción que regula en positivo a PEPCK y G6-P, también juega un papel clave en la sobreproducción de glucosa en ratones obesos [30]. La obesidad promueve la sobreexpresión de PPAR γ , lo que resulta en un aumento en la transcripción de las enzimas de la gluconeogénesis [30]. Finalmente, estudios en los que se ha eliminado el receptor de insulina en el hígado, grasa y músculo de forma independiente, ha demostrado un papel clave de la resistencia hepática a la insulina en el desarrollo de hiperglicemia e intolerancia a la glucosa [13]. La figura 3 esquematiza los efectos de la resistencia a la insulina en la diabetes tipo 2.

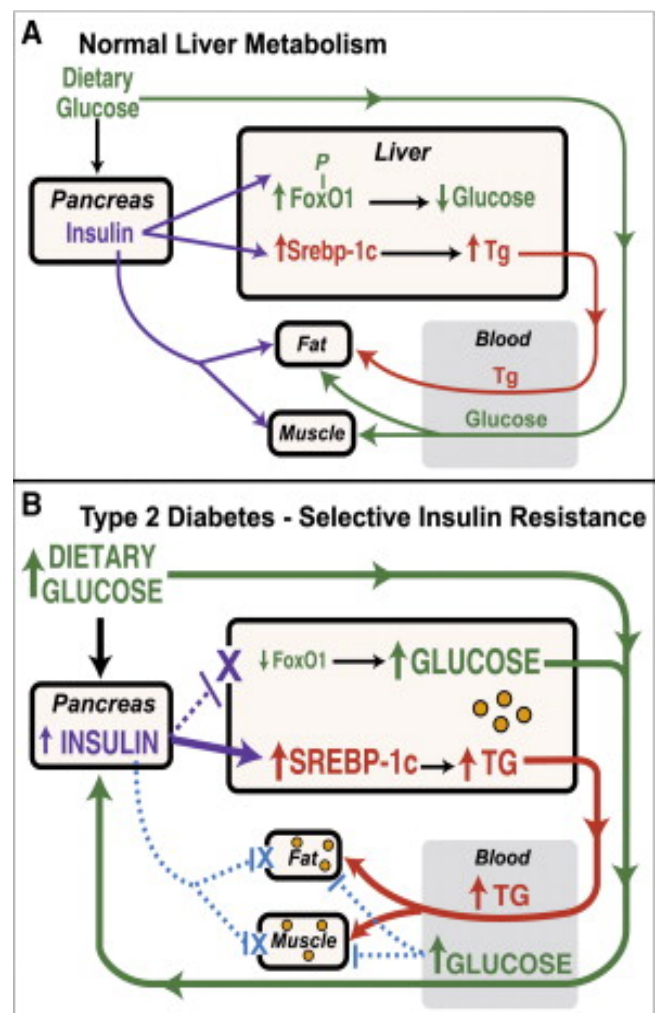


Figura 3. Efecto de la Resistencia a la insulina en el hígado sobre el metabolismo de la glucosa y lipídico. Modificado de [29]. Tg: triglicéridos.

Al igual que en tejido adiposo, una alimentación en base a una dieta rica en grasas también genera un estado pro inflamatorio en el hígado [31]. En el hígado dicho estado se caracteriza por un aumento en la transcripción de genes blanco de NFκB, como IL6 y TNFα. Ratones que sobreexpresan IκκB en el hígado (y por lo tanto presentan mayor actividad de NFκB) desarrollan diabetes tipo 2, una profunda resistencia a la insulina en el hígado e incluso resistencia sistémica a la insulina [31].

La obesidad y la resistencia a la insulina no solo se asocian a problemas en el metabolismo de la glucosa, sino también con el desarrollo de hígado graso [27, 32, 33], dislipidemia, aterosclerosis y enfermedades cardiovasculares [34-36], ovario poliquístico [37-39] y algunos tipos de cáncer [36, 40, 41], entre otros. La figura 4 detalla las complicaciones asociadas a la obesidad.

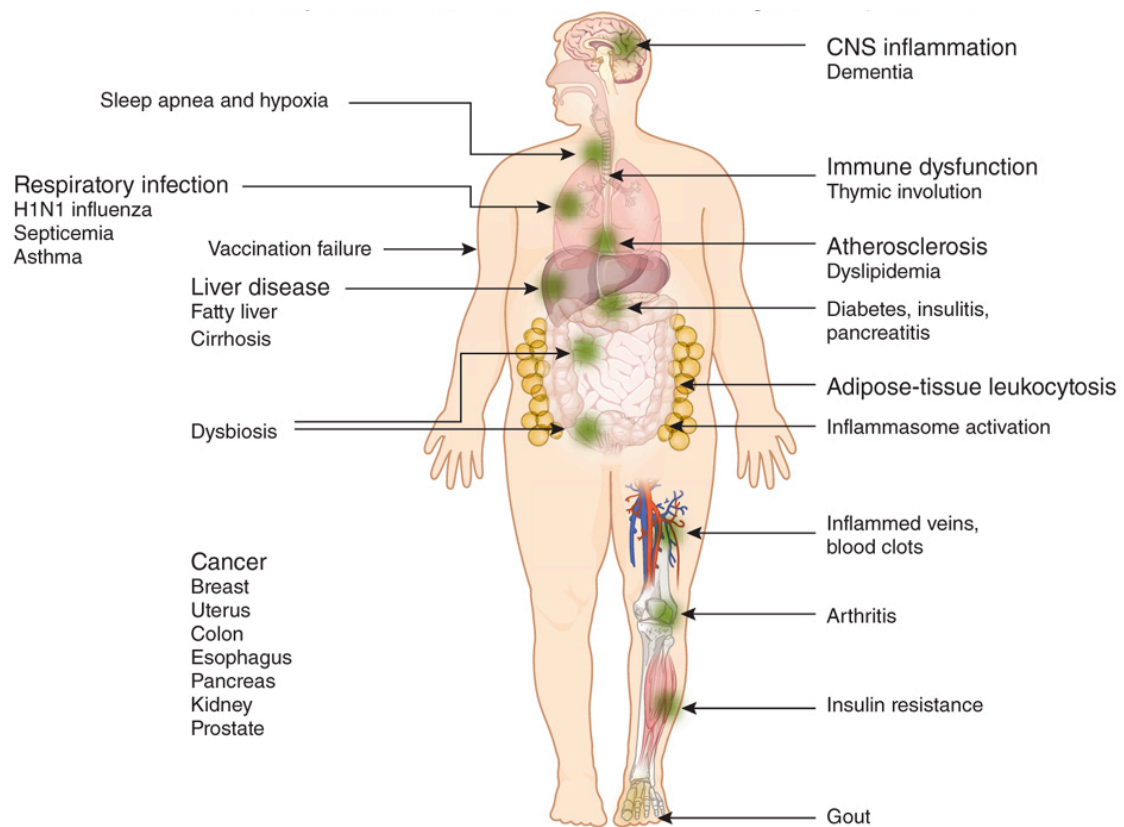


Figura 4. Patologías asociadas a la obesidad, con énfasis en las complicaciones de sustrato inflamatorio. Tomado de [41].

El auge de la restricción calórica.

En vista de los problemas de salud generados por la obesidad y las patologías asociadas a ella, no es sorprendente que se busquen intervenciones para paliar sus efectos negativos. La restricción calórica es la única intervención que consistentemente aumenta el tiempo de vida y disminuye los problemas metabólicos asociados al envejecimiento y a la obesidad en una multitud de especies [42, 43]. Esta intervención consiste en disminuir entre un 20 y un 40% la cantidad de calorías ingeridas sin limitar la cantidad de nutrientes. Los efectos de la restricción calórica en levaduras, ratones e incluso primates están bien documentados [42]. Por ejemplo, en un estudio realizado en monos rhesus, la restricción calórica mejoró el metabolismo de la glucosa, el perfil lipídico, disminuyó la hipertensión arterial [44, 45], la temperatura corporal y los niveles de insulina [46]. La restricción calórica también retardó la aparición de diabetes, cáncer, enfermedades cardiovasculares y atrofia cerebral. El efecto más marcado fue la dramática disminución en la incidencia de diabetes tipo 2 en el grupo sometido a restricción calórica [44]. La figura 5 presenta algunos de estos hallazgos. También existe evidencia parcial sobre el efecto de la restricción calórica en humanos [42, 47]. Los estudios de restricción calórica en pacientes obesos también son prometedores. Un estudio realizado en Pensilvania, Estados Unidos, mostró que cuanto mayor es la restricción calórica, mayor es la mejoría en la tolerancia a la glucosa y la sensibilidad a la insulina independientemente de la pérdida de peso [48].

Sin embargo, es improbable que la población general, y más aun la población obesa, se someta de forma voluntaria a una dieta reducida en calorías para mejorar su salud. Por lo tanto, encontrar fármacos que mimeticen los efectos de la restricción calórica se convirtió en un punto central en la búsqueda de tratamientos para las enfermedades metabólicas [49, 50]. De hecho, en la cultura popular se comenzó a denominar la búsqueda de dichos fármacos como la búsqueda de la “fuente de la juventud” [51, 52], o del “santo grial” [53].

Tanto la obesidad como la restricción calórica suponen un desbalance energético que tiene profundas consecuencias en la fisiología celular y del organismo. La necesidad de entender como una ingesta elevada o disminuida de calorías afecta a la homeóstasis energética, determinaron un gran aumento en la investigación sobre los mecanismos moleculares que coordinan la

disponibilidad de sustratos energéticos con la fisiología celular. Así, cuando los nutrientes son suficientes, las células ponen en marcha mecanismos de crecimiento y almacenaje de energía. En cambio, cuando los nutrientes son insuficientes, las células deben adaptarse al stress nutricional para no depletar las reservas energéticas [54]. ¿En definitiva, cuales son los mecanismos intracelulares que median los efectos deletéreos de la obesidad y los beneficiosos de la restricción calórica? Las respuestas a estas preguntas provienen de estudios mecanísticos en levaduras, mosca y modelos murinos.

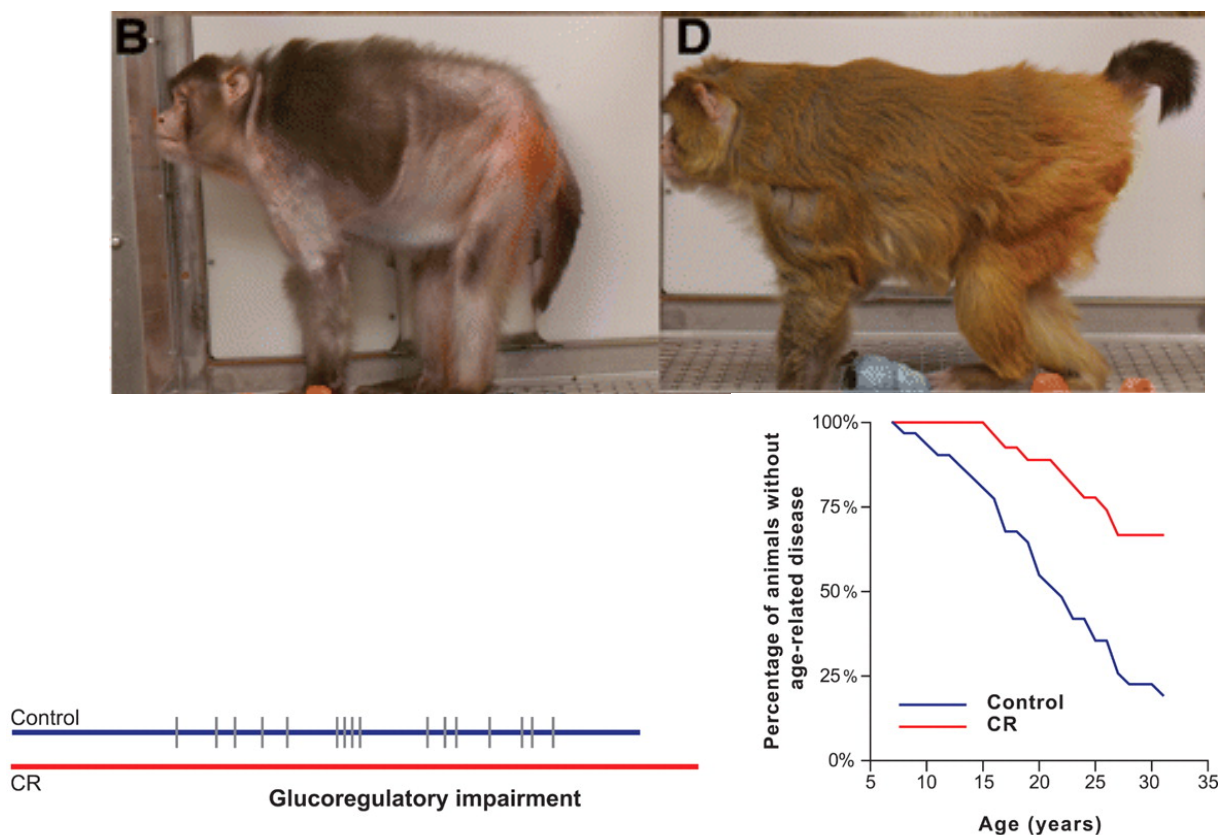


Figura 5. Efecto de la restricción calórica en monos rhesus (*Macaca mulatta*). Panel superior: apariencia de monos ancianos de la misma edad. A la izquierda un mono representativo del grupo control y a la derecha un mono representativo del grupo sometido a restricción calórica (CR). Panel inferior izquierdo: índice de desarrollo de diabetes tipo II. Panel inferior derecho: curvas de supervivencia en ambos grupos. Modificado de [44].

El acalorado debate sobre Sir2, restricción calórica y longevidad

Un estudio que causó un gran revuelo en el campo del envejecimiento y la restricción calórica fue el publicado en el año 2000 por el laboratorio de Leonard Guarente en el MIT, en el que los autores mostraron que en levadura, la ausencia de la proteína sir2 evita algunos efectos de la restricción calórica [55]. sir2 es una histona deacetilasa cuya actividad enzimática depende de nicotinamida adenina dinucleótido en su forma oxidada (NAD⁺) [56] y es inhibida por nicotinamida [57]. Trabajos posteriores mostraron que la restricción calórica provoca una disminución de nicotinamida en levadura y consecuentemente la activación de sir2 [58]. A partir del 2005, varios grupos han reportado resultados que desafían la importancia de sir2 en los efectos de la restricción calórica en levadura. Por ejemplo, varios trabajos del grupo de Brian Kennedy mostraron que la restricción calórica es capaz de prolongar la vida de *S. cerevisiae* en ausencia de sir2 [59, 60]. Los partidarios de la importancia de sir2 en la restricción calórica respondieron a estas críticas mostrando que en ausencia de sir2, su homólogo HST2 promueve la longevidad a través del mismo mecanismo que sir2 [61], aunque este hallazgo también ha sido cuestionado [62]. *Saccharomyces cerevisiae* presenta varias desacetilasas, pero la única conservada en todos los reinos es sir2 [63]. Algunos trabajos en *Drosophila melanogaster* apoyaron el rol de los ortólogos de Sir2 como base mecánica de los efectos de la restricción calórica [64]. Finalmente, el ortólogo de sir2 de mamíferos, SIRT1, también ha sido implicada en algunos de los efectos de la restricción calórica en ratones [65]. El grupo de Sinclair mostró que la restricción calórica en ratones promueve un aumento en la expresión de SIRT1 en varios tejidos, incluyendo cerebro, hígado y grasa, en parte mediado por el descenso en la concentración de insulina e IGF-1 en plasma [66]. Sin embargo, algunos de estos resultados son controversiales, ya que otros trabajos encontraron que la expresión de SIRT1 disminuye en hígados de ratones sometidos a restricción calórica [67]. Debido a que en ratones, la ausencia de SIRT1 es cuasi-letal en homocigosis en cepas puras, ha sido difícil estudiar el efecto de la restricción calórica en ausencia de SIRT1. La sobreexpresión de SIRT1 mejora varios aspectos del metabolismo, aunque es controversial si mimetiza aspectos de animales sometidos a restricción calórica [68]. Un modelo de ratón que sobreexpresa SIRT1 en el tejido adiposo blanco, pardo y cerebro muestra niveles disminuidos de insulina en plasma, mejor tolerancia a la glucosa, niveles más bajos de glucosa en ayuno, mayor consumo de oxígeno, mayor

tasa metabólica y mayor actividad física, todos ellos característicos de ratones sometidos a restricción calórica [68]. Otro modelo de sobreexpresión de SIRT1 reveló efectos positivos en ratones obesos, como mejora de la tolerancia a la glucosa y mejor sensibilidad a la insulina, pero menor consumo de oxígeno y menos actividad locomotora [69]. Finalmente, en un tercer modelo de sobreexpresión de SIRT1, los ratones también mostraron mejora en la tolerancia a la glucosa, y una dramática reducción de acumulación de grasas en el hígado (esteatosis hepática) bajo una dieta rica en grasas [70]. Todos los artículos concuerdan en que la activación de SIRT1 promueve mejoras en el metabolismo. Finalmente, en el año 2011, un artículo publicado en la revista Nature mostró que en las cepas de *C. Elegans* y *D. Melanogaster* que sobreexpresan sir2 no son longevas, aduciendo los resultados previos a falta de controles en la homogenización del “background” genético [71].

La búsqueda de activadores de SIRT1

Previo a el acalorado debate sobre la importancia de sir2 en los mecanismos que median el efecto de la restricción calórica, el grupo liderado por David Sinclair identificó al polifenol resveratrol como un activador de sir2, y demostró que la suplementación de resveratrol es suficiente para prolongar la longevidad replicativa de *Saccharomyces cerevisiae* [72]. Además, el resveratrol y otras moléculas pequeñas que activan sir2 también mimetizan los efectos de la restricción calórica en *Drosophila melanogaster* y *Caenorhabditis elegans* de forma sir2-dependiente [73]. La administración de resveratrol a ratones obesos mejoró la sensibilidad a la insulina, el perfil lipídico, y reprodujo la expresión génica de ratones en dieta normal. Más aun, la administración de resveratrol prolongó la expectativa de vida de los ratones alimentados una dieta rica en grasa [74]. Un grupo independiente confirmó los efectos beneficiosos del resveratrol *in vivo*, y mostró que en modelos celulares, la acción del resveratrol es dependiente de SIRT1 [75]. A partir de estos trabajos el grupo de Sinclair postuló que el resveratrol activa a SIRT1 directamente, mimetizando los mecanismos de la restricción calórica y generando efectos beneficiosos. Empero, la controversia no tardó en llegar. Una vez más, el grupo de Brian Kennedy mostró que el efecto del resveratrol en la activación de SIRT1 *in vitro* es artefactual, y se debe a la presencia de un grupo hidrofóbico en el

péptido utilizado como sustrato, y que el resveratrol no activa a sir2 en levadura *in vivo* [76]. El requisito del grupo hidrofóbico en el péptido sustrato para que el resveratrol active a SIRT1 fue confirmado por grupos independientes [77, 78]. También aparecieron trabajos que sugirieron efectos del resveratrol independientes de SIRT1 [79, 80]. Finalmente, el grupo de Linda Partridge presentó evidencia firme que el efecto de resveratrol en *C. elegans* es dependiente de la cepa utilizada, y por primera vez sugiere que el efecto de este polifenol es dependiente de la activación de la kinasa activada por AMP (AMPK) [81]. En la última parte del debate, un trabajo realizado en la compañía farmacéutica SIRTRIS reportó activadores de SIRT1 más potentes y estructuralmente no relacionados al resveratrol, y mostró que estos compuestos (por ejemplo el SRT1720 y el SRT1420), denominados STACs (por SirT1 Activating Compounds), mejoran el metabolismo de la glucosa y la sensibilidad a la insulina de ratones obesos [82, 83] y ratones en dieta normal [84]. Uno de estos STACs, el SRT2104 ha sido probado en adultos mayores, mostrándose cierto efecto beneficioso en el metabolismo lipídico [85]. No obstante, nuevamente surgieron datos que apuntaban a que estos STACS no son activadores directos de SIRT1 [86]. Finalmente, el grupo de Chung del National Institute of Health reportó que el resveratrol es un inhibidor de la fosfodiesterasa 4 (PDE4) y de forma indirecta un activador de SIRT1. En este trabajo, los autores muestran que la inhibición de PDE4 promueve la acumulación de AMP cíclico, la activación de la GTPasa pequeña EPAC, la vía CaMKK β -AMPK, lo que finalmente genera un aumento en los niveles de NAD⁺ y la activación de SIRT1 [87]. La figura 6, tomada de [88], esquematiza el modelo propuesto por Park et al [87].

En resumen, el resveratrol y otros miméticos de la restricción calórica tienen efectos positivos en el metabolismo *in vivo*, al igual que la sobreexpresión de SIRT1. Sin embargo, se han propuesto varios mecanismos de acción de estos fármacos, y el tema es aun un área de debate.

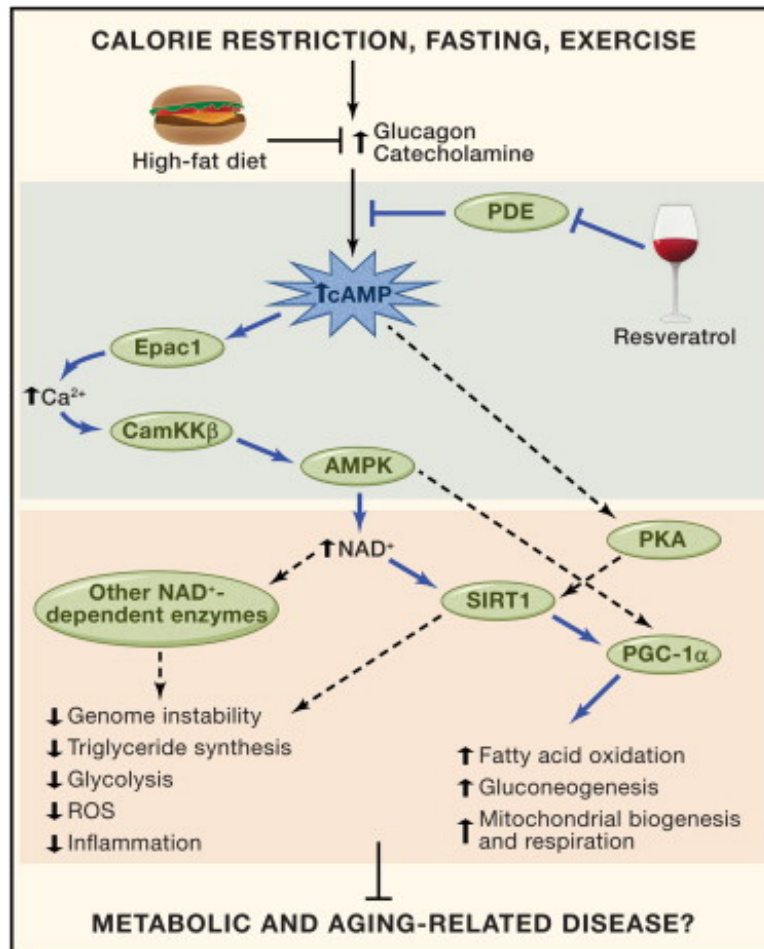


Figura 6. Mecanismo propuesto de la acción del resveratrol y la restricción calórica . Tomado de [88].

Obesidad, restricción calórica y AMPK

En el año 2007, dos grupos independientes mostraron que la proteína AMPK es fundamental para que la restricción calórica prolongue la longevidad de *C. elegans*. Por un lado, el grupo de Brunet de la Universidad de Stanford mostró que el efecto de la restricción calórica en *C. elegans* es mediado en gran parte por la enzima AMPK y su sustrato Daf-16, homólogo del factor de transcripción FOXO [89]. Por otro lado, el artículo de Schulz *et al.* mostró que la restricción de glucosa provoca un aumento en la longevidad de *C. elegans* que es independiente de Sir2 pero requiere la presencia de AMPK [90]. De manera similar, la metformina, un activador de AMPK, promueve la longevidad en el gusano a través de AMPK [91]. En mamíferos, la restricción calórica

promueve la activación de AMPK en el miocardio, al tiempo que mejora la salud cardiovascular [92].

Es interesante notar que el trabajo del grupo de Sinclair que describe los efectos beneficiosos del resveratrol en ratones obesos apunta a la posible participación de AMPK [74], y al menos otros dos trabajos mostraron que el resveratrol activa AMPK [79, 93]. Mas adelante, un trabajo de Um et al. mostró que muchos de los efectos metabólicos del resveratrol no tienen efecto en ratones que carecen de las subunidades catalíticas $\alpha 1$ o $\alpha 2$ de AMPK [94]. Los datos presentados en dicho trabajo revelaron que en ausencia de AMPK, el resveratrol no previene la pérdida de peso, la mejora en la tolerancia a la glucosa y sensibilidad a la insulina, el aumento en la tasa metabólica y la biogénesis mitocondrial [94]. Mas aun, la activación de AMPK con dosis pequeñas de metformina produce mejoras en la salud de ratones adultos [95]. Mas aun, la activación de AMPK es un tratamiento habitual en la practica clínica como tratamiento para pacientes con diabetes tipo 2 [96-99]. La metformina, y otros activadores de AMPK, como el AICAR, mejoran el transporte de glucosa en el músculo [100], suprime la producción de glucosa en el hígado [99] y disminuye la lipólisis [100].

Proteínas que sensan la disponibilidad de energía: AMPK y SIRTUINAS

En los párrafos anteriores discutimos la relevancia de SIRT1 y AMPK en el mecanismo de acción de la restricción calórica y las dietas ricas en grasas y el metabolismo. A continuación describiremos en más detalle su estructura y regulación.

En la célula, las vías catabólicas producen energía, ATP, mientras que las vías anabólicas consumen energía y producen ADP o AMP. A pesar que ambos grupos de reacciones fluctúan, dependiendo de la actividad celular y la concentración de sustratos, el rango ATP:ADP se mantiene en un rango muy estrecho [101]. Uno de los principales sistemas que mantienen la relación entre ATP y ADP casi constante es la kinasa activada por AMP (AMPK). Cualquier factor de estrés celular que disminuya la relación ATP:ADP activa a AMPK. En organismos unicelulares como *S. Cerevisiae*, y en células en cultivo, la actividad de AMPK aumenta bajo condiciones de restricción de glucosa [102, 103]. Es importante notar sin embargo, que en mamíferos, la regulación por restricción de glucosa ocurre fundamentalmente en las células β del páncreas, en el hipotálamo y en el hígado, ya que allí se expresan el transportador de glucosa GLUT2 y la isoforma IV de hexokinasa, llamada glucokinasa que presenta un K_m alto por glucosa. Estas características permiten que la célula responda a fluctuaciones muy pequeñas de glucosa [104, 105].

AMPK posee tres subunidades, la subunidad catalítica (α), y dos subunidades regulatorias (β y γ). La subunidad gamma de AMPK contiene cuatro motivos CBS que unen nucleótidos (AMP, ADP y ATP). Uno de estos bolsillos permanece vacío, otro es ocupado continuamente por AMP y los otros dos unen ATP y sus productos de hidrólisis ADP y AMP [106]. Cuando la disponibilidad energética de una célula es alta, los dos sitios de unión a nucleótido estarían ocupados por ATP. En cambio, cuando la cantidad de ATP disminuye, ya sea por baja disponibilidad de sustratos oxidables o por un aumento brusco en el consumo de energía, el ATP unido a la subunidad gamma sería desplazado por ADP o AMP [106]. Esto resulta en la activación de AMPK a través de tres mecanismos: activación alostérica, cambios conformacionales que promueven un evento de fosforilación en el “loop” de activación de la proteína, y prevención de la desfosforilación de ese sitio [106]. La subunidad α contiene, como otras kinasas, un loop de activación. La treonina 172, ubicada en dicho loop, es fosforilada por las kinasas LKB1 [107-109] y CaMKK β [110, 111]. La fosforilación en este sitio es básicamente constitutiva [101], aunque es

rápidamente desfosforilado. también de manera constitutiva [101]. La unión de AMP o ADP a la subunidad gama genera un cambio conformacional que promueve la fosforilación de la treonina 172, y mas importante, inhibe su desfosforilación. Estos eventos resultan en un aumento de la actividad kinasa de AMPK. Además, la unión de AMP, pero no ADP, genera una activación alostérica adicional, que aumenta aun mas la actividad de la enzima [101, 106].

La subunidad beta de AMPK tiene un módulo que une glucógeno y azucres ramificados y se presume que esta subunidad es responsable de que dichos compuestos inhiban la actividad de AMPK [112].

Actualmente se propone que en condiciones de estrés moderado, un aumento en la concentración de ADP es responsable de la activación de AMPK, mientras que en el caso de un estrés energético severo, la capacidad del AMP de activar alostericamente a AMPK es fundamental [113].

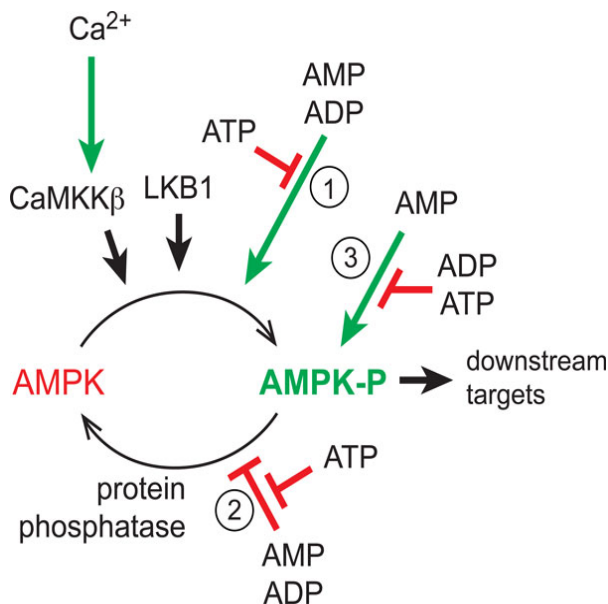


Figura 7. Esquema de los tres mecanismos de regulación de AMPK. Tomado de [113].

SIRT1

La generación de ATP en células eucariotas esta ligada a reacciones catabólicas como la oxidación de carbohidratos (glucólisis), ácidos grasos (β -oxidación) y degradación de proteínas, que

generan sustratos que nutren el ciclo de Krebs en la mitocondria. En ese organelo, la cadena de transferencia de electrones se acopla a la fosforilación oxidativa, que genera ATP a partir de ADP. Una de las moléculas claves en la transferencia de electrones es la coenzima nicotinamida adenina dinucleótido (NAD⁺). Durante momentos de abundancia de sustratos oxidables, la concentración relativa de NADH aumenta, mientras que la de NAD⁺ disminuye. En cambio, en momentos en los que los sustratos oxidables son escasos, la forma reducida disminuye su concentración [114]. Por ende, la concentración de NAD⁺, y la relación NAD⁺/NADH es un indicador del estatus energético de la célula.

La familia de sirtuinas de los mamíferos toma su nombre por su homología con la proteína sir2 de *S. Cerevisiae*, y esta compuesta por siete miembros. El factor común a estas siete enzimas es un dominio catalítico conservado que une NAD⁺. SIRT1, SIRT6 y SIRT7 se localizan en el núcleo [115, 116], aunque una subpoblación de SIRT1 puede desplazarse también al citosol [117]. SIRT2 es citosólica, mientras que SIRT3, SIRT4 y SIRT5 son mitocondriales (figura 8). La mayoría de las sirtuinas, incluyendo SIRT1, presentan actividad deacilasa, es decir, remueven grupos acilo (acetilos, malonilo y succinilo), ubicados en residuos lisina [116, 118], como se muestra en la figura 9. Para la reacción es imprescindible la unión y consumo de NAD⁺. Como resultado de la reacción catalizada por SIRT1, el grupo acetilo de la proteína se transfiere a parte de la molécula de NAD, que es clivada y genera nicotinamida y 1-O-ADP ribosa [119]. Una excepción es SIRT4 presenta únicamente baja actividad ADP-ribosil transferasa [120]. Cabe destacar que a diferencia de lo que ocurre en las reacciones de oxido-reducción, las sirtuinas consumen NAD⁺ durante la reacción enzimática. A continuación nos concentraremos en SIRT1, la sirtuina central en el desarrollo de esta tesis.

Mucho de lo que sabemos acerca de la estructura de SIRT1 es en base a estudios comparativos, ya que aun no ha sido posible cristalizar la enzima completa. Todas las sirtuinas presentan una región catalítica conservada, de aproximadamente 275 aminoácidos, flanqueada por los dominios N y C terminales, que son de tamaño variable [63]. La región catalítica presenta una forma elongada con un pliegue de tipo Rossmann, característico de las proteínas que unen NAD⁺ y NADH. También presentan un pequeño dominio de unión a Zinc que esta menos conservado.

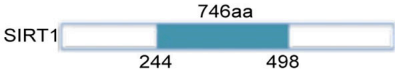
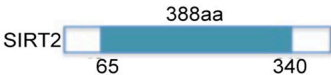
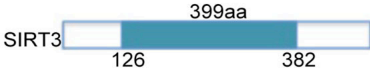
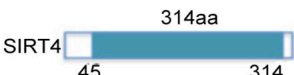
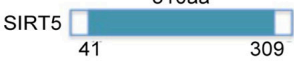
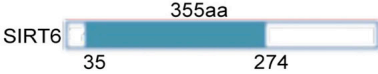

Classes		Enzymatic activity	Targets and Substrate	Localization	Function	Involvement in cancer
I	 <p>SIRT1 746aa 244 498</p>	Deacetylase	p53, FOXO, MyoD, Ku70, PPAR γ , NF κ B, PCAF, H3K9, H3K14,	Nuclear/ cytoplasmatic	Glucose metabolism, differentiation, neuroprotection, insulin secretion	Acute myeloid leukemia, colon, bladder, prostate, glioma, nonmalignant skin, ovarian
	 <p>SIRT2 388aa 65 340</p>	Deacetylase	α -Tubulin FOXO	Nuclear/ cytoplasmatic	Cell-cycle control, tubulin deacetylation	Glioma
	 <p>SIRT3 399aa 126 382</p>	Deacetylase	GHD complex 1, AceCS2	Mitochondrial	ATP-production, regulation of mitochondrial proteins deacetylation, fatty-acid oxidation	Breast cancer
	 <p>SIRT4 314aa 45 314</p>	ADP-ribosyl-transferase	GHD, ANT	Mitochondrial	Insulin secretion	Breast cancer
	 <p>SIRT5 310aa 41 309</p>	Deacetylase	CPSI	Mitochondrial	Urea cycle	Pancreatic, breast cancer
	 <p>SIRT6 355aa 35 274</p>	Deacetylase ADP-ribosyl-transferase	Hif1 α , helicase NF κ B, DNA polimerasi β	Nuclear	Telomeres and telomeric functions, DNA repair	Colon, breast cancer
	 <p>SIRT7 400aa 90 331</p>	Deacetylase	RNA polymerase type 1, EIA SMAD6	Nuclear	RNA pol I transcription	Breast cancer

Figura 8. La familia de las sirtuinas en mamíferos. Tomado de [116].

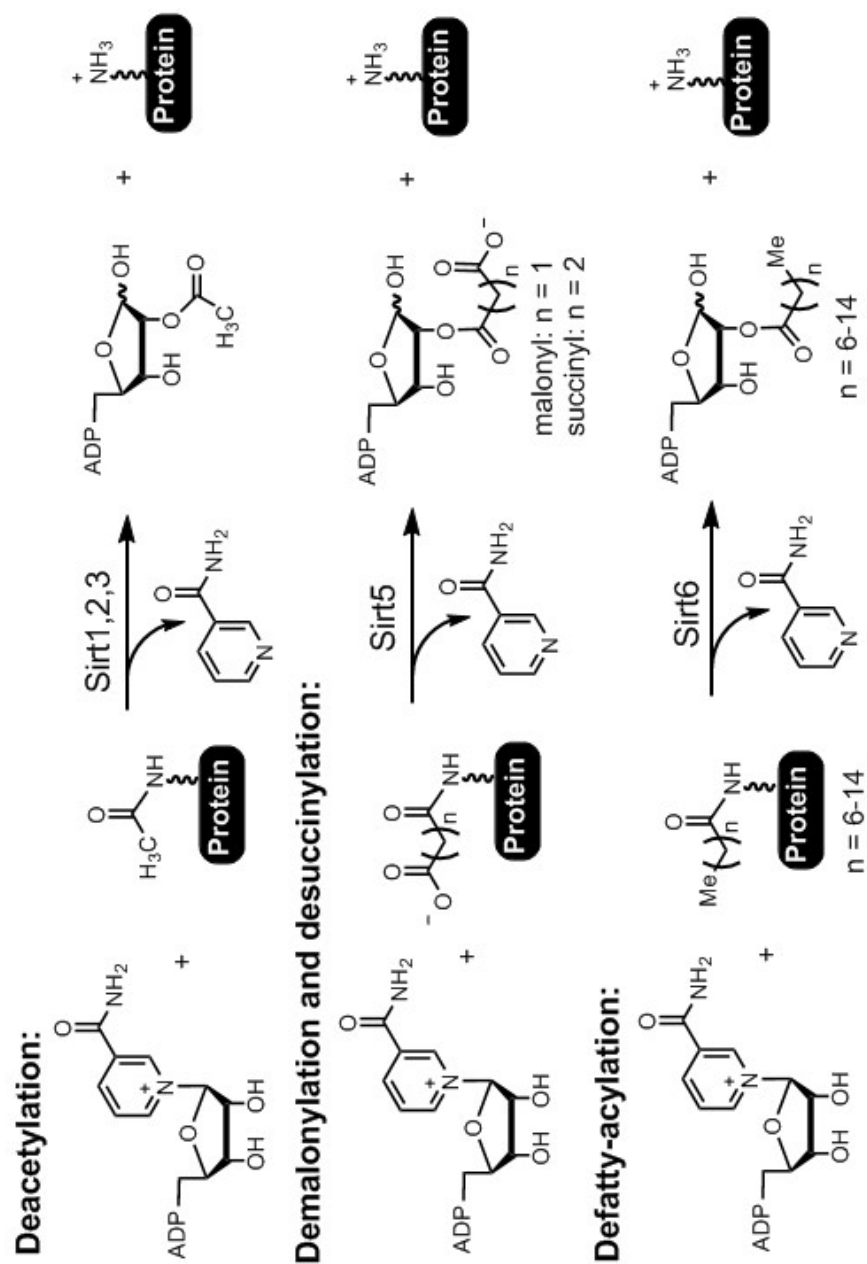


Figura 9. Reacciones enzimáticas catalizadas por la familia de las sirtuinas. Tomado de [118].

Ambos dominios están unidos por varios *loops*, que se pliegan formando un surco profundo al que entran por lados opuestos el aminoácido acetilado y la molécula de NAD⁺ [63]. Estudios de biología molecular han revelado el interesante hecho que la región catalítica de SIRT1 no presenta actividad enzimática *per se*, y que los dominios amino y carboxi terminales son imprescindibles para la actividad enzimática [121]. Así mismo, se ha determinado que el dominio N-terminal regula la tasa catalítica (catalytic rate) de la enzima, mientras que el dominio C-terminal disminuye el Km por NAD⁺ [121]. Es también particularmente interesante que un sector del dominio C-terminal, denominado ESA (por Essential for SIRT1 activity) se pliega de forma que interacciona con la región catalítica, y esa interacción intramolecular es necesario para la catálisis [122].

Procesos metabólicos regulados por SIRT1

En el tejido adiposo

El primer efecto metabólico descrito para SIRT1 fue su capacidad de promover la movilización de grasas desde el tejido adiposo en condiciones de ayuno [123]. El mecanismo propuesto incluye la asociación de SIRT1 con el complejo represor NCoR-SMRT en los promotores de genes vinculados a la diferenciación de los adipocitos [123]. Mas adelante otro grupo mostró que el factor de transcripción PPAR γ , central en la diferenciación del tejido adiposo blanco, es sustrato de SIRT1 [124]. PPAR γ es acetilado en las lisinas 268 y 293 y desacetilado por SIRT1. La desacetilación de PPAR γ promueve la asociación con el cofactor prdm16, un determinante de la expresión de genes propios del tejido adiposo pardo. En definitiva, la desacetilación de PPAR γ promueve que el tejido graso blanco adquiera características de tejido adiposo pardo, lo que tiene efectos beneficiosos, como un aumento en la sensibilidad a la insulina y mejor tolerancia a la glucosa. Los autores también mostraron que los niveles de acetilación de PPAR γ cambian en respuesta a situaciones fisiológicas, aumentando cuando los animales son expuestos a temperaturas bajas, y disminuyendo en animales alimentados una dieta rica en grasas [124].

En el páncreas

SIRT1 se expresa preferencialmente en las células β del páncreas [125]. Los ratones que sobreexpresan SIRT1 en este tipo celular presentan mejor tolerancia a la glucosa y una mayor secreción de insulina en respuesta a glucosa [126]. Por el contrario, los ratones knock out (KO) para SIRT1 presentan niveles bajos de insulina en plasma y no son capaces de secretar insulina en respuesta a glucosa. Es intrigante que estos ratones también presentan mejor tolerancia a la glucosa [125]. Desde un punto de vista mecanístico, SIRT1 promueve la secreción de insulina vía la represión de la expresión de la proteína desacoplante 2 (UCP-2) [125]. En acuerdo con estos datos, el resveratrol promueve la secreción de insulina por parte de las células β del páncreas de forma dependiente de SIRT1 [127].

En el hígado

Un tema de gran debate ha sido el papel de SIRT1 en la producción hepática de glucosa. El primer reporte sobre este tema mostró que en células SIRT1 desacetila al factor de transcripción PGC1 α , e induce los genes de enzimas gluconeogénicas PEPCK y G6P mientras que reduce la expresión del gen de la enzima glicolítica glucocinasa (GK) [128]. Posteriormente el mismo grupo mostró que una disminución de la expresión de SIRT1 en el hígado provoca hipoglicemia y mejor tolerancia a la glucosa. De manera adicional, los ratones producen mas glucosa a partir del sustrato gluconeogénico piruvato [129] Además, el *knock down* de SIRT1 en el hígado provoca la disminución en la expresión de los genes PEPCK y G6P y el aumento de los genes para GK y piruvato kinasa [129]. En el mismo sentido, la incubación de hepatocitos con resveratrol provocó un aumento en la producción de glucosa a través de la desacetilación del factor de transcripción FOXO1 [130]. Otro factor importante en la regulación de la gluconeogénesis es STAT3, un inhibidor de este proceso, al reprimir la transcripción de PGC1 α [131]. En condiciones de ayuno, SIRT1 desacetila a STAT3, lo que provoca la desrepresión de PEPCK y G6P [132]. Mas aun, la disminución en la expresión del SIRT1 en el hígado de ratas con diabetes tipo 2 provocó un aumento en la sensibilidad a la insulina y la disminución de la expresión de los genes

gluconeogénicos y la producción de glucosa [133]. Además, una dieta rica en fructosa provocó un aumento en la expresión de PEPCK y mayor producción de glucosa, efecto abolido mediante la inhibición de SIRT1 [134]. De manera adicional, un trabajo de Singh et al. reveló que el efecto pro-gluconeogénico de la hormona tiroidea requiere la desacetilación de FOXO mediada por SIRT1 [135].

Sin embargo, un trabajo posterior reveló que SIRT1 también desacetila al coactivador de CREB CRCT2, provocando su ubiquitinación y degradación, lo que suprime la transcripción de PEPCK y G6P. De hecho los autores de este trabajo muestran que el knock-out de SIRT1 en el hígado provoca un aumento en la producción de glucosa [136]. En el mismo sentido, otro artículo presenta datos que sugieren que parte del mecanismo de acción de la droga antidiabética metformina es la inducción de SIRT1 y desacetilación de CRCT2 [137]. Mas aun, un trabajo en el que se sobreexpresa SIRT1 en el hígado de ratones obesos reveló mayor sensibilidad a la insulina, disminución de la expresión de PEPCK y menor producción de glucosa [138]. También se ha presentado evidencia que SIRT1 inhibe la producción de glucosa a través de la vía AKT/FOXO. En este trabajo, los autores muestran que un ratón que carece de SIRT1 en el hígado presenta peor tolerancia a la insulina y mayor producción de glucosa a partir de piruvato [139].

En definitiva, diferentes modelos de disminución y estimulación de la actividad SIRT1 han generado resultados conflictivos en torno al papel de SIRT1 en la producción hepática de glucosa, tema que aun no ha sido saldado.

Procesos inflamatorios

SIRT1 es en general un inhibidor de los procesos inflamatorios. SIRT1 desacetila a la subunidad RelA/p65 del factor de transcripción NFκB, inhibiendo la transcripción de sus genes blanco [140], y promueve la interacción de NFκB con el correpresor TLE1, sumando otra forma de inhibición de NFκB [141]. Como se mencionó más arriba, la obesidad se caracteriza por un estado pro inflamatorio generalizado. En el hígado, la sobreexpresión de SIRT1 o la ausencia de su inhibidor endógeno DBC1 disminuye la expresión de las citoquinas pro inflamatorias TNF-α e IL-6 [142] [70]. Por el contrario, la ausencia de SIRT1 en el hígado se correlaciona con una mayor infiltración de macrófagos y un aumento en la expresión de varias moléculas pro inflamatorias

[143]. De forma similar, la ausencia de SIRT1 en el tejido adiposo blanco provoca la infiltración de macrófagos, mientras que en ratones alimentados con dietas ricas en grasas, la sobreexpresión de SIRT1 previene la infiltración de macrófagos en la grasa [144]. La sobreexpresión de SIRT1 también protege a las células β del páncreas de los efectos deletéreos de las citoquinas IFN- γ e IL1 β a través de la inhibición de NF κ B [126]. De manera adicional, en macrófagos el *knock-down* de SIRT1 aumenta la actividad de la vías de señalización pro inflamatorias mediadas por JNK y NF κ B, promueve la expresión de genes inflamatorios y aumenta la secreción de TNF- α inducida por LPS [145]. En definitiva, SIRT1 regula varios aspectos de los procesos inflamatorios en una variedad de tejidos.

Regulación transcripcional de SIRT1

El promotor de SIRT1 contiene secuencias de unión a varios factores de transcripción [146]. Como detallaremos a continuación, la transcripción de SIRT1 es sujeta a regulación positiva y negativa. En términos generales, la evidencia experimental muestra que durante periodos de ayuno varios factores de transcripción aumentan la transcripción de SIRT1 [146]. El promotor de SIRT1 contiene un elemento de respuesta a AMPc (CRE, cAMP response element). En condiciones de ayuno se produce un aumento en la señalización por glucagón y glucocorticoides. Ambas hormonas promueven un aumento en la concentración de AMPc, que resulta en la activación de CREB y un aumento en la transcripción de SIRT1. Este mecanismo de activación se observo en hígado, músculo, y tejido adiposo blanco y pardo[147]. También se ha mostrado que el aumento en la expresión de SIRT1 provocado por ayuno es mediado en parte por PPAR α [148]. En cultivos celulares, la falta de nutrientes también lleva a un aumento en la expresión de SIRT1 mediada en parte por FOXO3a y p53 [149]. Finalmente, el promotor de SIRT1 también contiene secuencias de unión a FOXO1. *In vitro* FOXO1 que estimula la expresión de SIRT1 [150], aunque la relevancia fisiológica en la transcripción de SIRT1 es aun desconocida.

Por otro lado, el factor de transcripción ChREBP (carbohydrate response element binding protein, en español proteína de unión al elemento de respuesta a carbohidratos) media la represión de la expresión de SIRT1 bajo condiciones en las que los nutrientes no son escasos [147]. El promotor de SIRT1 contiene una región conservada de unión a ChREBP. Es interesante que

durante el ayuno, el promotor de SIRT1 es ocupado por CREB, que estimula su transcripción, mientras que en presencia de alimento, la presencia de CREB en el promotor disminuye al tiempo que la ocupación por ChREBP aumenta [147]. Este mecanismo de intercambio de factores de transcripción provee un mecanismo sencillo y atractivo que explica el ajuste de los niveles de SIRT1 a la disponibilidad energética [147]. La enzima Poly-ADP-ribosil-polimerasa 2 (PARP2) también se une a la región proximal del promotor de SIRT1 e inhibe su expresión [151]. De hecho, el músculo e hígado de ratones que carecen de PARP2, presentan un contenido elevado de SIRT1. Estos ratones también presentan un fenotipo característico de actividad SIRT1 elevada, es decir, protección contra la esteatosis hepática, mayor biogénesis mitocondrial, y tendencia a la intolerancia a la glucosa [151]. Por otro lado, experimentos en cultivos celulares sugieren que PPAR γ reprime la transcripción de SIRT1 durante la senescencia celular [152]. Es interesante destacar que este trabajo muestra que SIRT1 es reclutada por PPAR γ a su propio promotor, lo que sugiere que SIRT1 es capaz de autorregular su expresión. La figura 10 resume los mecanismos de regulación transcripcional de SIRT1.

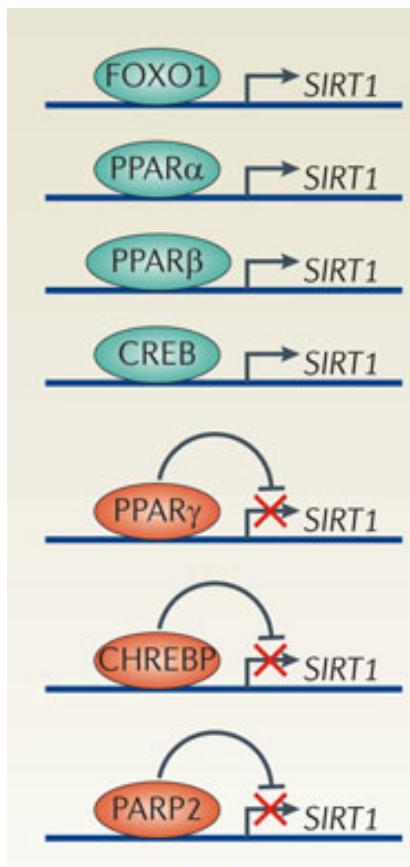


Figura 10. Algunos factores que regulan la transcripción de SIRT1. Tomado de [146].

Los niveles de NAD⁺ intracelulares son el resultado del balance entre su síntesis y su degradación. En mamíferos, CD38 es la principal enzima que degrada NAD⁺ [153]. En el año 2007, el laboratorio del Dr. Chini fue el primero en mostrar que la manipulación de los niveles intracelulares de NAD⁺ efectivamente modulan la actividad de SIRT1 [154, 155]. En ausencia de CD38, los niveles de NAD⁺ y la actividad de SIRT1 aumentan notablemente [155]. Por otro lado, la degradación de NAD⁺ mediado por la NAD⁺asa CD38 resulta en una reducción de la actividad SIRT1 [156]. Posteriormente se mostró también que la ausencia de PARP1 Poly-ADP-ribosil-polimerasa, una enzima que consume NAD⁺, los niveles de NAD⁺ aumentan y la actividad SIRT1 también [157].

En células eucariotas el NAD⁺ es sintetizado por dos vías: la síntesis *de novo* y la vía de rescate. En mamíferos, esta última es la predominante. El paso limitante en la síntesis de NAD⁺ es catalizado por la enzima Nicotinamida fosforibosil transferasa (NAMPT) [158]. La sobreexpresión de NAMPT resulta en un aumento en la concentración de NAD⁺ y en la actividad SIRT1. Mas aun, dos enzimas de la síntesis de NAD⁺ (NAMPT y NMAT) interaccionan con SIRT1 en promotores de genes y colaboran en la regulación de éstos. Este dato también abre la posibilidad de que los niveles de NAD⁺ [159] sean regulados de forma local y en estrecha asociación a la presencia de SIRT1 [160]. Mas recientemente, se ha mostrado que la suplementación con precursores de la biosíntesis de NAD⁺ aumenta la actividad SIRT1 [161, 162]. Mas aun, un aumento en los niveles de NAD⁺, ya sea promovido por la disminución de la degradación [155, 157], o un aumento en la síntesis [161, 162], mejora la tolerancia a la glucosa, la sensibilidad a la insulina e incluso protege del sobrepeso en ratones alimentados con dietas ricas en grasas [155, 161, 162].

Ha sido difícil de evaluar si la concentración de NAD⁺ cambia en situaciones fisiológicas lo suficiente como para afectar la actividad SIRT1. En el 2009 Canto et al. propusieron que en el músculo, la activación de AMPK provocada por ejercicio genera un aumento en los niveles de NAD⁺ y en la relación NAD⁺/NADH que repercute en un aumento en la actividad de SIRT1 [163]. Este artículo fue el primero en proponer un vínculo entre AMPK y SIRT1. En dicho

trabajo [163], los datos que muestran que la activación de AMPK provoca un aumento en la actividad SIRT1 son sólidos, sin embargo, el mecanismo propuesto de activación de SIRT1 es a mi entender poco convincente. Los autores proponen que la activación de AMPK provoca un aumento en la relación NAD⁺/NADH y en la concentración total de NAD⁺. A su vez, proponen que esto se debe al aumento en la β-oxidación propiciada por la activación de AMPK [163], algo que *a priori* parece contradictorio (a mayor oxidación de sustratos, mayor reducción de NAD⁺). Tampoco proponen mecanismos que expliquen porque los niveles totales de NAD⁺ aumentan, y no hay una prueba de que los cambios en la concentración de NAD⁺ que reportan, que son bastante pequeños, tengan un efecto directo sobre la actividad de SIRT1 [163].

También se ha reportado que en el hígado, el ayuno provoca un aumento en los niveles de NAD⁺, y desacetilación de PGC1α, sustrato de SIRT1 [128]. Sin embargo otros autores no observaron aumento de NAD⁺ en condiciones similares [67, 142].

El único proceso fisiológico en el que es claro que los niveles de NAD⁺ oscilan es durante el ciclo circadiano [164-166]. Los cambios en los niveles de NAD⁺ son producto de la oscilación en la transcripción de NAMPT [165, 166], que es regulado por CLOCK, BMAL y SIRT1 [167]. A su vez, la actividad SIRT1 también cicla, y la acetilación/desacetilación de PER2 e histonas contribuyen a la función del reloj circadiano [167, 168].

DBC1

En el año 2008 dos trabajos mostraron que la proteína nuclear Deleted in breast cancer 1 (DBC1) es un inhibidor endógeno de SIRT1 [169, 170]. Esta proteína no debe confundirse con otra, llamada “Deleted in bladder cancer-1” que utiliza la misma sigla. Para los efectos de esta tesis, la sigla DBC1 se referirá siempre a “Deleted in breast cancer 1”. DBC1 toma su nombre por localizarse en la región cromosómica 8p22, originalmente identificada como ausente en algunos tipos de cáncer de mama [171]. Sin embargo, reportes recientes no han corroborado el hallazgo inicial, y no han verificado la ausencia de DBC1 en varios tipos de cáncer [172].

DBC1 es una proteína nuclear de expresión ubicua [142], aunque es posible que se transloque al citosol y a la mitocondria durante la apoptosis [173]. Desde el punto de vista estructural presenta varios dominios. En el extremo C-terminal contiene una región “coiled coil” que se presume importante para la interacción con otras proteínas. DBC1 también contiene un dominio Nudix de unión a nucleótidos. Este dominio caracteriza a una familia de hidrolasas con baja especificidad de sustratos, aunque es probable que DBC1 no presente actividad enzimática. El rol de este dominio y la posible modulación de DBC1 por unión a nucleótidos es un tema completamente abierto [172]. DBC1 también presenta un dominio tipo S1 de unión a ARN [172]. De hecho, DBC1 es parte de un complejo que asocia la transcripción dependiente de la ARN polimerasa II con el splicing de los ARNs (153). Finalmente, el dominio N-terminal de DBC1, que contiene un cierre de leucina (leucine zipper, LZ), es el responsable de la interacción con varios receptores nucleares y enzimas [169, 174-179]. (Ver figura 11 por un esquema de la estructura de DBC1).

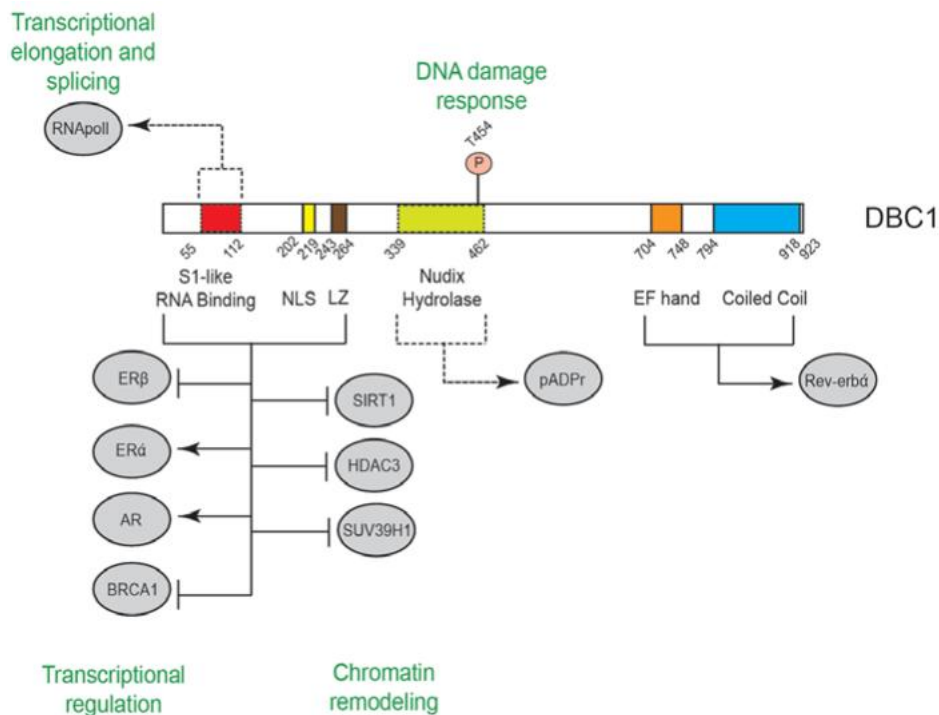


Figura 11. Diagrama de la estructura de DBC1. Se indican los dominios, los elementos que interaccionan y las funciones que desempeñan. Tomado de [186]

DBC1 interacciona con la región catalítica de SIRT1 [169]. De forma más reciente se propuso que el mecanismo por el cual DBC1 inhibe a SIRT1 implica el desplazamiento de una interacción intramolecular indispensable para la actividad de SIRT1 [122]. DBC1 y un péptido de 25 aminoácidos de la región C-terminal de SIRT1 compiten por la unión a la región catalítica de SIRT1 [122] (figura 11). La interacción entre SIRT1 y DBC1 parece ser directa, ya que ambas proteínas interactúan *in vitro*. La región de DBC1 responsable de la interacción con SIRT1 se identificó con gran precisión, e involucra una estructura tipo “cierre de leucina” presente en su región N-terminal [169].

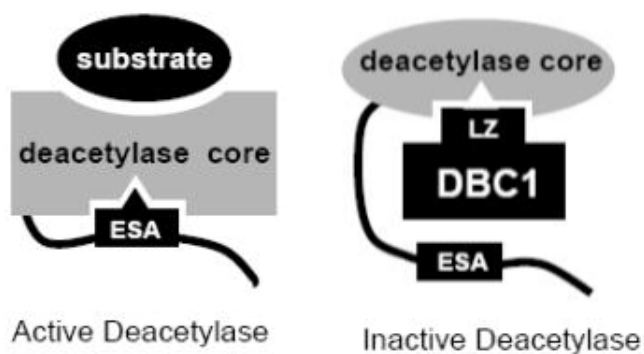


Figura 11. Esquema del mecanismo propuesto de inhibición de SIRT1 por DBC1. ESA: Essential for SIRT1 activity, LZ: cierre de leucina. Modificado de [122].

Escande et al. revelaron mediante experimentos de co-inmunoprecipitación que más del 50% de SIRT1 nuclear se encuentra unida a DBC1 en condiciones basales [142]. Escande et al. también mostró que la interacción entre SIRT1 y DBC1 es dinámica y que varía con el estado energético del individuo [142]. En el año 2010 el laboratorio del Dr. Chini mostró por primera vez medidas directas de la actividad de SIRT1 en condiciones de ayuno y dieta rica en grasas [142]. Como otros autores habían sugerido, la actividad de SIRT1 aumenta durante la ausencia de alimentos y disminuye cuando la carga calórica es excesiva [142]. También mostró que en estas condiciones los niveles de SIRT1 y de NAD⁺ no varían, pero la interacción con DBC1 sí. Durante el ayuno, el complejo SIRT1-DBC1 se disocia, mientras que en ratones alimentados una dieta rica en grasas la interacción entre ambas proteínas aumenta [142]. Este fenómeno también se observa en condiciones *in utero*. Los fetos de ratones preñadas alimentadas con una dieta rica en grasas presentan una disminución en la expresión de SIRT1 y una mayor asociación con DBC1, lo que promueve el desarrollo de hígado graso en los fetos [180].

Los ratones KO para DBC1 presentan mayor actividad SIRT1, que se refleja en una disminución en la acetilación de p53 [142]. Al igual que los ratones que sobreexpresan SIRT1 en el hígado [70], están protegidos contra el desarrollo de esteatosis hepática, y presentan menor inflamación en el hígado [142]. Sin embargo, los ratones machos para DBC1 presentan peor tolerancia a la glucosa, aunque el mecanismo detrás de este fenotipo no era claro al comienzo de esta tesis [124].

Al día de hoy se conocen dos modificaciones post-traduccionales en DBC1. Por un lado, DBC1 es fosforilado en la treonina 454 por las kinasas ATM/ATR (ataxia telangiectasia-mutated y ataxia telangiectasia and Rad3-related) [181, 182]. La fosforilación de DBC1 en dicho sitio promueve la interacción con SIRT1. La interacción de SIRT1 con DBC1 desplaza la interacción entre SIRT1 y p53, lo que redundaría en la acetilación e inhibición de p53 [170, 181]. De esta forma, la interacción entre SIRT1 y DBC1 impide que se desencadene la entrada en apoptosis [169, 181, 182]. Por otro lado, las lisinas 112 y 215 son blanco de la acetiltransferasa hMOF. La acetilación de estas lisinas provoca la disociación de DBC1 y SIRT1. Es muy interesante que SIRT1 desacetila esos sitios, lo que promueve su inhibición a través de la interacción con DBC1. La interacción entre hMOF y DBC1 disminuye en condiciones de daño al ADN, provocando una disminución en la acetilación de DBC1 [183]. Ambas vías de señalización contribuyen a que DBC1 inhiba la apoptosis a través de SIRT1 en situaciones de daño al ADN. Otro trabajo en la misma línea presenta evidencia que DBC1 reprime la anoiquis (apoptosis promovida por pérdida de anclaje) al estimular la actividad kinasa de IKK β y la actividad transcripcional de NF κ B [184].

DBC1 también une e inhibe otras enzimas nucleares. A través de su dominio N terminal, en particular a través del cierre de leucina, DBC1 se une a la desacetilasa de histonas HDAC3 [176]. El dominio N-terminal también es responsable de unir a la metiltransferasa SUV39H1, aunque en este caso la región no incluye al cierre de leucina [175]. La unión de DBC1 a todas estas enzimas resulta en la inhibición de las mismas [169, 170, 175, 176]. La acetilación y metilación son modificaciones epigenéticas con un rol central en la regulación de la expresión génica y la apertura de la cromatina [185]. Es posible entonces que DBC1 regule de forma indirecta el destino celular al modificar la información epigenética de la célula. De hecho, la respuesta inflamatoria en macrófagos promueve la degradación de DBC1, provocando la activación de desacetilasas y remodelación de la cromatina [186].

De manera adicional, DBC1 interacciona y regula la actividad transcripcional de varios receptores nucleares. Entre ellos se encuentran el receptor de andrógeno [174], los receptores de estrógeno α [179, 187] y β [177], el receptor de hormonas tiroideas [187], el receptor de glucocorticoides [187], y el receptor de hem Rev-erb α [188]. DBC1 funciona como co-activador ligando-dependiente del receptor de estrógenos α , del receptor de glucocorticoides y del receptor de hormonas tiroideas [187]. DBC1 también es parte de un complejo co-activador del receptor de andrógeno [174]. Además, DBC1 reprime la actividad del receptor de estrógenos β [177] y del factor de transcripción BRCA1 [178]. DBC1 también interacciona con el receptor de Hem Rev-erb α [188], que participa en la represión de varios genes vinculados al ciclo circadiano y al metabolismo, como PEPCK y PGC1 α (169,170). La interacción entre DBC1 y los receptores nucleares se da a través de la región N-terminal de DBC1 [172, 189], siendo la única excepción la interacción con Rev-erb α , que se da a través de la región C-terminal de DBC1 [188]. La interacción entre Rev-erb α y DBC1 resulta en un aumento en la estabilidad de Rev-erb α , lo que repercute en un aumento en la capacidad de este receptor de reprimir la transcripción de algunos de sus genes blanco [188].

Al comenzar el trabajo de tesis nos propusimos abordar varios aspectos debatidos o desconocidos relativos al complejo SIRT1-DBC1. En primer lugar, si la interacción entre ambas proteínas es regulada por vías de señalización endógenas. En segundo lugar, si los fármacos que activan SIRT1 lo hacen alterando la asociación a DBC1. Tercero, dado que al menos tres de las proteínas que interaccionan con DBC1 (SIRT1, HDAC3 y Rev-erb α) regulan la transcripción de PEPCK, decidimos evaluar la posibilidad de que DBC1 participe en la regulación de la transcripción de esta enzima, fundamental para la gluconeogénesis.

HIPÓTESIS DE TRABAJO

La hipótesis general de esta tesis fue que el complejo SIRT1-DBC1 es regulado por vías de señalización, es blanco de drogas y que ambas proteínas cumplen un papel importante en la regulación del metabolismo energético en el hígado.

Los resultados obtenidos se presentan en los siguientes artículos:

-Role of deleted in breast cancer 1 (DBC1) protein in SIRT1 deacetylase activation induced by protein kinase A and AMP-activated protein kinase.

Nin V, Escande C, Chini CC, Giri S, Camacho-Pereira J, Matalonga J, Lou Z, Chini EN.

J Biol Chem. 2012 Jul 6;287(28):23489-501

-Deleted in breast cancer 1 (DBC1) protein regulates hepatic gluconeogenesis.

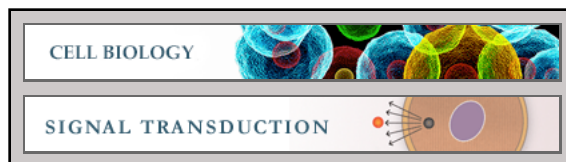
Nin V, Chini CC, Escande C, Capellini V, Chini EN.

J Biol Chem. 2014 Feb 28;289(9):5518-27

Cell Biology:

**Role of Deleted in Breast Cancer 1 (DBC1)
Protein in SIRT1 Deacetylase Activation
Induced by Protein Kinase A and
AMP-activated Protein Kinase**

Veronica Nin, Carlos Escande, Claudia C.
Chini, Shailendra Giri, Juliana
Camacho-Pereira, Jonathan Matalonga,
Zhenkun Lou and Eduardo N. Chini
J. Biol. Chem. 2012, 287:23489-23501.
doi: 10.1074/jbc.M112.365874 originally published online May 2, 2012



Access the most updated version of this article at doi: [10.1074/jbc.M112.365874](https://doi.org/10.1074/jbc.M112.365874)

Find articles, minireviews, Reflections and Classics on similar topics on the [JBC Affinity Sites](http://www.jbc.org/).

Alerts:

- [When this article is cited](#)
- [When a correction for this article is posted](#)

[Click here](#) to choose from all of JBC's e-mail alerts

Supplemental material:

<http://www.jbc.org/content/suppl/2012/05/01/M112.365874.DC1.html>

This article cites 71 references, 23 of which can be accessed free at
<http://www.jbc.org/content/287/28/23489.full.html#ref-list-1>

Role of Deleted in Breast Cancer 1 (DBC1) Protein in SIRT1 Deacetylase Activation Induced by Protein Kinase A and AMP-activated Protein Kinase^{*S}

Received for publication, March 23, 2012, and in revised form, April 24, 2012. Published, JBC Papers in Press, May 2, 2012, DOI 10.1074/jbc.M112.365874

Veronica Nin^{†1,2}, Carlos Escande^{†1,3}, Claudia C. Chini[‡], Shailendra Giri[§], Juliana Camacho-Pereira^{†4}, Jonathan Matalonga[‡], Zhenkun Lou[¶], and Eduardo N. Chini^{‡#5}

From the [†]Department of Anesthesiology and Kogod Aging Center, [§]Department of Experimental Pathology, and [¶]Division of Oncology Research, Department of Oncology, Mayo Clinic, Rochester, Minnesota 55905

Background: DBC1 is a key regulator of SIRT1 activity, although it is unknown how the SIRT1-DBC1 interaction is regulated.

Results: PKA and AMPK activate SIRT1 by disrupting the interaction between SIRT1 and DBC1.

Conclusion: We provide mechanistic evidence on how the SIRT1-DBC1 complex is regulated.

Significance: The SIRT1-DBC1 complex constitutes a target for the development of drugs to activate SIRT1.

The NAD⁺-dependent deacetylase SIRT1 is a key regulator of several aspects of metabolism and aging. SIRT1 activation is beneficial for several human diseases, including metabolic syndrome, diabetes, obesity, liver steatosis, and Alzheimer disease. We have recently shown that the protein deleted in breast cancer 1 (DBC1) is a key regulator of SIRT1 activity *in vivo*. Furthermore, SIRT1 and DBC1 form a dynamic complex that is regulated by the energetic state of the organism. Understanding how the interaction between SIRT1 and DBC1 is regulated is therefore essential to design strategies aimed to activate SIRT1. Here, we investigated which pathways can lead to the dissociation of SIRT1 and DBC1 and consequently to SIRT1 activation. We observed that PKA activation leads to a fast and transient activation of SIRT1 that is DBC1-dependent. In fact, an increase in cAMP/PKA activity resulted in the dissociation of SIRT1 and DBC1 in an AMP-activated protein kinase (AMPK)-dependent manner. Pharmacological AMPK activation led to SIRT1 activation by a DBC1-dependent mechanism. Indeed, we found that AMPK activators promote SIRT1-DBC1 dissociation in cells, resulting in an increase in SIRT1 activity. In addition, we observed that the SIRT1 activation promoted by PKA and AMPK occurs without changes in the intracellular levels of NAD⁺. We propose that PKA and AMPK can acutely activate SIRT1 by inducing dissociation of SIRT1 from its endogenous inhibitor DBC1. Our experiments provide new insight on the *in vivo* mechanism of SIRT1 regulation and a new avenue for the

development of pharmacological SIRT1 activators targeted at the dissociation of the SIRT1-DBC1 complex.

SIRT1 is an NAD⁺-dependent deacetylase that regulates gene expression and protein function by deacetylating lysine residues in proteins. It has been shown to regulate many aspects of cell and tissue metabolism, including liver gluconeogenesis (1, 2), insulin secretion (3–5), insulin sensitivity (5), fatty acid oxidation (6), and adipogenesis (7). Although the literature regarding the physiological processes regulated by SIRT1 is vast, our knowledge about how this key enzyme is regulated in the cellular context is scarce. In this regard, several possible regulatory mechanisms have been described.

One of the proposed mechanisms of SIRT1 regulation involves alterations in the intracellular concentration of NAD⁺. Because SIRT1 enzymatic activity is dependent on NAD⁺ (8), changes in the concentration of this nucleotide can lead to changes in SIRT1 activity. Indeed, modification of the two main enzymes responsible for the control of intracellular NAD⁺ levels, namely NamPT (9) and CD38 (10–12), can lead to changes in SIRT1 activity (11, 13, 14). However, the specificity of this mechanism seems low as there are several other NAD⁺-consuming enzymes in the cell. Moreover, it remains unknown whether global changes in NAD⁺ are reflected by similar changes in the nuclei where most SIRT1 is localized.

Several authors have shown that SIRT1 can be regulated at the transcriptional level (7, 15, 16). Although this mechanism could certainly explain long term changes in SIRT1 activity, it does not account for transient changes in its activity. Several post-transcriptional modifications can also affect SIRT1 activity. In this regard, it has been described that SUMOylation (17) and phosphorylation by several kinases (18–23) can increase SIRT1 activity. The kinases cyclin-dependent kinase 1 (22), casein kinase, (23, 24), and the c-Jun N-terminal kinase (JNK) (21) have been shown to directly phosphorylate SIRT1. On the other hand, it has been reported that the cAMP-dependent protein kinase (PKA) activates SIRT1 indirectly (19), the effects

* This work was supported, in whole or in part, by National Institutes of Health Grant DK-084055 from the NIDDK. This work was also supported by grants from the American Federation of Aging Research and the Mayo Foundation and by the Strickland Career Development Award.

^S This article contains supplemental Figs. S1–S5.

[†] Both authors contributed equally to this work.

[‡] Author contribution to this manuscript is part of Ph.D. research.

[§] Supported by American Heart Association Postdoctoral Fellowship Award 11POST7320060.

[¶] Supported by Fundação de Amparo À Pesquisa do Estado do Rio de Janeiro, Brazil.

^{#5} To whom correspondence should be addressed: Laboratory of signal transduction, Department of Anesthesiology and Kogod Aging Center, Mayo Clinic, Rochester, MN, 55905. Tel.: 507-255-0992; Fax: 507-255-7300; E-mail: chini.eduardo@mayo.edu.

DBC1 Is Necessary for SIRT1 Activation by PKA and AMPK

being mediated by an unidentified kinase. In addition, it has been proposed that AMP-dependent protein kinase (AMPK)⁶ modulates NAD⁺ intracellular levels and consequently SIRT1 activity (25). Interestingly, some of the effects of PKA appear to be mediated by AMPK (26, 27). Moreover, PKA activation can lead to a fast activation of AMPK in several tissues and cell models (26, 28–30).

In addition, SIRT1 is regulated by protein-protein interactions. Recently, we and others demonstrated that *in vivo* SIRT1 is largely associated with its endogenous inhibitor deleted in breast cancer 1 (DBC1) (31–33). DBC1 is a nuclear protein that, in addition to SIRT1, binds to several nuclear receptors and enzymes, including the estrogen receptors α (34) and β (35), the androgen receptor (36), the transcription factor BRCA1 (37), and the deacetylase HDAC3 (38).

SIRT1 and DBC1 form a dynamic complex in cells and *in vivo* (31). Moreover, the binding between SIRT1 and DBC1 is regulated by the energetic state of the organism (31). So far it is unknown which are the molecular pathways that modulate the interaction between SIRT1 and DBC1 and consequently SIRT1 activity *in vivo*.

Here, we show that the activation of the cAMP/PKA pathway leads to SIRT1 activation through an AMPK-dependent mechanism. Furthermore, this activation is DBC1-dependent and involves dissociation of the SIRT1-DBC1 complex. We propose that AMPK activation, either pharmacological or induced by PKA, results in the dissociation of SIRT1 from DBC1 and activation of SIRT1. Our results provide insight into the mechanisms that regulate the interaction between SIRT1 and DBC1 and may lead to newer pharmacological approaches to activate SIRT1.

EXPERIMENTAL PROCEDURES

Reagents and Antibodies—Unless otherwise specified, all reagents and chemicals were from Sigma-Aldrich. Anti-human SIRT1, anti-phosphorylated SIRT1 (Ser-47), anti-phosphorylated AMPK (Thr-172), anti-AMPK antibodies, and AICAR were from Cell Signaling Technology. Anti-DBC1 antibodies were from Bethyl Laboratories. Antibodies for p53, acetylated p53, and tubulin were from Abcam. Anti-actin antibody was from Sigma. PKA activator 6-MB-cAMP and exchange protein activated by cAMP (EPAC) activator 8-(4-chlorophenylthio)-2'-O-methyl-cAMP were from Biolog. A769662 was from Santa Cruz Biotechnology Inc. Resveratrol and recombinant SIRT1 were from Enzo Life Sciences. 1,1,2-Trichloro-1,2,2-trifluoroethane was from Fisher.

Cell Culture and Transfections—HepG2, HEK 293T, and DBC1 and AMPK wild type (WT) and knock-out (KO) MEFs were cultured in Dulbecco's modified Eagle's medium (5 g/liter glucose), and A549 cells were maintained in RPMI 1640 medium, all of them supplemented with 10% FBS and penicillin/streptomycin (Invitrogen). For all the experiments, the cul-

tures were serum-starved for 1 h before the treatments. AMPK $\alpha 1/\alpha 2$ WT and KO MEFs were a kind gift from Dr. Keith R. Laderoute. SIRT1 KO MEFs were kindly provided by Dr. David Sinclair.

Transient overexpression of SIRT1 and DBC1 was performed under the conditions and using the vectors described previously (31). The dominant-negative mutant of human AMPK $\alpha 1$ catalytic subunit (D157A) was kindly provided by Dr. David Carling. The constitutively active form of AMPK $\alpha 1$ was kindly provided by Dr. Benoit Viollet. Transient overexpression of these constructs was performed using Lipofectamine 2000 (Invitrogen) for 48 h following the manufacturer's instructions.

siRNA—All siRNAs were from Dharmacon (Lafayette, CO). The siRNA duplex against DBC1 was 21 bp as follows: DBC1 siRNA sense strand, 5'-AAACGGAGCCUACUGAACAAU. SMARTpool siRNAs were used to knock down SIRT1. Nontargeting siRNA number 3 was used as a control (D001210-03-20). Transfections were performed with 150 nM siRNA using Darmaphect 1 (Dharmacon) according to the manufacturer's instructions. Cells were harvested 72 h after the transfection.

Immunoprecipitation and Western Blot—Cultured cells were lysed in NETN buffer (20 mM Tris-HCl, pH 8.0, 100 mM NaCl, 1 mM EDTA, and 0.5% Nonidet P-40) supplemented with 5 mM NaF, 50 mM 2-glycerophosphate, 1 mM Na₃VO₄, and a protease inhibitor mixture (Roche Applied Science). Homogenates were incubated at 4 °C for 30 min under constant agitation and then centrifuged at 11,200 $\times g$ for 10 min at 4 °C. For immunoprecipitation, 1–1.5 mg of protein were incubated with 20 μ l of Protein A/G (Santa Cruz Biotechnology Inc.) and 1 μ g of antibody for 1 h at 4 °C under constant rotation. Nonspecific IgG (Santa Cruz Biotechnology Inc.) was used as a control. Finally, immunoprecipitates were washed two times with cold NETN before addition of 2 \times Laemmli buffer. Cell lysates and immunoprecipitates were analyzed by Western blot with the indicated antibodies. Western blots were developed using secondary antibodies or protein A-HRP and SuperSignal West Pico chemiluminescent substrate (Pierce).

SIRT1 Activity Measurement—SIRT1 activity was measured with a fluorometric assay (Enzo Life Sciences catalogue number BML-AK555-0001). Cells were extracted with NETN buffer as described above, and then the protein concentration in the lysates was quantified and equalized with deacetylase buffer (50 mM Tris-HCl, pH 8, 137 mM NaCl, 2.7 mM KCl, 1 mM MgCl₂, and 1 mg/ml BSA). Samples were incubated for 10 min at 30 °C to allow for NAD⁺ degradation and incubated for 10 additional min with 2 μ M DTT. Finally, 30–50 mg of protein of each sample were transferred to 6 wells of a 96-well plate, and a solution of deacetylase buffer containing 100 μ M substrate and 5 μ M trichostatin A was added to the wells. Half the wells included 100 μ M NAD⁺. The reaction proceeded for 2 h at room temperature, and then the developer, prepared according to the manufacturer's recommendations, was added for 1 h. Finally, the fluorescence was read with excitation of 360 nm and emission at 460 nm. SIRT1 activity was calculated as NAD⁺-dependent fluorescence. All the activity measurements were determined in the initial linear portion of the reaction.

NAD⁺ Extraction and Quantification—Cells were placed on ice, washed with ice-cold PBS twice, harvested, and spun down.

⁶ The abbreviations used are: AMPK, AMP-activated protein kinase; DBC1, deleted in breast cancer 1; AICAR, 5-amino-1- β -D-ribofuranosylimidazole-4-carboxamide; 6-MB-cAMP, N⁶-monobutyl-cAMP; EPAC, exchange protein activated by cAMP; cpt-cAMP, 8-(4-chlorophenylthio)-adenosine 3,5'-cyclic monophosphate-cAMP; MEF, mouse embryonic fibroblast; CA, constitutively active; ANOVA, analysis of variance.

The cell pellet was extracted on ice with ice-cold 10% TCA and sonicated three times, and then the TCA was extracted with 2 volumes of an organic phase consisting of 1,1,2-trichloro-1,2,2-trifluoroethane and trioctylamine in a 3:1 ratio. Both phases were vigorously vortexed for 15 s and then allowed to separate for 3 min. The pH of the top aqueous layer containing NAD^+ was adjusted with 1 M Tris, pH 8. The NAD^+ concentration was measured by means of an enzymatic cycling assay. Briefly, the aqueous layer was incubated with a 20 mM Na_2HPO_4 , pH 8 buffer containing 0.76% ethanol, 4 mM flavin mononucleotide (FMN), 27 units/ml alcohol dehydrogenase, 0.4 unit/ml diaphorase, and 8 μM rezasurin. A standard curve for NAD^+ was included. The fluorescence in the samples was followed with excitation at 544 nm and emission at 590 nm. Measurements were made in triplicates.

Autoradiography—293T cells were transfected with FLAG-SIRT1 or with FLAG-SIRT1 and constitutively active (CA) AMPK. After 48 h of transfection, the medium was replaced with phosphate-free DMEM supplemented with $\text{H}_3^{32}\text{PO}_4$ (0.5 mCi/ml). Cells were incubated in this medium for 2 h. After that, the medium was replaced with regular DMEM. Cells were stimulated with the AMPK activator resveratrol for 2 h. After that, SIRT1 was immunoprecipitated, and ^{32}P incorporation was evidenced by electrophoresis and autoradiography.

Site-directed Mutagenesis—Mutagenesis was performed on FLAG-SIRT1 using a QuikChange II site-directed mutagenesis kit from Agilent Technologies following the manufacturer's instructions.

Statistics—Values are presented as mean \pm S.E. of three to five experiments unless otherwise indicated. The significance of differences between means was assessed by ANOVA or two-tailed Student's *t* test as indicated. A *p* value less than 0.05 was considered significant.

RESULTS

Measurement of SIRT1 Activity in Cells—Cellular SIRT1 activity and activation were determined with a SIRT1 fluorometric kit (Enzo Life Sciences) according to the manufacturer's instructions. This assay has been extensively characterized in our laboratory (14, 31). The substrate used is a small peptide derived from p53 that includes an acetylated lysine, corresponding to Lys-382 of human p53; this residue is the target of SIRT1 enzymatic activity. Independent investigators have shown that this assay is a reliable tool to measure cellular SIRT1 activity and regulation (19, 31, 39–41). However, a controversy regarding the validity of this assay arose when it was shown that *in vitro* some compounds produce fluorescence artifacts that could be misinterpreted as changes in SIRT1 activity (42). In fact, the Fluor-de-Lys SIRT1 assay was used to propose that the polyphenol resveratrol is a direct SIRT1 activator (43, 44). It was later shown that the direct activation of SIRT1 by resveratrol was an artifact as a consequence of the interaction between resveratrol and the 7-amino-4-methylcoumarin fluorescent probe linked to the acetylated peptide (42). Nevertheless, these artifacts occur only when SIRT1 activity is measured *in vitro* and in the presence of small molecules (42, 45, 46) and not when used to measure SIRT1 activity in cell extracts. This has been clearly established by different independent investigators,

including us (14, 31, 39–41). Here, we further characterize the assay to demonstrate that indeed it constitutes a highly reliable way to measure SIRT1 activation in cells.

A brief scheme of the basic steps used to measure cellular SIRT1 activity is provided in Fig. 1A. Determination of cellular SIRT1 activity by this method depends on the addition of exogenous NAD^+ , and this activity is inhibited when the cellular extracts are also incubated with nicotinamide, suramin, or EX527, three very well known inhibitors of SIRT1 (Fig. 1B). The fact that cellular determination of SIRT1 activity by this method requires the addition of NAD^+ constitutes at the same time a limitation and an advantage because it provides a way to measure changes in SIRT1 activity regardless of changes in intracellular NAD^+ levels. This is especially relevant when one wants to determine whether post-translational modifications like phosphorylation or protein-protein interactions may alter SIRT1 activity.

To prove that the cellular activity measured by the Fluor-de-Lys assay quantitatively correlates with the level of SIRT1 expression in the cells, we performed a dose-response curve. For that, we transfected different amounts of a SIRT1-coding plasmid in 293T cells and then measured SIRT1 activity. As can be seen in Fig. 1C, the amount of SIRT1 in the cell lysates increased with increasing concentrations of plasmid. We measured SIRT1 activity in these samples, and we found that the increase in protein levels correlates with the activity measured by the assay. In fact, when we plotted SIRT1 activity *versus* the expression level of SIRT1, we found that these parameters correlate perfectly with an r^2 of 0.9945 (Fig. 1C, *right panel*). To further prove that the activity measured is linearly dependent on SIRT1 concentration, we assessed different amounts of protein lysates from SIRT1-positive cells. As can be seen in supplemental Fig. S1, SIRT1 activity correlates perfectly with the amount of protein assessed (r^2 of 0.994). These experiments show that the activity measured by this method is a quantitative reflection of the SIRT1 content in cells.

Furthermore, to assess the specificity of the assay, we measured SIRT1 activity in WT and SIRT1 KO MEFs. SIRT1 activity was undetectable in SIRT1 KO MEFs (Fig. 1D), clearly showing that the enzymatic activity measured by the Fluor-de-Lys assay is not present in cellular extracts that lack SIRT1. The same result was obtained when SIRT1 was knocked down by siRNA transfection in HepG2 cells (Fig. 1E).

In addition, we evaluated whether the assay was able to detect changes in SIRT1 activity regardless of changes in the expression level of SIRT1. To do so, we evaluated the effect of the SIRT1 negative regulator DBC1 on SIRT1 activity. As we had shown previously (31), knockdown of DBC1 led to an increase in cellular SIRT1 activity, an event that was not observed if SIRT1 was absent (Fig. 1E). Moreover, when SIRT1 was cotransfected with DBC1, we observed inhibition of the SIRT1 cellular activity. This inhibition was lost when SIRT1 was cotransfected with $\Delta\text{LZ-DBC1}$, a deletion mutant of DBC1 that was shown previously by us (31, 33) not to bind to SIRT1 (Fig. 1F). Also, cellular SIRT1 activity was higher in DBC1 KO MEFs than in the WT control cells (Fig. 1G). This result is specific for DBC1 KO MEFs because there was no difference in SIRT1 activity between WT cells and AMPK ($\alpha 1\alpha 2$) KO cells

DBC1 Is Necessary for SIRT1 Activation by PKA and AMPK

A Steps followed to measure cellular SIRT1 activation:

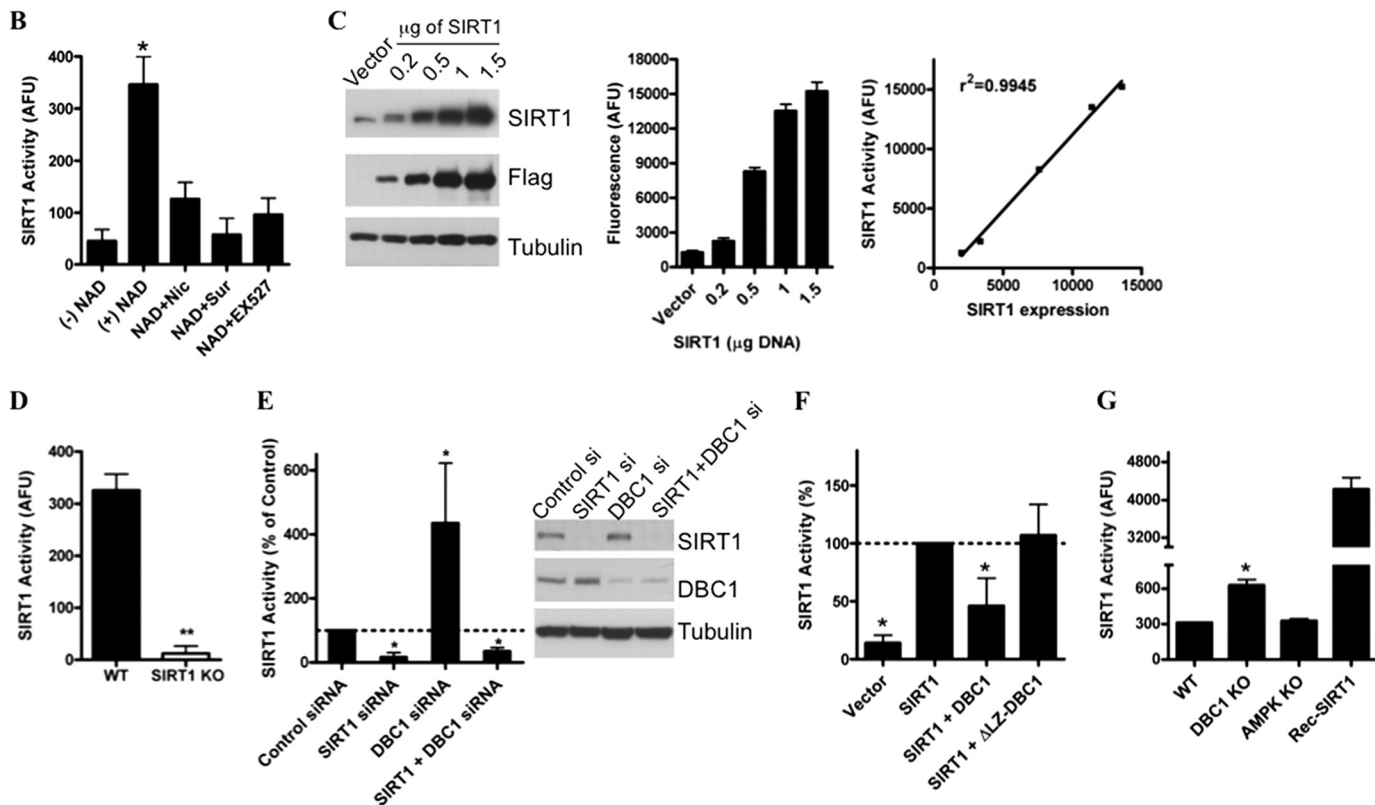
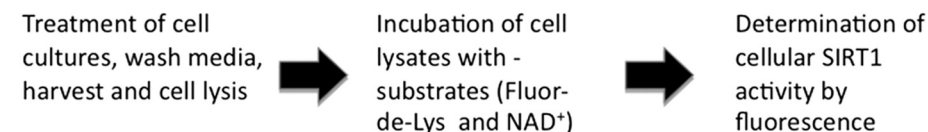


FIGURE 1. Characterization of assay used to measure cellular SIRT1 activity. *A*, basic scheme showing the steps followed to measure cellular SIRT1 activity. Detailed information is provided under "Experimental Procedures." *B*, measurement of endogenous cellular SIRT1 activity in 293T cells. Activity was measured in cellular extracts in the absence of exogenous NAD⁺ (–NAD⁺), with the addition of 100 μM NAD⁺ (+NAD), or with NAD⁺ plus 2 mM nicotinamide (NAD+Nic), with NAD⁺ plus 100 μM suramin (NAD+Sur), or NAD⁺ plus 10 μM EX527 (NAD+EX527). *C*, 293T cells were transfected with different amounts of a FLAG-SIRT1-coding plasmid. Cell lysates were immunoblotted with anti-SIRT1, anti-FLAG, and anti-tubulin antibodies. The graph on the left is the cellular SIRT1 activity measured 24 h after the transfection. The graph on the right shows the relationship between SIRT1 expression levels and cellular SIRT1 activity. *D*, SIRT1 activity was measured in MEFs obtained from WT and SIRT1 KO mice. *E*, SIRT1 and DBC1 were knocked down in HepG2 cells with specific siRNAs, and SIRT1 activity was assessed. Activity is shown as fold change with respect to the control. *, *p* < 0.05 (ANOVA test, *n* = 3). Cell lysates were immunoblotted with anti-SIRT1, anti-DBC1, and anti-tubulin antibodies. *F*, cellular SIRT1 activity was measured in 293T cells transfected with FLAG-SIRT1, FLAG-SIRT1 + Myc-DBC1, or FLAG-SIRT1 + ΔLZ Myc-DBC1, a mutant DBC1 that does not have the leucine zipper domain and does not bind to SIRT1. *, *p* < 0.05 (ANOVA test, *n* = 3). *G*, cellular SIRT1 activity was measured in MEFs from WT, DBC1 KO, and AMPK (α1α2) KO mice. The activity of 1 unit of purified recombinant human SIRT1 was measured in parallel for the same time. *, *p* < 0.05 (ANOVA test, *n* = 3). Error bars represent S.D. AFU, arbitrary fluorescence units.

(Fig. 1G). More importantly, we also found that the cellular SIRT1 activity measured in cell lysates is within the linear range of detection of the assay, and further changes could be determined as shown by the measurement in parallel of recombinant purified SIRT1 activity (Fig. 1G). Taken together, the results shown here plus what we and others have previously and independently shown (31, 39–41) provide very strong evidence that the Fluor-de-Lys SIRT1 assay is an extremely valuable assay to measure cellular SIRT1 activation.

cAMP/PKA Pathway Activates SIRT1—We (31) and other investigators (2, 47) have shown previously that SIRT1 is activated in the liver and in cells upon starvation. In fact, we have shown that starvation increases SIRT1 activity by displacing it from DBC1 (31). However, the molecular pathways that lead to the dissociation of the SIRT1-DBC1 complex are not known. One of the main kinases activated by starvation is PKA (48). In

fact, while this manuscript was in preparation, Gerhart-Hines *et al.* (19) showed that PKA stimulation leads to SIRT1 activation by a not completely elucidated mechanism. Similar to what was found by Gerhart-Hines *et al.* (19), we observed that treatment of cells with forskolin or cpt-cAMP, a permeant analog of cAMP, produces a rapid and transient activation of SIRT1 in several cell lines (Fig. 2, A–C). Because it has been proposed that changes in NAD⁺ can lead to changes in SIRT1 activity (49), we measured intracellular NAD⁺ levels after forskolin and cpt-cAMP treatments. We did not detect changes in the intracellular levels of NAD⁺ under these experimental conditions (Fig. 2D), suggesting that SIRT1 activation is achieved by a different mechanism.

To confirm the specificity of the activity measurements, we transfected HepG2 cells with control and SIRT1 siRNAs. We did not detect any SIRT1 activity in the SIRT1 siRNA-treated

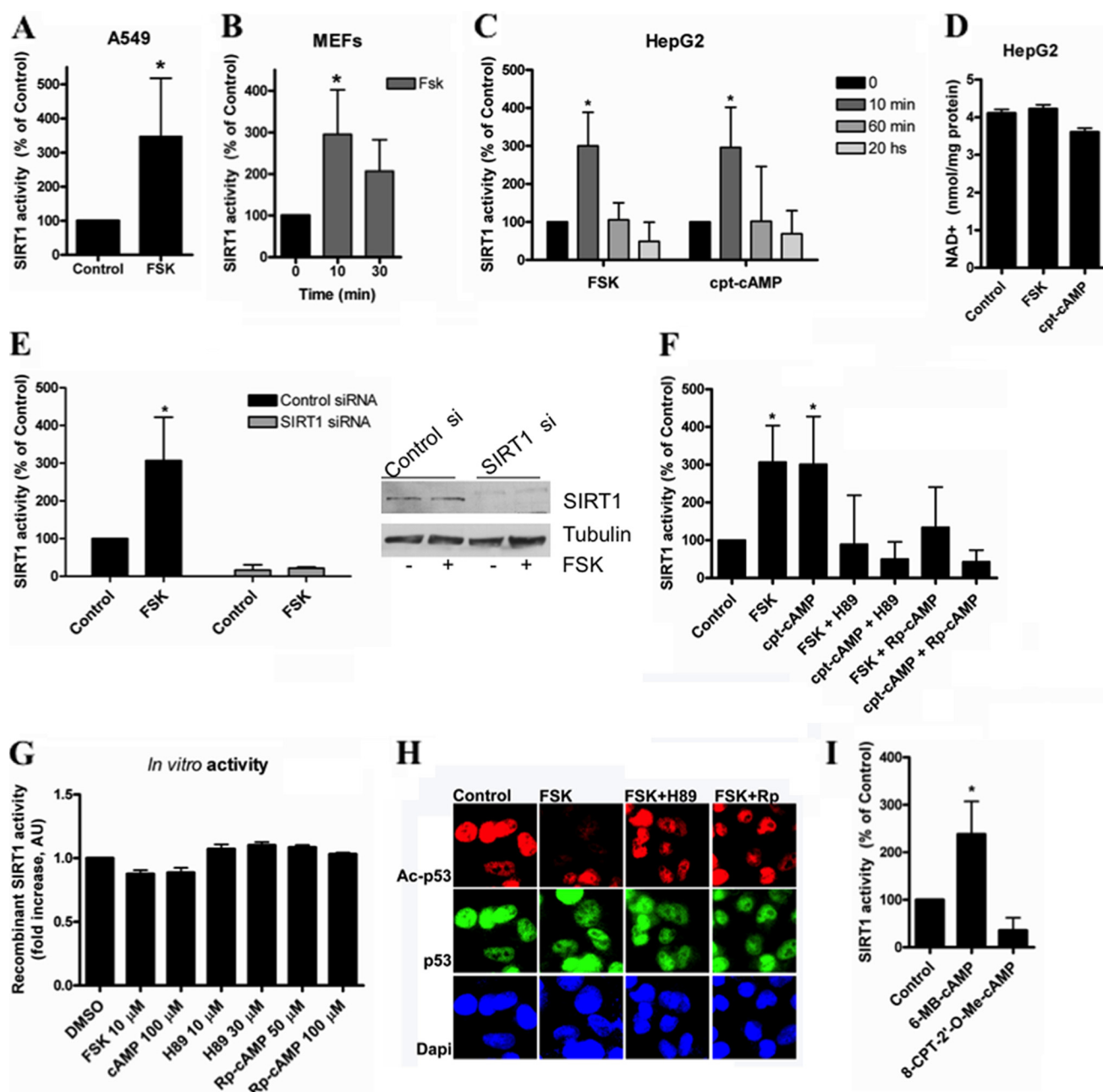


FIGURE 2. cAMP/PKA increase SIRT1 activity by mechanism that is independent of changes in NAD levels. SIRT1 activity was measured in A549 cells (A), mouse embryonic fibroblasts (B), and HepG2 cells (C) treated with 10 μ M forskolin (FSK) or 100 μ M cpt-cAMP for the indicated times. *, $p < 0.01$ (ANOVA, $n = 3-9$). SIRT1 activity was normalized to time 0. D, -fold change in NAD⁺ concentration in HepG2 cells after forskolin (10 μ M) or cpt-cAMP (100 μ M) incubation for 10 min ($n = 3$). E, SIRT1 was knocked down in HepG2 cells with specific siRNA, and SIRT1 activity was assessed after stimulation with 10 μ M forskolin for 10 min. Activity is shown as -fold change with respect to the control. *, $p < 0.05$ (ANOVA test, $n = 3$). Cell lysates were immunoblotted with anti-SIRT1 and anti-tubulin antibodies. F, cells were pretreated for 45 min with the PKA inhibitor H89 (30 μ M) or (R_p)-cAMP (100 μ M) and then stimulated with 10 μ M forskolin or 100 μ M cpt-cAMP for 10 min. SIRT1 activity was normalized to the control. * shows significant difference with respect to the control ($p < 0.01$, ANOVA, $n = 3$). G, human recombinant purified SIRT1 activity in the presence of different compounds was measured *in vitro*. 0.2 unit of SIRT1 was incubated with the compounds at the indicated concentrations. H, HepG2 cells were pretreated for 45 min with the PKA inhibitor H89 (30 μ M) or (R_p)-cAMP (Rp; 100 μ M) and then stimulated with 10 μ M forskolin for 10 min. Immunofluorescence for Ac-p53 and total p53 was analyzed using specific antibodies. I, cells were incubated with the PKA activator 6-MB-cAMP (100 μ M) and the EPAC activator 8-CPT-2'-O-Me-cAMP; (100 μ M) for 10 min before harvesting. SIRT1 activity was measured and normalized to the control. *, $p < 0.01$ (t test, $n = 3$). Error bars represent S.D. AU, arbitrary units.

cultures either in the control cells or after treatment with forskolin (Fig. 2E).

cAMP can regulate cellular functions by a direct effect on target proteins (50), or it can activate a signal transducer like PKA or the EPACs (50). To further explore the mechanism by which cAMP activates SIRT1, we studied which of these differ-

ent mechanisms account for the cAMP-mediated SIRT1 activation. The cAMP-induced SIRT1 activation was prevented by the PKA inhibitors H89 and (R_p)-cAMP (Fig. 2F), suggesting that in cells this effect is mediated by PKA. As a control, we tested whether these compounds directly interfered with the SIRT1 assay. We found that none of the PKA activators or

DBC1 Is Necessary for SIRT1 Activation by PKA and AMPK

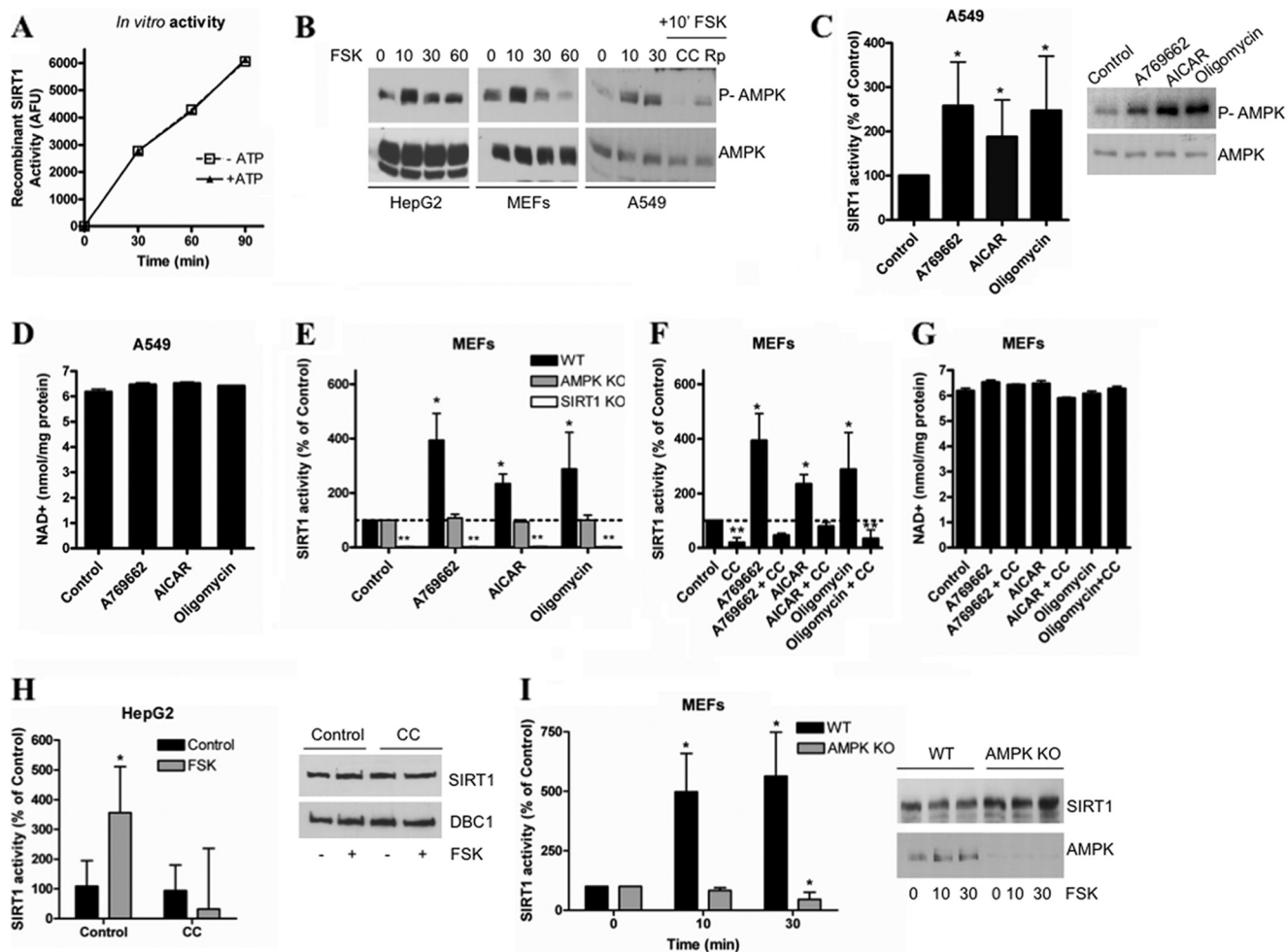


FIGURE 3. SIRT1 activation by PKA is AMPK-dependent. *A*, activity of human recombinant purified SIRT1 (0.2 unit) was measured using a fluorometric assay after performing a kinase assay with the catalytic subunit of PKA in the presence or absence of 200 μM ATP. *B*, AMPK activation was measured by immunoblot using anti-Thr(P)-172 antibody in different cell lines after treatment with 10 μM forskolin (FSK) for different times. Compound C (CC; 10 μM) and (R_p)-cAMP (R_p ; 100 μM) were added 2 h prior to the addition of forskolin. *C*, SIRT1 activity in A549 cells was measured after a 2-h incubation with A769662 (100 μM), AICAR (2 mM), and oligomycin (5 μM). Activity was expressed as the percentage of activity with respect to the control. *, $p < 0.05$ (ANOVA test, $n = 3$). AMPK activation by the different compounds was confirmed by Western blot (right) with anti-Thr(P)-172 antibody. *D*, determination of intracellular NAD⁺ levels in A549 cells treated as described in *C*. *E*, SIRT1 activity was measured in MEFs from WT, AMPK KO, and SIRT1 KO mice. Cells were incubated with A769662 (100 μM), AICAR (2 mM), or oligomycin (5 μM) for 2 h before measuring SIRT1 activity. SIRT1 activity was normalized to the respective control for each cell type. SIRT1 KO cells showed no detectable activity. * and **, $p < 0.05$ (ANOVA test, $n = 3$). *F*, SIRT1 activity was determined in MEFs from WT mice. The AMPK inhibitor compound C (10 μM) was added to the cells 2 h before starting the treatments. Cells were incubated with A769662 (100 μM), A769662 + compound C, AICAR (2 mM), AICAR + compound C, oligomycin (5 μM), and oligomycin + compound C for 2 h before measuring SIRT1 activity. SIRT1 activity was normalized to control. * and **, $p < 0.05$ (ANOVA test, $n = 3$). *G*, intracellular NAD⁺ levels in WT MEFs treated as described in *F*. *H*, AMPK was inhibited in HepG2 cells by a pretreatment with compound C (10 μM) for 2 h, and SIRT1 activity was assessed after stimulation with 10 μM forskolin for 10 min. Activity is shown as -fold change with respect to the control. *, $p < 0.05$ (ANOVA test, $n = 3$). *I*, SIRT1 activity was measured in AMPK WT and KO ($\alpha 1\alpha 2$) MEFs treated with 10 μM forskolin for the indicated times. *, $p < 0.05$ (ANOVA test, $n = 3$). Error bars represent S.D. AFU, arbitrary fluorescence units; P-AMPK, phosphorylated AMPK.

inhibitors had a direct effect on SIRT1 activity *in vitro* (Fig. 2G). To provide additional evidence that SIRT1 is activated by the cAMP/PKA pathway, we performed an immunofluorescence assay for endogenous p53 acetylation. We used an antibody against acetylated Lys-382 on p53, a site that is deacetylated by SIRT1 (51). Although forskolin treatment induced p53 deacetylation, H89 and (R_p)-cAMP prevented the deacetylation induced by forskolin (Fig. 2H), confirming the results obtained using the Fluor-de-Lys assay.

To further assess the role of PKA and to evaluate a possible contribution of EPAC, we treated cell cultures with 6-MB-cAMP, a direct and specific activator of PKA, and with 8-CPT-2'-O-Me-cAMP, a specific activator of EPAC. We observed that only the PKA stimulator produced activation of SIRT1

(Fig. 2I), confirming that the cAMP/PKA pathway can transiently activate SIRT1. Taken together, these results indicate that the cAMP/PKA pathway can activate endogenous cellular SIRT1.

AMPK Mediates Effect of cAMP/PKA on SIRT1 Activation—We measured recombinant SIRT1 activity *in vitro* after a kinase assay that included the catalytic subunit of PKA with or without ATP. We found that PKA does not affect SIRT1 activity directly (Fig. 3A), suggesting that another kinase mediates the effect of PKA on SIRT1 activation. Interestingly, we observed that when cells were treated with forskolin the AMPK was also transiently activated in a pattern that followed the same temporal curve observed for SIRT1 activation (Fig. 3B). This fast AMPK activation by forskolin was observed in several cell lines, including

MEFs, HepG2, and A549. Preincubation of A549 cell cultures with the AMPK inhibitor compound C prevented the activation of AMPK, confirming the specificity of the antibody (Fig. 3B). In addition, preincubation of the cells with the PKA inhibitor (R_p)-cAMP also prevented the forskolin-induced increase in AMPK phosphorylation, suggesting that the AMPK activation observed is dependent on PKA (Fig. 3B). In light of these observations, we tested whether AMPK was mediating the PKA-induced SIRT1 activation.

AMPK is a kinase that has a key role in metabolism and has been shown to regulate SIRT1 activity (25). In fact, it was recently shown that incubation of cells with AMPK activators for long periods (typically 8–12 h) leads to SIRT1 activation through an increase in the intracellular levels of NAD^+ (25). Our results showed a fast SIRT1 activation that occurred independently of changes in NAD^+ levels, suggesting that SIRT1 is activated through a different mechanism. Therefore, we tested whether short treatments (1–2 h) with AMPK activators can induce an increase in SIRT1 activity without changes in the intracellular levels of NAD^+ .

To test our hypothesis, we used several AMPK activators: A769662 (52), AICAR (53), and oligomycin (54). We found that a short incubation of A549 cells with all these AMPK activators promoted SIRT1 activation (Fig. 3C) without any changes in NAD^+ levels (Fig. 3D). We measured the *in vitro* recombinant SIRT1 activity in the presence of the AMPK activators and confirmed that the AMPK activators have no direct effect on SIRT1 activity *in vitro* (supplemental Fig. S2). Resveratrol was excluded from the *in vitro* SIRT1 activity assay due to the artifact it has been reported to produce in the fluorescence assay. To confirm that the effect of the AMPK activators was indeed AMPK-dependent, we incubated AMPK WT and KO MEFs with AMPK activators and then measured SIRT1 activity. None of the AMPK activators induced SIRT1 activity on the AMPK KO MEFs in contrast to the WT cells (Fig. 3E). As a control for the assay, SIRT1 activity was also measured in SIRT1 KO MEFs (Fig. 3E), and we detected no activity in these cells. Finally, to further confirm our results, we measured the effect of the AMPK activators on SIRT1 activity in WT MEFs pretreated with the AMPK inhibitor compound C. We found that in these conditions the AMPK activators did not induce SIRT1 activation (Fig. 3F). All the observed changes in SIRT1 activity occurred independently of changes in NAD^+ levels (Fig. 3G). To demonstrate that the assay we used to measure NAD^+ is able to detect even small changes in NAD^+ , we performed a time course with the NamPT inhibitor FK866. As shown in supplemental Fig. S3, the methodology used in this study was sensitive to small variations in NAD^+ concentration. Furthermore, we have previously detected changes in NAD^+ and NAD^+ metabolites in several cells and tissues using the same method (10, 11, 14, 31, 55–57). Taken together, these results demonstrate that AMPK can activate SIRT1 without detectable changes in cellular NAD^+ levels.

Finally, we directly tested the role of AMPK in the cAMP/PKA-mediated SIRT1 activation. For this, we used HepG2 cells pretreated with the AMPK inhibitor compound C. In agreement with our hypothesis, when AMPK activation was blocked by compound C, forskolin no longer induced SIRT1 activation

(Fig. 3H). Moreover, the response to forskolin was abrogated in AMPK ($\alpha1\alpha2$) KO MEFs but not in WT MEFs (Fig. 3I). From these experiments, we concluded that the activation of SIRT1 induced by cAMP/PKA is dependent on AMPK activation.

DBC1 Is Required for SIRT1 Activation Induced by PKA and AMPK—We have observed previously that, *in vivo*, fasting promotes an increase in SIRT1 activity by disrupting the interaction between SIRT1 and DBC1 without changes in NAD^+ levels or in the expression levels of SIRT1 (31). We then explored whether DBC1 was required for the AMPK- and PKA-induced SIRT1 activation. For this, we stimulated AMPK with A769662, AICAR, and oligomycin in DBC1 WT and KO MEFs. As shown in Fig. 4A, none of the AMPK activators were able to induce an increase in SIRT1 activity in cells that lacked DBC1 in contrast with the clear induction of SIRT1 activity in WT cells. We further confirmed that SIRT1 activation was AMPK-mediated in these cells by preincubating them with compound C. Again, the activation promoted by the AMPK activators was prevented by pretreatment with compound C (Fig. 4A).

Next, we investigated whether the SIRT1 response to cAMP/PKA activation was also dependent on DBC1. For this, we stimulated the cAMP/PKA pathway in cells that lacked DBC1 and in cells treated with siRNA specific for DBC1. Our results show that forskolin did not activate SIRT1 in the absence of DBC1 either in DBC1 KO MEFs (Fig. 4B) or in HepG2 cells where DBC1 was knocked down (Fig. 4C). Altogether, our results indicate that DBC1 is required for the AMPK- and PKA-induced SIRT1 activation.

AMPK and PKA Activation Promote Dissociation of SIRT1 from DBC1—Because DBC1 is required for the AMPK effect on SIRT1, we examined the effect of the AMPK activation on the interaction between endogenous SIRT1 and DBC1. We performed co-immunoprecipitation in A549 cells treated with the AMPK activators A769662, oligomycin, and resveratrol. Resveratrol was used at high concentrations that have been shown previously to activate AMPK (54) due to impairment in mitochondrial function (58) (see also supplemental Fig. S4). As shown in Fig. 5A, all of these compounds promoted a robust dissociation of the SIRT1-DBC1 complex, an event that was partially blocked by preincubation with the AMPK inhibitor compound C (Fig. 5B).

We also evaluated the effect of a CA form of AMPK or a dominant-negative form of AMPK on the interaction between transfected SIRT1 and DBC1 (Fig. 5C). Our results show that cellular AMPK activity inversely correlates with the amount of interaction between SIRT1 and DBC1. In other words, the transfection of the CA form of AMPK decreased the interaction between SIRT1 and DBC1, whereas the dominant-negative form increased the interaction between these two proteins. This set of experiments demonstrates that AMPK modulates the interaction between SIRT1 and DBC1.

Next, we tested whether the cAMP/PKA pathway also modulates the SIRT1-DBC1 complex. We activated PKA with forskolin and 6-MB-cAMP and evaluated the interaction between SIRT1 and DBC1. Treatment of A549 cells with these compounds resulted in a clear loss of the interaction between SIRT1 and DBC1 (Fig. 6A), an event that was blocked by preincubation with the PKA inhibitor H89 (Fig. 6B). To further prove that

DBC1 Is Necessary for SIRT1 Activation by PKA and AMPK

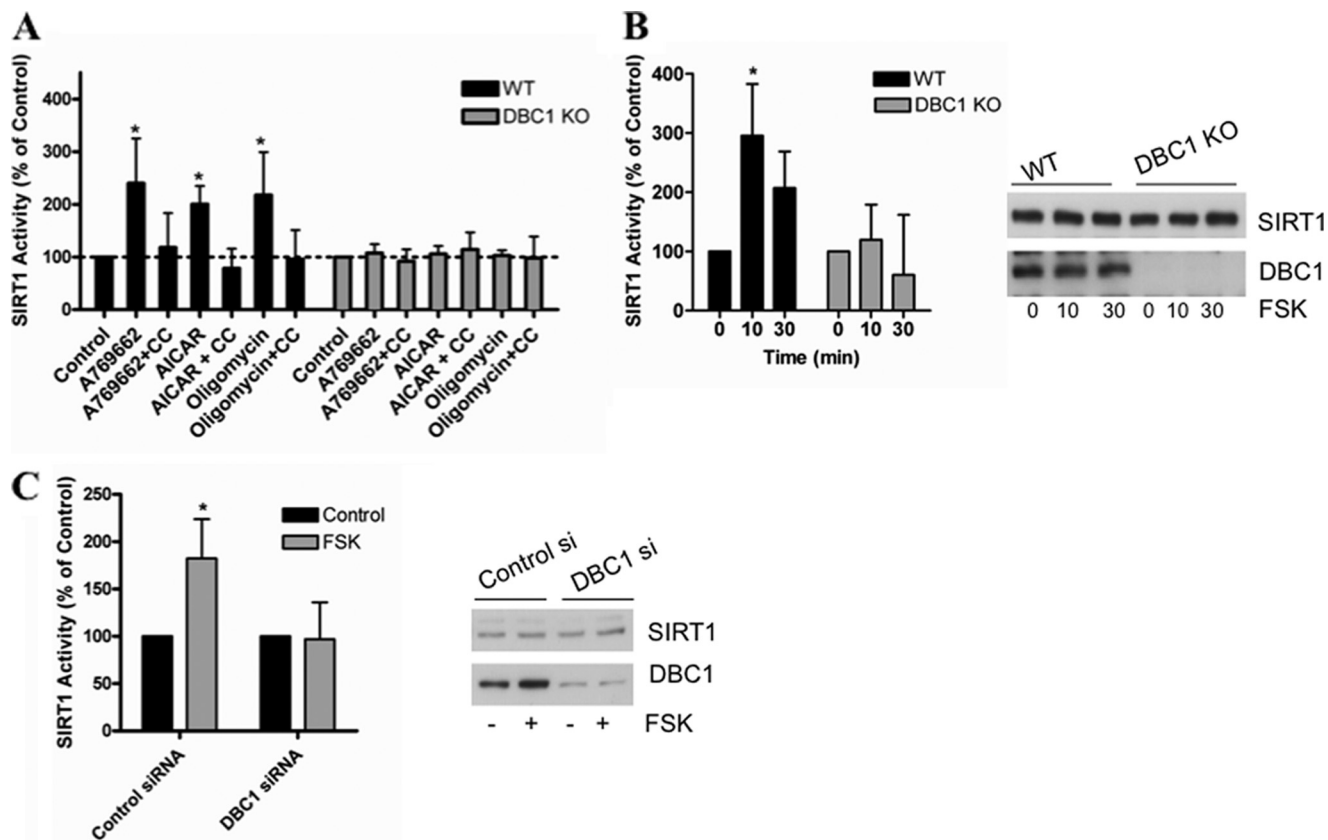


FIGURE 4. SIRT1 activation by cAMP/PKA/AMPK pathway depends on DBC1. A, SIRT1 activity was measured in WT and DBC1 KO MEFs. Cells were incubated with A769662 (100 μ M) or A769662 + compound C (CC), AICAR (2 mM) or AICAR + compound C, and oligomycin (5 μ M) or oligomycin + compound C for 2 h before measuring SIRT1 activity. Compound C was used at 10 μ M and was preincubated for 2 h. Activity in the WT cells was normalized to the WT control, and activity in the KO cells was normalized to the KO control. SIRT1 activity in the control was always higher in DBC1 KO than in WT MEFs (see Fig. 1). *, $p < 0.05$ (ANOVA test, $n = 3$). B, DBC1 was knocked down in HepG2 cells with siRNA, and SIRT1 activity was assessed after stimulation with 10 μ M forskolin (FSK) for 10 min. Activity is shown as -fold change with respect to the control. *, $p < 0.05$ (ANOVA test, $n = 3$). C, SIRT1 activity in DBC1 WT and KO MEFs treated with 10 μ M forskolin for the indicated times. *, $p < 0.05$ (ANOVA test, $n = 3$). Error bars represent S.D.

PKA activates SIRT1 in an AMPK-dependent manner, we tested the effect of compound C on the dissociation promoted by forskolin. As shown in Fig. 6C, preincubation of cells with compound C blocked the dissociation induced by forskolin, indicating that indeed AMPK is part of the signaling pathway that connects PKA and SIRT1.

SIRT1 Is Phosphorylated in Response to AMPK Activation—Phosphorylation is a key modification that regulates SIRT1 function as it has been clearly shown in numerous reports (18, 20–24). However, there is no evidence to support that either PKA or AMPK phosphorylates SIRT1 directly *in vivo*. Gerhart-Hines *et al.* (19) showed that Ser-434 phosphorylation on mouse SIRT1 is necessary for PKA regulation, although the authors speculate that the site is unlikely to be a direct target of PKA. On the other hand, two independent investigators failed to observe SIRT1 phosphorylation by AMPK *in vitro* or in cells (25, 59). Therefore, it is unlikely that either PKA or AMPK is directly phosphorylating SIRT1. However, PKA and AMPK activation could result in SIRT1 phosphorylation by an intermediate kinase. To determine whether AMPK activation results in SIRT1 phosphorylation, we performed autoradiography in cells loaded with 32 P. As can be seen in Fig. 7A, transfection of a constitutively active form of AMPK resulted in incorporation of 32 P into SIRT1. Moreover, treatment of cells with

resveratrol also resulted in incorporation of 32 P into SIRT1 (Fig. 7B). These data indicate that SIRT1 phosphorylation could be involved in the SIRT1 activation by PKA and AMPK.

To date, several phosphorylation sites have been reported on SIRT1. We directly tested the phosphorylation of serine 47 because this site has been suggested to mediate activation of SIRT1 (13). For this, we used a specific antibody against phosphorylated serine 47. We found that treatment with resveratrol or A769662 resulted in an increase in phosphorylation in serine 47 that was blocked by preincubation with compound C (Fig. 7, C and D). The specificity of the phosphoantibody was assessed by immunoblotting of the wild type SIRT1 and the mutant form of SIRT1 in which serine 47 was replaced by arginine (S47R). As can be seen in Fig. 7E, the antibody did not recognize the mutant that lacks serine 47. In light of these findings, we tested the relevance of this site in the regulation of SIRT1 by PKA and AMPK. In particular, we tested the ability of the S47R mutant to dissociate from DBC1 in response to AMPK activation. However, we found that AMPK activators were still able to dissociate the complex between DBC1 and the S47R SIRT1 mutant (data not shown), suggesting that more than one site may be needed to regulate the interaction by AMPK.

In an attempt to map additional sites on SIRT1 that might be a target of regulation by PKA/AMPK and to evaluate the impor-

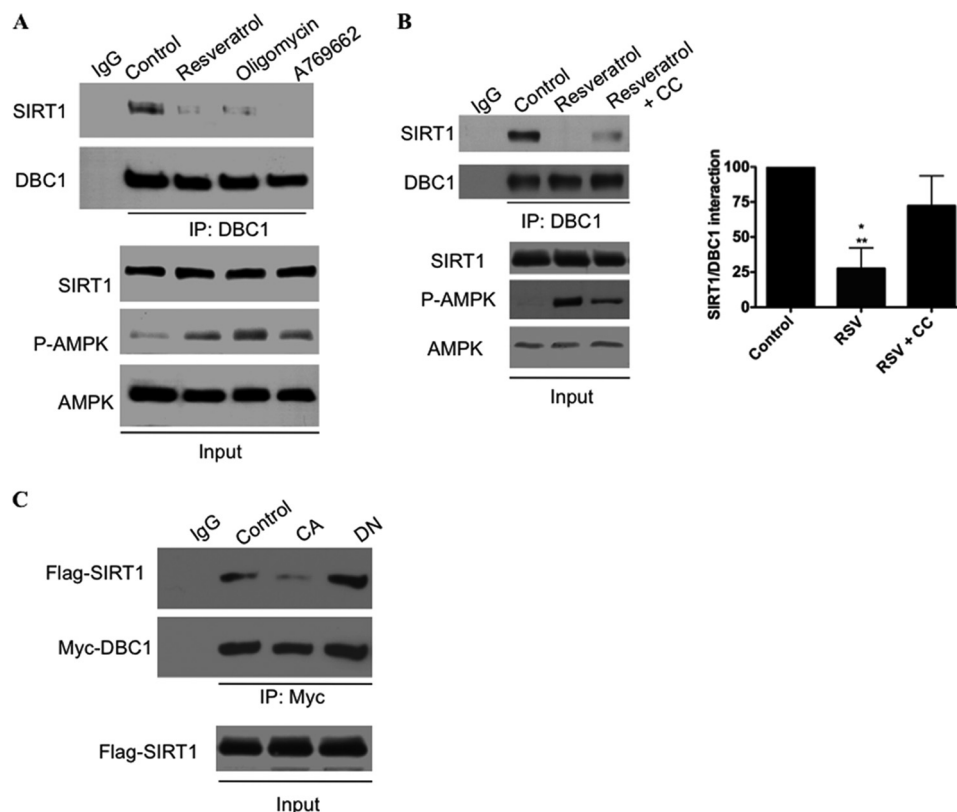


FIGURE 5. AMPK activation induces dissociation of SIRT1 from DBC1. *A* and *B*, SIRT1-DBC1 interaction was evaluated by co-immunoprecipitation in A549 cells. *A*, cells were treated with resveratrol (100 μ M), oligomycin (5 μ M), or A769662 (100 μ M) for 2 h before performing immunoprecipitation (IP) for DBC1. Proteins were immunoblotted with anti-SIRT1, anti-DBC1, anti-phosphorylated AMPK (P-AMPK) (Thr-172), and anti-AMPK antibodies. *B*, cells were treated with resveratrol (RSV; 100 μ M) or resveratrol + compound C (CC; 10 μ M) for 2 h before performing immunoprecipitation. Immunoprecipitates were immunoblotted with anti-SIRT1 and anti-DBC1 antibodies. The graph shows the average of three independent experiments. * Denotes difference to control, and ** denotes difference to RSV + CC. Error bars represent S.D. *C*, SIRT1-DBC1 interaction was evaluated by co-immunoprecipitation in 293T cells after transfection of FLAG-SIRT1, Myc-DBC1, and CA AMP α or dominant-negative AMPK α (DN). Immunoprecipitates were immunoblotted with anti-FLAG and anti-Myc antibodies.

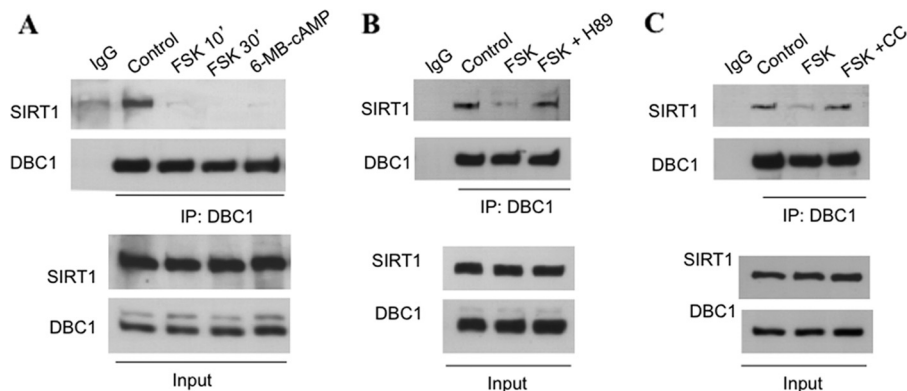


FIGURE 6. cAMP-PKA activation promotes dissociation of SIRT1 from DBC1 by AMPK-dependent mechanism. *A–C*, co-immunoprecipitation (IP) of SIRT1 with DBC1 in A549 cells. DBC1 was immunoprecipitated from cell lysates, and immunoprecipitates were immunoblotted with anti-SIRT1 and anti-DBC1 antibodies. In *A*, cells were stimulated with forskolin (FSK) + isobutylmethylxanthine (IBMX) (10 and 70 μ M, respectively) for the indicated times or the PKA activator 6-MB-cAMP (100 μ M) for 10 min ('). *B*, cells were pretreated with the PKA inhibitor H89 (30 μ M for 45 min) and then stimulated with forskolin and isobutylmethylxanthine (10 and 70 μ M, respectively) for 10 min. *C*, cells were pretreated with compound C (CC; 10 μ M) for 2 h and then stimulated as in *B*.

tance of the dissociation of SIRT1 and DBC1 in the activation of SIRT1 mediated by PKA/AMPK, we performed point mutations of other reported phosphosites (for a complete list of mutations, see supplemental Fig. S5). First, we tested the ability of the single phosphomutants to dissociate from DBC1 upon activation of PKA and AMPK. We found that AMPK activators were still able to dissociate DBC1 from all the SIRT1 single phosphomutants. We therefore speculated that that a combi-

nation of phosphosites could be responsible for the regulation of the binding between SIRT1 and DBC1. Interestingly, the triple mutant S47R,S605R,S615R did not dissociate from DBC1 in response to PKA activation (Fig. 7F). Furthermore, the activity of the triple mutant was insensitive to PKA activation (Fig. 7G). The results shown in Fig. 7, F and G, clearly show that the dissociation from DBC1 is required for the SIRT1 activation promoted by the cAMP/PKA pathway. Moreover, our data

DBC1 Is Necessary for SIRT1 Activation by PKA and AMPK

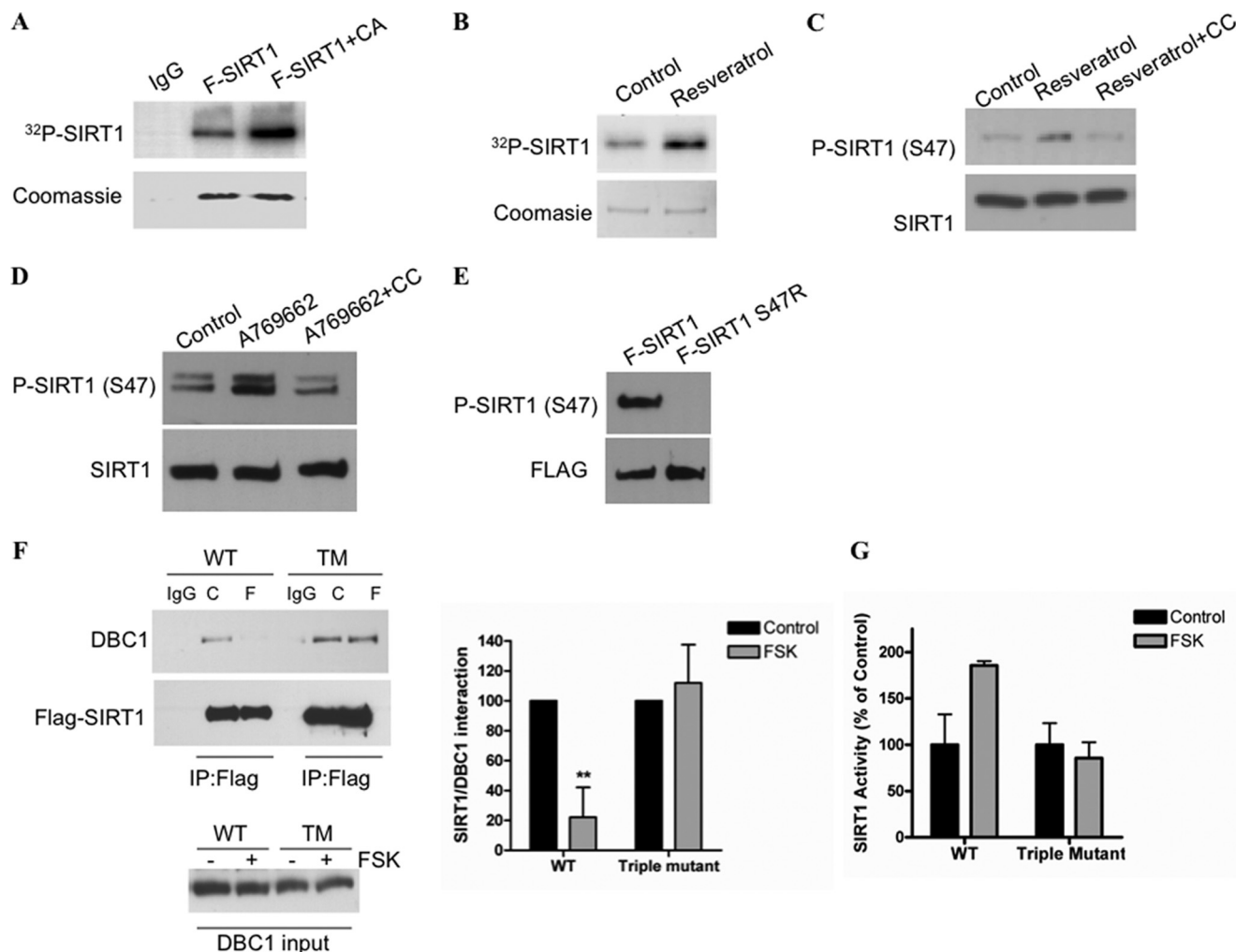


FIGURE 7. Activation of AMPK and PKA leads to SIRT1 phosphorylation. *A*, 293T cells were transfected with FLAG-SIRT1 or FLAG-SIRT1 plus a CA form of AMPK. The cell cultures were loaded with $\text{H}_3\text{-}^{32}\text{PO}_4$, FLAG-SIRT1 was immunoprecipitated, and the radioactivity incorporated was visualized by autoradiography. *B*, 293T cells were transfected with FLAG-SIRT1, loaded with $\text{H}_3\text{-}^{32}\text{PO}_4$, and later treated with 10 μM resveratrol for 2 h. SIRT1 phosphorylation was visualized by autoradiography. *C*, A549 cells were incubated with resveratrol (10 μM) or resveratrol and compound C (CC; 10 μM) for 2 h. Compound C was added 45 min before resveratrol. Samples were immunoblotted with anti-phospho (P)-SIRT1 (Ser-47). *D*, HepG2 cells were incubated with A769662 (100 μM) or A769662 and compound C (10 μM) for 2 h. *E*, Western blot with anti-phospho-SIRT1 (Ser-47) in 293T cells transfected with WT SIRT1 (FLAG (F)-SIRT1) or FLAG-S47RSIRT1. *F*, WT and the triple mutant (TM; S47R,S605R,S615R) SIRT1 were transfected in 293T cells. After 24 h, cells were incubated with forskolin (FSK; 10 μM) for 20 min. FLAG-SIRT1 was immunoprecipitated (IP), and the interaction was evaluated by immunoblot with anti-DBC1 and anti-FLAG antibodies. The graph shows the average of four experiments (**, $p < 0.001$; ANOVA test). *G*, SIRT1 activity was measured in the same experimental conditions described in *B*. Error bars represent S.D.

identified the sites 47, 605, and 615 as residues involved in the regulation of the interaction between SIRT1 and DBC1. Although we do not have evidence that the activation of SIRT1 involves phosphorylation of serines 605 and 615, we provide evidence that suggest that these sites modulate the binding between SIRT1 and DBC1. A scheme representing our main findings is shown in Fig. 8.

DISCUSSION

The beneficial effects of SIRT1 activation have been studied extensively (60). Mounting evidence from independent groups shows that SIRT1 activation leads to protection against metabolic syndrome, cardiovascular diseases, and cancer (60) among other diseases. However, a much more complex issue is how to achieve SIRT1 activation *in vivo*. We have recently shown that, *in vivo*, most SIRT1 is bound to its regulator DBC1 and that this interaction is dynamic and can be displaced (31).

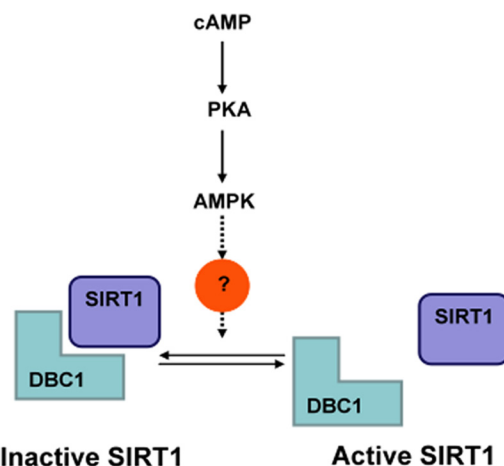


FIGURE 8. Proposed mechanism of SIRT1 regulation by PKA and AMPK.

In fact, we also showed that when DBC1 is absent and therefore SIRT1 is more active mice are protected against metabolic syndrome (31). It therefore becomes of key importance to understand how the SIRT1-DBC1 complex is regulated because it may lead to the development of new strategies to activate SIRT1 pharmacologically.

In this work, we attempted to characterize in detail the mechanism involved in the regulation of the interaction between SIRT1 and DBC1 and therefore SIRT1 activity. We found that SIRT1 activity is positively regulated by the protein kinases PKA and AMPK. We showed that PKA activation leads to a fast and transient SIRT1 activation. This activation was AMPK-dependent, involved the dissociation of SIRT1 from DBC1, and occurred independently of changes in NAD^+ levels.

While this article was in preparation, Gerhart-Hines *et al.* (19) also showed SIRT1 activation by PKA. These authors propose that SIRT1 activation by PKA involves phosphorylation of SIRT1 and changes in the affinity of SIRT1 for NAD^+ . Although our findings do not exclude this possibility, we showed that SIRT1 must dissociate from DBC1 to be activated by PKA. Also, a recent paper shows that the polyphenol resveratrol induces cellular SIRT1 activation via activation of the cAMP/EPAC pathway and AMPK (61). Therefore, our group and two independent groups have shown that an increase in cAMP leads to SIRT1 activation. Our study provides further information about the specific mechanism of SIRT1 activation, which is mediated by modulation of the SIRT1-DBC1 interaction.

Recent publications, including this one, have reported changes in SIRT1 activity that are independent of alterations in the concentration of NAD^+ (19, 31). Since our first observation of an increase in SIRT1 activity *in vivo* without detectable changes in NAD^+ concentration (31), evidence has accumulated to prove that it is possible to induce SIRT1 activation without detectable changes in intracellular NAD^+ levels (19). During physiological processes, it may be necessary to activate SIRT1 and not other NAD^+ -consuming enzymes. However, an increase in the cytoplasmic and nuclear levels of NAD^+ could result in higher activity of several sirtuins and the poly(ADP-ribose) polymerases. Therefore, one can foresee that there must be an alternative, specific mode of SIRT1 regulation.

The results presented here provide mechanistic insight into the PKA-induced SIRT1 activation. Our results point to AMPK as a kinase that is downstream of PKA. In support of this notion, we observed that forskolin induces a transient activation of AMPK that parallels the increase in SIRT1 activity, that the AMPK inhibitor compound C abolishes the effect of forskolin in SIRT1 activity, and that in AMPK KO MEFs SIRT1 is insensitive to cAMP elevations. In line with our observations, others have also reported that PKA can transiently activate AMPK (26–30, 62). This activation seems to occur through the kinase LKB1, which activates AMPK by phosphorylation of serine 172 (63). PKA phosphorylates LKB1 directly at serine 431 (62, 64), and phosphorylation at this site is needed for some of the LKB1 functions (64, 65). Another possible mechanism that may lead to AMPK activation by the cAMP/PKA pathway is through regulation of cAMP degradation. Once cAMP levels increase in cells, the level of this second messenger quickly returns to basal levels due to its degradation by phosphodiesterases. Phos-

phodiesterases degrade cAMP into 5'-AMP (66), and therefore its action could result in a fast accumulation of AMP. Therefore, it seems plausible that agents that activate the cAMP/PKA pathway could result in activation of AMPK either by activation of LKB1, an increase in AMP levels, or both.

In this work, we present evidence that SIRT1 is phosphorylated upon AMPK activation. However, it remains unknown which kinase is responsible for SIRT1 phosphorylation upon PKA and AMPK activation. Our data identified serines 47, 605, and 615 as key residues involved in the regulation of the interaction between SIRT1 and DBC1. We provide evidence of phosphorylation of serine 47, but it remains to be elucidated whether serines 605 and 615 are also phosphorylated when PKA and AMPK are activated. As mentioned before, two independent groups failed to detect SIRT1 phosphorylation by AMPK (25, 59), which suggests that the regulation of this process is extremely complex. However, sequence analysis of human SIRT1 suggests that SIRT1 could be a target for AMPK phosphorylation. The consensus sequence for AMPK phosphorylation as first proposed by Carling and Hardie (67) consists of an arginine in the -2, -3, or -4 position and a hydrophobic residue at -1 relative to the serine or threonine target of phosphorylation. Later on, a study by Dale *et al.* (68) described the importance of a leucine at positions -5 and +4 (although other hydrophobic amino acids are accepted too) besides the basic amino acid at -3 or -4. More recently, another study identified that AMPK favors a serine with a valine or arginine at -2 (69). However, it is also important to note that not all known substrates for AMPK have the perfect consensus sequence but a variation of it. FOXO3 for example is phosphorylated by AMPK at Ser-413, which is not flanked by a leucine at position -5 or +4, and Ser-588 that lacks a basic residue at -3 or -4 (59). Using the above data as a reference, we searched the human SIRT1 sequence for serines and threonines in potential AMPK consensus sequence. Interestingly, the serine residue in position 605, one of the sites that is involved in SIRT1 activation by PKA, is flanked by a lysine at -4, a leucine at -5, and a valine at -2 in addition to a hydrophobic amino acid at -1, which is very close to the optimal sequence for AMPK phosphorylation. This fact suggests that further effort should be made to determine whether SIRT1 is a direct target for AMPK.

Of interest is that Kang *et al.* (70) recently found that the amino acids 631–655 in SIRT1 (what they call the essential for SIRT1 activity region) are necessary for SIRT1 activation. Moreover, these authors proposed that this region is important for the regulation of SIRT1 by DBC1. Interestingly, two of the amino acids, 605 and 615, which are involved in the PKA/AMPK-induced activation of SIRT1, are in close proximity to this region. Therefore, amino acids 605 and 615 may play a role in the activation of SIRT1 by PKA and AMPK by regulating the essential for SIRT1 activity region of SIRT1.

Serine 47 in SIRT1 has been shown to be target of JNK1 (21). Furthermore, Gao *et al.* (18) recently showed that JNK1 leads to SIRT1 phosphorylation and a fast increase in SIRT1 activity upon glucose treatment that correlates very well with the time course that we observed for PKA-dependent SIRT1 activation. It could be that AMPK and JNK1 are acting in conjunction to promote SIRT1 dissociation from DBC1.

DBC1 Is Necessary for SIRT1 Activation by PKA and AMPK

Finally, we want to highlight how important it is to understand how the interaction between SIRT1 and DBC1 is regulated to study the regulation of SIRT1. The fact that in the absence of DBC1 the cAMP/PKA and AMPK pathways are incapable of activating SIRT1 suggests that a possible phosphorylation of SIRT1 *per se* is not enough to sustain an increase in its activity. Furthermore, our observations place the SIRT1-DBC1 complex as a key physiological target for SIRT1 regulation.

In summary, our results provide a novel mechanism of SIRT1 activation by a cAMP/PKA/AMPK/DBC1-dependent pathway. It also provides the evidence that the interaction between SIRT1 and DBC1 can be regulated by endogenous cell signaling pathways and opens the possibility that other signals may also promote SIRT1 activation through the dissociation of the SIRT1-DBC1 complex. For instance, it was recently shown that the ataxia telangiectasia mutated kinase (ATM) phosphorylates DBC1 and increases the interaction between SIRT1 and DBC1 (71). Finally, mounting evidence indicates that modulation of SIRT1 activity can be achieved without the nonspecific changes in global cellular NAD⁺ levels. The understanding of specific mechanisms of SIRT1 activation as described here may provide a clearer picture about the regulation of cellular SIRT1 and its physiological consequences.

REFERENCES

- Liu, Y., Dentin, R., Chen, D., Hedrick, S., Ravnskjaer, K., Schenk, S., Milne, J., Meyers, D. J., Cole, P., Yates, J., 3rd, Olefsky, J., Guarente, L., and Montminy, M. (2008) A fasting inducible switch modulates gluconeogenesis via activator/coactivator exchange. *Nature* **456**, 269–273
- Rodgers, J. T., Lerin, C., Haas, W., Gygi, S. P., Spiegelman, B. M., and Puigserver, P. (2005) Nutrient control of glucose homeostasis through a complex of PGC-1 α and SIRT1. *Nature* **434**, 113–118
- Bordone, L., Motta, M. C., Picard, F., Robinson, A., Jhala, U. S., Apfeld, J., McDonagh, T., Lemieux, M., McBurney, M., Szilvasi, A., Easlson, E. J., Lin, S. J., and Guarente, L. (2006) Sirt1 regulates insulin secretion by repressing UCP2 in pancreatic β cells. *PLoS Biol.* **4**, e31
- Moynihan, K. A., Grimm, A. A., Plueger, M. M., Bernal-Mizrachi, E., Ford, E., Cras-Mneur, C., Permutt, M. A., and Imai, S. (2005) Increased dosage of mammalian Sir2 in pancreatic β cells enhances glucose-stimulated insulin secretion in mice. *Cell Metab.* **2**, 105–117
- Schenk, S., McCurdy, C. E., Philp, A., Chen, M. Z., Holliday, M. J., Bandyopadhyay, G. K., Osborn, O., Baar, K., and Olefsky, J. M. (2011) Sirt1 enhances skeletal muscle insulin sensitivity in mice during caloric restriction. *J. Clin. Investig.* **121**, 4281–4288
- Gerhart-Hines, Z., Rodgers, J. T., Bare, O., Lerin, C., Kim, S. H., Mostoslavsky, R., Alt, F. W., Wu, Z., and Puigserver, P. (2007) Metabolic control of muscle mitochondrial function and fatty acid oxidation through SIRT1/PGC-1 α . *EMBO J.* **26**, 1913–1923
- Picard, F., Kurtev, M., Chung, N., Topark-Ngarm, A., Senawong, T., Machado De Oliveira, R., Leid, M., McBurney, M. W., and Guarente, L. (2004) Sirt1 promotes fat mobilization in white adipocytes by repressing PPAR- γ . *Nature* **429**, 771–776
- Imai, S., Armstrong, C. M., Kaeberlein, M., and Guarente, L. (2000) Transcriptional silencing and longevity protein Sir2 is an NAD-dependent histone deacetylase. *Nature* **403**, 795–800
- Revollo, J. R., Grimm, A. A., and Imai, S. (2007) The regulation of nicotinamide adenine dinucleotide biosynthesis by Nampt/PBEF/visfatin in mammals. *Curr. Opin. Gastroenterol.* **23**, 164–170
- Aksoy, P., White, T. A., Thompson, M., and Chini, E. N. (2006) Regulation of intracellular levels of NAD: a novel role for CD38. *Biochem. Biophys. Res. Commun.* **345**, 1386–1392
- Barbosa, M. T., Soares, S. M., Novak, C. M., Sinclair, D., Levine, J. A., Aksoy, P., and Chini, E. N. (2007) The enzyme CD38 (a NAD glycohydrolase, EC 3.2.2.5) is necessary for the development of diet-induced obesity. *FASEB J.* **21**, 3629–3639
- Chini, E. N. (2009) CD38 as a regulator of cellular NAD: a novel potential pharmacological target for metabolic conditions. *Curr. Pharm. Des.* **15**, 57–63
- Revollo, J. R., Grimm, A. A., and Imai, S. (2004) The NAD biosynthesis pathway mediated by nicotinamide phosphoribosyltransferase regulates Sir2 activity in mammalian cells. *J. Biol. Chem.* **279**, 50754–50763
- Aksoy, P., Escande, C., White, T. A., Thompson, M., Soares, S., Benech, J. C., and Chini, E. N. (2006) Regulation of SIRT1 mediated NAD dependent deacetylation: a novel role for the multifunctional enzyme CD38. *Biochem. Biophys. Res. Commun.* **349**, 353–359
- Chen, D., Bruno, J., Easlson, E., Lin, S. J., Cheng, H. L., Alt, F. W., and Guarente, L. (2008) Tissue-specific regulation of SIRT1 by calorie restriction. *Genes Dev.* **22**, 1753–1757
- Haigis, M. C., and Sinclair, D. A. (2010) Mammalian sirtuins: biological insights and disease relevance. *Annu. Rev. Pathol.* **5**, 253–295
- Yang, Y., Fu, W., Chen, J., Olashaw, N., Zhang, X., Nicosia, S. V., Bhalla, K., and Bai, W. (2007) SIRT1 sumoylation regulates its deacetylase activity and cellular response to genotoxic stress. *Nat. Cell Biol.* **9**, 1253–1262
- Gao, Z., Zhang, J., Kheterpal, I., Kennedy, N., Davis, R. J., and Ye, J. (2011) Sirtuin 1 (SIRT1) protein degradation in response to persistent c-Jun N-terminal kinase 1 (JNK1) activation contributes to hepatic steatosis in obesity. *J. Biol. Chem.* **286**, 22227–22234
- Gerhart-Hines, Z., Dominy, J. E., Jr., Bltler, S. M., Jedrychowski, M. P., Banks, A. S., Lim, J. H., Chim, H., Gygi, S. P., and Puigserver, P. (2011) The cAMP/PKA pathway rapidly activates SIRT1 to promote fatty acid oxidation independently of changes in NAD⁺. *Mol. Cell* **44**, 851–863
- Guo, X., Williams, J. G., Schug, T. T., and Li, X. (2010) DYRK1A and DYRK3 promote cell survival through phosphorylation and activation of SIRT1. *J. Biol. Chem.* **285**, 13223–13232
- Nasrin, N., Kaushik, V. K., Fortier, E., Wall, D., Pearson, K. J., de Cabo, R., and Bordone, L. (2009) JNK1 phosphorylates SIRT1 and promotes its enzymatic activity. *PLoS One* **4**, e8414
- Sasaki, T., Maier, B., Koclega, K. D., Chruszcz, M., Gluba, W., Stukenberg, P. T., Minor, W., and Scoble, H. (2008) Phosphorylation regulates SIRT1 function. *PLoS One* **3**, e4020
- Zschoernig, B., and Mahlknecht, U. (2009) Carboxy-terminal phosphorylation of SIRT1 by protein kinase CK2. *Biochem. Biophys. Res. Commun.* **381**, 372–377
- Kang, H., Jung, J. W., Kim, M. K., and Chung, J. H. (2009) CK2 is the regulator of SIRT1 substrate-binding affinity, deacetylase activity and cellular response to DNA damage. *PLoS One* **4**, e6611
- Cant, C., Gerhart-Hines, Z., Feige, J. N., Lagouge, M., Noriega, L., Milne, J. C., Elliott, P. J., Puigserver, P., and Auwerx, J. (2009) AMPK regulates energy expenditure by modulating NAD⁺ metabolism and SIRT1 activity. *Nature* **458**, 1056–1060
- Yin, W., Mu, J., and Birnbaum, M. J. (2003) Role of AMP-activated protein kinase in cyclic AMP-dependent lipolysis in 3T3-L1 adipocytes. *J. Biol. Chem.* **278**, 43074–43080
- Wu, H. M., Yang, Y. M., and Kim, S. G. (2011) Rimobant, a cannabinoid receptor type 1 inverse agonist, inhibits hepatocyte lipogenesis by activating liver kinase B1 and AMP-activated protein kinase axis downstream of G $\alpha_{i/o}$ inhibition. *Mol. Pharmacol.* **80**, 859–869
- Kimball, S. R., Siegfried, B. A., and Jefferson, L. S. (2004) Glucagon represses signaling through the mammalian target of rapamycin in rat liver by activating AMP-activated protein kinase. *J. Biol. Chem.* **279**, 54103–54109
- Williamson, D. L., Kubica, N., Kimball, S. R., and Jefferson, L. S. (2006) Exercise-induced alterations in extracellular signal-regulated kinase 1/2 and mammalian target of rapamycin (mTOR) signalling to regulatory mechanisms of mRNA translation in mouse muscle. *J. Physiol.* **573**, 497–510
- Djouder, N., Tuerk, R. D., Suter, M., Salvioni, P., Thali, R. F., Scholz, R., Vaahomeri, K., Auchli, Y., Rechsteiner, H., Brunisholz, R. A., Viollet, B., T. P., Wallimann, T., Neumann, D., and Krek, W. (2010) PKA phosphorylates and inactivates AMPK α to promote efficient lipolysis. *EMBO J.* **29**, 469–481
- Escande, C., Chini, C. C., Nin, V., Dykhouse, K. M., Novak, C. M., Levine, J., van Deursen, J., Gores, G. J., Chen, J., Lou, Z., and Chini, E. N. (2010)

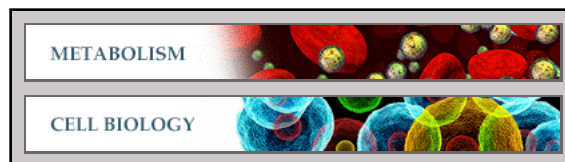
- Deleted in breast cancer-1 regulates SIRT1 activity and contributes to high-fat diet-induced liver steatosis in mice. *J. Clin. Invest.* **120**, 545–558
32. Zhao, W., Kruse, J. P., Tang, Y., Jung, S. Y., Qin, J., and Gu, W. (2008) Negative regulation of the deacetylase SIRT1 by DBC1. *Nature* **451**, 587–590
 33. Kim, J. E., Chen, J., and Lou, Z. (2008) DBC1 is a negative regulator of SIRT1. *Nature* **451**, 583–586
 34. Trauernicht, A. M., Kim, S. J., Kim, N. H., and Boyer, T. G. (2007) Modulation of estrogen receptor α protein level and survival function by DBC-1. *Mol. Endocrinol.* **21**, 1526–1536
 35. Koyama, S., Wada-Hiraike, O., Nakagawa, S., Tanikawa, M., Hiraike, H., Miyamoto, Y., Sone, K., Oda, K., Fukuhara, H., Nakagawa, K., Kato, S., Yano, T., and Taketani, Y. (2010) Repression of estrogen receptor β function by putative tumor suppressor DBC1. *Biochem. Biophys. Res. Commun.* **392**, 357–362
 36. Fu, J., Jiang, J., Li, J., Wang, S., Shi, G., Feng, Q., White, E., Qin, J., and Wong, J. (2009) Deleted in breast cancer 1, a novel androgen receptor (AR) coactivator that promotes AR DNA-binding activity. *J. Biol. Chem.* **284**, 6832–6840
 37. Hiraike, H., Wada-Hiraike, O., Nakagawa, S., Koyama, S., Miyamoto, Y., Sone, K., Tanikawa, M., Tsuruga, T., Nagasaka, K., Matsumoto, Y., Oda, K., Shoji, K., Fukuhara, H., Saji, S., Nakagawa, K., Kato, S., Yano, T., and Taketani, Y. (2010) Identification of DBC1 as a transcriptional repressor for BRCA1. *Br. J. Cancer* **102**, 1061–1067
 38. Chini, C. C., Escande, C., Nin, V., and Chini, E. N. (2010) HDAC3 is negatively regulated by the nuclear protein DBC1. *J. Biol. Chem.* **285**, 40830–40837
 39. Nakahata, Y., Kaluzova, M., Grimaldi, B., Sahar, S., Hirayama, J., Chen, D., Guarente, L. P., and Sassone-Corsi, P. (2008) The NAD⁺-dependent deacetylase SIRT1 modulates CLOCK-mediated chromatin remodeling and circadian control. *Cell* **134**, 329–340
 40. van der Veer, E., Ho, C., O'Neil, C., Barbosa, N., Scott, R., Cregan, S. P., and Pickering, J. G. (2007) Extension of human cell lifespan by nicotinamide phosphoribosyltransferase. *J. Biol. Chem.* **282**, 10841–10845
 41. Chen, Z., Peng, I. C., Cui, X., Li, Y. S., Chien, S., and Shyy, J. Y. (2010) Shear stress, SIRT1, and vascular homeostasis. *Proc. Natl. Acad. Sci. U.S.A.* **107**, 10268–10273
 42. Borra, M. T., Smith, B. C., and Denu, J. M. (2005) Mechanism of human SIRT1 activation by resveratrol. *J. Biol. Chem.* **280**, 17187–17195
 43. Howitz, K. T., Bitterman, K. J., Cohen, H. Y., Lamming, D. W., Lavu, S., Wood, J. G., Zipkin, R. E., Chung, P., Kisielewski, A., Zhang, L. L., Scherer, B., and Sinclair, D. A. (2003) Small molecule activators of sirtuins extend *Saccharomyces cerevisiae* lifespan. *Nature* **425**, 191–196
 44. Wood, J. G., Rogina, B., Lavu, S., Howitz, K., Helfand, S. L., Tatar, M., and Sinclair, D. (2004) Sirtuin activators mimic caloric restriction and delay ageing in metazoans. *Nature* **430**, 686–689
 45. Beher, D., Wu, J., Cumine, S., Kim, K. W., Lu, S. C., Atangan, L., and Wang, M. (2009) Resveratrol is not a direct activator of SIRT1 enzyme activity. *Chem. Biol. Drug Des.* **74**, 619–624
 46. Pacholec, M., Bleasdale, J. E., Chruncyk, B., Cunningham, D., Flynn, D., Garofalo, R. S., Griffith, D., Griffor, M., Loulakis, P., Pabst, B., Qiu, X., Stockman, B., Thanabal, V., Varghese, A., Ward, J., Withka, J., and Ahn, K. (2010) SIRT1720, SIRT2183, SIRT1460, and resveratrol are not direct activators of SIRT1. *J. Biol. Chem.* **285**, 8340–8351
 47. Rodgers, J. T., and Puigserver, P. (2007) Fasting-dependent glucose and lipid metabolic response through hepatic sirtuin 1. *Proc. Natl. Acad. Sci. U.S.A.* **104**, 12861–12866
 48. Jiang, G., and Zhang, B. B. (2003) Glucagon and regulation of glucose metabolism. *Am. J. Physiol. Endocrinol. Metab.* **284**, E671–E678
 49. Cantó, C., and Auwerx, J. (2012) Targeting sirtuin 1 to improve metabolism: all you need is NAD⁺? *Pharmacol. Rev.* **64**, 166–187
 50. Murray, A. J. (2008) Pharmacological PKA inhibition: all may not be what it seems. *Sci. Signal* **1**, re4
 51. Vaziri, H., Dessain, S. K., Ng Eaton, E., Imai, S. I., Frye, R. A., Pandita, T. K., Guarente, L., and Weinberg, R. A. (2001) hSIR2(SIRT1) functions as an NAD-dependent p53 deacetylase. *Cell* **107**, 149–159
 52. Moreno, D., Knecht, E., Viollet, B., and Sanz, P. (2008) A769662, a novel activator of AMP-activated protein kinase, inhibits non-proteolytic components of the 26S proteasome by an AMPK-independent mechanism. *FEBS Lett.* **582**, 2650–2654
 53. Corton, J. M., Gillespie, J. G., Hawley, S. A., and Hardie, D. G. (1995) 5-Aminoimidazole-4-carboxamide ribonucleoside. A specific method for activating AMP-activated protein kinase in intact cells? *Eur. J. Biochem.* **229**, 558–565
 54. Hawley, S. A., Ross, F. A., Chevtzoff, C., Green, K. A., Evans, A., Fogarty, S., Towler, M. C., Brown, L. J., Ogunbayo, O. A., Evans, A. M., and Hardie, D. G. (2010) Use of cells expressing γ subunit variants to identify diverse mechanisms of AMPK activation. *Cell Metab.* **11**, 554–565
 55. Barata, H., Thompson, M., Zielinska, W., Han, Y. S., Mantilla, C. B., Prakash, Y. S., Feitoza, S., Sieck, G., and Chini, E. N. (2004) The role of cyclic-ADP-ribose-signaling pathway in oxytocin-induced Ca²⁺ transients in human myometrium cells. *Endocrinology* **145**, 881–889
 56. Chini, E. N., Nagamune, K., Wetzel, D. M., and Sibley, L. D. (2005) Evidence that the cADPR signalling pathway controls calcium-mediated microneme secretion in *Toxoplasma gondii*. *Biochem. J.* **389**, 269–277
 57. Nagamune, K., Hicks, L. M., Fux, B., Brossier, F., Chini, E. N., and Sibley, L. D. (2008) Abscisic acid controls calcium-dependent egress and development in *Toxoplasma gondii*. *Nature* **451**, 207–210
 58. Gledhill, J. R., Montgomery, M. G., Leslie, A. G., and Walker, J. E. (2007) Mechanism of inhibition of bovine F₁-ATPase by resveratrol and related polyphenols. *Proc. Natl. Acad. Sci. U.S.A.* **104**, 13632–13637
 59. Greer, E. L., Oskoui, P. R., Banko, M. R., Maniar, J. M., Gygi, M. P., Gygi, S. P., and Brunet, A. (2007) The energy sensor AMP-activated protein kinase directly regulates the mammalian FOXO3 transcription factor. *J. Biol. Chem.* **282**, 30107–30119
 60. Guarente, L. (2011) Franklin H. Epstein Lecture: sirtuins, aging, and medicine. *N. Engl. J. Med.* **364**, 2235–2244
 61. Park, S. J., Ahmad, F., Philp, A., Baar, K., Williams, T., Luo, H., Ke, H., Rehmann, H., Taussig, R., Brown, A. L., Kim, M. K., Beaven, M. A., Burgin, A. B., Manganiello, V., and Chung, J. H. (2012) Resveratrol ameliorates aging-related metabolic phenotypes by inhibiting cAMP phosphodiesterases. *Cell* **148**, 421–433
 62. Collins, S. P., Reoma, J. L., Gamm, D. M., and Uhler, M. D. (2000) LKB1, a novel serine/threonine protein kinase and potential tumour suppressor, is phosphorylated by cAMP-dependent protein kinase (PKA) and prenylated *in vivo*. *Biochem. J.* **345**, 673–680
 63. Hardie, D. G. (2005) New roles for the LKB1→AMPK pathway. *Curr. Opin. Cell Biol.* **17**, 167–173
 64. Sapkota, G. P., Kieloch, A., Lizcano, J. M., Lain, S., Arthur, J. S., Williams, M. R., Morrice, N., Deak, M., and Alessi, D. R. (2001) Phosphorylation of the protein kinase mutated in Peutz-Jeghers cancer syndrome, LKB1/STK11, at Ser431 by p90^{RSK}, is cAMP-dependent protein kinase, but not its farnesylation at Cys⁴³³, is essential for LKB1 to suppress cell growth. *J. Biol. Chem.* **276**, 19469–19482
 65. Shelly, M., Cancedda, L., Heilshorn, S., Sumbre, G., and Poo, M. M. (2007) LKB1/STRAD promotes axon initiation during neuronal polarization. *Cell* **129**, 565–577
 66. Lugnier, C. (2006) Cyclic nucleotide phosphodiesterase (PDE) superfamily: a new target for the development of specific therapeutic agents. *Pharmacol. Ther.* **109**, 366–398
 67. Carling, D., and Hardie, D. G. (1989) The substrate and sequence specificity of the AMP-activated protein kinase. Phosphorylation of glycogen synthase and phosphorylase kinase. *Biochim. Biophys. Acta* **1012**, 81–86
 68. Dale, S., Wilson, W. A., Edelman, A. M., and Hardie, D. G. (1995) Similar substrate recognition motifs for mammalian AMP-activated protein kinase, higher plant HMG-CoA reductase kinase-A, yeast SNF1, and mammalian calmodulin-dependent protein kinase I. *FEBS Lett.* **361**, 191–195
 69. Gwinn, D. M., Shackelford, D. B., Egan, D. F., Mihaylova, M. M., Mery, A., Vasquez, D. S., Turk, B. E., and Shaw, R. J. (2008) AMPK phosphorylation of raptor mediates a metabolic checkpoint. *Mol. Cell* **30**, 214–226
 70. Kang, H., Suh, J. Y., Jung, Y. S., Jung, J. W., Kim, M. K., and Chung, J. H. (2011) Peptide switch is essential for Sirt1 deacetylase activity. *Mol. Cell* **44**, 203–213
 71. Yuan, J., Luo, K., Liu, T., and Lou, Z. (2012) Regulation of SIRT1 activity by genotoxic stress. *Genes Dev.* **26**, 791–796

Metabolism:
**Deleted in Breast Cancer 1 (DBC1) Protein
Regulates Hepatic Gluconeogenesis**

Veronica Nin, Claudia C. S. Chini, Carlos
Escande, Verena Capellini and Eduardo N.
Chini

J. Biol. Chem. 2014, 289:5518-5527.

doi: 10.1074/jbc.M113.512913 originally published online January 10, 2014



Access the most updated version of this article at doi: [10.1074/jbc.M113.512913](https://doi.org/10.1074/jbc.M113.512913)

Find articles, minireviews, Reflections and Classics on similar topics on the [JBC Affinity Sites](http://www.jbc.org/).

Alerts:

- [When this article is cited](#)
- [When a correction for this article is posted](#)

[Click here](#) to choose from all of JBC's e-mail alerts

Supplemental material:

<http://www.jbc.org/content/suppl/2014/01/10/M113.512913.DC1.html>

This article cites 41 references, 17 of which can be accessed free at
<http://www.jbc.org/content/289/9/5518.full.html#ref-list-1>

Deleted in Breast Cancer 1 (DBC1) Protein Regulates Hepatic Gluconeogenesis*[§]

Received for publication, August 23, 2013, and in revised form, January 8, 2014. Published, JBC Papers in Press, January 10, 2014, DOI 10.1074/jbc.M113.512913

Veronica Nin¹, Claudia C. S. Chini, Carlos Escande, Verena Capellini, and Eduardo N. Chini²

From the Department of Anesthesiology and Kogod Center on Aging, Mayo Clinic, Rochester, Minnesota 55905

Background: Gluconeogenesis is an important physiological pathway in response to fasting and stress.

Results: DBC1 regulates gluconeogenesis and PEPCK expression by a mechanism that is at least in part explained by the Rev-erb α and the deacetylase SIRT1.

Conclusion: A new role for DBC1 as a regulator of PEPCK expression is described.

Significance: We aim to understand the molecular mechanisms of glucose metabolism and response to fasting.

Liver gluconeogenesis is essential to provide energy to glycolytic tissues during fasting periods. However, aberrant up-regulation of this metabolic pathway contributes to the progression of glucose intolerance in individuals with diabetes. Phosphoenolpyruvate carboxykinase (PEPCK) expression plays a critical role in the modulation of gluconeogenesis. Several pathways contribute to the regulation of PEPCK, including the nuclear receptor Rev-erb α and the histone deacetylase SIRT1. Deleted in breast cancer 1 (DBC1) is a nuclear protein that binds to and regulates both Rev-erb α and SIRT1 and, therefore, is a candidate to participate in the regulation of PEPCK. In this work, we provide evidence that DBC1 regulates glucose metabolism and the expression of PEPCK. We show that DBC1 levels decrease early in the fasting state. Also, DBC1 KO mice display higher gluconeogenesis in a normal and a high-fat diet. DBC1 absence leads to an increase in PEPCK mRNA and protein expression. Conversely, overexpression of DBC1 results in a decrease in PEPCK mRNA and protein levels. DBC1 regulates the levels of Rev-erb α , and manipulation of Rev-erb α activity or levels prevents the effect of DBC1 on PEPCK. In addition, Rev-erb α levels decrease in the first hours of fasting. Finally, knockdown of the deacetylase SIRT1 eliminates the effect of DBC1 knockdown on Rev-erb α levels and PEPCK expression, suggesting that the mechanism of PEPCK regulation is, at least in part, dependent on the activity of this enzyme. Our results point to DBC1 as a novel regulator of gluconeogenesis.

Hepatic gluconeogenesis plays a key role in the maintenance of systemic glucose levels during health and disease. During fasting, circulating hormones promote the *de novo* synthesis of

glucose (1, 2), ensuring delivery of energy to glucose-dependent tissues. However, up-regulation of glucose production in the liver may also play a role in the development of hyperglycemia in diabetes (3). Regulation of gluconeogenesis mainly targets the expression of the enzyme phosphoenolpyruvate carboxykinase (PEPCK³, also known as PCK1) because this enzyme catalyzes a committed step in the gluconeogenic pathway (1, 4). PEPCK is regulated by several signaling systems, including the glucagon-cAMP and the insulin-AKT pathways (1). In addition, like many other metabolically relevant enzymes, PEPCK displays a circadian regulation (5). Central to the metabolic circadian rhythms are the nuclear receptors Rev-erbs (6). Rev-erb α , the most studied member of the family, is a heme receptor (7, 8) that represses transcription of target genes via an interaction with the nuclear corepressor (NCoR) (6). Two studies have demonstrated that Rev-erb α is a transcriptional repressor of PEPCK in liver cells (8, 9), and a central role for Rev-erb α in the control of hepatic metabolism has been proposed (10, 11).

The relative abundance of Rev-erb α present in a cell is in part controlled by its ubiquitin-mediated proteasomal degradation (12). We have shown recently that deleted in breast cancer 1 (DBC1) binds and stabilizes Rev-erb α , preventing its degradation (13). In fact, in DBC1 KO mice, the hepatic levels of Rev-erb α are lower than in wild-type littermates. More importantly, our previous study demonstrated that DBC1 regulates circadian rhythms that are Rev-erb α -dependent (13).

DBC1 is a nuclear protein that binds and regulates the activity of several nuclear receptors (14) and enzymes involved in epigenetic processes, such as the methyltransferase SUV39H1 (15) and the deacetylases HDAC3 (16) and SIRT1 (17, 18). Not much is known about the molecular cues that modulate the interaction between DBC1 and its partners. However, we have shown previously that the interaction between DBC1 and SIRT1 is disrupted under fasting conditions (19) and that the kinases AMP-activated protein kinase (AMPK) and PKA regulate the interaction between both proteins (20). SIRT1, a NAD-dependent deacetylase, regulates glucose metabolism in the liver through deacetylation of several targets, although different models provide conflicting results (21–27). It appears that

* This work was supported, in whole or in part, by NIDDK, National Institutes of Health Grant DK-084055. This work was also supported by grants from the American Federation of Aging Research and from the Mayo Foundation, by the Strickland Career Development Award, by Mayo-UOFM Decade of Discovery Grant 63-01, and by Minnesota Obesity Council grant DK-50456-15.

[§] This article contains supplemental Figs. 1 and 2.

¹ This paper constitutes part of the doctoral studies of V. N.

² To whom correspondence should be addressed: Laboratory of Signal Transduction, Dept. of Anesthesiology, Cancer Center, Center for GI Signaling, and Kogod Center on Aging, Mayo Clinic, Rochester MN 55905. Tel.: 507-255-0992; Fax: 507-255-7300; E-mail: chini.eduardo@mayo.edu.

³ The abbreviations used are: PEPCK, phosphoenol pyruvatecarboxikinase; DBC, deleted in breast cancer.

SIRT1 deacetylates PGC1 α (21) and FOXO (Forkhead box) (28), increasing their transcriptional activity. We previously showed that mice knocked out for DBC1 display higher SIRT1 activity (19) and are protected against high-fat diet-induced liver steatosis (19), suggesting that DBC1 plays an important role in the regulation of liver metabolism (19).

In this study, we explored whether DBC1 is important for glucose metabolism and PEPCK regulation and the mechanisms involved in this process. Our data reveal that DBC1 is a novel regulator of PEPCK expression and gluconeogenesis by a mechanism that involves, at least in part, both Rev-erb α and SIRT1.

EXPERIMENTAL PROCEDURES

Reagents and Antibodies—Unless specified otherwise, all reagents and chemicals were purchased from Sigma-Aldrich. The Rev-erb α antagonist SR8278 was from Tocris Bioscience. Anti-human SIRT1 and anti-mouse SIRT1, phospho-AKT, AKT, tubulin, and GAPDH antibodies were from Cell Signaling Technology. Anti-DBC1 antibodies were from Bethyl Laboratories. The anti-mouse PEPCK antibody was from Cayman Chemical. Anti-human PCK1, anti-Rev-erb α , and anti HA antibodies were from Abcam. Anti-actin and anti-FLAG antibodies were from Sigma.

Animal Handling and Studies—All mice used in this study were maintained at the Mayo Clinic animal facility. All experimental protocols were approved by the Institutional Animal Care and Use Committee at the Mayo Clinic (protocol A33209 and A52112), and studies were performed according to the methods approved in the protocols. The production and characterization of DBC1 KO mice has been described before (19). All studies were performed in animals that were between 12 and 36 weeks old. Mice were fed normal chow or a 60% high-fat diet as described before (19). A glucose tolerance test was performed after 16 h of fasting. Mice were injected intraperitoneally with 1.5 g of dextrose/kg. To perform the insulin sensitivity test and the pyruvate tolerance test, DBC1 WT or KO mice were fasted for 6 h. After this, mice were challenged with a single dose of either 0.5 units/kg of insulin or 1.5 g/kg of pyruvate intraperitoneally. All mice had access to water during the fasting period. Blood glucose was measured from the tip of the tail vein using an AlphaTRAK blood glucose monitoring system (Abbott). For the glucose tolerance test and the pyruvate tolerance test, the area under the curve was calculated as the net incremental area over the baseline. For the insulin sensitivity test, the blood glucose values were normalized to time 0, and the total area under the curve was calculated. For shorter fasting periods, food was removed 1 h before the start of the dark cycle.

Cell Culture—HepG2 and 293T cells were cultured in Dulbecco's modified Eagle's medium (5 g/liter glucose) with 10% FBS, glutamine, and penicillin/streptomycin (Invitrogen). In all experiments with HepG2 cells, the cells were switched to serum-free medium 16 h before harvesting. Transfection of HA/Myc or FLAG-Rev-erb α in 293T cells was performed in 6-well plates using Lipofectamine 2000 (Invitrogen) and 1 μ g of total DNA. To generate 293T stable cell lines overexpressing FLAG-DBC1 or HA/Myc-Rev-erb α , cells were cotransfected

with a vector that confers resistance to puromycin and the vector with the cDNA for DBC1 or Rev-erb α using Lipofectamine 2000. 48 h after transfection, the cells were diluted and selected with puromycin for 15 days. Individual cells were grown to generate clones, which were screened by immunofluorescence and Western blot analysis with anti-tag antibodies.

siRNA—All siRNAs were from Dharmacon (Lafayette, CO). The siRNA duplex against DBC1 was 5'-CAGUUGCAUGACUACUUUUU (sense). SMARTpool siRNAs were used to knock down SIRT1. Non-targeting siRNA 3 was used as a control (D001210-03-20). Transfections in HepG2 and 293T were performed with 100 nM siRNA on day 1. Cells were split on the following day, transfected again on the third day, and harvested 96 h after the first transfection.

Western Blot Analysis—Mouse tissues and cultured cells were lysed in NETN buffer (20 mM Tris-HCl (pH 8.0), 100 mM NaCl, 1 mM EDTA, and 0.5% Nonidet P-40) supplemented with 5 mM NaF, 50 mM 2-glycerophosphate, 1 mM Na₃VO₄, and protease inhibitor mixture (Roche). For experiments to detect acetylation, 5 μ M trichostatin A and 5 mM nicotinamide were also added. Homogenates were incubated at 4 °C for 30 min under constant agitation and then centrifuged at 11,200 \times g for 10 min at 4 °C. Cell and tissue lysates were analyzed by Western blot analysis with the indicated antibodies. Western blots were developed using secondary antibodies and SuperSignal West Pico chemiluminescent substrate (Pierce). Films were scanned, and bands were quantified by densitometry using ImageJ (<http://rsbweb.nih.gov/ij/>).

Real-time PCR—Total RNA was prepared and retrotranscribed as described before (13). TaqMan probes for DBC1, PEPCK, and GAPDH were obtained from Applied Biosystems. The relative amount of mRNA was calculated using the $\Delta\Delta C_T$ method using GAPDH as an internal control.

Site-directed Mutagenesis—Point mutations were performed using a QuikChange directed mutagenesis kit (Stratagene) following the instructions of the manufacturer.

Statistics—Values are presented as mean \pm S.D. of three to five experiments unless indicated otherwise. The significance of differences between means was assessed by one-way analysis of variance or two-tailed Student's *t* test. A *p* value of less than 0.05 was considered significant.

RESULTS

Lack of DBC1 Results in Elevated Gluconeogenesis—To characterize the role of DBC1 in glucose homeostasis, we first performed glucose tolerance tests in WT and DBC1 KO mice fed regular chow. We observed that DBC1 KO male mice reached higher levels of blood glucose than WT mice after an intraperitoneal challenge of glucose (Fig. 1A). We also observed that DBC1 KO mice display higher blood glucose levels in the fed state (Fig. 1B) than WT mice, although glycemia was not different in the fasted state (Fig. 1A). We then evaluated whether insulin release and insulin sensitivity were responsible for the differences in glucose tolerance between WT and DBC1 KO mice. We found that insulin release was similar between genotypes (Fig. 1C). There was no significant difference in insulin sensitivity (Fig. 1D). Because the glycemia is a balance between glucose clearance and glucose production, we sought to assess

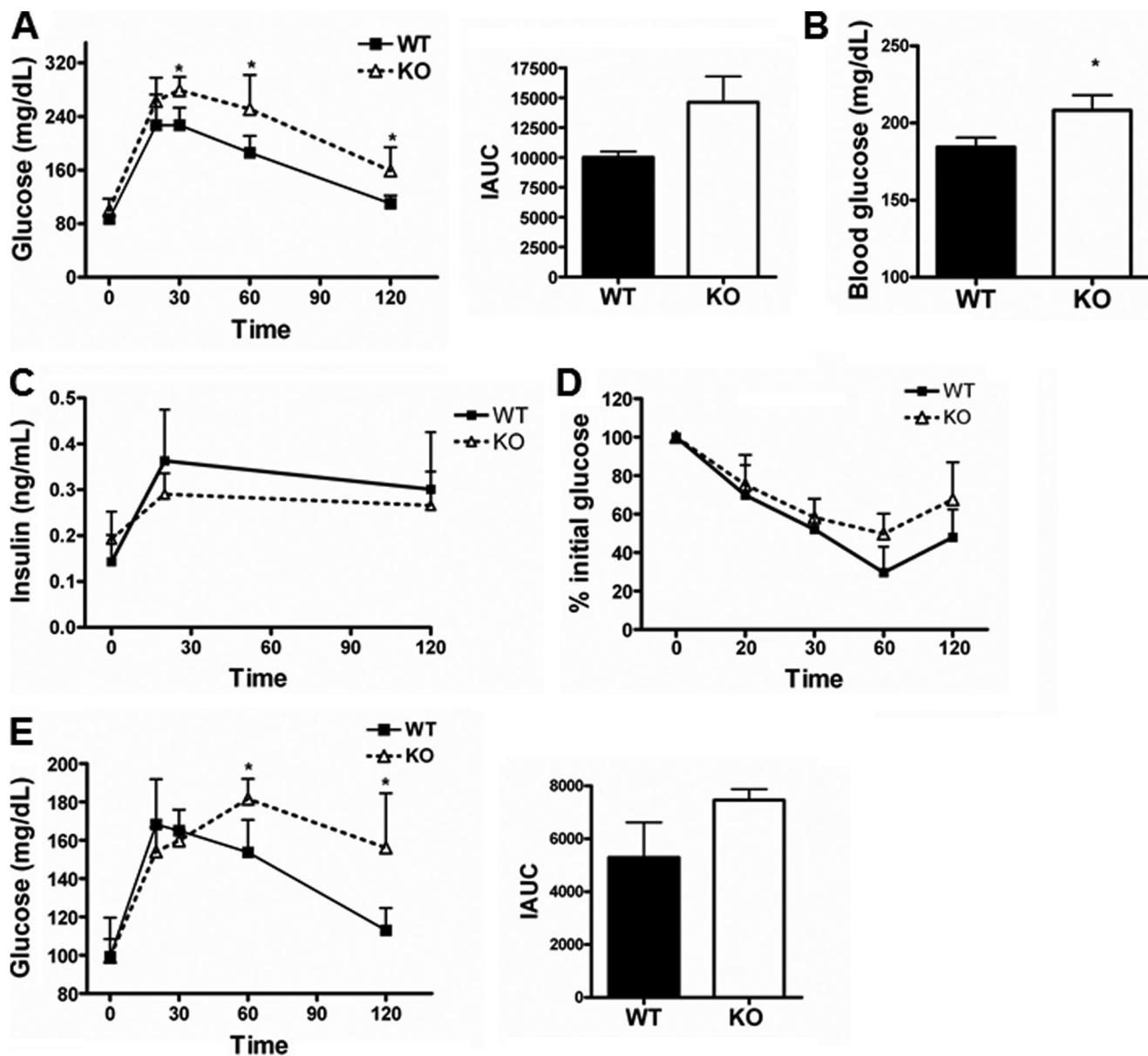


FIGURE 1. **DBC1 KO mice are more gluconeogenic than WT littermates.** *A*, glucose tolerance test and net incremental area under the curve (IAUC) in WT and DBC1 KO mice fed regular chow. *B*, blood glucose in WT and DBC1 KO mouse males fed *ad libitum*. *C*, insulin release after a glucose challenge. *D*, insulin sensitivity in WT and DBC1 KO mice. *E*, pyruvate tolerance test and net incremental area under the curve in WT and DBC1 KO mice fed regular chow. *, $p < 0.05$; $n = 4-8$.

the contribution of gluconeogenesis to the observed glucose intolerance. To this end, we compared the response of wild-type and DBC1 KO mice to a pyruvate challenge, a precursor for glucose synthesis. As can be seen in Fig. 1*E*, KO mice reached higher levels of blood glucose than their WT littermates (Fig. 1*B*). These findings point to elevated gluconeogenesis in the DBC1 KO mice compared with the WT counterparts.

Increased gluconeogenesis is a hallmark of type II diabetes and is usually accompanied by obesity. To study glucose metabolism in obese mice, we fed DBC1 WT and KO mice a hypercaloric high-fat diet. We performed a glucose tolerance test after 16 weeks of high-fat diet and found that both genotypes became glucose-intolerant, although the glucose tolerance was more altered in DBC1 KO mice (Fig. 2*A*). Akin to what we observed when mice were fed normal chow, feed glycemia was higher in the DBC1 knockout mice (180 mg/dl) compared with

wild-type mice (140 mg/dl), although insulin sensitivity was similar between genotypes (Fig. 2*B*). However, when we performed a pyruvate tolerance test, the response of DBC1 KO mice on the high-fat diet was exaggerated in comparison with WT mice (Fig. 2*C*). Therefore, the effect of the high-fat diet on gluconeogenesis was more pronounced in mice lacking DBC1. Taken together, our results demonstrate that the absence of DBC1 leads to glucose intolerance driven mainly by elevated gluconeogenesis.

DBC1 Regulates PEPCK Expression—To confirm that the phenotype we observed was driven by elevated gluconeogenesis and not insulin sensitivity, we evaluated the expression level of AKT and PEPCK in the livers of WT and KO mice. The levels of phospho-AKT and AKT were similar in *ad libitum* conditions in both genotypes (Fig. 3*A*). In contrast, PEPCK levels were higher in KO mice than in WT mice under basal conditions and

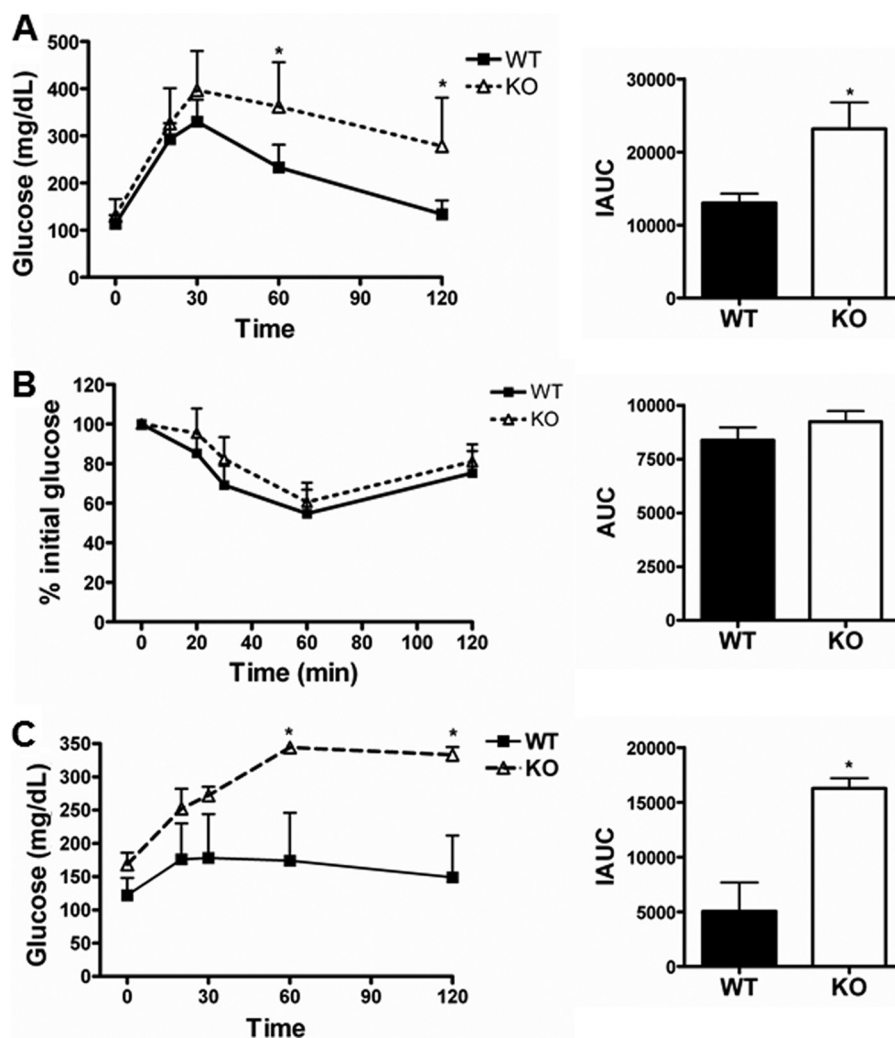


FIGURE 2. **Effect of a high-fat diet on glucose metabolism of DBC1 KO mice.** *A*, glucose tolerance test and net incremental area under the curve (IAUC) in WT and DBC1 KO mice fed a high-fat diet. *B*, insulin sensitivity and net area under the curve (AUC) in WT and DBC1 KO mice fed a high-fat diet. *C*, pyruvate tolerance test and net incremental area under the curve in WT and DBC1 KO mice fed a high-fat diet. *, $p < 0.05$.

after 6 and 24 h of fasting (Fig. 3, *B* and *C*). These results are in agreement with glucose synthesis as the main cause of the glucose intolerance presented by the DBC1 KO mice. In addition to elevated levels of PEPCK, we also observed that the protein levels of PGC1- α , a coactivator that potentiates PEPCK transcription, were also increased in DBC1 KO livers (Fig. 3*B*). The fact that the expression of both PGC1- α and PEPCK is higher in KO mice is not surprising, considering that several signaling pathways regulate both genes. In fact, we hypothesized that DBC1 is upstream of a factor that is common to the regulation of PEPCK and PGC1- α . Among the transcription factors involved in the regulation of PEPCK, the heme receptor Rev-erb α has recently gained attention. We showed previously that DBC1 regulates the stability and the function of Rev-erb α (13), a repressor of PEPCK and PGC1- α (8). In fact, we showed that DBC1 stabilizes Rev-erb α and that the livers of DBC1 KO mice express lower levels of this nuclear receptor (13). So far, a possible function for DBC1 and Rev-erb α during fasting and gluconeogenesis has not been established. We speculated that if alterations in these proteins were involved in the onset of PEPCK transcription, these should occur early during fasting.

To test this hypothesis, mice were fasted for a short period (3 h), and the levels of DBC1 and Rev-erb α were assessed by Western blot analysis. We found that DBC1 levels decreased about 40% in this condition (Fig. 3*D*). We also detected a similar decrease in Rev-erb α , specifically in the band that migrates at ~80 kDa (Fig. 3*D*). It is important to note that the decrease in DBC1 levels is transient. After 24 h of fasting, its levels are similar to the fed state (Fig. 3*C*).

To confirm that DBC1 regulates the expression of PEPCK, we manipulated the levels of DBC1 and assessed whether there were changes in PEPCK levels. First, we knocked down DBC1 and, akin to what was observed in mice lacking DBC1, the expression of PEPCK was increased (Fig. 4*A*). This was accompanied by an increase in the amount of mRNA for PEPCK (Fig. 4*B*). Then we overexpressed DBC1 and observed a decrease in the protein and mRNA levels of PEPCK (Fig. 4, *C* and *D*), supporting our initial hypothesis that DBC1 is involved in the regulation of PEPCK.

DBC1 Regulates PEPCK Expression, at Least in Part, through Rev-erb α —To investigate whether Rev-erb α is involved in the regulation of PEPCK by DBC1, we first expanded our previous

DBC1 Regulates Gluconeogenesis

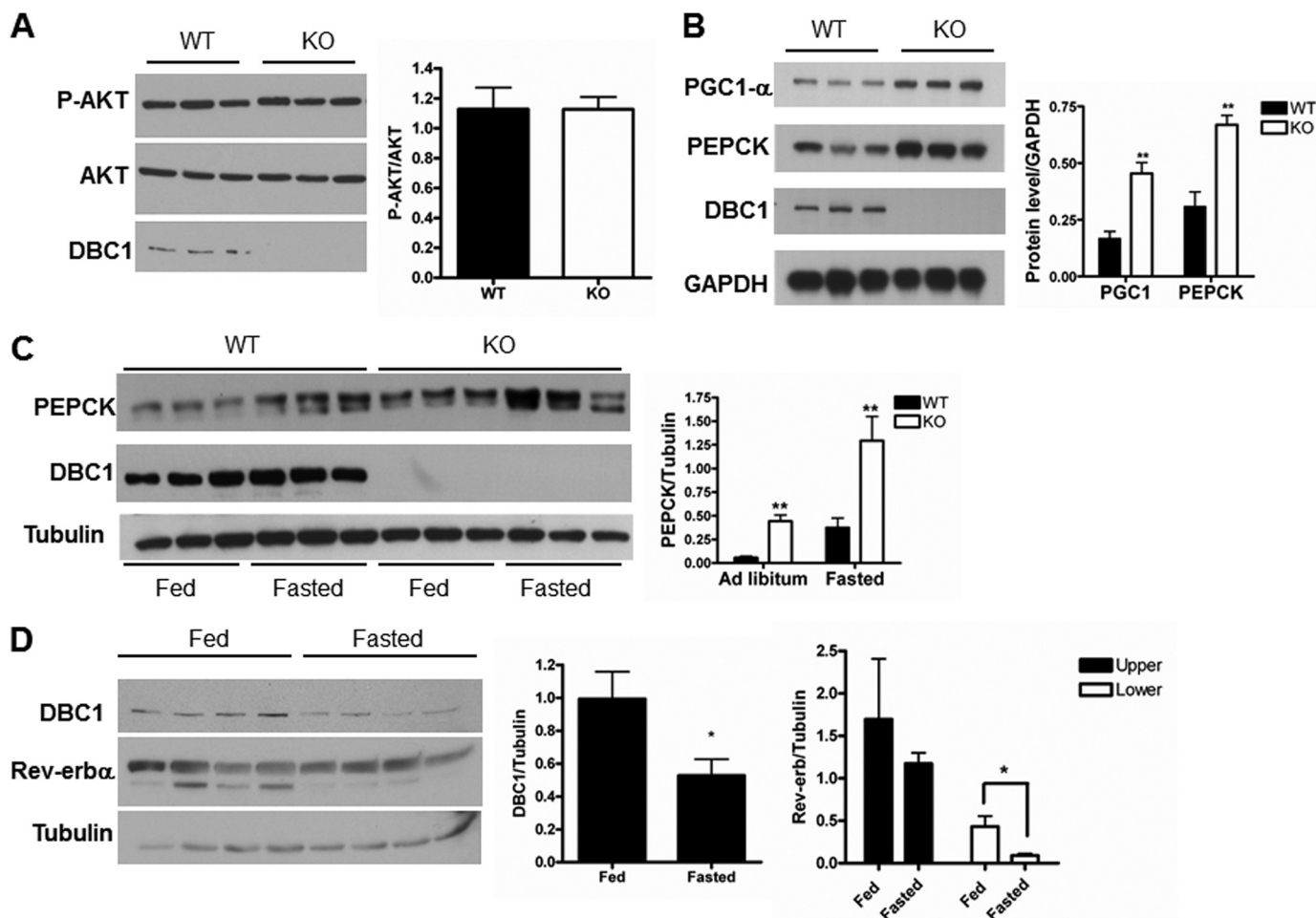


FIGURE 3. DBC1 KO mice display similar levels of P-AKT and elevated expression of PEPCK than WT mice. *A*, liver extracts of DBC1 WT and KO mice fed *ad libitum* were immunoblotted for P-AKT and AKT. The densitometry is shown in the *right panel*. *B*, DBC1 WT and KO mice were fasted for 6 h, and the liver extracts were immunoblotted with specific antibodies against PGC1 α , PEPCK, DBC1, and GAPDH. The *graph* in the *right panel* shows the quantification of the bands by densitometry. **, $p < 0.005$. *C*, DBC1 WT and KO mice were fasted for 24 h or fed *ad libitum*, and the expression of the indicated proteins was determined by Western blot analysis. The *graph* in the *right panel* shows the quantification of the bands by densitometry. *D*, liver extracts of WT mice fasted for 3 h were immunoblotted with specific antibodies against DBC1, Rev-erb α , and tubulin. The *graph* in the *right panel* shows the quantification of the bands by densitometry. *, $p < 0.05$.

observations that manipulation of DBC1 levels affects the levels of Rev-erb α (13). Indeed, in agreement with our previous report (13) in 3T3 cells, we observed that knock down of DBC1 in HepG2 cells also resulted in a decrease in endogenous Rev-erb α (Fig. 5A) and that overexpression of DBC1 in 293T cells was accompanied by an increase in the endogenous levels of this nuclear receptor (Fig. 5B). The changes in the levels of Rev-erb α were not dramatic, and, therefore, we decided to evaluate whether they were enough to participate in the regulation of PEPCK by DBC1. With this in mind, we tested whether a Rev-erb α antagonist would rescue the decrease in PEPCK induced by overexpression of DBC1. We treated stable cell lines expressing either an empty vector (control) or overexpressing FLAG-DBC1 with the Rev-erb α antagonist SR8278 (29) for 24 h, and then the levels of PEPCK were evaluated. In accordance with our hypothesis, the treatment of the FLAG-DBC1 stable cell line with SR8278 increased PEPCK expression to a level comparable with the untreated control cells (Fig. 5C). In addition, we tested whether the small decrease in Rev-erb α induced by knockdown of DBC1 had a functional effect. For this, we generated a stable cell line that overexpresses a

HA/Myc-Rev-erb α in a vector that contains multiple nuclear localization motives. Our idea was that, by forcing Rev-erb α to remain in the nucleus, there would be more stable functional Rev-erb α , even in the absence of DBC1. Certainly, when we treated this cell line with a DBC1 siRNA, the levels of Myc/HA-Rev-erb α did not decrease (Fig. 5D). In this scenario, the up-regulation of PEPCK by DBC1 was lost. However, in the empty vector-transfected cell line, a similar decrease in DBC1 led to an increase in PEPCK. Taken together, our results support, at least in part, a role for Rev-erb α in the DBC1-mediated regulation of PEPCK.

SIRT1 Is Important for the Regulation of PEPCK and Rev-erb α by DBC1—DBC1 is an endogenous inhibitor of several nuclear enzymes. Among these, SIRT1 is a NAD-dependent deacetylase involved in the regulation of gluconeogenesis. To further understand the mechanism of PEPCK regulation by DBC1, we evaluated a possible contribution of SIRT1. We compared the levels of PEPCK expression in HepG2 cells treated with a control siRNA, a DBC1 siRNA, and a combination of DBC1 and SIRT1 siRNA. As shown in Fig. 6A, in the absence of SIRT1, DBC1 is no longer able to up-regulate PEPCK. More-

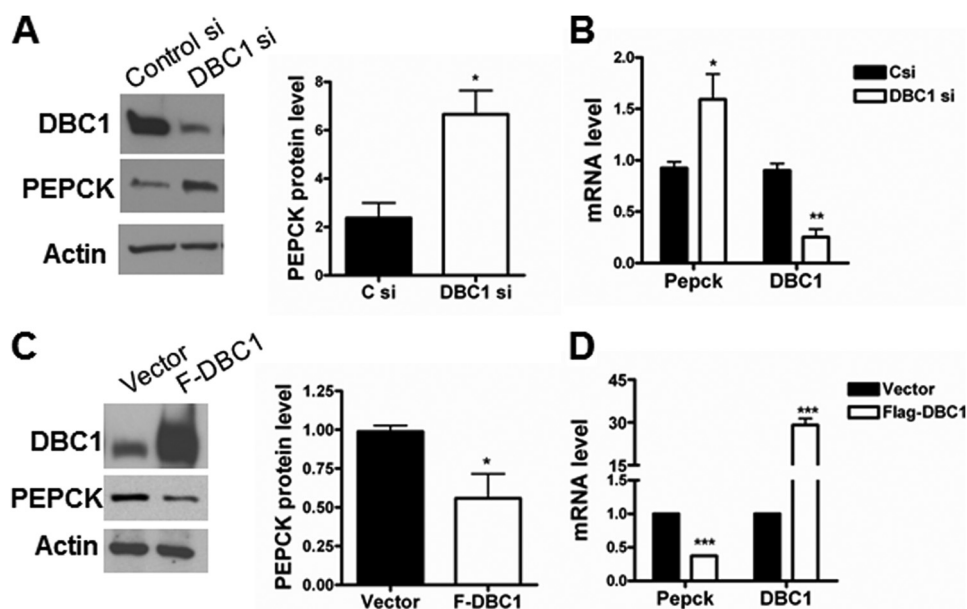


FIGURE 4. **DBC1 regulates the expression of PEPCK in cellular models.** *A*, HepG2 cells were knocked down with a control (*C si*) and DBC1 siRNA (*DBC1 si*), and the levels of PEPCK, DBC1, and actin were assessed by Western blot analysis. The graph in the right panel is the quantification by densitometry of PEPCK expression. *, $p < 0.05$; $n = 5$. *B*, the relative amount of PEPCK mRNA was determined by real-time PCR in control- (*Csi*) and DBC1 siRNA-transfected HepG2 cells. *, $p < 0.05$, **, $p < 0.005$; $n = 3$. *C*, FLAG-DBC1 was stably overexpressed in 293T cells. The levels of DBC1 and PEPCK were evaluated by Western blot analysis. The graph in the right panel is the quantification by densitometry of PEPCK expression. *, $p < 0.05$; $n = 5$. *D*, the relative level of PEPCK mRNA was determined by real-time PCR in the same F-DBC1 clone. ***, $p < 0.05$; $n = 3$.

over, the absence of SIRT1 led to a clear decrease in the levels of PEPCK. We also analyzed whether SIRT1 is required for the regulation of Rev-erb α . Again, we observed that, in the absence of SIRT1, a decrease in DBC1 does not result in a decrease in Rev-erb α (Fig. 6A). In addition, the treatment of cells overexpressing Rev-erb α with the sirtuin inhibitor nicotinamide resulted in increased levels of this nuclear receptor (Fig. 6B). To further explore the role of acetylation in the regulation of Rev-erb α , we transfected cells with Rev-erb α and the acetyltransferase p300 in the presence or absence of SIRT1. In agreement with our previous observations, expression of p300 increased the levels of Rev-erb α , and this effect was ablated by cotransfection with SIRT1 (Fig. 6C). p300 appears to increase levels of Rev-erb α by stabilization of the protein (supplemental Fig. 1). To assess the acetylation of Rev-erb α , we cotransfected cells with Rev-erb α and p300 and immunoprecipitated Rev-erb α . We could not detect acetylation under this condition (not shown). In addition, we could not detect acetylation of Rev-erb α immunoprecipitated from liver tissue (not shown). To dismiss the possibility that the negative results were due to technical issues, we incubated 293T cells transfected with Rev-erb α with deacetylase inhibitors and analyzed Rev-erb α posttranslational modifications by mass spectrometry. We found that lysines 400 and 591 were indeed acetylated. However, single mutants of these sites are still up-regulated by p300 (supplemental Fig. 2). Moreover, the protein levels of the single mutant (supplemental Fig. 2) and double mutant (Fig. 6D) are not lower than the WT, as one would expect if acetylation of Rev-erb α promoted its stabilization. Therefore, it is likely that p300 and SIRT1 regulate Rev-erb α levels by an indirect mechanism that involves acetylation/deacetylation events upstream of Rev-erb α . A schematic of the proposed mechanism by which DBC1 regulates transcription of PEPCK is shown in Fig. 7. Taken

together, our results unveil a novel role for DBC1 in the regulation of PEPCK expression and gluconeogenesis through a mechanism that, at least in part, involves Rev-erb α and, possibly, SIRT1.

DISCUSSION

Hepatic gluconeogenesis is an essential component of the homeostatic mechanisms that ensure proper supply of glucose to glycolytic tissues during times of food deprivation (2). However, deregulation of this process can lead to increased blood glucose levels and is an important contributor to the pathogenesis of diabetes (3). Therefore, understanding the molecular mechanisms involved in the regulation of gluconeogenesis will provide us with potential new targets to treat diabetes. A variety of hormones and dietary signals that control glucose synthesis target the expression of PEPCK, given that this enzyme catalyzes the first committed step of gluconeogenesis (4). In mouse models, overexpression of PEPCK is enough to induce glucose intolerance (30), and even a modest reduction in PEPCK expression is able to ameliorate fasting glucose levels and glucose tolerance (31).

In this report, we demonstrate a new role for the protein DBC1 in the regulation of gluconeogenesis. DBC1 levels decrease in the early hours of the fasting state, suggesting that such a decrease is one of the first events that lead to the onset of the gluconeogenic program. Mice that lack DBC1 mimic a fasted state and, therefore, display an increased production of glucose. Hence, one can infer that the natural role of DBC1 is to act as a suppressor of gluconeogenesis. Interestingly, Qiang *et al.* (32) showed that DBC1 knockout mice are glucose-intolerant in a normal and a high-fat diet, a phenotype that is in agreement with our findings. Ours is the first report that presents evidence that DBC1 levels are regulated in different metabolic states.

DBC1 Regulates Gluconeogenesis

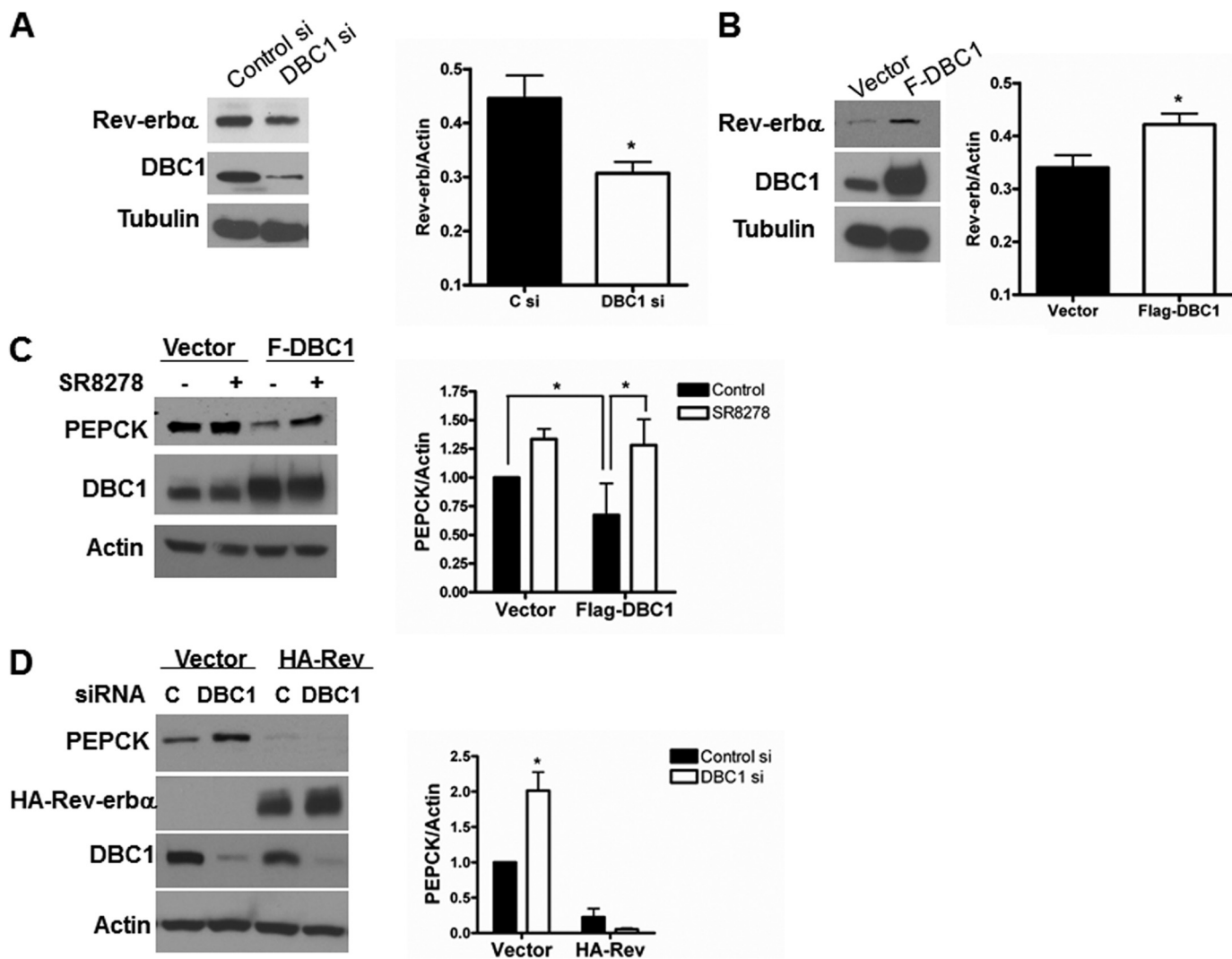


FIGURE 5. DBC1 regulates the steady levels of Rev-erb α . *A*, DBC1 was knocked down with specific siRNA in HepG2 cells. Expression of Rev-erb α and DBC1 was analyzed by Western blot analysis with specific antibodies. *, $p < 0.05$; $n = 6$. *C* si, control siRNA; *DBC1* si, DBC1 siRNA. *B*, a stable cell line overexpressing FLAG-DBC1 was generated in 293T cells, and the levels of Rev-erb α and DBC1 were analyzed by Western blot analysis with specific antibodies. *, $p < 0.05$; $n = 5$. *C*, the stable FLAG-DBC1 clone or the empty vector stable clone were treated with the Rev-erb α antagonist SR8278 (10 μ M) for 24 h. The expression of PEPCK was evaluated by Western blot analysis. The graph in the right panel shows the quantification of the bands by densitometry. *, $p < 0.05$; $n = 5$. *D*, a stable cell line overexpressing HA/Myc Rev-erb α was generated in 293T cells. Cells were knocked down with control (black bar) and DBC1-specific siRNA (white bar), and the levels of PEPCK and DBC1-specific siRNA were determined by Western blot analysis. The graph in the right panel shows the quantification of the bands by densitometry. *, $p < 0.05$.

Whether this regulation is transcriptional or posttranslational and which are the signaling pathways involved are a completely new avenue of research that warrants further investigation.

We have shown previously that DBC1 is important for the stability of Rev-erb α . In fact, DBC1 KO mice present lower levels of Rev-erb α in the liver and fat than wild-type littermates (13). Moreover, we demonstrated that DBC1 modulates Rev-erb α transcriptional repressor activity and that it is required for proper oscillations of clock genes, such as *bmal* (13). In this work, we unveil further implications of the DBC1-Rev-erb α axis, particularly in the regulation of PEPCK.

Rev-erb α has recently gained attention in the field of metabolism regulation because it connects circadian oscillations to metabolic adaptations (13). A recent report also implicates Rev-erb α in the secretion of glucagon (33). Although Rev-erb α has been linked mainly to the regulation of hepatic lipid metabolism (10, 34), previous articles show that this nuclear receptor

regulates PEPCK at the mRNA level (8, 9). We show that Rev-erb α levels decrease during the first hours of starvation, an event that can contribute to derepression of the PEPCK gene. Our findings support and expand the role of Rev-erb α in the regulation of PEPCK, stressing the importance of a DBC1-Rev-erb α axis in the control of metabolic processes. Solt *et al.* (35) recently reported the development of Rev-erb α agonists along with its effects on circadian behavior and some aspects of metabolism. The authors find that administration of the ligand SR9009 improve lipid metabolism. However, data on glucose metabolism are not provided. Noteworthy is that Cho *et al.* (10) showed that, in the absence of Rev-erb α and β , fasting glucose is elevated. In light of these findings and the ones presented here, it would be advisable to study the effect of Rev-erb α ligands on glucose metabolism, especially in the context of obesity.

Glucose synthesis is regulated in a circadian fashion by the repressor cryptochrome (36), and the activator Bmal (37).

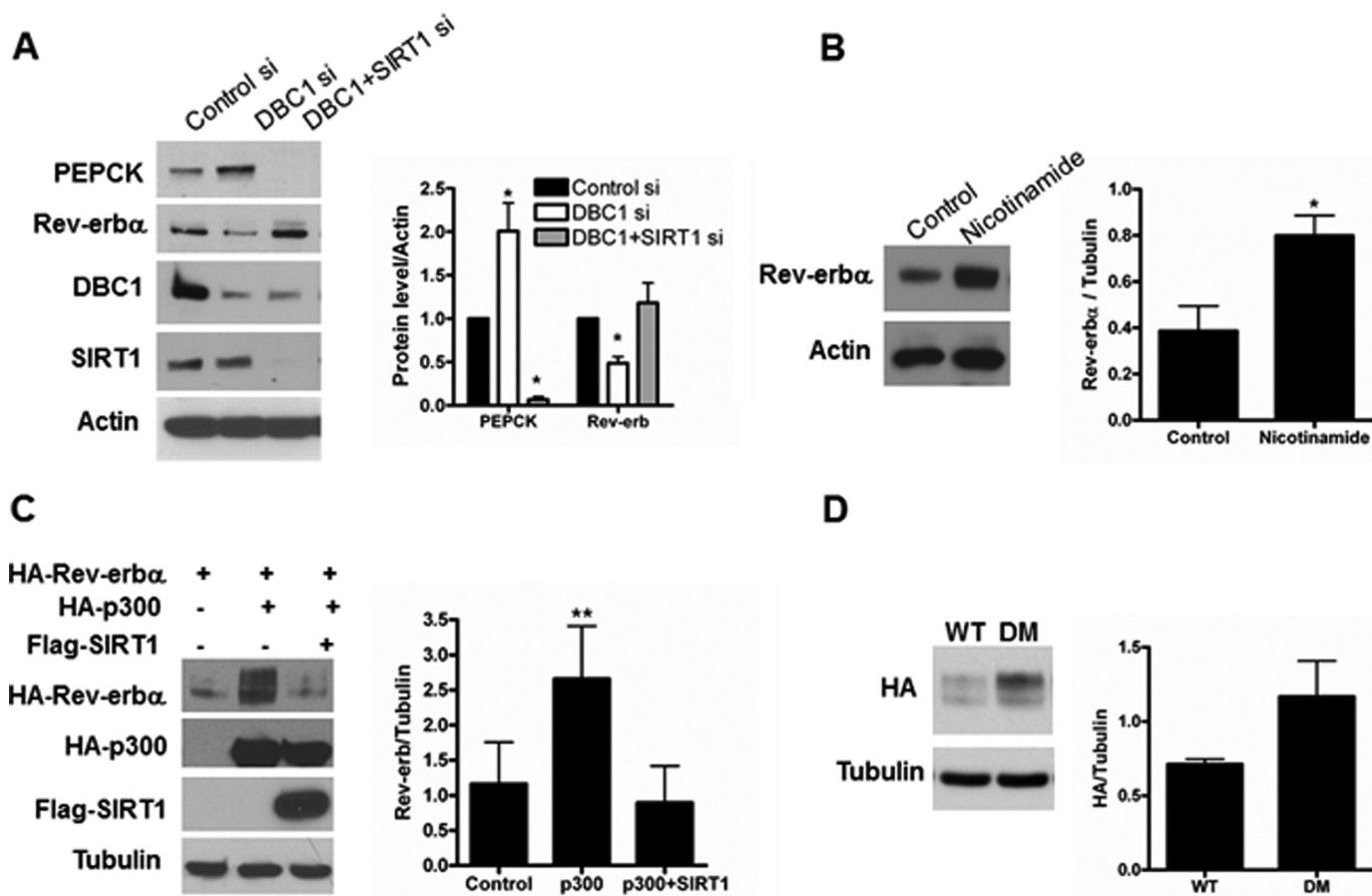


FIGURE 6. **SIRT1 is involved in the regulation of PEPCK and Rev-erb α .** *A*, DBC1 was knocked down alone or in combination with SIRT1 siRNA in HEPG2 cells, and the expression of PEPCK and Rev-erb α was evaluated by Western blot analysis. The *graph* in the *right panel* shows the quantification of the PEPCK and Rev-erb α levels normalized to actin. *, $p < 0.05$; $n = 4$. *B*, 293T cells were transfected with FLAG-Rev-erb α and treated with 5 mM nicotinamide for 16 h. The levels of Rev-erb α were assessed by Western blot analysis, and the quantification of the bands is shown in the *graph* in the *right panel*. *, $p < 0.05$; $n = 3$. *C*, 293T cells were transfected as indicated. 48 h later, the protein levels of HA-Rev-erb α , HA-p300, and SIRT1 were evaluated by Western blot analysis. The *graph* in the *right panel* shows the quantification of the bands by densitometry. **, $p < 0.01$; $n = 3$. *D*, 293T cells were transfected with Rev-erb α WT or the Rev-erb α K400A/K591A double mutant (DM), and the protein levels were assessed by Western blot analysis with anti-HA antibody.

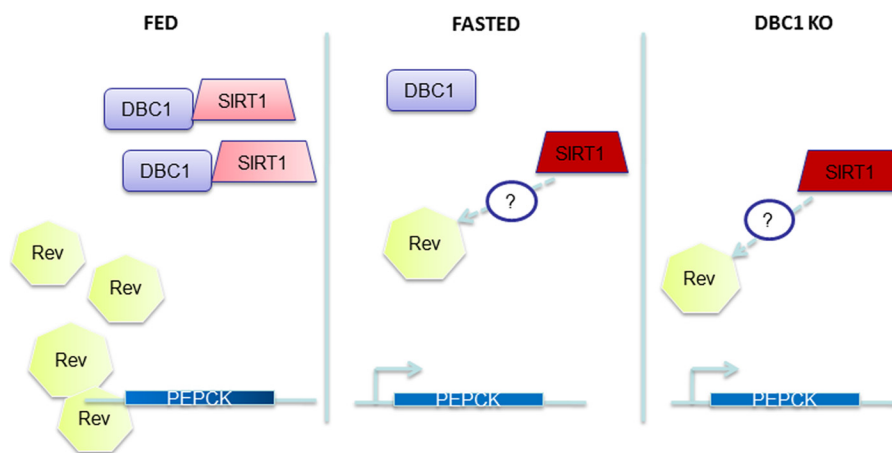


FIGURE 7. **Putative mechanism of DBC1 regulation of DBC1.** *Left*, we propose that, in the fed state, DBC1 is bound to SIRT1, inhibiting it (light red). Rev-erb α (Rev) represses the transcription of PEPCK. *Center*, in the fasted state, DBC1 levels decrease, and it dissociates from SIRT1, which leads to an increase in its activity (dark red) and a decrease in Rev-erb α levels. These events result in derepression of PEPCK. The mechanism by which SIRT1 regulates Rev-erb α is likely indirect and not completely understood. *Right*, in the DBC1 KO model, SIRT1 is active, and the levels of Rev-erb α are low, which results in PEPCK expression. The model does not exclude the possibility that other targets of DBC1, such as HDAC3, SIRT1, PGC1, and FOXO1 may also play a role in the mechanism of regulation of PEPCK by DBC1.

Hepatic Rev-erb α levels also oscillate in a circadian way (34), and we have shown oscillations of DBC1 in cells (13). It would be interesting to study whether DBC1 expression var-

ies *in vivo* during the circadian cycle and if this is, in turn, connected to the oscillations in Rev-erb α and glucose synthesis.

Finally, we observed that SIRT1 regulates Rev-erb α protein levels, an observation that, to our knowledge, has not been reported before. In agreement with our observations, Viera *et al.* (33) suggested that, in a pancreatic cell line, SIRT1 is involved in the regulation of Rev-erb α mRNA levels. On the other hand, Rev-erb α regulates the expression of SIRT1 (38), which points to a loop of cross-regulation between these two proteins. We provide evidence that acetylation/deacetylation processes regulate Rev-erb α protein levels. However, whether SIRT1 regulates Rev-erb α by directly deacetylating it, or through an indirect mechanism, requires further research. One possibility is that activation of SIRT1 results in repression of p300, as has been shown by Bouras *et al.* (39), and that this, in turn, results in destabilization of Rev-erb α . The precise mechanism by which SIRT1 regulates Rev-erb α , and the physiologic consequences of this regulation, warrant further investigation.

We want to stress that the DBC1-Rev-erb α -SIRT1 pathway described in this paper may not be the only one mediating the regulation of PEPCK by DBC1. In the fasted state, and in the DBC1 KO mice, increased SIRT1 activity could result in deacetylation of PGC1 α (21) and FOXO (28), which would also result in higher glucose production. Moreover, it is possible that DBC1 also regulates gluconeogenesis through histone deacetylase 3 (HDAC3), which is inhibited by DBC1 (16) and has been shown to promote glucose production (40, 41). In addition, it could also be that changes in the levels of DBC1, or changes to its binding partners, result in alterations in the epigenetic landscape of the PEPCK promoter. Finally, one can envision that DBC1 is a coordinator of all these different pathways that converge on PEPCK.

In conclusion, we describe, for the first time, a key role for the nuclear protein DBC1 as a regulator of gluconeogenesis. DBC1 may play a major role in the development of glucose intolerance and may also have a physiological role in plasma glucose maintenance during starvation. We believe that our studies reveal a new pathway involved in the regulation of gluconeogenesis and may provide a better understanding of the mechanisms that maintain body glucose homeostasis during normal physiology and disease states.

REFERENCES

- Desvergne, B., Michalik, L., and Wahli, W. (2006) Transcriptional regulation of metabolism. *Physiol. Rev.* **86**, 465–514
- Hellerstein, M. K., Neese, R. A., Linfoot, P., Christiansen, M., Turner, S., and Letscher, A. (1997) Hepatic gluconeogenic fluxes and glycogen turnover during fasting in humans. A stable isotope study. *J. Clin. Invest.* **100**, 1305–1319
- Gastaldelli, A., Baldi, S., Pettiti, M., Toschi, E., Camastra, S., Natali, A., Landau, B. R., and Ferrannini, E. (2000) Influence of obesity and type 2 diabetes on gluconeogenesis and glucose output in humans. A quantitative study. *Diabetes* **49**, 1367–1373
- Hanson, R. W., and Reshef, L. (1997) Regulation of phosphoenolpyruvate carboxykinase (GTP) gene expression. *Annu. Rev. Biochem.* **66**, 581–611
- Guillaumond, F., Gréchez-Cassiau, A., Subramaniam, M., Brangolo, S., Peteri-Brünback, B., Staels, B., Fiévet, C., Spelsberg, T. C., Delaunay, F., and Teboul, M. (2010) Kruppel-like factor KLF10 is a link between the circadian clock and metabolism in liver. *Mol. Cell Biol.* **30**, 3059–3070
- Duez, H., and Staels, B. (2009) Rev-erb- α . An integrator of circadian rhythms and metabolism. *J. Appl. Physiol.* **107**, 1972–1980
- Raghuram, S., Stayrook, K. R., Huang, P., Rogers, P. M., Nosie, A. K., McClure, D. B., Burris, L. L., Khorasanizadeh, S., Burris, T. P., and Rastinejad, F. (2007) Identification of heme as the ligand for the orphan nuclear receptors REV-ERB α and REV-ERB β . *Nat. Struct. Mol. Biol.* **14**, 1207–1213
- Yin, L., Wu, N., Curtin, J. C., Qatanani, M., Szwegold, N. R., Reid, R. A., Waitt, G. M., Parks, D. J., Pearce, K. H., Wisely, G. B., and Lazar, M. A. (2007) Rev-erb α , a heme sensor that coordinates metabolic and circadian pathways. *Science* **318**, 1786–1789
- Grant, D., Yin, L., Collins, J. L., Parks, D. J., Orband-Miller, L. A., Wisely, G. B., Joshi, S., Lazar, M. A., Willson, T. M., and Zuercher, W. J. (2010) GSK4112, a small molecule chemical probe for the cell biology of the nuclear heme receptor Rev-erb α . *ACS Chem. Biol.* **5**, 925–932
- Cho, H., Zhao, X., Hatori, M., Yu, R. T., Barish, G. D., Lam, M. T., Chong, L. W., DiTacchio, L., Atkins, A. R., Glass, C. K., Liddle, C., Auwerx, J., Downes, M., Panda, S., and Evans, R. M. (2012) Regulation of circadian behaviour and metabolism by REV-ERB- α and REV-ERB- β . *Nature* **485**, 123–127
- Bugge, A., Feng, D., Everett, L. J., Briggs, E. R., Mullican, S. E., Wang, F., Jager, J., and Lazar, M. A. (2012) Rev-erb α and Rev-erb β coordinately protect the circadian clock and normal metabolic function. *Genes Dev.* **26**, 657–667
- Yin, L., Joshi, S., Wu, N., Tong, X., and Lazar, M. A. (2010) E3 ligases Arf-bp1 and Pam mediate lithium-stimulated degradation of the circadian heme receptor Rev-erb α . *Proc. Natl. Acad. Sci. U.S.A.* **107**, 11614–11619
- Chini, C. C., Escande, C., Nin, V., and Chini, E. N. (2013) DBC1 (deleted in breast cancer 1) modulates the stability and function of the nuclear receptor Rev-erb α . *Biochem. J.* **451**, 453–461
- Chini, E. N., Chini, C. C., Nin, V., and Escande, C. (2013) Deleted in breast cancer-1 (DBC-1) in the interface between metabolism, aging and cancer. *Biosci. Rep.* **33**, e00058
- Li, Z., Chen, L., Kabra, N., Wang, C., Fang, J., and Chen, J. (2009) Inhibition of SUV39H1 methyltransferase activity by DBC1. *J. Biol. Chem.* **284**, 10361–10366
- Chini, C. C., Escande, C., Nin, V., and Chini, E. N. (2010) HDAC3 is negatively regulated by the nuclear protein DBC1. *J. Biol. Chem.* **285**, 40830–40837
- Zhao, W., Kruse, J. P., Tang, Y., Jung, S. Y., Qin, J., and Gu, W. (2008) Negative regulation of the deacetylase SIRT1 by DBC1. *Nature* **451**, 587–590
- Kim, J. E., Chen, J., and Lou, Z. (2008) DBC1 is a negative regulator of SIRT1. *Nature* **451**, 583–586
- Escande, C., Chini, C. C., Nin, V., Dykhouse, K. M., Novak, C. M., Levine, J., van Deursen, J., Gores, G. J., Chen, J., Lou, Z., and Chini, E. N. (2010) Deleted in breast cancer-1 regulates SIRT1 activity and contributes to high-fat diet-induced liver steatosis in mice. *J. Clin. Invest.* **120**, 545–558
- Nin, V., Escande, C., Chini, C. C., Giri, S., Camacho-Pereira, J., Matalonga, J., Lou, Z., and Chini, E. N. (2012) Role of deleted in breast cancer 1 (DBC1) protein in SIRT1 deacetylase activation induced by protein kinase A and AMP-activated protein kinase. *J. Biol. Chem.* **287**, 23489–23501
- Rodgers, J. T., Lerin, C., Haas, W., Gygi, S. P., Spiegelman, B. M., and Puigserver, P. (2005) Nutrient control of glucose homeostasis through a complex of PGC-1 α and SIRT1. *Nature* **434**, 113–118
- Wei, D., Tao, R., Zhang, Y., White, M. F., and Dong, X. C. (2011) Feedback regulation of hepatic gluconeogenesis through modulation of SHP/Nr0b2 gene expression by Sirt1 and FoxO1. *Am. J. Physiol. Endocrinol. Metab.* **300**, E312–320
- Rodgers, J. T., and Puigserver, P. (2007) Fasting-dependent glucose and lipid metabolic response through hepatic sirtuin 1. *Proc. Natl. Acad. Sci. U.S.A.* **104**, 12861–12866
- Erion, D. M., Yonemitsu, S., Nie, Y., Nagai, Y., Gillum, M. P., Hsiao, J. J., Iwasaki, T., Stark, R., Weismann, D., Yu, X. X., Murray, S. F., Bhanot, S., Monia, B. P., Horvath, T. L., Gao, Q., Samuel, V. T., and Shulman, G. I. (2009) SirT1 knockdown in liver decreases basal hepatic glucose production and increases hepatic insulin responsiveness in diabetic rats. *Proc. Natl. Acad. Sci. U.S.A.* **106**, 11288–11293
- Nie, Y., Erion, D. M., Yuan, Z., Dietrich, M., Shulman, G. I., Horvath, T. L., and Gao, Q. (2009) STAT3 inhibition of gluconeogenesis is downregulated by SirT1. *Nat. Cell Biol.* **11**, 492–500
- Wang, R. H., Kim, H. S., Xiao, C., Xu, X., Gavrilova, O., and Deng, C. X.

- (2011) Hepatic Sirt1 deficiency in mice impairs mTorc2/Akt signaling and results in hyperglycemia, oxidative damage, and insulin resistance. *J. Clin. Invest.* **121**, 4477–4490
27. Banks, A. S., Kon, N., Knight, C., Matsumoto, M., Gutiérrez-Juárez, R., Rossetti, L., Gu, W., and Accili, D. (2008) SirT1 gain of function increases energy efficiency and prevents diabetes in mice. *Cell Metab.* **8**, 333–341
 28. Frescas, D., Valenti, L., and Accili, D. (2005) Nuclear trapping of the forkhead transcription factor FoxO1 via SIRT-dependent deacetylation promotes expression of glucogenetic genes. *J. Biol. Chem.* **280**, 20589–20595
 29. Kojetin, D., Wang, Y., Kamenecka, T. M., and Burris, T. P. (2011) Identification of SR8278, a synthetic antagonist of the nuclear heme receptor REV-ERB. *ACS Chem. Biol.* **6**, 131–134
 30. Valera, A., Pujol, A., Pelegrin, M., and Bosch, F. (1994) Transgenic mice overexpressing phosphoenolpyruvate carboxykinase develop non-insulin-dependent diabetes mellitus. *Proc. Natl. Acad. Sci. U.S.A.* **91**, 9151–9154
 31. Linares, A., Perales, S., Palomino-Morales, R. J., Castillo, M., and Alejandro, M. J. (2006) Nutritional control, gene regulation, and transformation of vascular smooth muscle cells in atherosclerosis. *Cardiovasc. Hematol. Disord. Drug Targets* **6**, 151–168
 32. Qiang, L., Wang, L., Kon, N., Zhao, W., Lee, S., Zhang, Y., Rosenbaum, M., Zhao, Y., Gu, W., Farmer, S. R., and Accili, D. (2012) Brown remodeling of white adipose tissue by SirT1-dependent deacetylation of PPAR γ . *Cell* **150**, 620–632
 33. Vieira, E., Marroquí, L., Figueroa, A. L., Merino, B., Fernandez-Ruiz, R., Nadal, A., Burris, T. P., Gomis, R., and Quesada, I. (2013) Involvement of the clock gene Rev-erb α in the regulation of glucagon secretion in pancreatic α -cells. *PLoS ONE* **8**, e69939
 34. Feng, D., Liu, T., Sun, Z., Bugge, A., Mullican, S. E., Alenghat, T., Liu, X. S., and Lazar, M. A. (2011) A circadian rhythm orchestrated by histone deacetylase 3 controls hepatic lipid metabolism. *Science* **331**, 1315–1319
 35. Solt, L. A., Wang, Y., Banerjee, S., Hughes, T., Kojetin, D. J., Lundasen, T., Shin, Y., Liu, J., Cameron, M. D., Noel, R., Yoo, S. H., Takahashi, J. S., Butler, A. A., Kamenecka, T. M., and Burris, T. P. (2012) Regulation of circadian behaviour and metabolism by synthetic REV-ERB agonists. *Nature* **485**, 62–68
 36. Zhang, E. E., Liu, Y., Dentin, R., Pongsawakul, P. Y., Liu, A. C., Hirota, T., Nusinow, D. A., Sun, X., Landais, S., Kodama, Y., Brenner, D. A., Montminy, M., and Kay, S. A. (2010) Cryptochrome mediates circadian regulation of cAMP signaling and hepatic gluconeogenesis. *Nat. Med.* **16**, 1152–1156
 37. Rudic, R. D., McNamara, P., Curtis, A. M., Boston, R. C., Panda, S., Hogenesch, J. B., and Fitzgerald, G. A. (2004) BMAL1 and CLOCK, two essential components of the circadian clock, are involved in glucose homeostasis. *PLoS Biol.* **2**, e377
 38. Woldt, E., Sebt, Y., Solt, L. A., Duhem, C., Lancel, S., Eeckhoutte, J., Heselink, M. K., Paquet, C., Delhay, S., Shin, Y., Kamenecka, T. M., Schaart, G., Lefebvre, P., Nevière, R., Burris, T. P., Schrauwen, P., Staels, B., and Duez, H. (2013) Rev-erb- α modulates skeletal muscle oxidative capacity by regulating mitochondrial biogenesis and autophagy. *Nat. Med.* **19**, 1039–1046
 39. Bouras, T., Fu, M., Sauve, A. A., Wang, F., Quong, A. A., Perkins, N. D., Hay, R. T., Gu, W., and Pestell, R. G. (2005) SIRT1 deacetylation and repression of p300 involves lysine residues 1020/1024 within the cell cycle regulatory domain 1. *J. Biol. Chem.* **280**, 10264–10276
 40. Sun, Z., Miller, R. A., Patel, R. T., Chen, J., Dhir, R., Wang, H., Zhang, D., Graham, M. J., Unterman, T. G., Shulman, G. I., Sztalryd, C., Bennett, M. J., Ahima, R. S., Birnbaum, M. J., and Lazar, M. A. (2012) Hepatic Hdac3 promotes gluconeogenesis by repressing lipid synthesis and sequestration. *Nat. Med.* **18**, 934–942
 41. Mihaylova, M. M., Vasquez, D. S., Ravnskjaer, K., Denechaud, P. D., Yu, R. T., Alvarez, J. G., Downes, M., Evans, R. M., Montminy, M., and Shaw, R. J. (2011) Class IIa histone deacetylases are hormone-activated regulators of FOXO and mammalian glucose homeostasis. *Cell* **145**, 607–621

CONTRIBUCIONES, PERSPECTIVAS Y CONTROVERSIAS

Esta sección será dividida en relación a los diferentes aspectos que fueron abordados en el desarrollo de la tesis con respecto a DBC1, su interacción con SIRT1 y los procesos biológicos regulados por ambas proteínas.

Regulación de la interacción entre SIRT1 y DBC1: preguntas y controversias

En los últimos años, nuestro trabajo [190] junto con otros [181-183] han empezado a generar datos que demuestran que la interacción entre SIRT1 y DBC1 es dinámica y regulada por claves fisiológicas. Dentro de estos, el nuestro es el único que evalúa la interacción entre SIRT1 y DBC1 en contextos relevantes para el metabolismo [190]. En este sentido, un resultado central de la tesis es que el complejo SIRT1-DBC1 se disocia en condiciones que mimetizan el ayuno. ¿Cuáles son algunas de las preguntas que surgen a partir de los datos presentados? Para poner nuestros datos en un contexto más fisiológico, sería interesante investigar si el glucagón y otras hormonas elevadas durante el ayuno generan la misma respuesta que la forskolina en términos de activación de SIRT1 y disociación del complejo SIRT1-DBC1. En este sentido, una posibilidad es generar una curva temporal de la interacción entre SIRT1 y DBC1 *in vivo* luego de inyecciones de glucagón, o al menos *ex vivo* en *slices* de hígado. Otra posibilidad consistiría en estudiar que sucede con la interacción entre SIRT1 y DBC1 y la actividad de SIRT1 en ratones que carecen del receptor para glucagón [191]. Finalmente, la expansión de estos estudios a otros tejidos importantes para la homeostasis energética, como el páncreas, el músculo y el tejido adiposo nos permitiría comprender las características tejido-específicas de la regulación de SIRT1 y del complejo SIRT1-DBC1.

La insulina también juega un papel central en la regulación de la homeostasis energética y tiene una gran capacidad inhibitoria de la gluconeogénesis hepática. Esta hormona no ejerce su función a través de la vía del AMPc sino a través de kinasas, en particular la kinasa AKT [192]. Al

día de hoy no hay evidencia que vincule los niveles de insulina con la actividad enzimática de SIRT1, o la interacción entre SIRT1 y DBC1.

Uno de los datos que presentamos en el primer trabajo de la tesis muestra que la activación de PKA estimula la actividad de SIRT1 [190]. Es relevante notar que un grupo de investigación independiente también mostró que la activación de PKA promueve un aumento en la actividad SIRT1 con una curva temporal similar a la observada por nosotros [193]. Estos autores identifican la serina 434 como blanco directo de PKA [193]. Sin embargo, nuestros estudios *in vitro* no coinciden en este aspecto [190]. Es posible que otros estudios aporten mas información relevante a este punto, sin embargo, hasta ahora, no se han presentado nuevos artículos que echen luz sobre este tema. Los autores de este trabajo también muestran que a pesar que la activación de SIRT1 por PKA es transitoria, tiene un efecto sobre la transcripción de genes vinculados a la oxidación de ácidos grasos en fibroblastos embrionarios en cultivo [193]. Es interesante que en concordancia con nuestros datos, Gerhart-Hinez también proponen que la activación de SIRT1 es independiente de cambios en los niveles de NAD⁺ intracelular [193], una particularidad bastante novedosa y anti-paradigmática en el campo de las sirtuinas. Un aspecto contradictorio entre ambos trabajos es que nuestros datos apuntan a que la activación de SIRT1 mediada por PKA es indirecta y mediada por AMPK [190], mientras que Gerhart-Hinez proponen que la activación es directa, mediada por la fosforilación de la región catalítica de SIRT1 [193]. Es mas, nuestro trabajo es el primero en mostrar que AMPK activa a SIRT1 en ausencia de cambios en el NAD⁺ intracelular [190]. De hecho, nuestros datos apuntan con firmeza que la activación farmacológica de AMPK redundante en la activación de SIRT1, y que incluso el resveratrol, un fármaco que marcó un antes y un después en el campo de las sirtuinas, actúa mediante esta vía [190].

Un artículo mas reciente propone que el resveratrol actúa como inhibidor de la fosfodiesterasa 4, una enzima que cliva AMPc [87]. Park et al. mostraron que el resveratrol provoca un aumento en los niveles de AMPc que resultan en la activación de AMPK vía EPAC (una GTPasa pequeña cuya actividad es regulada por AMPc) [87]. Cabe notar que nuestros datos apuntan a PKA y no a EPAC como intermediario de la acción del AMPc sobre SIRT1 [190]. Ambos trabajos utilizan modelos celulares diferentes, por lo que, tomando los datos en conjunto, es posible generar un panorama en el que el AMPc y el resveratrol promuevan la activación de

SIRT1 a través de mecanismos que dependen del tipo celular, pero que generan el mismo resultado.

Además de la activación aguda que produce el AMPc sobre la actividad SIRT1, el factor de transcripción CREB, que es activado por la vía del AMPc y PKA, provoca un aumento en la transcripción de SIRT1 [147]. Por lo tanto, un aumento en los niveles de este segundo mensajero promueven primero una activación transitoria de SIRT1, mientras que a largo plazo, lo mismo se consigue aumentando los niveles de proteína. En este escenario es factible cuestionarse si la vía del AMPc/PKA regula a través de CREB también la transcripción de DBC1.

Hasta ahora, los datos generados por varios laboratorios independientes, incluido el de realización de esta tesis, proponen que AMPK regula la actividad de SIRT1. Sin embargo, un tema de debate aun no saldado es la posible fosforilación *directa* de SIRT1 por AMPK. En el primer trabajo que mostró que AMPK regula la actividad de SIRT1, los autores defienden que AMPK no fosforila directamente a SIRT1 [163]. Los datos se presentan en el material suplementario del trabajo, donde muestran una gráfica de incorporación de fósforo radiactivo en un ensayo kinasa *in vitro*. Si bien el nivel de incorporación de radiactividad en SIRT1 es mucho menor que en el control positivo, los datos presentados en el trabajo muestran que SIRT1 incorpora radiactividad [163]. Sin embargo, los autores proponen que AMPK no fosforila directamente a SIRT1 [163]. Nuestros resultados muestran claramente que la co-transfección de AMPK y SIRT1 en células HEK-293 resulta en la incorporación de radiactividad en SIRT1, al igual que el tratamiento con resveratrol [190]. De hecho, la serina 605 de SIRT1, se encuentra en una secuencia que contiene muchos de los aspectos de las secuencias consenso de AMPK, y nuestros datos apuntan a que este residuo es necesario para que el AMPc provoque la disociación de SIRT1 y DBC1 [190]. Mas aun, datos no publicados de nuestro laboratorio muestran que AMPK fosforila a SIRT1 en ensayos *in vitro*. Un trabajo mas reciente presenta evidencia que AMPK fosforila directamente a SIRT1 en la treonina 344, que resulta en la inhibición de SIRT1 [194]. En mi opinión, es importante estudiar mas a fondo la posibilidad que SIRT1 sea un sustrato de AMPK, los posibles sitios de fosforilación, y la relevancia fisiológica de dichos sitios.

La superfamilia de desacetilasas de histonas es vasta, y esta compuesta por cuatro clases. Las familia de desacetilasas de histonas clásicas (clases I, II y IV), son independientes de NAD⁺,

mientras que la familia III, también conocida como sirtuinas, presentan actividad enzimática NAD⁺ dependiente [195]. Es interesante que de las diecisiete desacetilasas presentes en mamíferos, HDAC3 y SIRT1 comparten sustratos, regulan algunos procesos fisiológicos en común, y comparten formas de regulación. A modo de ejemplo, ambas proteínas desacetilan a p53 [196, 197], FOXO [198, 199], NFκB [140, 200] y MEF2 [201, 202]. Tanto SIRT1 como HDAC3 regulan la producción de glucosa hepática [198, 203] (ver introducción por una descripción detallada de los mecanismos por los que SIRT1 regula la gluconeogénesis). Mas aun, ambas desacetilasas son inhibidas por DBC1 [169, 170, 176]. No obstante, hasta la fecha no hay datos sobre los mecanismos moleculares que regulan la interacción entre HDAC3 y DBC1. A la vista de la similitud entre HDAC3 y SIRT1 recién discutida, es razonable hipotetizar que la vía del AMPc incide sobre la interacción entre DBC1 y HDAC3 de forma similar a lo que ocurre con SIRT1.

Como se menciona en la introducción, DBC1 es una proteína con múltiples interactores. No obstante, es muy poco lo que se conoce acerca de las señales que regulan la interacción entre DBC1 y sus *partners*. En este sentido, la atención se ha centrado en la interacción SIRT1-DBC1. La interacción entre DBC1 y algunos receptores nucleares es ligando dependiente, mientras que otras es ligando independiente [172, 189]. Sin embargo, no sabemos si todos los posibles interactores compiten entre si por su unión a DBC1, ni las constantes de asociación entre DBC1 y las proteínas con las que interactúa, o que efecto tiene la disociación de DBC1 y un interactor en particular sobre las otras interacciones. ¿Es posible que existan *pools* intranucleares de DBC1, por ejemplo, un *pool* DBC1-receptor nuclear, otro DBC1-enzimas que modifican el código epigenético y uno DBC1-ARNpol II? ¿Qué papel juega DBC1 en los procesos regulados por hormonas? ¿Participa DBC1 en la regulación del splicing de todos los ARNm o de algunos, en todas las células, en todas las etapas del desarrollo?

Otro aspecto que podría afectar la interacción entre DBC1, SIRT1 y otros interactores son modificaciones post-traduccionales en DBC1. Se ha descrito, por ejemplo, que la fosforilación de DBC1 en la treonina 454 por las kinasas ATM/ATR promueve la interacción con SIRT1 [181, 182]. Un dato importante que aportaría a nuestra comprensión acerca de la regulación de la interacción entre SIRT1 y DBC1 por la vía del AMPc es estudiar si DBC1 es un blanco directo

de PKA. En este sentido, es alentador que la serina 249 de DBC1 se encuentra en una secuencia con características de la secuencia consenso para PKA. Esta serina es parte del dominio cierre de leucina de DBC1, que como hemos mencionado es fundamental para la interacción con SIRT1 [142, 169]. En la misma línea, resulta imprescindible evaluar si DBC1 puede ser blanco de otras kinasas, entre ellas AMPK.

Regulación de los niveles de DBC1: interrogantes

La experiencia de nuestro laboratorio indica que DBC1 es una proteína muy estable. Por lo tanto, la observación que un periodo de ayuno corto resultara en una disminución de DBC1 en el hígado fue muy sorprendente [204]. Este dato en particular abre varias preguntas cuyas respuestas sin duda aportaran a comprender mejor la regulación de DBC1. Una posibilidad es que la disminución en la señalización por insulina, o la activación de la señalización por glucagón, desestabilicen a DBC1. Otra posibilidad es que DBC1 sea ubiquitinada y por lo tanto degradada vía el proteasoma. ¿Es DBC1 blanco de modificaciones post-traduccionales que la hacen blanco de ubiquitin-ligasas? ¿si es así, cuales son?. Otra posibilidad es que la transcripción de DBC1 se detenga abruptamente. No existen datos en la literatura que indiquen como se regula la transcripción de DBC1. Una estrategia sencilla para evaluar esta posibilidad es estudiar las características del promotor de DBC1. En particular, la búsqueda de secuencias consenso para factores de transcripción, en particular, regulados por hormonas o sensibles a los cambios energéticos del organismo permitiría comenzar a abordar este punto.

En cultivos celulares, los niveles de ARNm para DBC1 ciclan en un patrón de estilo circadiano [188]. Los niveles proteicos también cambian, aunque las variaciones no coinciden completamente con los cambios en el ARNm [188]. En conjunto, estos datos apuntan a que existe una regulación compleja de los niveles de DBC1, por un lado a nivel de transcripción, y probablemente también a nivel de estabilidad de la proteína.

Dado que la restricción calórica ha demostrado generar beneficios en la salud de varios organismos (ver la introducción por una discusión detallada y referencias), varios grupos de investigación han intentado identificar moléculas que mimeticen los efectos de la restricción calórica [205]. Es importante notar que la restricción calórica afecta simultáneamente a varias vías intracelulares, entre ellas la de mTOR [206], SIRT1 [55] y AMPK [89]. Por ende, la búsqueda de miméticos de la restricción calórica puede orientarse a cualquiera de dichos blancos [205]. En lo que respecta a la búsqueda de activadores de SIRT1, los ensayos utilizados hasta el momento son ensayos *in vitro* [72, 83]. Sin embargo, como mencionamos con anterioridad, nuestros datos apuntan a que la disociación de DBC1 es parte central del mecanismo de acción de algunos fármacos activadores de SIRT1 [190]. Cabe preguntarse si este mecanismo de búsqueda de activadores de SIRT1 no deja por fuera una potencial clase de activadores, los que dependen de DBC1. ¿Es posible diseñar fármacos que apunten a la disociación del complejo? Sería de gran utilidad contar con una estructura cristalina del complejo SIRT1-DBC1, o al menos entre SIRT1 y el cierre de leucina de DBC1. De manera adicional, contar con un ensayo que permita probar fármacos sobre el complejo SIRT1-DBC1 es fundamental. Chiba et al. [207] desarrollaron un bioensayo que detecta fármacos que activan una respuesta similar a la desencadenada por la restricción calórica. Los autores analizaron los promotores de genes regulados en positivo en el hígado de animales sometidos a restricción calórica, e identificaron un motivo presente en los promotores de dichos genes al que denominaron DFRCR-REs (por Dwarfism and Calorie Restriction Responsive Elements). Con esta información construyeron un plásmido que incluye un motivo DFRCR-RE en el promotor de un gen reportero [207], y demostraron que es sensible a la restricción calórica tanto *in vivo* como en cultivos celulares [207]. Con este método es posible probar que drogas promueven la expresión de un programa símil-restricción calórica, pero además es posible transfectar el plásmido en células que carecen de DBC1 y probar las drogas en ausencia de DBC1.

DBC1 regula al menos tres enzimas vinculadas a modificaciones epigenéticas: SIRT1, HDAC3 y la metiltransferasa SUV39H1 [175]. Esto sugiere que DBC1 participa en la regulación del “paisaje” epigenético de la cromatina (epigenetic landscape), que tiene profundas consecuencias en la fisiología celular. Algunos datos preliminares que no fueron incluidos en los trabajos presentados sugieren que en ausencia de DBC1 la acetilación y metilación de histonas en el promotor de PEPCK esta alterada. ¿Cómo juega esto en relación a la interpretación de los resultados?. Es posible que DBC1 regule la expresión de PEPCK a varios niveles: el primer nivel sería regular la acetilación y metilación de histonas en el promotor de PEPCK, el siguiente nivel sería a través del reclutamiento de enzimas y factores nucleares al promotor. Por un lado, nuestro trabajo plantea la importancia de SIRT1 y Rev-erba [204], pero es posible que DBC1 también regule la acetilación de FOXO1 a través de HDAC3 [198], y la acetilación de PPARγ vía SIRT1. Mas aun, es atractivo especular que DBC1 orqueste todo esto a nivel del promotor de PEPCK para promover una regulación coordinada de la expresión del gen. En la actualidad existen aproximaciones globales que permiten estudiar las modificaciones epigenéticas a gran escala [208, 209]. Aplicar estas técnicas en un futuro al modelo de ratón KO para DBC1 revelará hasta que grado DBC1 regula la información epigenética del organismo.

La acetilación es una modificación postraduccional importante también por fuera de la cromatina. Varios trabajos muestran que miles de proteínas celulares son acetiladas [210], de hecho, es posible que la acetilación de proteínas sea tan común como la fosforilación [211]. Mas aun, estudios comparativos entre *Drosophila* y humanos han demostrado que las regiones en las que aparecen lisinas acetiladas están muy conservadas [212, 213] y que regulan importantes procesos, como la traducción de proteínas, el plegamiento proteico, empaquetamiento del ADN y función mitocondrial [212]. De hecho, Zhao et al. presentaron el impactante hecho de que en el hígado todas las enzimas de glicólisis, gluconeogénesis, ciclo de Krebs, el ciclo de la urea, y del metabolismo del glicógeno y ácidos grasos están acetiladas [213]. Sería interesante aplicar técnicas de estudio global de acetilación para evaluar el acetiloma regulado por DBC1.

Para terminar, cabe destacar que al comienzo del desarrollo de esta tesis el conocimiento acumulado sobre DBC1 era relativamente pequeño. Nuestro trabajo aporta datos acerca de rol de esta proteína en varios campos de debate y aporta al panorama emergente que posiciona a DBC1 como una molécula central en la regulación y coordinación de procesos metabólicos.

De manera paralela al desarrollo del tema principal de la tesis, durante el trabajo de doctorado también se colaboro en otras dos líneas de investigación. Una de ellas es el papel de DBC1 en el tejido adiposo blanco, en especial su papel en la diferenciación y senescencia celular y en la sensibilidad a la insulina. La participación en esta línea resultó en la coautoría de los siguientes trabajos, el último de ellos en vías de publicación:

-Deleted in Breast Cancer 1 regulates cellular senescence during obesity

Carlos Escande, Verónica Nin, Tamar Pirtskhalava, Claudia C. Chini¹, Maria Thereza Barbosa, Angela Mathison, Raul Urrutia, Tamar Tchkonina, James L. Kirkland, Eduardo N. Chini.

Aging Cell. 2014 Jul 3. doi: 10.1111/accel.12235. [Epub ahead of print]

-Deleted in Breast Cancer 1 limits adipose tissue fat accumulation and plays a key role in the development of metabolic syndrome phenotype.

Escande C, Nin V, Pirtskhalava T, Chini CC, Tchkonina T, Kirkland JL, Chini EN.

Diabetes. 2014 Jul 22. pii: DB_140192. [Epub ahead of print]

SHORT TAKE

Deleted in Breast Cancer 1 regulates cellular senescence during obesity

Carlos Escande,^{1,2,3} Veronica Nin,^{1,2} Tamar Pirtskhalava,² Claudia C. Chini,^{1,2} Maria Thereza Barbosa,¹ Angela Mathison,⁴ Raul Urrutia,^{4,5} Tamar Tchkonina,² James L. Kirkland² and Eduardo N. Chini^{1,2}

¹Department of Anesthesia, Mayo Clinic, Rochester, MN, USA

²Robert and Arlene Kogod Center on Aging, Mayo Clinic, Rochester, MN, USA

³Institut Pasteur Montevideo, Montevideo, Uruguay

⁴Laboratory of Epigenetics and Chromatin Dynamics, Mayo Clinic, Rochester, MN, USA

⁵Epigenomic Translational Program, Mayo Clinic Center for Individualized Medicine, Rochester, MN, USA

Summary

Chronic obesity leads to inflammation, tissue dysfunction, and cellular senescence. It was proposed that cellular senescence during obesity and aging drives inflammation and dysfunction. Consistent with this, clearance of senescent cells increases healthspan in progeroid mice. Here, we show that the protein Deleted in Breast Cancer-1 (DBC1) regulates cellular senescence during obesity. Deletion of DBC1 protects preadipocytes against cellular senescence and senescence-driven inflammation. Furthermore, we show protection against cellular senescence in DBC1 KO mice during obesity. Finally, we found that DBC1 participates in the onset of cellular senescence in response to cell damage by mechanism that involves binding and inhibition of HDAC3. We propose that by regulating HDAC3 activity during cellular damage, DBC1 participates in the fate decision that leads to the establishment of cellular senescence and consequently to inflammation and tissue dysfunction during obesity.

Key words: aging; hdacs; mice; obesity; senescence; signaling; Sir2.

Introduction

Obesity, a major health problem in the USA and many developed countries (Flegal *et al.*, 2012), is associated with an increase in cellular senescence and inflammation (Tchkonina *et al.*, 2010). Cellular senescence has been proposed to promote chronic, “sterile” inflammation through the senescence-associated secretory phenotype (SASP) (Tchkonina *et al.*, 2010). Supporting this notion, some of us found that

eliminating senescent cells from progeroid mice improves healthspan (Baker *et al.*, 2011). The physiological and molecular events that lead to cellular senescence, however, are still poorly understood. We have been studying the role of the protein Deleted in Breast Cancer-1 (DBC1) in energy metabolism (Chini *et al.*, 2013). DBC1 regulates several nuclear proteins, including SIRT1 and HDAC3 (Escande *et al.*, 2010; Chini *et al.*, 2013). Both SIRT1 and HDAC3 regulate cellular senescence (Ghosh, 2008; Feng *et al.*, 2009). We investigated whether DBC1 plays a role in cellular senescence and the SASP during obesity. We found that preadipocytes isolated from WT and DBC1 KO mice after 12 weeks of high-fat diet feeding exhibit less senescence, indicated by lower levels of p16^{Ink4a} and p21, as well as the SASP markers, MCP-1, TNF- α , and IL-6 (Fig. 1A). Also, we found fewer γ -H2.AX (a marker of activated DNA damage responses)-positive preadipocytes isolated from DBC1 KO mice (Fig. 1B). Several markers of antioxidant defense mechanisms were up-regulated in preadipocytes from DBC1 KO mice (Fig. 1C). Consistent with our *in vitro* results, DBC1 KO mice have less cellular senescence in adipose tissue during high-fat diet feeding measured by cytoplasmic (Fig. S1A) SA- β Gal activity and p16^{Ink4a} expression (Fig. 1D–F). The effect of DBC1 on cellular senescence may not be linked to chronological aging, as there was no difference between WT and DBC1 KO mice fed with normal chow during 16 months (Fig. 1G–H). Nevertheless, DBC1 KO mice had less inflammation in fat tissue (Fig. 1H). We are currently investigating whether there is a difference on cellular senescence that may appear later in life.

Next, we investigated whether deletion of DBC1 protects against DNA damage-induced cellular senescence. We induced DNA damage by H₂O₂ treatment in 3T3-L1 preadipocytes stable expressing scrambled shRNA (Control shRNA) or DBC1 shRNA. We found increased cellular SA- β Gal activity in the control shRNA cells exposed to H₂O₂, but not in cells expressing DBC1 shRNA (Fig. 2A). Control cells showed a dose-dependent increase in expression of p53 and p21 after H₂O₂ treatment. However, there were no changes in p53 and p21 in cells expressing DBC1 shRNA (Fig. 2A). The effect of DBC1 on the response to H₂O₂-induced DNA damage was only related to cellular senescence, as apoptosis was not affected by DBC1 knockdown (Fig. S1B). DBC1 binds and inhibits HDAC3 (Chini *et al.*, 2010). Indeed, HDAC3 regulates DNA damage response (Bhaskara *et al.*, 2010) and inhibits expression of the senescence mediator p16^{Ink4a} (Zheng *et al.*, 2012). We found that the effect of DBC1 knockdown on senescence was completely abrogated by cotransfection with HDAC3 siRNA, but not by SIRT1 siRNA (Fig. 2C and Fig. S1C). Indeed, DBC1 knockdown increased HDAC3 activity in 3T3-L1 cells (Fig. 2D). Furthermore, HDAC3 siRNA, restored p21 expression driven by H₂O₂ treatment in DBC1 shRNA-expressing cells (Fig. 2E and Fig. S1D). Also, knockdown of DBC1 resulted in less γ -H2.AX-positive cells (Fig. 2F and Fig. S1E), an effect that was lost when HDAC3 was knocked down together with DBC1 (Fig. 2F). Interestingly, treatment with H₂O₂ led to a rapid increase in DBC1 binding to HDAC3 (Fig. 2G), which correlated with an increase in histone H3 acetylation (Ac-H3K9, Fig. 2H), a target site for HDAC3 (Bhaskara *et al.*, 2010). Finally, we found that DBC1 is present in both p16 and p21 promoter regions in

Correspondence

Eduardo N. Chini, Laboratory of Signal Transduction, Department of Anesthesiology, Cancer Center, Center for GI Signaling, and Kogod Center on Aging, Mayo Clinic, Rochester, MN 55905, USA. Tel.: +1 507 255 0992; fax: +1 507 255 7300; e-mail: chini.eduardo@mayo.edu

Accepted for publication 29 April 2014



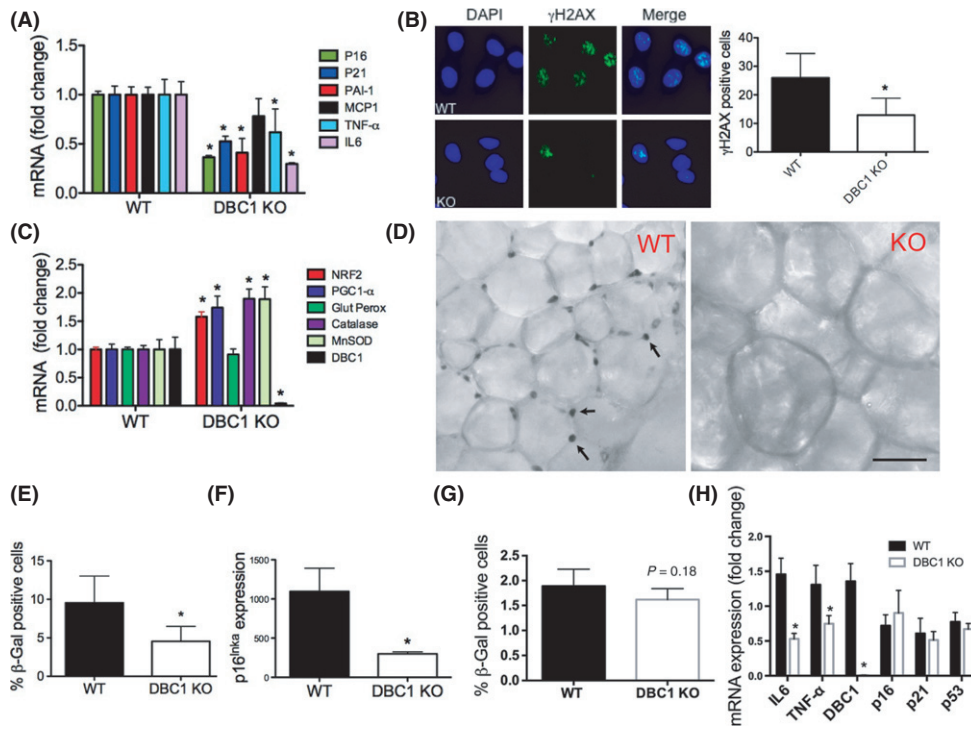


Fig. 1 Deletion of DBC1 protects against cellular senescence during obesity (A) Cellular senescence and SASP marker gene expression by RT-PCR in cultured inguinal mouse preadipocytes after HFD. (B) Left, γ -H2.AX immunostaining in preadipocytes from WT and DBC1 KO mice. Right, quantification of γ -H2.AX foci-positive cells ($*P < 0.05$; *t*-test; *n* = 4 mice/group). (C) ROS and mitochondrial function marker gene expression by RT-PCR in cultured preadipocytes ($*P < 0.05$; *t*-test; *n* = 4 mice/ group). (D) SA- β Gal activity in inguinal adipose tissue of WT and DBC1 KO mice after 12 weeks on a high-fat diet. Arrowheads point to positive cells. (E) Quantitation of cellular SA- β Gal activities in the inguinal fat of the mice described in D ($P < 0.05$; *t*-test; *n* = 4 mice/ group). (F) Expression of the senescence marker, p16^{INK4a}, by RT-PCR in inguinal fat under the conditions described in D. (G–H) Senescence and inflammation markers in inguinal fat tissue of WT and DBC1 KO female mice at 16 months of age fed with normal chow diet. (G) Quantitation of SA- β Gal activity. (H) Expression of senescence and inflammation markers by RT-PCR. ($P < 0.05$; *t*-test; *n* = 4 mice/ group)

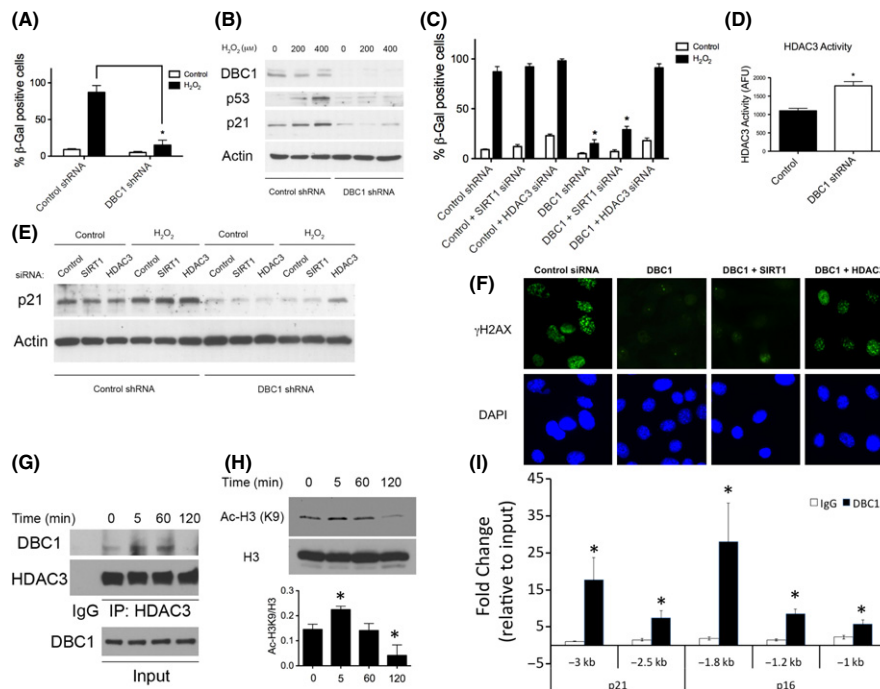


Fig. 2 DBC1 regulates cellular senescence by an HDAC3-mediated mechanism (A) Quantitation of cellular SA- β Gal activity in 3T3-L1 preadipocytes following H_2O_2 treatment (200 μ M; $*P < 0.05$; *t*-test; *n* = 5). (B) Protein expression of p53 and p21 in 3T3-L1 preadipocytes stably transfected with scrambled or DBC1 shRNA and treated with 200 μ M H_2O_2 . (C) Quantitation of SA- β Gal staining in 3T3-L1 after treatment with H_2O_2 (200 μ M). Cells stably transfected with control or DBC1 shRNA were transfected with control, SIRT1, or HDAC3 siRNA before H_2O_2 treatment. Senescence was evaluated by cellular SA- β Gal activity ($*P < 0.05$; *t*-test; *n* = 5). (D) HDAC3 deacetylase activity measured after immunoprecipitation of HDAC3 preadipocytes stably transfected with control or DBC1 shRNA. (E) Representative effect of SIRT1 and HDAC3 knockdown on the effect of DBC1 in p21 expression after H_2O_2 treatment. (*n* = 3) (F) Effect of DBC1, SIRT1, and HDAC3 siRNA on γ -H2.AX foci in 3T3-L1 preadipocytes after incubation with H_2O_2 (200 μ M) (*n* = 3). (G) Time-dependent interaction between HDAC3 and DBC1 after treatment of 3T3-L1 preadipocytes with 200 μ M of H_2O_2 . (H) Upper, time dependence of histone H3 lysine residue 9 acetylation (K9) after treatment of preadipocytes with 200 μ M H_2O_2 . Lower, densitometry analysis of K9 histone 3 acetylation ($*P < 0.05$; *t*-test; *n* = 3). (I) Chromatin immunoprecipitation (ChIP) for the p21 and p16 promoter regions in 3T3-L1 preadipocytes using an antibody against DBC1. Nonspecific IgG was used as control. The results shown are the average \pm SEM of 4 independent ChIP. ($*P < 0.01$; *t*-test)

3T3-L1 cells (Fig. 2I), with a binding profile similar to the one of HDAC3 (Fig. S1F), which suggests that DBC1 binding to the chromatin is bridged by HDAC3. DBC1 is regulated by the checkpoint kinase ATM (Yuan et al., 2012), and HDAC3 is required for the DNA damage response (Bhaskara et al., 2010). We propose that during the cellular stress driven by obesity, DBC1 has an active role in the onset of cellular senescence and inflammation. It is plausible that in the event of chronic damage or stress, DBC1 plays a role in checkpoint control, contributing to a switch in cell fate and promoting cellular senescence.

Acknowledgments

Supported by grants: NIH (NIDDK) DK084055 (to ENC), NIH (NIA) AG26094 (to ENC), AG41122 and AG13925 (to JLK), and AHA 11POST7320060 (to CE).

Funding

Supported by grants: NIH (NIDDK) DK084055 (to ENC), NIH (NIA) AG26094 (to ENC), AG41122 and AG13925 (to JLK), and AHA 11POST7320060 (to CE).

Conflict of interest

None declared.

Author contributions

CE executed most experiments; VN measured senescence in tissue. CC helped in siRNA experiments. MTB did senescence experiments and quantitation in cells. TP did isolation of mouse preadipocytes. AM and RU provided expertise with ChIP experiments. CE, TT, JLK, and ENC planned the experimental strategy. CE, TT, JLK, and ENC wrote the manuscript.

References

- Baker DJ, Wijshake T, Tchkonja T, LeBrasseur NK, Childs BG, van de Sluis B, Kirkland JL, van Deursen JM (2011) Clearance of p16Ink4a-positive senescent cells delays ageing-associated disorders. *Nature* **479**, 232–236.
- Bhaskara S, Knutson SK, Jiang G, Chandrasekharan MB, Wilson AJ, Zheng S, Yenamandra A, Locke K, Yuan JL, Bonine-Summers AR, Wells CE, Kaiser JF, Washington MK, Zhao Z, Wagner FF, Sun ZW, Xia F, Holson EB, Khabele D, Hiebert SW (2010) Hdac3 is essential for the maintenance of chromatin structure and genome stability. *Cancer Cell* **18**, 436–447.
- Chini CC, Escande C, Nin V, Chini EN (2010) HDAC3 is negatively regulated by the nuclear protein DBC1. *J. Biol. Chem.* **285**, 40830–40837.
- Chini EN, Chini CC, Nin V, Escande C (2013). Deleted in breast cancer-1 (DBC-1) in the interface between metabolism, aging and cancer. *Biosci. Rep.* **33**, 637–643.

- Escande C, Chini CC, Nin V, Dykhouse KM, Novak CM, Levine J, van Deursen J, Gores GJ, Chen J, Lou Z, Chini EN (2010) Deleted in breast cancer-1 regulates SIRT1 activity and contributes to high-fat diet-induced liver steatosis in mice. *J Clin Invest.* **120**, 545–558.
- Feng Y, Wang X, Xu L, Pan H, Zhu S, Liang Q, Huang B, Lu J (2009) The transcription factor ZBP-89 suppresses p16 expression through a histone modification mechanism to affect cell senescence. *FEBS J.* **276**, 4197–4206.
- Flegal KM, Carroll MD, Kit BK, Ogden CL (2012) Prevalence of obesity and trends in the distribution of body mass index among US adults, 1999–2010. *JAMA* **307**, 491–497.
- Ghosh HS (2008) The anti-aging, metabolism potential of SIRT1. *Curr. Opin. Investig. Drugs* **9**, 1095–1102.
- Tchkonja T, Morbeck DE, Von Zglinicki T, Van Deursen J, Lustgarten J, Scrbale H, Khosla S, Jensen MD, Kirkland JL (2010) Fat tissue, aging, and cellular senescence. *Aging Cell* **9**, 667–684.
- Yuan J, Luo K, Liu T, Lou Z (2012) Regulation of SIRT1 activity by genotoxic stress. *Genes Dev.* **26**, 791–796.
- Zheng S, Li Q, Zhang Y, Balluff Z, Pan YX (2012) Histone deacetylase 3 (HDAC3) participates in the transcriptional repression of the p16 (INK4a) gene in mammary gland of the female rat offspring exposed to an early-life high-fat diet. *Epigenetics* **7**, 183–190.

Supporting Information

Additional Supporting Information may be found in the online version of this article at the publisher's web-site.

Fig. S1 (A) DAPI counterstaining of fat tissue SA-βGal staining described in Figure 1D, showing cytoplasmic localization of the βGal signal. (B) Effect of DBC1 knockdown on apoptosis triggered by H₂O₂ in 3T3-L1 preadipocytes. Cells were incubated with 200 μM H₂O₂ for 2 h, washed and let them recover for 4 more hours. Apoptosis was determined by nuclear shape using DAPI as nuclear marker. Pictures were taken blindly before and after treatment and apoptosis was independently evaluated by counting cells in the field based in nuclear shape, size, and DNA condensation. Results shown represent average ± SEM of 3 independent experiments. (C) Western blot for DBC1, HDAC3, and SIRT1 in H₂O₂-treated 3T3-L1 preadipocytes transfected with the different siRNAs and collected at the time of H₂O₂ treatment. (D) Densitometry analysis for p21 expression in three independent experiments corresponding to the results shown in Figure 2E. (E) Quantitation of the effect of DBC1, SIRT1, and HDAC3 siRNA on γ-H2.AX foci in 3T3-L1 preadipocytes after incubation with H₂O₂ (200 μM) shown in Figure 2F. Connecting lines show significant differences between conditions (*P* < 0.05, ANOVA, *n* = 3). (F) Chromatin immunoprecipitation (ChIP) for the p21 and p16 promoter regions in 3T3-L1 preadipocytes using an antibody against HDAC3. Nonspecific IgG was used as control. The results shown are the average ± SEM of 4 independent ChIP. (**P* < 0.01; *t*-test).

Data. S1 Methods.

Carlos Escande,^{1,2,3} Veronica Nin,^{1,2} Tamar Pirtskhalava,¹ Claudia C.S. Chini,^{1,2} Tamar Tchkonja,¹ James L. Kirkland,¹ and Eduardo N. Chini^{1,2}



Deleted in Breast Cancer 1 Limits Adipose Tissue Fat Accumulation and Plays a Key Role in the Development of Metabolic Syndrome Phenotype

Q:1,2

Diabetes 2014;63:1–11 | DOI: 10.2337/db14-0192

Obesity is often regarded as the primary cause of metabolic syndrome. However, many lines of evidence suggest that obesity may develop as a protective mechanism against tissue damage during caloric surplus and that it is only when the maximum fat accumulation capacity is reached and fatty acid spillover occurs into peripheral tissues that metabolic diseases develop. In this regard, identifying the molecular mechanisms that modulate adipocyte fat accumulation and fatty acid spillover is imperative. Here we identify the deleted in breast cancer 1 (DBC1) protein as a key regulator of fat storage capacity of adipocytes. We found that knockout (KO) of DBC1 facilitated fat cell differentiation, lipid accumulation, and increased fat storage capacity of adipocytes in vitro and in vivo. This effect resulted in a “healthy obesity” phenotype. DBC1 KO mice fed a high-fat diet, although obese, remained insulin sensitive, had lower free fatty acid in plasma, were protected against atherosclerosis and liver steatosis, and lived longer. We propose that DBC1 is part of the molecular machinery that regulates fat storage capacity in adipocytes and participates in the “turn-off” switch that limits adipocyte fat accumulation and leads to fat spillover into peripheral tissues, leading to the deleterious effects of caloric surplus.

Metabolic syndrome constitutes a leading cause of death in the world (1). Several conditions, including type 2 diabetes, liver steatosis, cardiovascular disease, stroke,

dementia, and cancer, are believed to be modulated by the metabolic dysfunction encountered in metabolic syndrome (2). Obesity has been proposed to be a component or a risk factor for metabolic syndrome and many other human conditions. Fat tissue can be the largest organ in the body (3), and its function has a crucial role in the physiology of the entire organism (3).

Although obesity is commonly seen as a cause of metabolic dysfunction, experimental evidence supports the notion that, in the context of caloric surplus, individuals may be protected against the development of metabolic dysfunction as long as they maintain functional adipocyte fat storage capacity and low levels of fat tissue inflammation (4). Once fat storage capacity is surpassed or fat tissue becomes dysfunctional, fatty acid spillover occurs, leading to ectopic fat accumulation in peripheral tissues and lipotoxicity, and eventually, systemic metabolic disease (5,6). In fact, it has been proposed that obesity is protective against metabolic diseases until fat accumulation capacity is reached and fatty acid spillover begins (4,7). Several lines of evidence support this idea:

First, lipodystrophic humans and animals are highly susceptible to the development of insulin resistance, liver steatosis, and cardiac diseases (8,9).

Second, an increase in adipocyte storage capacity, such as overexpression of adiponectin in *ob/ob* mice and overexpression of PEPCK in fat tissue, leads to an increase in weight and fat gain under high-caloric feeding but

¹Kogod Aging Center, Mayo Clinic, Rochester, MN

²Department of Anesthesiology, Mayo Clinic, Rochester, MN

³Institut Pasteur Montevideo, Montevideo, Uruguay.

Corresponding author: Eduardo N. Chini, chini.eduardo@mayo.edu.

Received 3 February 2014 and accepted 17 July 2014.

This article contains Supplementary Data online at <http://diabetes.diabetesjournals.org/lookup/suppl/doi:10.2337/db14-0192/-/DC1>.

© 2014 by the American Diabetes Association. Readers may use this article as long as the work is properly cited, the use is educational and not for profit, and the work is not altered.

preservation of insulin sensitivity and metabolic health (10,11).

Finally, it has been observed in humans that obesity may be protective against metabolic syndrome as long as fat accumulation occurs preferentially in subcutaneous fat (12,13). In fact, fatty acid spillover had been shown to inversely correlate with obesity in diabetic subjects (7). Because adipocyte fat accumulation and obesity can delay the development of metabolic diseases, it is key to identify the molecular pathways that are involved in the “turn on-off” switch that limits adipose tissue fat storage capacity and can modulate fatty acid spillover and the development of metabolic dysfunction.

In recent years, we have been studying the role of the deleted in breast cancer-1 (DBC1) protein. DBC1 binds and regulates many nuclear proteins, including SIRT1 (14–16), HDAC3 (17), Rev-erb α (18), ER- α (19) and ER- β (20), BRCA1 (21), SUV39H1 (22), and IKK- β (23). We were the first to show that DBC1 is a SIRT1 inhibitor *in vivo* and that DBC1 plays a key role in metabolism (15). DBC1 knockout (KO) mice are protected against liver steatosis and nonalcoholic steatohepatitis (15). On the basis of our findings, we proposed that DBC1 might constitute a key regulator of metabolism during metabolic disorders.

Here we describe the role of DBC1 in the development of fat tissue dysfunction and the development of metabolic diseases during caloric surplus. We found that DBC1 KO mice become more obese than their wild-type (WT) litter mates when fed a high-fat diet. Interestingly, we found that despite being more obese, DBC1 KO mice had low free fatty acid (FFA) levels in blood, preserved insulin sensitivity, less atherosclerosis, less liver steatosis, and lived longer during high-fat diet feeding compared with their WT litter mates. Furthermore, we found preserved adipocyte fat storage capacity in DBC1 KO mice under caloric surplus. We propose that DBC1 modulates fat tissue function, fat accumulation, fatty acid spillover, and peripheral tissue damage. We propose that DBC1 is a key molecular component of the “on-off” switch that controls total adipocyte fat accumulation and fat tissue function and links obesity to its deleterious metabolic effects. Manipulation of this pathway may help prevent the negative effect of caloric surplus and obesity in health.

RESEARCH DESIGN AND METHODS

Reagents and Antibodies

Unless otherwise specified, all reagents and chemicals were purchased from Sigma-Aldrich. Antibodies purchased were SIRT1, vascular cell adhesion molecule (VCAM)-1, and activated caspase 3 (Cell Signaling Technology), PEPCK (Cayman Chemical Company), F4/80 (Abcam), DBC1 (Bethyl Laboratories), p53 and p21 (Santa Cruz Biotechnology, Inc.), and actin (Sigma-Aldrich). Human aortic endothelial cells and EGM2 culture media were purchased from Lonza.

Animal Handling and Experiments

The mice used in this study were females and were maintained in the Mayo Clinic Animal Breeding facility.

All experimental protocols were approved by the Mayo Clinic Institutional Animal Care and Use Committee. For the metabolic studies, mice were fed *ad libitum* a normal control diet (diet No. 3807; KLIBA-NAFAG), a high-fat diet (AIN-93G, modified to provide 60% of calories from fat; Dyets, Inc.), or a Western diet (TD.88137; 42% fat, 0.2% cholesterol; Harlan Laboratories). Body weight was recorded weekly. Food intake was measured for 7 consecutive days, with no difference detected between groups. Fat accumulation was measured by MRI (EcoMRI; EchoMedical Systems, Houston, TX) or by microcomputed tomography (micro-CT) scan (vivaCT40; SCANCO Medical, Zurich, Switzerland). For insulin tolerance testing, mice were food starved for 6 h before receiving a single intraperitoneal insulin injection (0.5 units/kg). Glycemia was measured from the tail vein. For survival experiments, mice were fed the normal chow diet until 6 months of age and were switched to the high-fat diet. Kaplan-Meier curves were generated using more than 20 mice per group. In all experiments, only litter mates were used.

PREADIPOCYTE CULTURE AND DIFFERENTIATION

Fat depots were removed under sterile conditions. Fat tissue was minced into fragments, digested with 1 mg/mL type II collagenase (Worthington Biochemical Corp.) for 60 min at 37°C, and filtered through a 100- μ m nylon mesh. After digestion, mature adipocytes were separated from stromal vascular cells by centrifugation at 1,000g for 10 min. The pellets were resuspended in α -minimum essential medium containing 10% calf serum and antibiotics. Cells were placed in a humidified incubator (3% oxygen). After 16 h, adherent preadipocytes were replated at a density of 5×10^4 cells/cm².

To induce differentiation, subconfluent preadipocytes were exposed to differentiation medium containing DMEM/F12, 10% FBS, 1 μ g/mL insulin, 250 nmol/L dexamethasone, 0.5 mmol/L isobutylmethylxanthine, and 2.5 μ mol/L rosiglitazone in 5% oxygen. After 48 h, all ingredients except insulin and FBS were removed from the medium. Cells were differentiated for 5–10 days.

Immunoprecipitation and Western Blotting

Mouse tissues and cultured cells were lysed in NETN buffer (20 mmol/L Tris-HCl, pH 8.0; 100 mmol/L NaCl; 1 mmol/L EDTA; and 0.5% NP-40) supplemented with 5 mmol/L NaF, 50 mmol/L 2-glycerophosphate, and a protease inhibitor cocktail (Roche Diagnostics). For each immunoprecipitation, 1 mg protein was used.

SIRT1 Activity Measurement

SIRT1 activity was measured from SIRT1 immunoprecipitates from tissue as previously described (15).

Atherosclerosis Model

Mice were fed the Western-style diet starting at 8 weeks of age. After 8–20 weeks of the diet, the aorta was dissected to the iliac bifurcation, opened longitudinally, and pinned in place on black wax. Lipid-rich regions were

Q:3

Q:4

stained with Oil Red O. Image analysis was performed using ImageJ software (National Institutes of Health). Lesion area was calculated for each animal as a percentage of the total aortic area, and the lesion number was expressed as plaques per aorta. All quantifications were performed blindly by independent personnel.

Ex Vivo Glycerol Production in Fat Tissue

The method used to measure glycerol production by adipose tissue in vitro was a modification of a method described by Vaughan (24). Inguinal fat pads (50–75 mg) were incubated for 2 h at 37°C in 3 mL Krebs-Ringer bicarbonate HEPES buffer (pH 7.4), containing 3% BSA (fatty acid-free) and 5 mmol/L pyruvate. Glycerol levels were analyzed in the medium before and after the incubation using a glycerol determination kit (Cayman Chemical Company). Glycerol production from external pyruvate was calculated by comparing glycerol levels in the media after 2 h incubation, with or without 5 mmol/L pyruvate, for each fat depot.

Determination of Metabolically Relevant Molecules in Plasma

The following molecules were assayed in plasma from mice after starvation for 6 h: triglycerides (Infinity; Thermo Scientific), cholesterol (CardioChek; Chek Diagnostics),

insulin (BD Biosciences), glycerol (Cayman Chemical Company), and adiponectin (R&D Biosystems).

Cell and Fat Tissue Coculture

Human aortic endothelial cells were plated with coverslips. The next day, inguinal fat tissue was dissected under sterile conditions. Tissue (1 g) was cut into small pieces and put in six-well plates. Tissue was incubated in the media before the cells were added. Coverslips with attached cells were placed into a ThinCert chamber (0.4- μ m pore size; Greiner Bio-One) and put inside the well with fat tissue. After overnight incubation, cells were fixed with 4% paraformaldehyde and further processed for standard immunofluorescence.

Statistics

Values are presented as mean \pm SEM of three to five experiments, unless otherwise indicated. The significance of differences between means was assessed by ANOVA or a two-tailed Student *t* test, as indicated. A *P* value of <0.05 was considered significant.

RESULTS

High-Fat Diet Promotes SIRT1-DBC1 Interaction and Decreases SIRT1 Activity in Fat Tissue

In previous work, we showed that DBC1 plays a key role in metabolism by regulating SIRT1 activity and function

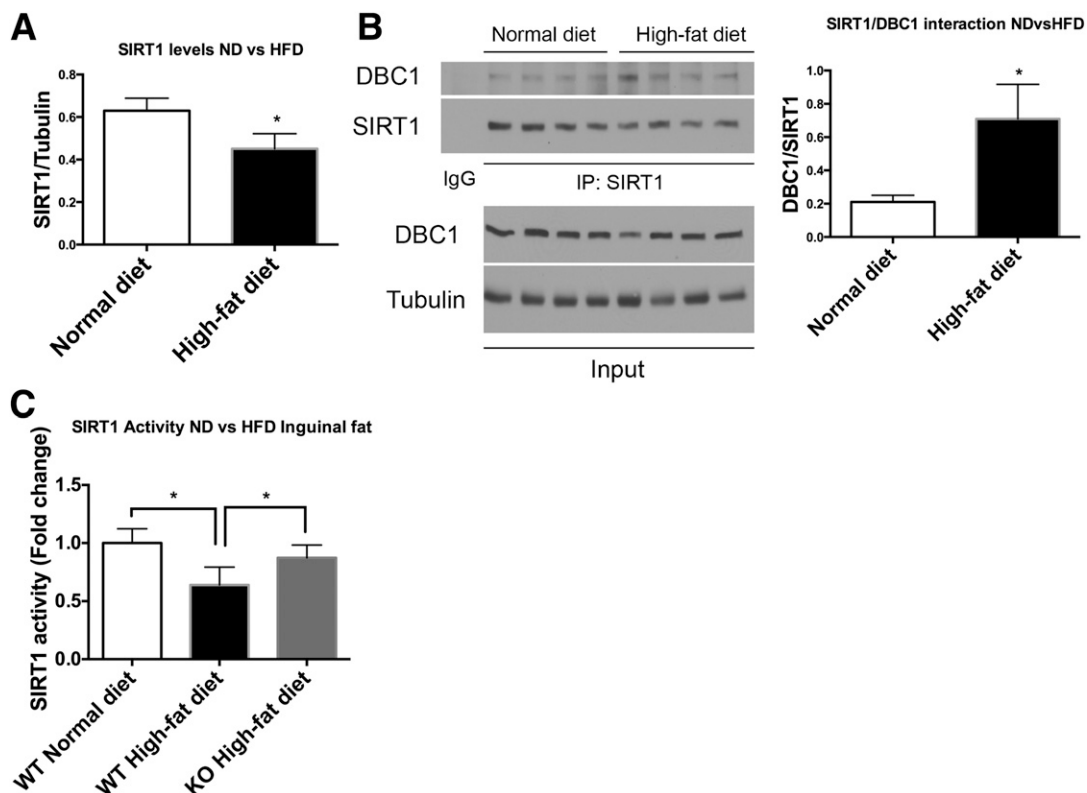


Figure 1—High-fat diet (HFD) feeding promotes SIRT1/DBC1 interaction and decreases SIRT1 activity in fat tissue. **A**: SIRT1 levels in inguinal fat tissue from 6-month-old mice fed the normal chow diet (ND) or the HFD for 20 weeks ($n = 5$ mice per group). $*P < 0.05$. **B**: Representative Western blot (left) of coimmunoprecipitation between SIRT1 and DBC1 in fat tissue from mice fed the ND or HFD, with each lane corresponding to a different mouse, and quantitation (right) of SIRT1/DBC1 interaction by densitometry ($n = 4$ mice per group). $*P < 0.05$. **C**: SIRT1 activity from immunoprecipitates of inguinal fat tissue in mice in fed the ND or HFD ($n = 5$ mice per group). $*P < 0.05$.

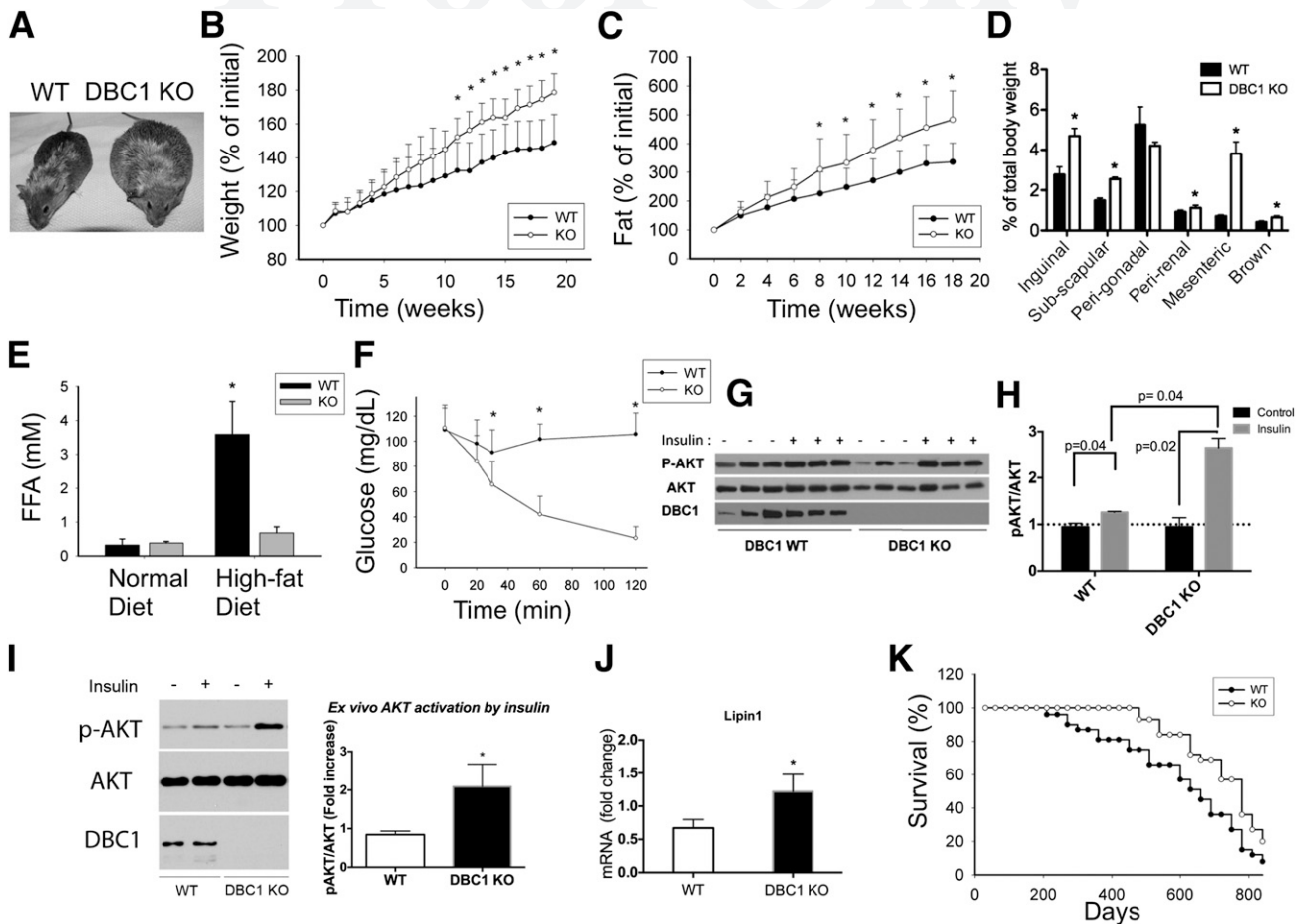


Figure 2—Deletion of DBC1 in vivo increases fat tissue accumulation capacity and prevents FFA spill over, protecting against insulin resistance. **A:** Representative photograph of WT (left) and DBC1 KO (right) siblings at 6 months of age and after 4 weeks of being fed the high-fat diet. **B:** Weight gain of WT and DBC1 KO mice fed the high-fat diet. The mice were switched from regular breeding chow to the high-fat diet starting at 6 months of age. Weight gain was monitored periodically during the treatment ($n = 16$ mice per group). $*P < 0.05$. **C:** Fat accumulation in the same mice described in **B**. Fat content in vivo was measured by MRI scanning ($n = 16$ mice per group). $*P < 0.05$. **D:** Quantification of different fat depots in WT and DBC1 KO mice after being fed the high-fat diet for 12 weeks. Fat tissue weight was expressed, corrected by total body weight ($n = 5$ mice per group). $*P < 0.05$. **E:** FFA levels in blood in WT and DBC1 KO adult mice fed regular breeding chow or after 12 weeks of the high-fat diet ($n = 8$ mice per group). $*P < 0.05$. **F:** Insulin tolerance test in WT and DBC1 mice fed the high-fat diet for 12 weeks. After 6 h of food starvation, mice were challenged with 0.5 units/kg of intraperitoneal insulin, and glycemia was monitored over time ($n = 8$ mice per group). $*P < 0.05$. **G:** Western blot shows phosphorylation of AKT (p-AKT) in inguinal fat tissue after WT and DBC1 KO mice fed the high-fat diet were challenged with 0.5 units/kg insulin for 15 min. **H:** Band intensity was measured by densitometry and expressed as the ratio of p-AKT to total AKT. **I:** Ex vivo insulin sensitivity in fat tissue from WT and DBC1 KO mice after 12 weeks of being fed the high-fat diet. Inguinal fat was incubated in Krebs-Ringer buffer with 5 mU/L insulin for 15 min. Tissue was later processed for Western blotting. *Left*, Representative Western blot of p-AKT after incubation with insulin. *Right*, Quantitation of p-AKT after insulin treatment expressed as the fold increase over control (no treatment) ($n = 5$ mice per group). $*P < 0.05$. **J:** Expression of lipin1 mRNA in inguinal fat tissue of WT and DBC1 KO after 12 weeks of the high-fat diet ($n = 4$). $*P < 0.05$. **K:** Survival curve of WT and DBC1 KO mice fed standard chow until 6 months of age and then fed the high-fat diet ($n = 22$ mice per group).

(15) and further found that a high-fat diet promotes SIRT1-DBC1 interaction and decreases SIRT1 activity in the liver. Here, we investigated whether DBC1 plays an active role in adipocyte and fat tissue function. We found that the high-fat diet leads to a decrease in SIRT1 expression in fat tissue (Fig. 1A) and that the data are consistent with previously published data (25). Interestingly, we found an increase in SIRT1 binding to DBC1 during the high-fat diet (Fig. 1B), with a consequent decrease in SIRT1 activity (Fig. 1C). The decrease in SIRT1 activity

in the fat tissue induced by the high-fat diet was prevented by deletion of DBC1 (Fig. 1C). These results suggested to us that DBC1 regulates SIRT1 activity in fat tissue during fat and caloric surplus and that DBC1 KO mice may be protected against fat tissue dysfunction induced by caloric surplus. Our findings that SIRT1 regulation by DBC1 during obesity may not be reflected during aging is worth noting: the expression of both SIRT1 and DBC1 decreases (Supplementary Fig. 1A) during aging, suggesting a different mechanism of regulation.

DBC1 KO In Vivo Promotes Increases in Adipocyte Fat Accumulation Capacity, Prevents FFA Spillover, and Protects Against Insulin Resistance

We fed adult WT and DBC1 KO female mice the high-fat diet for 20 weeks and observed that the DBC1 KO mice gained more weight than their WT litter mates. This trend was constant during the entire duration of the study and became statistically significant after 12 weeks of the high-fat diet (Fig. 2A and B). We observed the same trend when we measured fat accumulation by MRI (Fig. 2C). The post-mortem analysis of different fat depots showed a significant increase in inguinal, subscapular, mesenteric, perirenal, and brown fat (Fig. 2D). There were no significant changes in the total amount of perigonadal fat between WT and DBC1 KO mice when corrected by total body weight (Fig. 2D). Interestingly, we found that despite being more obese, DBC1 KO mice fed the high-fat diet had FFA levels that resembled those measured in mice fed the normal chow diet (Fig. 2E) and that they were also protected against fatty liver disease (Supplementary Fig. 1B). This was paralleled by protection against insulin resistance. We found that DBC1 KO mice were more sensitive to an insulin challenge by performing insulin tolerance test (Fig. 2F) and that AKT phosphorylation was increased in fat tissue in vivo after the mice were challenged with a dose of insulin (Figs. 2G and H). Also, AKT phosphorylation was increased in skeletal muscle in DBC1 KO mice (Supplementary Fig. 2A). Moreover, we found that DBC1 deletion preserves insulin sensitivity in fat by an ex vivo challenge with insulin (Fig. 2I), suggesting that DBC1 KO mice were preserving insulin sensitivity by preventing fat tissue dysfunction. Consistent with the increased fat accumulation and protection against insulin resistance, we found that lipin1 mRNA levels were increased in fat tissue from DBC1 KO mice (Fig. 2J). Lipin1 promotes fatty acid esterification, and its expression has been linked to insulin sensitivity and healthy fat accumulation in mice and humans (26,27).

We also monitored the longevity of WT and DBC1 KO mice fed the high-fat diet starting at 6 months of age and found that the DBC1 mice had an increased median life span, although the maximal life span was not significantly extended (Fig. 2K). Worth noticing, we found that increased fat accumulation and protection against fatty acid spillover was not restricted to mice fed the high-fat diet but also happened in old adult mice fed the normal chow diet their entire life. DBC1 KO mice that were 14 months old were heavier (Fig. 3A), had increased whole-body fat content (Fig. 3B), decreased FFA in plasma (Fig. 3C), and lower glucose levels in plasma (Fig. 3D) than their WT litter mates.

DBC1 KO Improves Fat Differentiation Capacity in Preadipocytes From Mice During Normal and High-Fat Diet Feeding

Next, we investigated if KO of DBC1 increases the fat differentiation potential of preadipocytes in mice. We purified and cultured preadipocytes from WT and DBC1

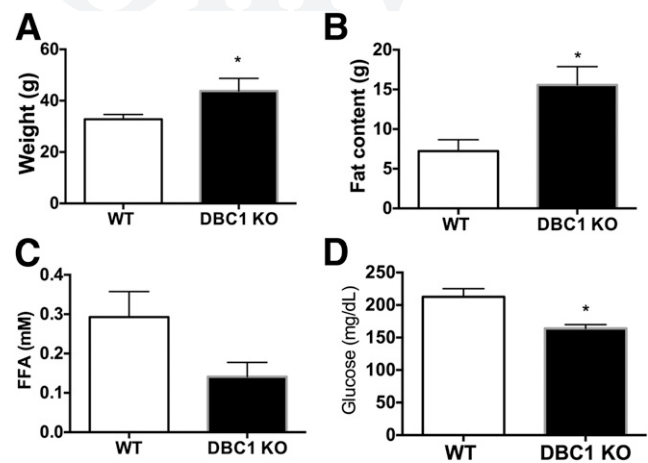


Figure 3—Deletion of DBC1 in vivo also prevents FFA spillover in old mice fed the normal chow diet. Weight (A), total body fat content measured by MRI (B), FFA in plasma (C), and glycemia (D) in 14-month-old mice fed the normal chow diet their entire life ($n = 4$ mice per group). * $P < 0.05$.

KO mice and found that DBC1 KO increases the differentiation potential of preadipocytes (Fig. 4A). Interestingly, this potential was also preserved during obesity. DBC1 KO increased the differentiation capacity in primary preadipocytes purified from the inguinal fat depot (Fig. 4B and C) and also from the epididymal fat depot (Fig. 4B and D) after 20 weeks of high-fat diet feeding. DBC1 KO in mice facilitates fat accumulation in fat tissue during obesity, which correlates with decreased FFA levels in plasma (Fig. 2). Because an increase in fat accumulation capacity could arise from increased lipid synthesis and esterification or from decreased lipolysis, we checked for lipolysis in vitro. Neither the main lipases (adipose triglyceride lipase and hormone-sensitive lipase) nor caveolin 1, another protein involved in lipolysis, were expressed differentially between WT and DBC1 KO differentiated adipocytes (Fig. 4E). Furthermore, we measured in vitro lipolysis in response to isobutylmethylxanthine in differentiated adipocytes and found no difference between WT and DBC1 KO cells (Fig. 4F).

ApoE^{-/-} DBC1^{-/-} Mice Have Increased Adipocyte Fat Accumulation Capacity and Decreased Inflammation in Fat Tissue

Cardiovascular diseases constitute the leading cause of death in adults, and there is a strong correlation between fat tissue dysfunction and cardiovascular morbidity. We investigated whether increased adipocyte fat storage capacity and a decrease in fatty acid spillover observed in the DBC1 KO mice could protect against cardiovascular dysfunction. For this, we crossed DBC1 KO mice with ApoE KO mice, to generate DBC1^{+/+}ApoE^{-/-} and DBC1^{-/-}ApoE^{-/-} mice. Pups from the different genotypes were obtained at Mendelian ratios, and there were no obvious phenotypic differences between genotypes. The ApoE KO mice are of particular value for these experiments because the atherosclerotic

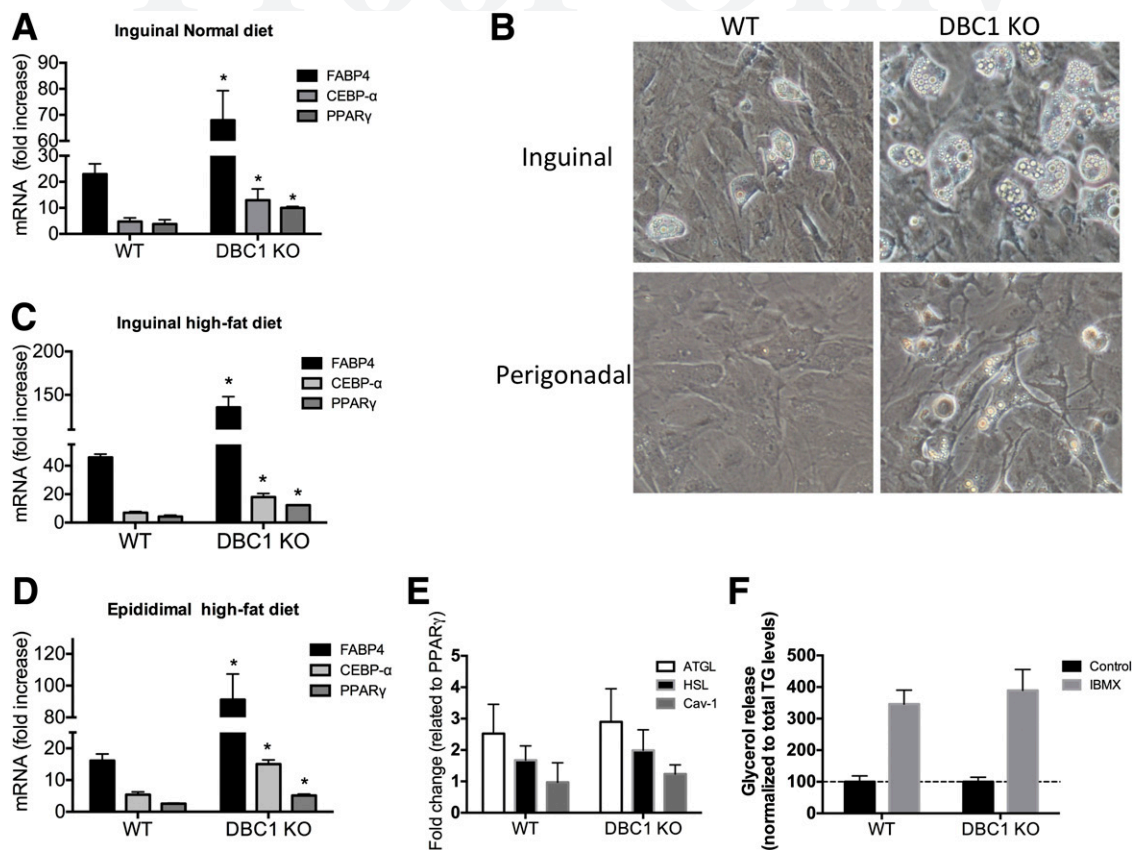


Figure 4—DBC1 KO increases fat differentiation capacity in preadipocytes isolated from mice fed the normal or high-fat diet. **A:** Gene expression analysis of adipogenesis markers by RT-PCR in inguinal preadipocytes isolated from mice fed the normal diet and after 5 days of differentiation ($n = 4$ mice per condition). $*P < 0.05$, t test. **B:** Representative image of differentiated primary adipocytes obtained from inguinal (upper panels) and perigonadal (lower panels) fat depots from WT and DBC1 KO mice. Cells were allowed to differentiate for 5 days after the addition of differentiation media. Gene expression analysis of adipogenesis markers by RT-PCR in inguinal (C) and perigonadal (D) mouse preadipocytes isolated from mice fed the high-fat diet and after 5 days of differentiation ($n = 4$ mice per condition). $*P < 0.05$, t test. **E:** Gene expression analysis of lipolysis markers by RT-PCR in inguinal mouse preadipocytes isolated from mice and after 5 days of differentiation. Results were normalized to peroxisome proliferator-activated receptor- γ (PPAR- γ) expression to correct for the difference in differentiation potential. **F:** In vitro lipolysis stimulated by isobutylmethylxanthine (IBMX; 100 $\mu\text{mol/L}$) in differentiated adipocytes from WT and DBC1 KO mice. Cells were incubated with IBMX or vehicle for 6 h. Glycerol content was determined from the cell culture media. Results were normalized to the total triglycerides (TG) content in the plate. (A high-quality color representation of this figure is available in the online issue.)

phenotype is modulated by adipocyte function in these animals (28,29). At the age of 8 weeks, female mice were challenged with a Western diet (42% fat and 0.2% cholesterol) for 20 weeks to induce atherosclerosis. We found that ApoE^{-/-}DBC1^{-/-} mice behaved very similar to what we had previously observed for DBC1 KO mice in fat accumulation and weight gain when fed the Western diet. In fact, the difference in weight and fat gain was even more striking between ApoE^{-/-}DBC1^{+/+} and ApoE^{-/-}DBC1^{-/-} mice (Figs. 5A), probably because ApoE^{-/-} is required for fat cell differentiation (30). We performed micro-CT scans in the mice after 20 weeks of the Western diet and observed increased fat content in different fat depots, including subcutaneous, abdominal, and visceral (Fig. 5B). We found that ApoE^{-/-}DBC1^{-/-} mice have decreased $\dot{V}O_2$, $\dot{V}CO_2$, and energy expenditure than the ApoE^{-/-}DBC1^{+/+} mice when fed the high-fat diet, consistent with the difference in weight (Supplementary

Fig. 3). We did not detect any significant difference in cholesterol, triglycerides, or insulin levels after 20 weeks of the Western diet (Table 1). However, adiponectin levels were significantly higher in the ApoE^{-/-}DBC1^{-/-} mice (Table 1).

Histological analysis of perigonadal and inguinal fat depots dissected from ApoE^{-/-}DBC1^{+/+} and ApoE^{-/-}DBC1^{-/-} mice after 20 weeks of being fed the Western diet showed a clear and significant difference in adipocyte cell size, with cells coming from ApoE^{-/-}DBC1^{-/-} between 3- and 10-times larger than those analyzed from control mice (Fig. 5C and D). We hypothesized that increased FFA esterification capacity in fat cells in the absence of DBC1 explained the increased fat cell size. To be able to accumulate more fatty acids, fat cells have to esterify them into triglycerides, and for that, glycerol must be available. We performed an ex vivo experiment where pieces of inguinal fat tissue were incubated with pyruvate,

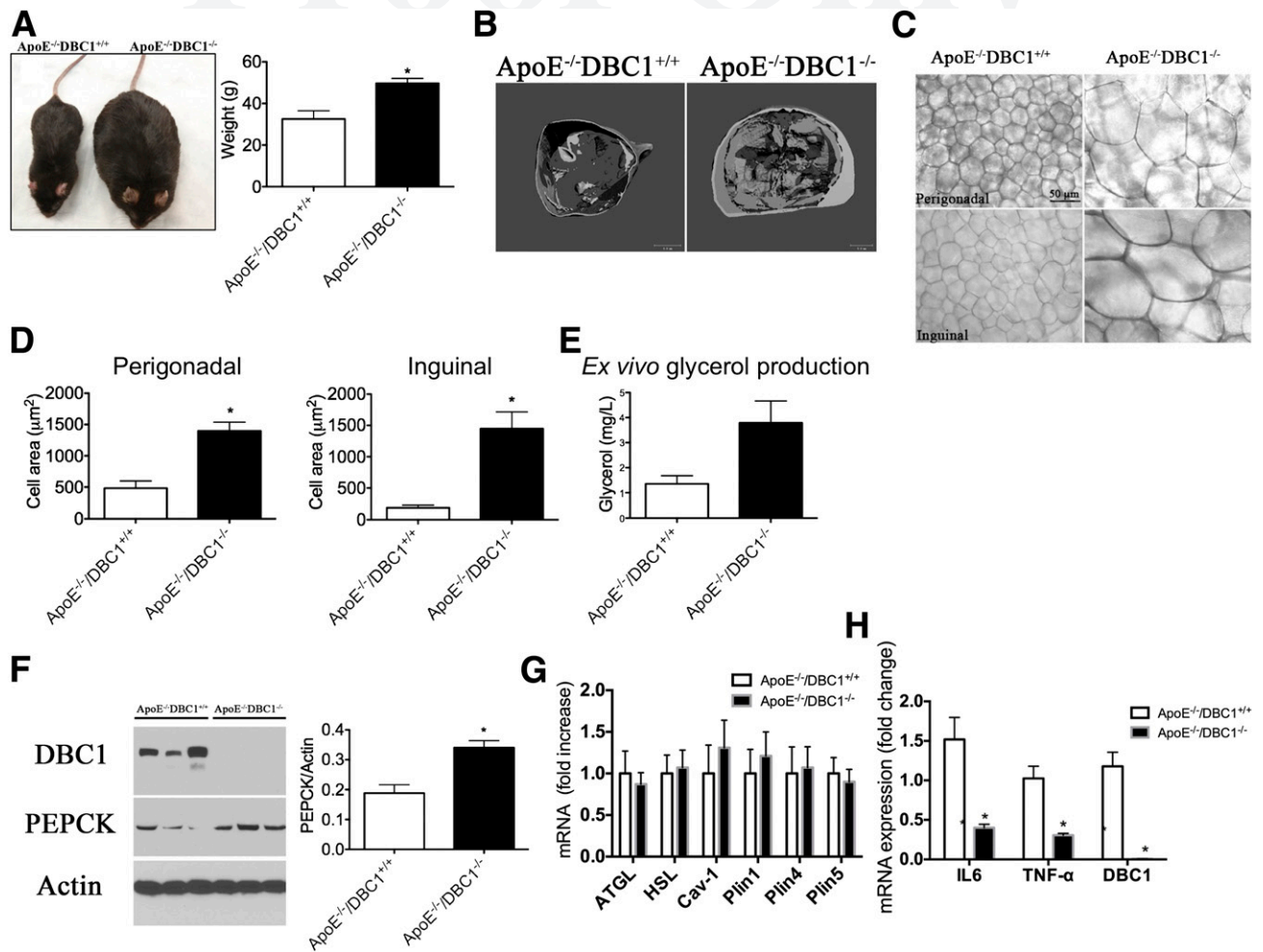


Figure 5— $ApoE^{-/-} DBC1^{-/-}$ mice have increased fat accumulation capacity and decreased inflammation in fat tissue. **A**: *Left*, Representative photograph of $ApoE^{-/-} DBC1^{+/+}$ (left side) and $ApoE^{-/-} DBC1^{-/-}$ (right side) mice after 20 weeks of being fed the Western diet. *Right*, Weight of $ApoE^{-/-} DBC1^{+/+}$ and $ApoE^{-/-} DBC1^{-/-}$ mice at the end of the treatment with the Western diet ($n = 8$ per group). *Shows significant difference at $P < 0.05$, t test. **B**: Representative CT scan shows fat tissue content and distribution of adult $ApoE^{-/-} DBC1^{+/+}$ and $ApoE^{-/-} DBC1^{-/-}$ mice after 20 weeks of being fed the Western diet. **C**: Representative picture of fat cell size in perigonadal (upper panels) and inguinal (lower panels) fat depots dissected from $ApoE^{-/-} DBC1^{+/+}$ and $ApoE^{-/-} DBC1^{-/-}$ mice after 20 weeks of being fed the Western Diet. **D**: Fat cell size measurement in perigonadal (left) and inguinal (right) fat tissue depots of $ApoE^{-/-} DBC1^{+/+}$ and $ApoE^{-/-} DBC1^{-/-}$ mice after 20 weeks of being fed the Western diet ($n = 3$ per group). *Shows significant difference at $P < 0.05$, t test. **E**: Ex vivo glycerol production and release from inguinal fat tissue in response to pyruvate in mice after 5 weeks of being fed the Western diet ($n = 5$ per group). *Shows significant difference at $P < 0.05$, t test. **F**: PEPCK expression in the same mice and conditions described in **D** ($n = 3$ per group). *Shows significant difference at $P < 0.05$, t test. **G**: Gene expression analysis of lipolysis markers in inguinal fat tissue of $ApoE^{-/-} DBC1^{+/+}$ and $ApoE^{-/-} DBC1^{-/-}$ mice after 20 weeks of being fed the high-fat diet ($n = 6$ per group). **H**: Gene expression analysis of inflammation markers in inguinal fat tissue of $ApoE^{-/-} DBC1^{+/+}$ and $ApoE^{-/-} DBC1^{-/-}$ after 20 weeks of being fed the high-fat diet ($n = 5$ per group). *Shows significant difference at $P < 0.05$, t test. (A high-quality color representation of this figure is available in the online issue.)

and the production of glycerol (glyceroneogenesis) was measured. We found that fat tissue from $ApoE^{-/-} DBC1^{-/-}$ mice had increased glyceroneogenesis capacity (Fig. 5E). Increased glyceroneogenesis was paralleled by increased expression of PEPCK (Fig. 5F), a key enzyme in this pathway. In fact, we previously described that DBC1 regulates gluconeogenesis and PEPCK expression in the liver (31). Interestingly, fat-specific overexpression of PEPCK promotes obesity and fat accumulation but also confers protection against insulin resistance (11), which is in agreement with our findings.

In agreement with our findings in cells in culture we found no difference in the lipolysis markers adipose triglyceride lipase, hormone-sensitive lipase, and caveolin 1 between $ApoE^{-/-} DBC1^{+/+}$ and $ApoE^{-/-} DBC1^{-/-}$ mice in adipose tissue (Fig. 5G). We also analyzed the expression of the lipid droplets-coating proteins perilipin 1, 4, and 5 and found no difference in their expression levels between $ApoE^{-/-} DBC1^{+/+}$ and $ApoE^{-/-} DBC1^{-/-}$ mice (Fig. 5G). Finally, we found that increased fat storage capacity led to decreased expression of inflammation markers in fat tissue (Fig. 5H). The expression of tumor

Q:11

Table 1—Triglycerides, insulin, adiponectin, and cholesterol levels in the plasma of ApoE^{-/-}DBC1^{+/+} and ApoE^{-/-}DBC1^{-/-} mice after 20 weeks of being fed the high-fat diet

	ApoE ^{-/-} DBC1 ^{+/+}		ApoE ^{-/-} DBC1 ^{-/-}	
	Average	SEM	Average	SEM
Cholesterol (mg/dL)	500		500	
Triglycerides (mg/dL)	776	213	784	150
Glycerol (mg/L)	56.8	9.3	80.3	12.0
Adiponectin (mg/L)*	9.84	0.42	14.63	0.92
Insulin (ng/mL)	0.16	0.05	0.40	0.13

*Shows significant difference, $P < 0.05$, t test ($n = 8$ per group).

necrosis factor- α and interleukin-6, two key inflammatory molecules involved in tissue dysfunction during obesity, was decreased in inguinal fat after the high-fat diet (Fig. 5H).

DBC1 KO Protects Mice Against Aortic Atherosclerosis, Inflammation, and Cellular and Tissue Damage

Finally, we determined the role of DBC1 in the development of atherosclerosis. We analyzed dissected aortas from ApoE^{-/-}DBC1^{+/+} and ApoE^{-/-}DBC1^{-/-} mice after 20 weeks of being fed the Western diet. Oil Red O staining of whole-mount aortas (Fig. 6A) showed a significant decrease in the total number of plaque formation (Fig. 6B) and in the total area with plaques (Fig. 6B) in ApoE^{-/-}DBC1^{-/-} compared with ApoE^{-/-}DBC1^{+/+} mice. We found a significant downregulation in the expression of several inflammation and damage markers at the mRNA level in the aortas of the ApoE^{-/-}DBC1^{-/-} compared with the ApoE^{-/-}DBC1^{+/+} mice. In particular, expression of p53, p21, p65, and MCP-1 were decreased in ApoE^{-/-}DBC1^{-/-} mice (Fig. 6C). Also, Western blot analysis from whole aortas showed decreased expression of markers of inflammation and tissue dysfunction such as VCAM-1, p53, and F4/80 (Fig. 6D). One of the early events in the development of atherosclerosis is the development of endothelial dysfunction (32). It has been proposed that FFAs play a role in the development of endothelial dysfunction and can cause endothelial apoptosis and endothelial insulin resistance (33).

To further investigate the mechanism by which DBC1 regulates the development of metabolic syndrome, we determine if prevention of fatty acid spillover induced by DBC1 KO protects against peripheral cell and tissue damage. In this regard, we performed coculture experiments with fat tissue and aortic endothelial cells in the presence of FFAs. Overnight incubation of aortic endothelial cells with 500 $\mu\text{mol/L}$ palmitate in the presence of inguinal fat obtained from ApoE^{-/-}DBC1^{+/+} mice led to cytotoxicity in endothelial cells and resulted in apoptosis. However, when the cells were cocultured with fat tissue obtained from ApoE^{-/-}DBC1^{+/+}, apoptosis in endothelial cells was significantly decreased (Fig. 6E and F). At the end of the experiment, we measured FFA levels in the

media and found that in the presence of fat coming from ApoE^{-/-}DBC1^{-/-} mice, FFA levels in the media were decreased, likely due to the increased fat buffering capacity from DBC1 KO adipocytes (Fig. 6G). In fact, as seen in our other experiments, ApoE^{-/-}DBC1^{-/-} mice also showed decreased FFA levels in plasma compared with ApoE^{-/-}DBC1^{+/+} controls (Fig. 6H). Taken together, our results indicate that DBC1 modulates fat tissue function, fatty acid spillover, and the development of features of metabolic syndrome.

DISCUSSION

Obesity-related systemic dysfunction, such as inflammation, insulin resistance, type 2 diabetes, liver steatosis, cardiovascular disease, and stroke, are among the leading causes of death in adults in Western countries (1), and only in the U.S. does obesity affect 35.7% of adults (1). Thus, understanding how obesity leads to tissue dysfunction is of key importance to the development of new therapeutic approaches.

Our work shows that DBC1 KO female mice are significantly more obese than their WT litter mates but remain “healthier” under a normal diet and also under diet-induced obesity. We propose that during obesity, metabolic diseases arise, at least in part, as a consequence of saturation of the storage capacity in fat tissue and spillover of fatty acids to the media, and we provide a new molecular pathway that links fat tissue dysfunction to metabolic syndrome. It is important to highlight that the phenotype of “healthy obesity” described in this work happens primarily in female adult mice but not in males. In fact, although male DBC1 KO mice tend to gain more weight than their WT litter mates, they do not differ in their insulin sensitivity when they are fed a high-fat diet, as we recently showed (31). This is an interesting point, because the “healthy obesity” phenotype observed in humans when there is increased subcutaneous fat deposition has been shown to happen primarily in women (34).

We recently showed that deletion of DBC1 protects against cellular senescence in adipose tissue during obesity (35). In fact, the absence of cellular senescence in DBC1 KO mice can be seen as another characteristic of the “healthy obesity” phenotype that we describe here, because it has been shown that obesity leads to an increase in cellular senescence in obese subjects (3). It would be interesting to determine whether individuals that display a healthy obesity phenotype also have protection against cellular senescence and also to determine whether there is any kind of change in the expression of DBC1 in these individuals. Our recent work also shows that the role of DBC1 in the regulation of cellular senescence in fat tissue might be restricted to high-caloric loads and not to aging, because we failed to see changes in senescence between WT and DBC1 KO during aging (35), although we could only study the mice until 18 months of age, and differences between mice might arise later in life.

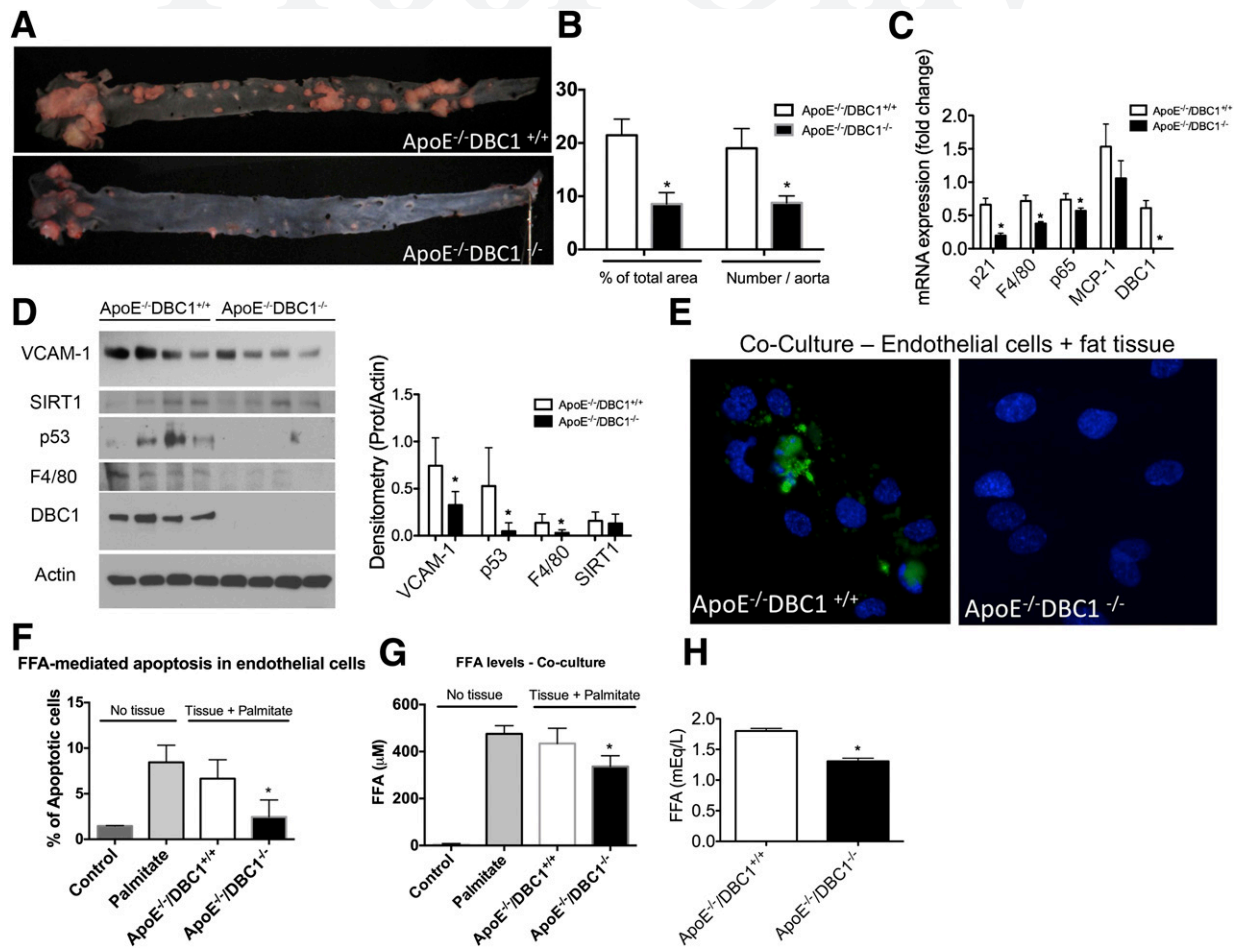


Figure 6—DBC1 KO protects against aortic atherosclerosis, inflammation, and cellular and tissue damage. **A**: Oil Red O staining of dissected aorta from ApoE^{-/-}DBC1^{+/+} (upper panel) and ApoE^{-/-}DBC1^{-/-} mice (lower panel) after 20 weeks of being fed the Western diet. **B**: Quantitation of the number of lesions and the total area with lesions described in **A** (n = 5 per group). *Shows significant difference at P < 0.05, t test. **C**: mRNA expression in whole aorta from ApoE^{-/-}DBC1^{+/+} and ApoE^{-/-}DBC1^{-/-} mice after 20 weeks of being fed the Western diet (n = 5 per group). *Shows significant difference at P < 0.05, t test. **D**: Left, Western blots from whole aortas dissected from ApoE^{-/-}DBC1^{+/+} and ApoE^{-/-}DBC1^{-/-} mice after 20 weeks of being fed the Western diet. Right, Quantitation of band intensity by densitometry (n = 4 per group). *Shows significant difference at P < 0.05, t test. **E**–**G**: Coculture of human aorta endothelial cells (HAEC) with ApoE^{-/-}DBC1^{-/-} fat depot results in protection against palmitate-induced cellular apoptosis. Inguinal fat depots were dissected from ApoE^{-/-}DBC1^{+/+} and ApoE^{-/-}DBC1^{-/-} mice and incubated in media containing 500 μmol/L sodium palmitate. HAEC cells were added to the media after 8 h, and cells and tissue were incubated together overnight. **E**: Representative image of caspase-3 activation (green label) after treatment with palmitate overnight in the presence of fat tissue. DAPI (blue label) was used for total cell number quantitation. **F**: The percentage of caspase-3-positive cells (i.e., apoptotic cells) in each condition was calculated by comparing the number of caspase-3-positive cells with the total number of cells. **G**: After the treatment, FFA levels in the media were measured (n = 3 per group). *Shows significant difference at P < 0.05, t test. **H**: FFA levels in plasma in ApoE^{-/-}DBC1^{+/+} and ApoE^{-/-}DBC1^{-/-} mice after 20 weeks of being fed the high-fat diet (n = 8 per group). *Shows significant difference at P < 0.05, t test.

In previous work we showed that DBC1 KO mice were protected against high-fat diet-induced liver steatosis by a molecular mechanism that involves SIRT1 activation in the liver (15). Our new findings suggest that protection against liver steatosis in the absence of DBC1 may be a consequence of intrinsic protection against fat deposition in the liver but also as a bystander effect of decreased FFA in plasma mediated by increased adipocyte storage capacity. Although we cannot rule out the possibility that other molecular targets of DBC1 besides SIRT1 are playing a role in the final phenotype observed, we found that DBC1 KO mice preserve SIRT1 activity during high-fat

diet-induced obesity. The role of SIRT1 in fat tissue development and function is still not completely clear. Some investigators have found that SIRT1 activation decreases body weight and fat tissue content (25,36), whereas others showed no significant effect in weight gain when mice were fed a high-fat diet (37). On the contrary, loss of function of SIRT1 decreases body weight and fat tissue content in mice fed a high-fat diet (38).

Regardless, whether the main molecular target of DBC1 in fat is SIRT1, we believe the DBC1 protein is part of a molecular switch that limits fat storage capacity, which in a chronic situation, will lead to fat tissue

damage, lipotoxicity, and peripheral tissue dysfunction. This will eventually lead to the development of type 2 diabetes, fatty liver disease, and cardiovascular diseases. Previous findings also support the idea that prevention of fatty acid spillover disconnects obesity from its deleterious effects. The transgenic mice that overexpress the hormone adiponectin on an *ob/ob* background show a similar phenotype as the DBC1 KO mice because they become more obese but preserve insulin sensitivity and show low levels of FFA in plasma (10). The antidiabetic drug rosiglitazone has metabolic effects that resemble the phenotype of DBC1 deletion. Rosiglitazone, a peroxisome proliferator-activated receptor- γ agonist, increases insulin sensitivity and lowers FFA levels and glycemia in animal models and in patients, although it also promotes weight gain through increased fat accumulation (39,40). Interestingly, it has been shown that DBC1 KO mice show phenotypic similarities with peroxisome proliferator-activated receptor- γ activation (41). Finally, mice that overexpress PEPCK specifically in fat tissue also show increased obesity due to fat accumulation but protection against insulin resistance (11). In agreement with this, we recently showed that DBC1 controls PEPCK expression by a mechanism that is dependent on SIRT1 (31). We found that DBC1 KO mice showed increased PEPCK expression in the liver, similar to what we show here for fat tissue, and as result of that, they have increased gluconeogenesis (31).

Our work brings a new insight into the link between obesity and metabolic diseases and provides a molecular mechanism that involves control of fat storage capacity and as a probable cause for the onset of metabolic syndrome. We propose that DBC1 acts as part of a molecular switch to stop fat accumulation in fat tissue, probably by regulating fat tissue inflammation, preadipocyte differentiation capacity, and also fatty acid esterification capacity in adipocytes. Pinpointing the exact molecular mechanism involved in the effect of DBC1 on fat tissue function is the goal of future work being conducted by our laboratory. Interestingly, the evolutionary role of an active molecular switch that prevents fat accumulation and leads to fatty acid spillover and the development of metabolic syndrome seems puzzling at first. However, we speculate that the main role of the DBC1-mediated fat tissue dysfunction and decrease in adipocyte storage capacity is to prevent the development of the “morbidly obese” phenotype that in the short-term would impair physical fitness in the wild. In contrast, the development of metabolic syndrome induced by the DBC1-mediated switch would cause health problems only much later in life.

In conclusion, there is growing evidence that supports the notion that obesity-driven metabolic diseases develop as a consequence of saturation of fat storage capacity in fat tissue. In the context of a high-caloric diet, obesity may act as a protective mechanism against diseases until fat tissue capacity is overloaded. Understanding the pathways that are involved in load capacity of fat tissue may provide new venues to treat obesity-driven metabolic

diseases. Our work establishes a molecular connection between fat load capacity in fat tissue and metabolic peripheral tissue damage. The relative contribution to the different pathways regulated by DBC1 to the overall phenotype found will be the subject of future investigation and may provide new ways for intervention against deleterious effects of obesity.

Acknowledgments. The authors thank Dr. Thomas A. White and Glenda Q:7 12 Evans for technical assistance with microCT scan.

Funding Support. This work was supported mainly by National Institutes of Health (National Institute of Diabetes and Digestive and Kidney Diseases) grant DK-084055 (E.N.C.). Support was also from National Institutes of Health (National Institute on Aging) grants AG-41122 and AG-13925 (J.L.K.), American Heart Association Post-doctoral Fellowship 11POST7320060, and Agencia Nacional de Investigación e Innovación (DCI-ALA/2011/023-502 “Contrato de apoyo a las políticas de innovación y cohesión territorial”) (C.E.).

Duality of Interest. No potential conflicts of interest relevant to this article were reported.

Author Contributions. C.E. planned the experimental strategy and executed most of the experiments. V.N. participated in the in vivo experiments and quantified all of the atherosclerotic lesions. T.P. participated in culture and differentiation of preadipocytes and fat depot isolation. C.C.S.C. participated in cell culture experiments, insulin sensitivity (AKT phosphorylation), and strategy design. T.T. and J.L.K. provided expertise in the adipocyte tissue experiments. C.E., T.T., J.L.K., and E.N.C. wrote the manuscript. E.N.C. conceptualized the main hypothesis of the study, planned the experimental strategy, and performed fat tissue isolation and some in vivo insulin sensitivity assessments. E.N.C. is the guarantor of this work and, as such, had full access to all the data in the study and takes responsibility for the integrity of the data and the accuracy of the data analysis. Q:8

References

1. Flegal KM, Graubard BI, Williamson DF, Gail MH. Cause-specific excess deaths associated with underweight, overweight, and obesity. *JAMA* 2007;298:2028–2037
2. National Institutes of Health (NIH) U. *Strategic Plan for NIH Obesity Research*. Bethesda, National Institutes of Health, 2004. Q:9
3. Tchkonina T, Morbeck DE, Von Zglinicki T, et al. Fat tissue, aging, and cellular senescence. *Aging Cell* 2010;9:667–684
4. Unger RH, Scherer PE. Gluttony, sloth and the metabolic syndrome: a roadmap to lipotoxicity. *Trends Endocrinol Metab* 2010;21:345–352
5. Wang MY, Grayburn P, Chen S, Ravazzola M, Orci L, Unger RH. Adipogenic capacity and the susceptibility to type 2 diabetes and metabolic syndrome. *Proc Natl Acad Sci U S A* 2008;105:6139–6144
6. Listenberger LL, Han X, Lewis SE, et al. Triglyceride accumulation protects against fatty acid-induced lipotoxicity. *Proc Natl Acad Sci U S A* 2003;100:3077–3082
7. Almandoz JP, Singh E, Howell LA, et al. Spillover of Fatty acids during dietary fat storage in type 2 diabetes: relationship to body fat depots and effects of weight loss. *Diabetes* 2013;62:1897–1903
8. Asterholm IW, Halberg N, Scherer PE. Mouse models of lipodystrophy key reagents for the understanding of the metabolic syndrome. *Drug Discov Today Dis Models* 2007;4:17–24
9. Savage DB. Mouse models of inherited lipodystrophy. *Dis Model Mech* 2009;2:554–562
10. Kim JY, van de Wall E, Laplante M, et al. Obesity-associated improvements in metabolic profile through expansion of adipose tissue. *J Clin Invest* 2007;117:2621–2637
11. Franckhauser S, Muñoz S, Pujol A, et al. Increased fatty acid re-esterification by PEPCK overexpression in adipose tissue leads to obesity without insulin resistance. *Diabetes* 2002;51:624–630

12. Wildman RP. Healthy obesity. *Curr Opin Clin Nutr Metab Care* 2009;12:438–443
13. Naukkarinen J, Heinonen S, Hakkarainen A, et al. Characterising metabolically healthy obesity in weight-discordant monozygotic twins. *Diabetologia* 2014;57:167–176
14. Kim JE, Chen J, Lou Z. DBC1 is a negative regulator of SIRT1. *Nature* 2008;451:583–586
15. Escande C, Chini CC, Nin V, et al. Deleted in breast cancer-1 regulates SIRT1 activity and contributes to high-fat diet-induced liver steatosis in mice. *J Clin Invest* 2010;120:545–558
16. Zhao W, Kruse JP, Tang Y, Jung SY, Qin J, Gu W. Negative regulation of the deacetylase SIRT1 by DBC1. *Nature* 2008;451:587–590
17. Chini CC, Escande C, Nin V, Chini EN. HDAC3 is negatively regulated by the nuclear protein DBC1. *J Biol Chem* 2010;285:40830–40837
18. Chini CC, Escande C, Nin V, Chini EN. DBC1 (Deleted in Breast Cancer 1) modulates the stability and function of the nuclear receptor Rev-erb α . *Biochem J* 2013;451:453–461
19. Trauernicht AM, Kim SJ, Kim NH, Boyer TG. Modulation of estrogen receptor alpha protein level and survival function by DBC-1. *Mol Endocrinol* 2007;21:1526–1536
20. Koyama S, Wada-Hiraike O, Nakagawa S, et al. Repression of estrogen receptor beta function by putative tumor suppressor DBC1. *Biochem Biophys Res Commun* 2010;392:357–362
21. Hiraike H, Wada-Hiraike O, Nakagawa S, et al. Identification of DBC1 as a transcriptional repressor for BRCA1. *Br J Cancer* 2010;102:1061–1067
22. Li Z, Chen L, Kabra N, Wang C, Fang J, Chen J. Inhibition of SUV39H1 methyltransferase activity by DBC1. *J Biol Chem* 2009;284:10361–10366
23. Park SH, Riley P 4th, Frisch SM. Regulation of anoikis by deleted in breast cancer-1 (DBC1) through NF-kappaB. *Apoptosis* 2013;18:649–962
24. Vaughan M. The production and release of glycerol by adipose tissue incubated in vitro. *J Biol Chem* 1962;237:3354–3358
25. Chalkiadaki A, Guarente L. High-fat diet triggers inflammation-induced cleavage of SIRT1 in adipose tissue to promote metabolic dysfunction. *Cell Metab* 2012;16:180–188
26. Donkor J, Sparks LM, Xie H, Smith SR, Reue K. Adipose tissue lipin-1 expression is correlated with peroxisome proliferator-activated receptor alpha gene expression and insulin sensitivity in healthy young men. *J Clin Endocrinol Metab* 2008;93:233–239
27. Reue K. The role of lipin 1 in adipogenesis and lipid metabolism. *Novartis Found Symp* 2007;286:58–68; discussion 68–71, 162–163, 196–203
28. Ohman MK, Shen Y, Obimba CI, et al. Visceral adipose tissue inflammation accelerates atherosclerosis in apolipoprotein E-deficient mice. *Circulation* 2008;117:798–805
29. Öhman MK, Luo W, Wang H, et al. Perivascular visceral adipose tissue induces atherosclerosis in apolipoprotein E deficient mice. *Atherosclerosis* 2011;219:33–39
30. Chiba T, Nakazawa T, Yui K, Kaneko E, Shimokado K. VLDL induces adipocyte differentiation in ApoE-dependent manner. *Arterioscler Thromb Vasc Biol* 2003;23:1423–1429
31. Nin V, Chini CC, Escande C, Capellini V, Chini EN. Deleted in breast cancer 1 (DBC1) protein regulates hepatic gluconeogenesis. *J Biol Chem* 2014;289:5518–5527
32. Stancu CS, Toma L, Sima AV. Dual role of lipoproteins in endothelial cell dysfunction in atherosclerosis. *Cell Tissue Res* 2012;349:433–446
33. Lu Y, Qian L, Zhang Q, et al. Palmitate induces apoptosis in mouse aortic endothelial cells and endothelial dysfunction in mice fed high-calorie and high-cholesterol diets. *Life Sci* 2013;92:1165–1173
34. Appleton SL, Seaborn CJ, Visvanathan R, et al.; North West Adelaide Health Study Team. Diabetes and cardiovascular disease outcomes in the metabolically healthy obese phenotype: a cohort study. *Diabetes Care* 2013;36:2388–2394
35. Escande C, Nin V, Pirtskhalava T, et al. Deleted in Breast Cancer 1 regulates cellular senescence during obesity. *Aging Cell* 2014 July 3 [Epub ahead of print]
36. Bordone L, Cohen D, Robinson A, et al. SIRT1 transgenic mice show phenotypes resembling calorie restriction. *Aging Cell* 2007;6:759–767
37. Pfluger PT, Herranz D, Velasco-Miguel S, Serrano M, Tschöp MH. Sirt1 protects against high-fat diet-induced metabolic damage. *Proc Natl Acad Sci U S A* 2008;105:9793–9798
38. Caron AZ, He X, Mottawea W, et al. The SIRT1 deacetylase protects mice against the symptoms of metabolic syndrome. *FASEB J* 2014 ;28:1306–1316.
39. Hallakou S, Doaré L, Foufelle F, et al. Pioglitazone induces in vivo adipocyte differentiation in the obese Zucker fa/fa rat. *Diabetes* 1997;46:1393–1399
40. Miyazaki Y, Glass L, Triplitt C, et al. Effect of rosiglitazone on glucose and non-esterified fatty acid metabolism in Type II diabetic patients. *Diabetologia* 2001;44:2210–2219
41. Qiang L, Wang L, Kon N, et al. Brown remodeling of white adipose tissue by SirT1-dependent deacetylation of Ppar γ . *Cell* 2012;150:620–632

La otra línea de investigación en la que se participo activamente fue el papel de CD38 en la regulación de los niveles de NAD⁺ y sus consecuencias en la actividad de las sirtuinas, la acetilación de proteínas y el ciclo circadiano. El resultado de la participación en estas líneas de investigación fue la coautoría en las siguientes publicaciones:

- Flavonoid apigenin is an inhibitor of the NAD⁺ ase CD38: implications for cellular NAD⁺ metabolism, protein acetylation, and treatment of metabolic syndrome.

Escande C, Nin V, Price NL, Capellini V, Gomes AP, Barbosa MT, O'Neil L, White TA, Sinclair DA, Chini EN.

Diabetes. 2013 Apr;62(4):1084-93.

- Altered behavioral and metabolic circadian rhythms in mice with disrupted NAD⁺ oscillation.

Sahar S, Nin V, Barbosa MT, Chini EN, Sassone-Corsi P.

Aging (Albany NY). 2011 Aug;3(8):794-802.

Flavonoid Apigenin Is an Inhibitor of the NAD⁺ase CD38

Implications for Cellular NAD⁺ Metabolism, Protein Acetylation, and Treatment of Metabolic Syndrome

Carlos Escande,¹ Veronica Nin,¹ Nathan L. Price,² Verena Capellini,¹ Ana P. Gomes,² Maria Thereza Barbosa,¹ Luke O'Neil,¹ Thomas A. White,¹ David A. Sinclair,² and Eduardo N. Chini¹

Metabolic syndrome is a growing health problem worldwide. It is therefore imperative to develop new strategies to treat this pathology. In the past years, the manipulation of NAD⁺ metabolism has emerged as a plausible strategy to ameliorate metabolic syndrome. In particular, an increase in cellular NAD⁺ levels has beneficial effects, likely because of the activation of sirtuins. Previously, we reported that CD38 is the primary NAD⁺ase in mammals. Moreover, CD38 knockout mice have higher NAD⁺ levels and are protected against obesity and metabolic syndrome. Here, we show that CD38 regulates global protein acetylation through changes in NAD⁺ levels and sirtuin activity. In addition, we characterize two CD38 inhibitors: quercetin and apigenin. We show that pharmacological inhibition of CD38 results in higher intracellular NAD⁺ levels and that treatment of cell cultures with apigenin decreases global acetylation as well as the acetylation of p53 and RelA-p65. Finally, apigenin administration to obese mice increases NAD⁺ levels, decreases global protein acetylation, and improves several aspects of glucose and lipid homeostasis. Our results show that CD38 is a novel pharmacological target to treat metabolic diseases via NAD⁺-dependent pathways. *Diabetes* 62:1084–1093, 2013

Obesity is a disease that has reached epidemic proportions in developed and developing countries (1–3). In the U.S., >60% of the population is overweight (1,3,4). Obesity is a feature of metabolic syndrome, which includes glucose intolerance, insulin resistance, dyslipidemia, and hypertension. These pathologies are well-documented risk factors for cardiovascular disease, type 2 diabetes, and stroke (4). It is therefore imperative to envision new strategies to treat metabolic syndrome and obesity.

Recently, the role of NAD⁺ as a signaling molecule in metabolism has become a focus of intense research. It was shown that an increase in intracellular NAD⁺ levels in tissues protects against obesity (5,6), metabolic syndrome, and type 2 diabetes (5–7). Our group was the first to demonstrate that an increase in NAD⁺ levels protects against high-fat diet-induced obesity, liver steatosis, and metabolic

syndrome (5). This concept was later expanded by others using different approaches, including inhibition of poly-ADP-ribose polymerase (PARP)1 (6) and stimulation of NAD⁺ synthesis (7).

The ability of NAD⁺ to affect metabolic diseases seems to be mediated by sirtuins (8). This family of seven NAD⁺-dependent protein deacetylases, particularly SIRT1, SIRT3, and SIRT6, has gained significant attention as candidates to treat metabolic syndrome and obesity (9). Sirtuins use and degrade NAD⁺ as part of their enzymatic reaction (8), which makes NAD⁺ a limiting factor for sirtuin activity (9). In particular, silent mating information regulation 2 homolog 1 (SIRT1) has been shown to deacetylate several proteins, including p53 (10), RelA/p65 (11), PGC1- α (12), and histones (13), among others. In addition, increased expression of SIRT1 (14), increased SIRT1 activity (15), and pharmacological activation of SIRT1 (16) protect mice against liver steatosis and other features of metabolic syndrome when mice are fed a high-fat diet. Given the beneficial consequences of increased SIRT1 activity, great efforts are being directed toward the development of pharmacological interventions aimed at activating SIRT1.

We previously reported that the protein CD38 is the primary NAD⁺ase in mammalian tissues (17). In fact, tissues of mice that lack CD38 contain higher NAD⁺ levels (17,18) and increased SIRT1 activity compared with wild-type mice (5,17). CD38 knockout mice are resistant to high-fat diet-induced obesity and other aspects of metabolic disease, including liver steatosis and glucose intolerance, by a mechanism that is SIRT1 dependent (5). These multiple lines of evidence suggest that pharmacological CD38 inhibition would lead to SIRT1 activation through an increase in NAD⁺ levels, resulting in beneficial effects on metabolic syndrome.

Recently, it was shown that in vitro, CD38 is inhibited by flavonoids, including quercetin (19). Flavonoids are naturally occurring compounds present in a variety of plants and fruits (20). Among them, quercetin [2-(3,4-dihydroxyphenyl)-3,5,7-trihydroxy-4H-chromen-4-one] and apigenin [5,7-dihydroxy-2-(4-hydroxyphenyl)-4H-1-benzopyran-4-one] have been shown to have beneficial effects against cancer (21–24). In fact, apigenin and quercetin ameliorate atherosclerosis (25) and reduce inflammation (26–28). However, the mechanisms of action of flavonoids remain largely unknown. We hypothesized that the effect of some flavonoids in vivo may occur through inhibition of CD38 and an increase in NAD⁺ levels in tissues, which lead to protection against metabolic syndrome.

Here, we show that CD38 expression and activity regulate cellular NAD⁺ levels and global acetylation of proteins, including SIRT1 substrates. We confirmed that quercetin is a CD38 inhibitor in vitro and in cells. Importantly, we

From the ¹Department of Anesthesiology and Kogod Aging Center, Mayo Clinic, Rochester, Minnesota; and ²Glenn Laboratories for the Biological Mechanisms of Aging, Genetics Department, Harvard Medical School, Boston, Massachusetts.

Corresponding author: Eduardo N. Chini, chini.eduardo@mayo.edu.

Received 22 August 2012 and accepted 9 October 2012.

DOI: 10.2337/db12-1139

This article contains Supplementary Data online at <http://diabetes.diabetesjournals.org/lookup/suppl/doi:10.2337/db12-1139/-DC1>.

© 2013 by the American Diabetes Association. Readers may use this article as long as the work is properly cited, the use is educational and not for profit, and the work is not altered. See <http://creativecommons.org/licenses/by-nc-nd/3.0/> for details.

demonstrate that apigenin is a novel inhibitor of CD38 *in vitro* and *in vivo*. Treatment of cells with apigenin or quercetin inhibits CD38 and promotes an increase in intracellular NAD⁺ levels. An increased NAD⁺ level decreases protein acetylation through sirtuin activation. Finally, treatment of obese mice with apigenin results in CD38 inhibition, higher NAD⁺ levels in the liver, and a decrease in protein acetylation. Apigenin treatment improves glucose homeostasis, glucose tolerance, and lipid metabolism in obese mice. Our results clearly demonstrate that CD38 is a novel therapeutic target for the treatment of metabolic diseases and that apigenin and quercetin as well as other CD38 inhibitors may be used to treat metabolic syndrome.

RESEARCH DESIGN AND METHODS

Reagents and antibodies. All reagents and chemicals were from Sigma-Aldrich. Antibodies for human SIRT1, mouse SIRT1, p65, acetylated p53 (K382), phosphorylated AMP-activated protein kinase (AMPK) (Thr172), AMPK, and acetyl-lysine were from Cell Signaling Technology. Antibody against Namp1 was from Bethyl Laboratories. Anti-human CD38 antibody was from R&D Biosystems, and anti-mouse CD38 was from Epitomics.

Cell culture. A549 cells were kept in RPMI 1640 media supplemented with 10% FBS and penicillin/streptomycin (Invitrogen). Primary CD38 wild-type and knockout mouse embryonic fibroblasts (MEFs) were kept in Dulbecco's modified

Eagle's medium supplemented with 10% FBS, penicillin/streptomycin, and glutamine. Primary MEFs were isolated from embryos (E18) from wild-type and CD38 knockout mice. Primary MEFs were used between passages 2 and 5. 293T and hepatocellular carcinoma (Hep)G2 cells were kept in Dulbecco's modified Eagle's medium supplemented with 10% FBS and penicillin/streptomycin.

Overexpression and small interfering RNA. Full-length human CD38 was subcloned into a modified pIRES2-enhanced green fluorescent protein vector. For overexpression, 293T cells were transfected for 48 h with Lipofectamine 2000 (Invitrogen) following the manufacturer's instructions.

For CD38 knockdown experiments, probe no. 2 of a TriFECTa kit against human CD38 was used (cat. no. HSC.RNAI.N001775.12.2; IDT). A549 cells were transfected with 40 nmol small interfering RNA (siRNA) duplex using Lipofectamine 2000 according to the manufacturer's instructions.

Determination of CD38 activity. Determination of CD38 activity in cells and tissues was performed as previously described (17). *In vitro* CD38 activity was measured using 0.1 unit of recombinant human CD38 (R&D Systems) in 0.25 mol/L sucrose and 40 mmol/L Tris-HCl (pH 7.4). The reaction was started by addition of 0.2 mmol/L substrate. Nicotinamide 1,N⁶-ethenoadenine dinucleotide was used to determine NAD⁺ase activity and nicotinamide guanine dinucleotide to determine cyclase activity. CD38 activity was expressed as arbitrary fluorescent units per minute (AFU/min).

NAD⁺ quantification. NAD⁺ extraction and quantification was performed as previously described (17). In brief, cells were lysed by sonication in ice-cold 10% trichloroacetic acid, and then the trichloroacetic acid was extracted with two volumes of an organic phase consisting of 1,1,2-trichloro-1,2,2-trifluoroethane and triethylamine. NAD⁺ concentration was measured by means of an enzymatic cycling assay (18).

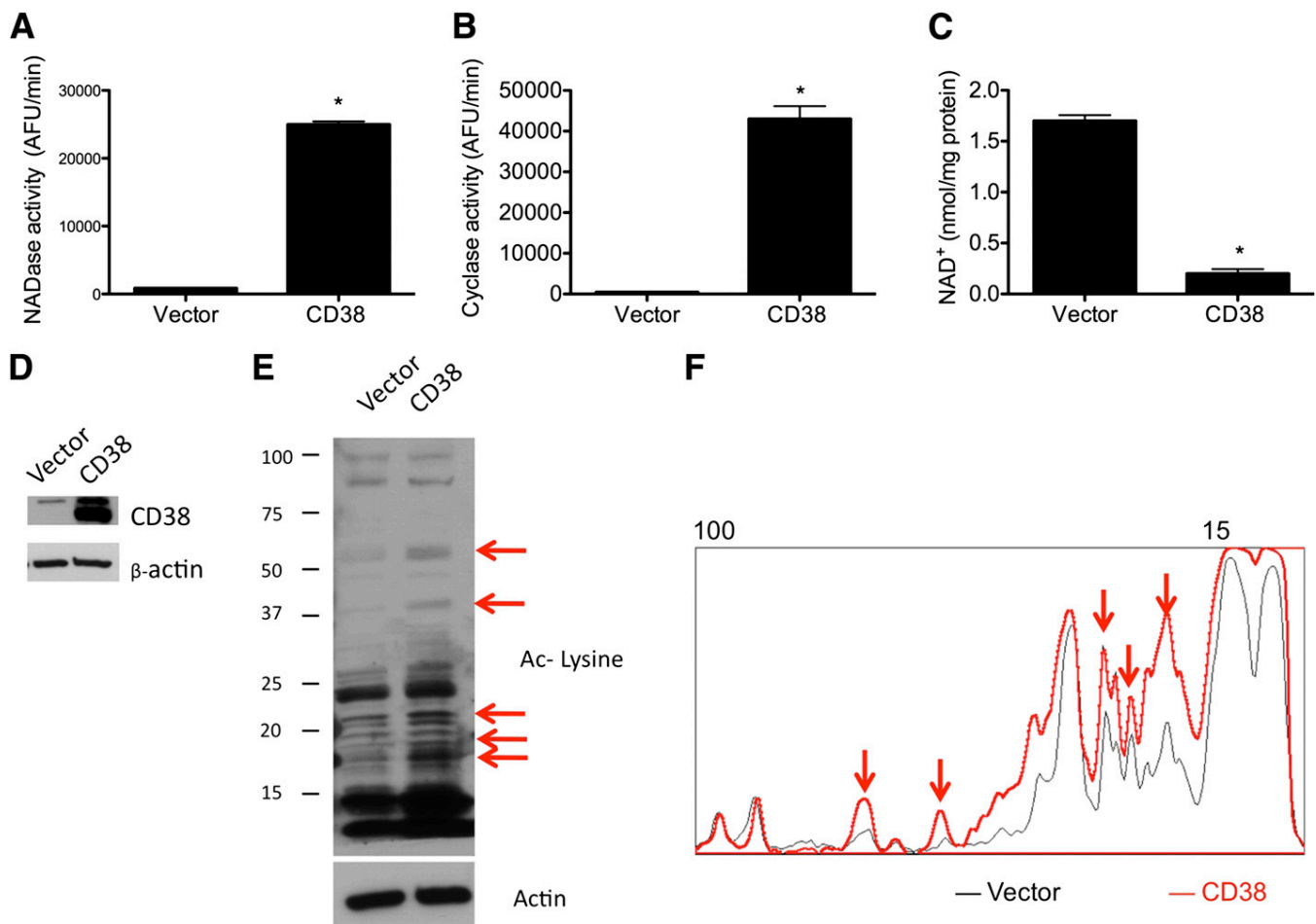


FIG. 1. CD38 overexpression decreases NAD⁺ and promotes protein acetylation in cells. 293T cells were transfected with empty vector or human CD38-coding vector. After 48 h, cells were harvested, and NAD⁺ase activity (A), ADP-ribosyl-cyclase activity (B), and total intracellular NAD⁺ levels (C) were measured in cell lysates. **P* < 0.05, *n* = 3. D: Western blot for CD38 in 293T cells transfected with empty vector or with human CD38. E: Western blot showing total protein acetylation in cells transfected with empty vector or with human CD38. Anti-acetylated (Ac) lysine antibody was used. Red arrows highlight the main bands that showed variations in intensity. F: Intensity profile of the Western blot shown in E. Western blots were scanned and intensity profile was obtained using ImageJ. Red arrows correspond with intensity of the same bands shown in E.

Determination of SIRT1 activity. SIRT1 activity was measured with a fluorimetric assay (Enzo) as previously described (15). One unit of human recombinant SIRT1 was incubated with different concentrations of apigenin plus 100 $\mu\text{mol/L}$ Fluor-de-Lys p53 tetra peptide and 100 $\mu\text{mol/L}$ NAD⁺. Fluor-de-Lys developer was prepared according to the manufacturer's recommendations and added to the reactions for 1 h. Fluorescence was read with an excitation of 360 nm and emission at 460 nm.

Mouse studies. All mice used in this study were maintained in the Mayo Clinic Animal facility. All experimental protocols were approved by the institutional animal care and use committee at Mayo Clinic (protocol no. A33209), and all studies were performed according to the methods approved in the protocol. For generation of obese mice, twelve 20-week-old C57BL/6 mice were placed on a high-fat diet (AIN-93G, modified to provide 60% of calories from fat; Dyets) ad libitum for 4 weeks. Body weight was recorded weekly. After 4 weeks of high-fat diet, mice were randomly divided in two groups and injected daily with 100 mg/kg i.p. apigenin or vehicle for 7 consecutive days while remaining on the high-fat diet. During the treatments, food intake and body weight were monitored daily. There was no difference in these parameters between groups. For the glucose tolerance experiments, mice were housed for 24 h without food, but with water ad libitum, and challenged with one dose of 1.5 g/kg i.p. dextrose. Area under the curve was calculated by the net incremental method (with baseline) and presented as incremental area under the curve.

Gene expression analysis. RNA from flash-frozen liver tissue was extracted with an RNeasy Mini Kit (Qiagen) according to the manufacturer's instructions. cDNA was synthesized with the iScript cDNA synthesis kit (BioRad) using 600 ng RNA. Quantitative RT-PCR reactions were performed using 1 $\mu\text{mol/L}$

primers and LightCycler 480 SYBR Green Master (Roche) on a LightCycler 480 detection system (Roche). Calculations were performed by a comparative method ($2^{-\Delta\Delta\text{CT}}$) using 18S rRNA as an internal control. Primers were designed using the IDT software, and the primer sequences were as follows: long-chain acyl-CoA dehydrogenase (LCAD), forward (Fw) GGTGGAAAACGGAATGAAAGG, reverse (Rv) GGCAATCGGACATCTTCAAAG; medium-chain acyl-CoA dehydrogenase (MCAD), Fw TGTTAATCGGTGAAGGAGCAG, Rv CTATCCA GGGCATACTTCGTG; CPT1a, Fw AGACAAGAACCCCAACATCC, Rv CAA AGGTGTCAAATGGGAAGG; and 18S, Fw CGGCTACCACATCCAAGGAA, Rv GCTGGAATTACCGCGGCT.

Lipid treatment. Cells were incubated with a mixture of oleic acid and palmitic acid in a 2:1 ratio in culture media supplemented with 1% fatty acid-free BSA (Sigma-Aldrich). Lipids were used at concentrations shown to induce steatosis but not apoptosis (15). Incubations with lipids were performed for 16–24 h.

Statistics. Values are presented as means \pm SEM of three to five experiments unless otherwise indicated. The significance of differences between means was assessed by ANOVA or two-tailed Student *t* test. A *P* value <0.05 was considered significant.

RESULTS

CD38 overexpression decreases NAD⁺ and promotes protein acetylation. We have previously shown that CD38 is the primary NAD⁺ase in mammalian tissues (17).

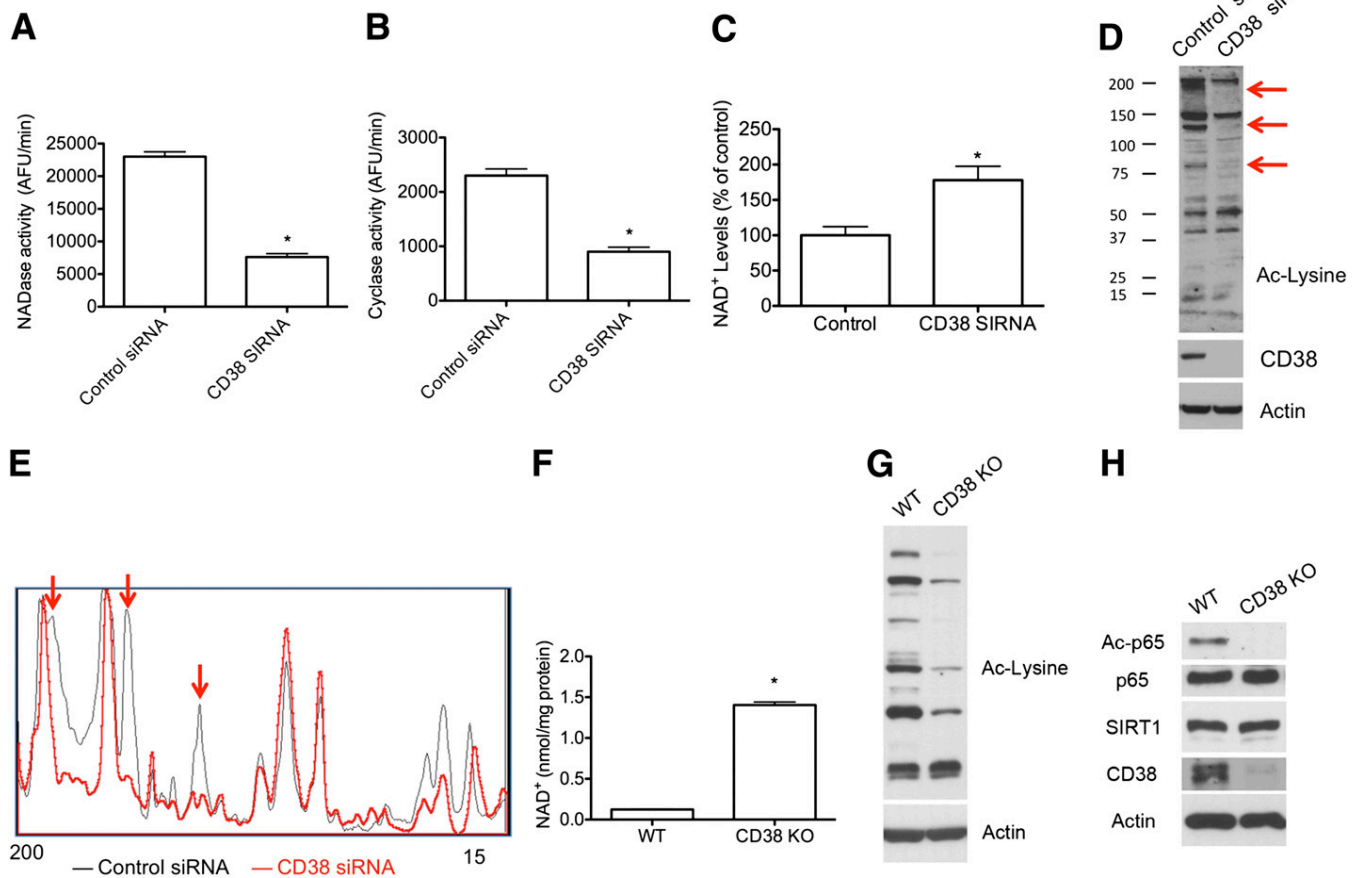


FIG. 2. CD38 downregulation increases NAD⁺ and decreases protein acetylation in cells. A549 cells were transfected with a scrambled siRNA (control siRNA) or human CD38 siRNA. After 72 h, cells were harvested and NAD⁺ase activity (A), ADP-ribosyl-cyclase activity (B), and total intracellular NAD⁺ levels (C) were measured from cell lysates. **P* < 0.05 , *n* = 3. D: Western blot showing total protein acetylation in cells transfected with control siRNA or with human CD38 siRNA. Anti-acetylated (Ac) lysine antibody was used. Red arrows highlight the main bands that showed variations in intensity. E: Intensity profile of the Western blot shown in D. Western blots were scanned and intensity profile was obtained using Image J. Red arrows correspond with intensity of the same bands showed in D. F–H: Primary MEFs were purified and cultured from wild-type (WT) and CD38 knockout (KO) mice. F: Intracellular NAD⁺ levels (**P* < 0.05 , *n* = 3). G: Western blot from wild-type and CD38 knockout MEFs showing total protein acetylation in these cells. H: Representative Western blot in wild-type and CD38 knockout MEFs. Acetylated RelA/p65 (K310), total RelA/p65, SIRT1, CD38, and actin antibodies were used.

CD38-deficient mice have increased NAD⁺ levels in multiple tissues (5,17). To further characterize the role of CD38 in the regulation of NAD⁺-dependent cellular events, we studied the effect of CD38 manipulation in cells. We found that cells that overexpress CD38 show a significant increase in NAD⁺ase and ADP ribosyl cyclase activities (Fig. 1A and B) and a consistent decrease in intracellular NAD⁺ levels (Fig. 1C). Interestingly, we found that overexpression of CD38 also led to an increase in global protein acetylation (Fig. 1E). The pattern of acetylated proteins was analyzed by plotting an intensity profile of the lanes in the Western blots (Fig. 1F). It is worth noting that CD38 overexpression promotes changes in the level of acetylation of several proteins (red arrows in Fig. 1E and F), while other bands remain unchanged. This is consistent with the fact that only sirtuin deacetylases depend on NAD⁺ for their activity (8); histone deacetylases of classes I and II have a different enzymatic mechanism that does not require NAD⁺ (29).

CD38 downregulation increases NAD⁺ and decreases protein acetylation. Next, we examined whether CD38 downregulation promotes the opposite effect on cellular NAD⁺ levels and global protein acetylation. This is of key relevance, since we (5) and other investigators (6,7) have shown that an increase in intracellular NAD⁺ levels protects against metabolic diseases and aging. We transfected cells with control or CD38 siRNA. Cells treated with CD38 siRNA had decreased NAD⁺ase and ADP ribosyl-cyclase activities (Fig. 2A and B) and a significant increase in intracellular NAD⁺ levels (Fig. 2C), consistent with the diminished CD38 NAD⁺ase activity. Moreover, the increase in NAD⁺ levels was accompanied by a decrease in global

protein acetylation (Fig. 2D and E). Finally, we isolated primary MEFs from wild-type and CD38 knockout mice and measured NAD⁺ levels and protein acetylation. We found that CD38 knockout MEFs have increased NAD⁺ levels (Fig. 2F) and decreased global protein acetylation (Fig. 2G). We also analyzed p65/RelA acetylation at K310, a site that is an accepted target for cellular SIRT1 activity (7,11). We found that CD38 knockout MEFs show no detectable p65/RelA (K310) acetylation compared with wild-type cells, despite having similar total p65/RelA protein (Fig. 2H) and similar SIRT1 levels. This indicates that SIRT1 activity is increased in the CD38 knockout MEFs.

Apigenin and quercetin inhibit CD38 activity in vitro. By use of high-throughput analysis to search for inhibitors of CD38, we found that several flavonoids, including quercetin and apigenin, inhibit CD38 in vitro. The complete screen will be published elsewhere. Recently, Kellenberger et al. (19) also published a list of flavonoids that act as CD38 inhibitors in vitro, many of which were also confirmed by our analysis. Quercetin was one of the compounds found by Kellenberger et al. (19) to inhibit CD38 in vitro. Apigenin, however, was demonstrated to be a novel CD38 inhibitor. We proceeded to further characterize these compounds in vitro and in cells.

The effect of apigenin and quercetin on CD38 activity in vitro was studied using the soluble ectodomain of human CD38 (17). We found that apigenin (Fig. 3A) inhibits in vitro CD38 activity with a half-maximal inhibitory concentration (IC₅₀) of $10.3 \pm 2.4 \mu\text{mol/L}$ for the NAD⁺ase activity and an IC₅₀ of $12.8 \pm 1.6 \mu\text{mol/L}$ for the ADP-ribosyl-cyclase activity (Fig. 3B and C). In vitro, quercetin (Fig. 3D) inhibits CD38 NAD⁺ase activity with an IC₅₀ of

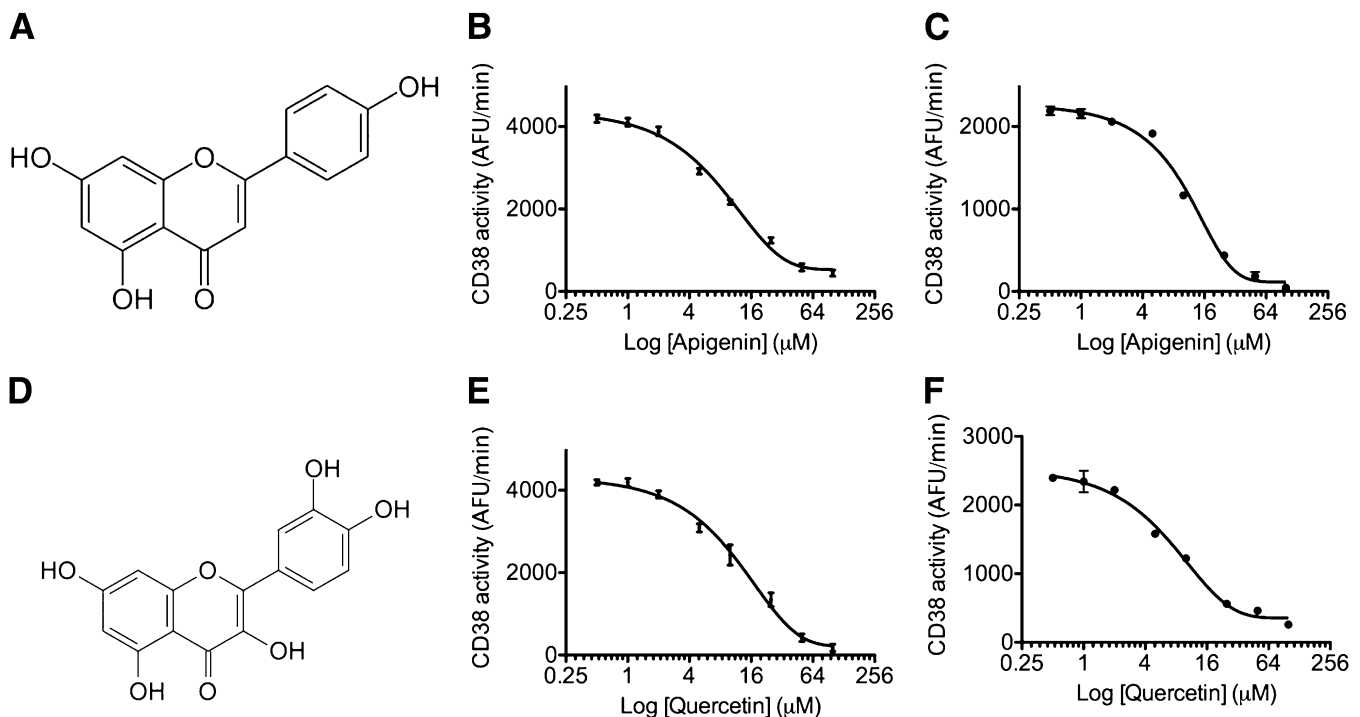


FIG. 3. The flavonoids apigenin and quercetin inhibit CD38 activity in vitro. **A:** Chemical structure of apigenin. **B and C:** In vitro NAD⁺ase (**B**) and ADP-ribosyl-cyclase (**C**) activity using human recombinant-purified CD38 and different concentrations of apigenin. **D:** Chemical structure of quercetin. **E and F:** In vitro CD38 NAD⁺ase activity (**E**) and ADP-ribosyl-cyclase activity (**F**) using human recombinant-purified CD38 and different concentrations of apigenin. In all the measurements, compounds were used in the 0.5–100 $\mu\text{mol/L}$ concentration range. Each measurement was done by triplicate. Data points were fitted to a standard competitive inhibition curve using a nonlinear regression program (GraphPad Prism) to yield the IC₅₀ value.

13.8 ± 2.1 μmol/L (Fig. 3E) and ADP-ribosyl-cyclase activity with an IC₅₀ of 15.6 ± 3.5 μmol/L (Fig. 3F).

CD38 inhibition by quercetin and apigenin increases NAD⁺ levels in cells. Although several flavonoids can inhibit purified recombinant CD38 in vitro (19), it is not known what effects these compounds have in cells. First, we measured the effect of quercetin on endogenous cellular CD38 activity. Inhibition of CD38 activity by quercetin in cells (IC₅₀ = 16.4 ± 1.8 μmol/L) resembles the effect on the recombinant protein (Fig. 4A). Furthermore, we found that quercetin promotes an increase in intracellular NAD⁺ in a dose-dependent manner (Fig. 4B). To further confirm this effect, we incubated cells in PBS and measured intracellular NAD⁺ levels over time. We found that in untreated cells, NAD⁺ levels decrease with time (Fig. 4C), probably as a result of the removal of NAD⁺ precursors from the culture media. However, when the cells were treated with quercetin, NAD⁺ levels were stable over time, suggesting that inhibition of CD38 is enough to maintain intracellular NAD⁺ levels in the absence of NAD⁺ precursors. Finally, in order to confirm that the effect of quercetin on cellular NAD⁺ levels was dependent on CD38, we measured NAD⁺ after incubation with quercetin in wild-type and CD38 knockout MEFs. We found that quercetin promotes an increase in NAD⁺ in the wild-type MEFs but does not further increase NAD⁺ levels in CD38 knockout MEFs (Fig. 4D), indicating that the effect of quercetin on NAD⁺ levels is CD38 dependent.

Apigenin also inhibits CD38 activity in cells (Fig. 5A). In fact, inhibition of cellular CD38 was very similar to that observed with the purified recombinant protein (IC₅₀ = 14.8 ± 2.2 μmol/L in cells and 10.3 ± 2.4 μmol/L in vitro). Apigenin treatment increased NAD⁺ levels in cells in a dose-dependent manner (Fig. 5B) and protected against NAD⁺ depletion when cells were incubated in PBS (Fig. 5C). Furthermore, treatment of CD38 knockout MEFs with apigenin had no effect on NAD⁺ levels (Fig. 5D), indicating that the effect of apigenin on NAD⁺ levels is mediated by CD38. Interestingly, we found that treatment of wild-type MEFs with apigenin decreased acetylation of RelA/p65 (Fig. 5E). However, in the CD38 knockout MEFs, RelA/p65 acetylation levels were undetectable in the control, and therefore we could not determine the effect of apigenin (Fig. 5E). These results are consistent with the effect of apigenin in intracellular NAD⁺ levels in these cells (Fig. 5D). Quercetin has been shown to activate SIRT1 in vitro (30), suggesting that it may activate SIRT1 activity by two different mechanisms. To rule out a possible direct effect of apigenin on SIRT1 activity, we measured in vitro recombinant SIRT1 activity in the presence of different concentrations of apigenin. We observed that apigenin does not activate SIRT1 directly (Fig. 5F). Combined, these results clearly demonstrate that apigenin inhibits CD38 in cells and by doing so promotes an increase in NAD⁺ levels that stimulates NAD⁺-dependent deacetylases.

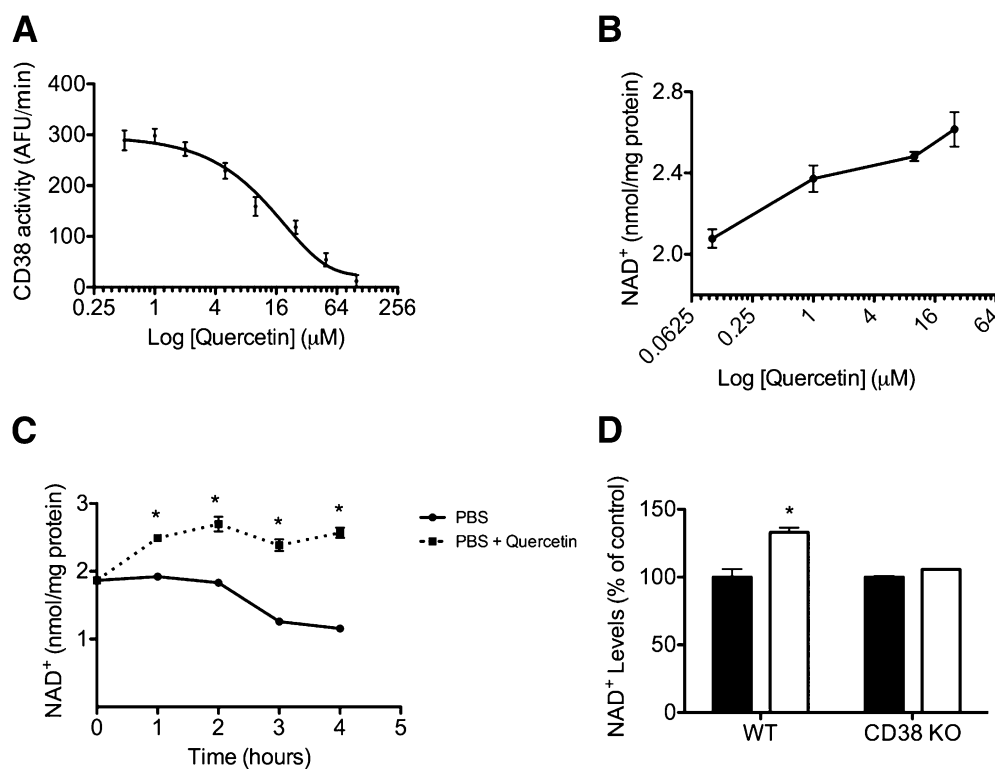


FIG. 4. CD38 inhibition by quercetin increases NAD⁺ levels in cells. **A:** Endogenous CD38 NAD⁺ase activity was measured in protein lysates from A549 cells. Quercetin was used in the 0.5–100 μmol/L concentration range. Each measurement was done in triplicate. Data points were fitted to a standard competitive inhibition curve using a nonlinear regression program (GraphPad Prism) to yield the IC₅₀ value. **B:** NAD⁺ dose-response curve in A549 cells treated with quercetin. Cells were incubated with quercetin for 6 h before NAD⁺ extraction. **P* < 0.05, *n* = 3. **C:** NAD⁺ time course in A549 cells incubated in PBS (●) or in PBS plus quercetin (50 μmol/L) (■). **P* < 0.05, *n* = 3. **D:** Intracellular NAD⁺ levels in wild-type (WT) and CD38 knockout (KO) MEFs treated with vehicle (control) (■) or with quercetin (50 μmol/L) (□) for 6 h. NAD⁺ levels were expressed as percent of change with respect to the control for both cells. Total NAD⁺ levels were significantly higher in CD38 knockout MEFs. (See Fig. 2F.) **P* < 0.05, *n* = 3.

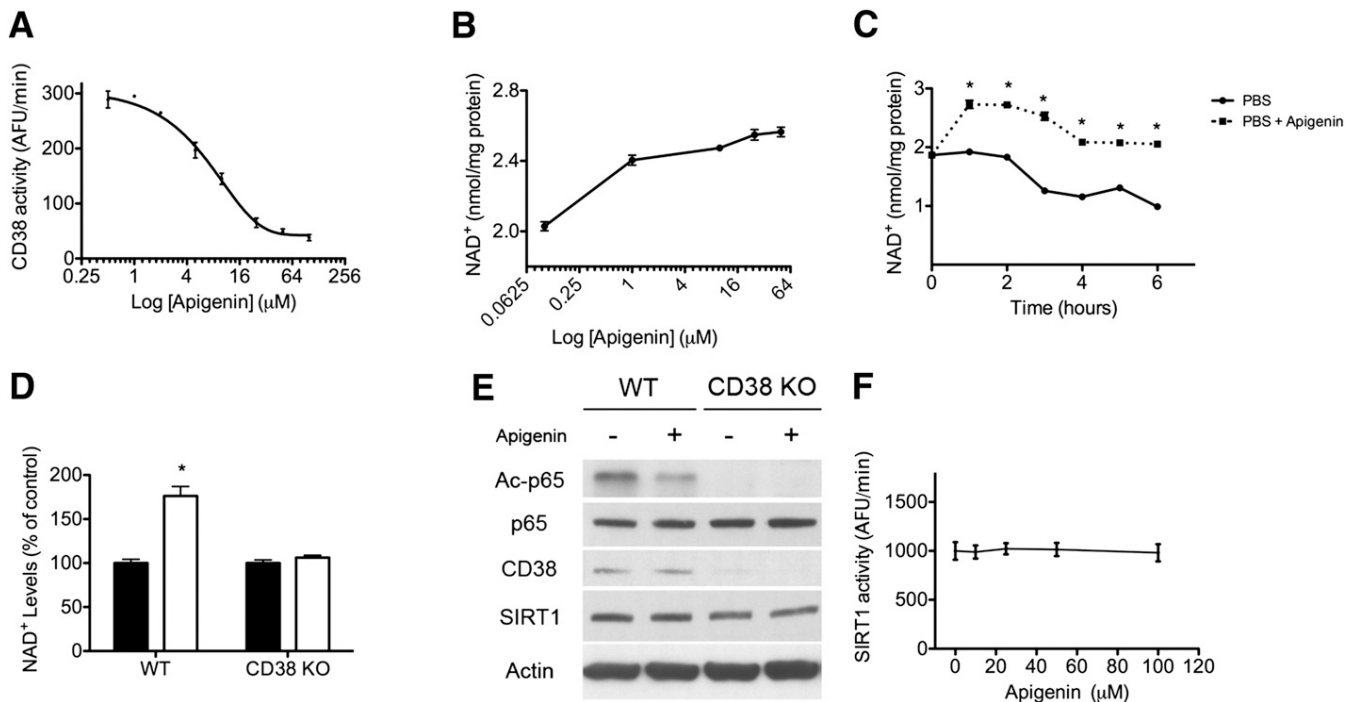


FIG. 5. CD38 inhibition by apigenin increases NAD⁺ and decreases protein acetylation in cells. **A:** Endogenous CD38 NAD⁺ase activity was measured in protein lysates from A549 cells. Apigenin was used in the 2.5–100 μmol/L concentration range. Each measurement was done in triplicate. Data points were fitted to a standard competitive inhibition curve using a nonlinear regression program (GraphPad Prism) to yield the IC₅₀ value. **B:** NAD⁺ dose-response curve in A549 cells treated with apigenin. Cells were incubated with apigenin for 6 h before NAD⁺ extraction. **C:** NAD⁺ time course in A549 cells incubated in PBS (●) or in PBS plus 25 μmol/L apigenin (■) (**P* < 0.05, *n* = 3). **D:** Intracellular NAD⁺ levels in wild-type (WT) and CD38 knockout (KO) MEFs treated with vehicle (control) (■) or with apigenin (25 μmol/L) (□) for 6 h. NAD⁺ levels were expressed as percent change with respect to the control for both cells. Total NAD⁺ levels were significantly higher in CD38 knockout MEFs. (See Fig. 2*F*.) **P* < 0.05, *n* = 3. **E:** Western blot of wild-type and CD38 knockout MEFs that were treated with vehicle or apigenin as described in **D**. Samples were immunoblotted for acetylated (Ac)-p65 (K310), total p65, CD38, SIRT1, and actin. **F:** In vitro SIRT1 activity using recombinant-purified human SIRT1. SIRT1 activity was measured in the presence of different concentrations of apigenin (0–100 μmol/L). Activity was determined in the linear portion of the reaction.

CD38 inhibition by apigenin increases NAD⁺ and decreases protein acetylation in mice. Apigenin and quercetin have been shown to ameliorate atherosclerosis in mice (25) and to protect against lipid accumulation in cells (25). However, the mechanism of action has not been elucidated. In fact, while most flavonoids activate AMPK, which could explain some of the metabolic effects observed, apigenin is a very poor AMPK activator (25).

Based on the results obtained in cells, we tested whether apigenin inhibits CD38 *in vivo* using a model of high-fat diet-induced obesity (5,15). We fed adult mice a high-fat diet for 4 weeks. After, we divided the mice randomly in two groups. Each group was injected daily with apigenin (100 mg/kg) or vehicle (DMSO) for a week. We found that mice that had been injected with apigenin had decreased CD38 activity in the liver (Fig. 6*A*), which correlated with an increase in hepatic NAD⁺ levels compared with control mice (Fig. 6*B*). We then examined whether the apigenin treatment had an effect on the level of expression of several proteins involved in NAD⁺ metabolism. As shown in Fig. 6*C*, we found no significant differences in the expression of CD38, SIRT1, or Nampt, the primary regulator of the NAD⁺ salvage pathway. Furthermore, we did not see any changes in phosphorylation or total levels of AMPK (Fig. 6*C*). However, when we analyzed the liver samples using an acetyl-lysine antibody, we found that the apigenin treatment resulted in a statistically significant decrease in global acetylation of proteins (Fig. 6*D* and *E*).

To determine the relevance of SIRT1 in the deacetylation of proteins triggered by apigenin treatment, we used human HepG2 cells: a well-accepted cellular model for studying hepatic cellular signaling (15,25,31). We found that treatment with apigenin decreases total protein acetylation—an effect that is lost in the presence of the SIRT1 inhibitor EX527 (Fig. 6*F*). Furthermore, treatment of HepG2 cells with apigenin decreased acetylation of p53 at K382 and also of RelA/p65 at K310: sites that are deacetylated by SIRT1 (Supplementary Fig. 1). This effect was reverted when cells were also incubated with the sirtuin inhibitor nicotinamide (Supplementary Fig. 1). Taken together, these results show that apigenin inhibits CD38 *in vivo* and is associated with increased NAD⁺ and decreased protein acetylation, likely through the activation of SIRT1.

CD38 inhibition by apigenin improves glucose homeostasis *in vivo* and promotes fatty acid oxidation in the liver. Finally, we tested whether apigenin protects against high-fat diet-induced hyperglycemia. We found that after 4 days of treatment, the mice treated with apigenin had significantly lower blood glucose levels compared with the control mice (Fig. 7*A*). Fasting blood glucose levels were also significantly lower after 1 week of treatment with apigenin (Fig. 7*B*). Moreover, we found that 1 week of treatment with apigenin was enough to improve glucose homeostasis in the mice (Fig. 7*C* and *D*). SIRT1 activation promotes fatty acid oxidation in the liver by inducing the expression of several

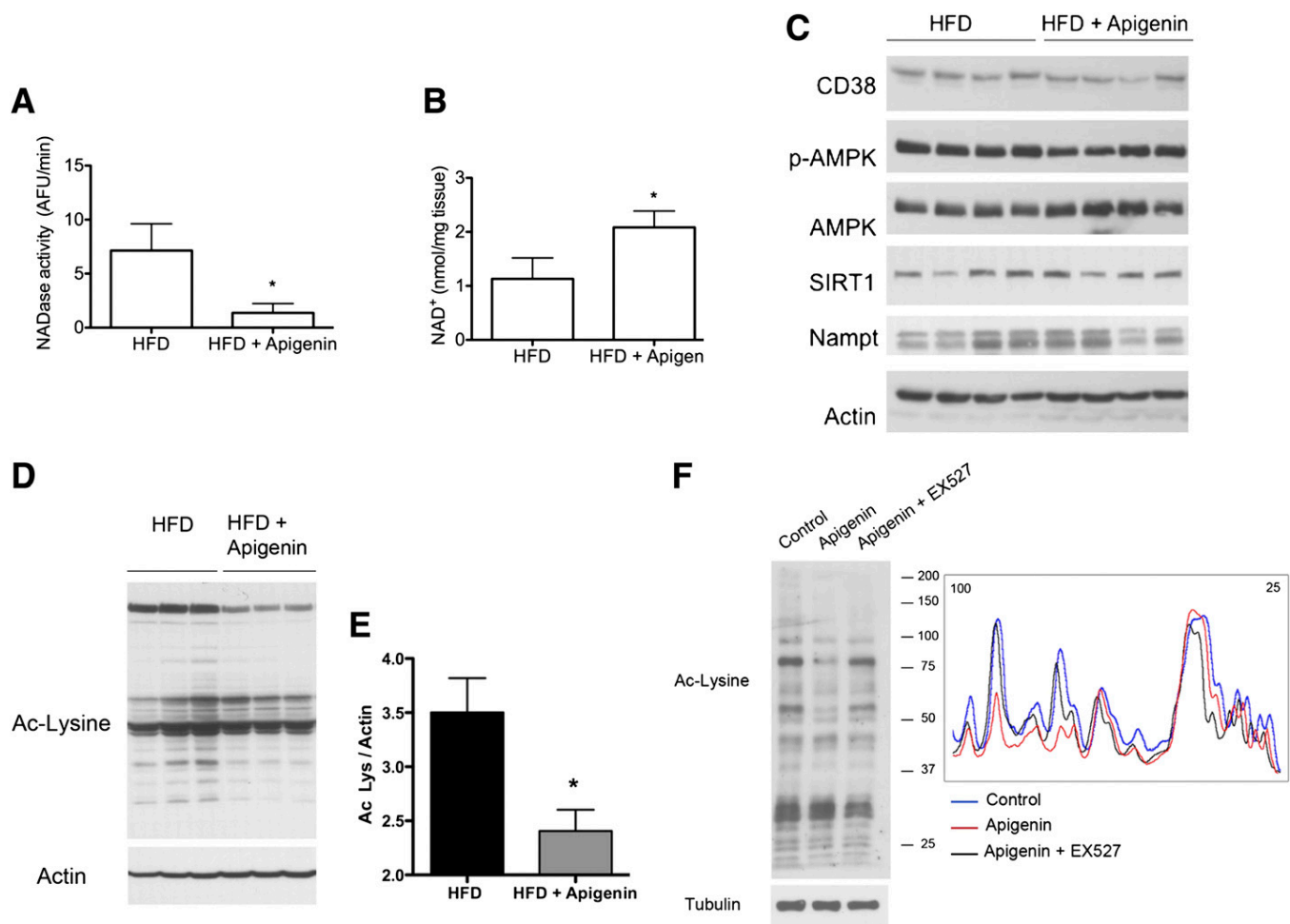


FIG. 6. CD38 inhibition by apigenin increases NAD^+ and decreases protein acetylation in vivo. *A–E*: Mice were fed a high-fat diet (HFD) for 4 weeks and then split in two groups. One group was injected with apigenin (100 mg/kg i.p.) and the other with vehicle (DMSO) with a single dose daily for 1 week. *A*: CD38 activity in the liver at the end of the treatment with apigenin ($*P < 0.05$, $n = 6$ animals per group). *B*: NAD^+ levels in the liver after the treatment ($*P < 0.05$, $n = 6$ animals per group). *C*: At the end of the treatment, liver samples were obtained and immunoblotted for CD38, phosphorylated (p)-AMPK (Thr172), AMPK, SIRT1, Nampt, and actin. *D*: Liver samples were immunoblotted for global acetylation of proteins using an anti-acetylated (Ac) lysine (Lys) antibody. Western blots were scanned and an intensity profile was obtained using Image J. The area under the curve is shown. ($*P < 0.05$, $n = 3$ per group.) *F*: Human HepG2 cells were incubated with vehicle (DMSO), apigenin (25 $\mu\text{mol/L}$), or apigenin plus EX527 (10 $\mu\text{mol/L}$) for 6 h. Cell lysates were immunoblotted for acetylated lysine to determine total protein acetylation levels (*left panel*). The intensity profile of the Western blot was obtained using Image J (*right panel*).

enzymes involved in fatty acid and cholesterol metabolism (32). In fact, SIRT1 activation in the liver prevents liver steatosis (5,14,15). Mice treated with apigenin had increased expression of the enzymes MCAD and LCAD in the liver (Fig. 8A), suggesting that apigenin treatment enhanced fatty acid oxidation. We confirmed these data by measuring total triglyceride content in the liver. Indeed, we found that the mice treated with apigenin had lower triglyceride levels in the liver compared with control mice (Fig. 8B), showing that apigenin promotes hepatic lipid oxidation. To further confirm this finding, we measured lipid accumulation in cells, using an in vitro model of hepatic steatosis (15). We found that apigenin decreases lipid accumulation in cells and that this effect was completely blocked by the SIRT1 inhibitor EX527 (Fig. 8C). Together, these results show that inhibition of CD38 by apigenin, and perhaps by other flavonoids, constitutes a pharmacological approach to activate sirtuins and treat high-fat diet-induced metabolic disorders. Furthermore, our results point to CD38 as a novel pharmacological target to treat metabolic diseases.

DISCUSSION

The alarming expansion of metabolic diseases has triggered a considerable effort in the development of pharmacological strategies to prevent and treat them. In this regard, the study of sirtuins and specifically SIRT1 has become of great relevance due to the many beneficial effects of their action (8,9). In fact, how to achieve SIRT1 activation in vivo is a subject of intense investigation. One of the strategies to achieve such activation has been the use of drugs that directly target SIRT1. Resveratrol (16) and SRT1720 (33) are two of the early SIRT1-activating compounds that improve metabolism and protect against metabolic disorders, although there is a debate about their mechanism of action (34–36). Another mechanism to achieve SIRT1 activation in vivo is to raise intracellular levels of NAD^+ either by increased synthesis or diminished degradation (5–7,18). Previously, we have shown that the enzyme CD38 is the principal regulator of intracellular NAD^+ levels in mammalian tissues (17). In fact, we were the first to show that increasing NAD^+ levels by deletion of

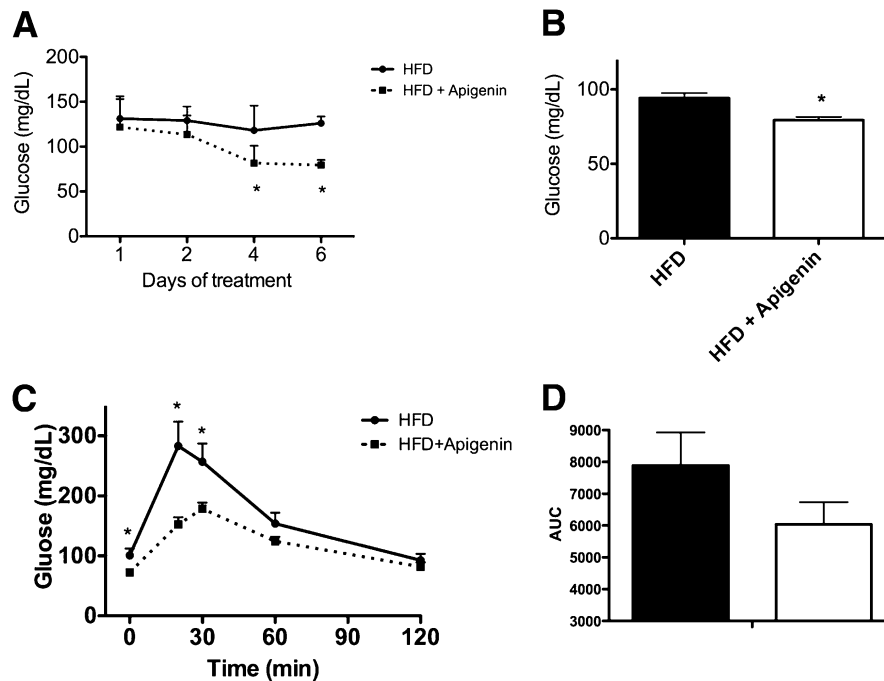


FIG. 7. CD38 inhibition by apigenin improves glucose homeostasis in vivo and improves lipid metabolism in the liver. Mice were fed a high-fat diet (HFD) for 4 weeks and then split in two groups. One group was injected with apigenin (100 mg/kg i.p.) and the other with vehicle (DMSO) with a single dose daily for 1 week. **A:** Blood glucose levels were measured during the week of apigenin treatment in ad libitum feeding conditions ($*P < 0.05$, $n = 6$ per group). **B:** Blood glucose levels were measured after 24 h of fasting on day 7 of treatment with apigenin ($*P < 0.05$, $n = 6$ per group). **C:** Glucose tolerance test in mice after 7 days of treatment with apigenin (■) or vehicle (●) ($*P < 0.05$, $n = 6$ per group). **D:** Area under the curve (AUC) calculated for the glucose tolerance test shown in C. ■, HFD; □, HFD plus apigenin.

CD38 protects against diet-induced obesity through SIRT1 activation (5). Other research groups later confirmed the importance of NAD⁺ in the prevention of metabolic diseases. Yoshino et al. (7) showed that administration of nicotinamide mononucleotide (a NAD⁺ precursor) to mice protects against high-fat diet-induced metabolic disorders. Bai et al. (6) obtained similar results using PARP1 knockout mice. Taken together, the evidence shows that pharmacological interventions that increase NAD⁺ are a promising avenue for treating metabolic disorders. However, the mechanism by which cellular NAD⁺ is increased may have different long-term outcomes. We followed survival of wild-type, CD38 knockout, and PARP1 knockout mice fed a high-fat diet. Preliminary studies with small numbers of mice suggest that CD38 knockout mice have increased average and maximum life span compared with wild-type mice when they are fed a high-fat diet. However, in the PARP1 knockout mice, which also have increased cellular NAD⁺ levels (6), the outcome was opposite this (Supplementary Fig. 2), with the PARP1 knockout mice having a decreased life span compared with the wild-type mice. This difference in survival could be explained by the fact that PARP1 is involved in genomic stability (37) and DNA repair both in the nucleus (37) and in mitochondria (38,39). This suggests that although CD38 and PARP1 knockout mice have similar protection against metabolic disorders, they may have distinct effects on longevity.

Here, we describe for the first time that the flavonoid apigenin is a CD38 inhibitor, and both apigenin and quercetin promote changes in intracellular NAD⁺ levels. This increase in NAD⁺ levels leads to changes in protein acetylation likely due to an increase in sirtuin activity. Furthermore, we show that apigenin improves glucose homeostasis and reduces lipid content in the liver in a

model of high-fat diet-induced obesity. Our results suggest that lipid oxidation is increased by a SIRT1-dependent mechanism. However, it could also happen that fatty acid synthesis or export is altered, since SIRT1 has been shown to regulate both processes (40,41). Our results demonstrate that CD38 is a promising pharmacological target to promote sirtuin actions and to treat metabolic diseases.

Flavonoids, including apigenin and quercetin, have broad beneficial effects (20). These two flavonoids ameliorate atherosclerosis in mouse genetic models (25). Although some of the beneficial effects of flavonoids on metabolism are believed to be AMPK mediated (25), this has not been clearly elucidated. Indeed, apigenin is a very weak AMPK activator in vivo (25), which suggests an additional mechanism of action. Our findings provide mechanistic evidence that flavonoids can promote an increase in NAD⁺ levels through inhibition of CD38, resulting in changes in protein acetylation, most likely through stimulation of SIRT1 (Fig. 8D). Although we show here that CD38 inhibition affects SIRT1 activity, it is likely that other sirtuins will also be stimulated by CD38 inhibition. Interestingly, CD38 is also present and active in the mitochondria (42,43), where it may regulate mitochondrial NAD⁺ levels and mitochondrial sirtuin activity.

It is likely that, similar to what happens with many other natural compounds, apigenin and quercetin have other cellular targets besides CD38. However, we clearly show that the increase in cellular NAD⁺ levels promoted by these compounds depends on CD38. More importantly, our findings support the idea that pharmacological inhibition of CD38 can be achieved as a strategy to treat obesity and obesity-related diseases. Further research will help to develop highly selective CD38 inhibitors that may be used as an approach to treat metabolic syndrome in humans.

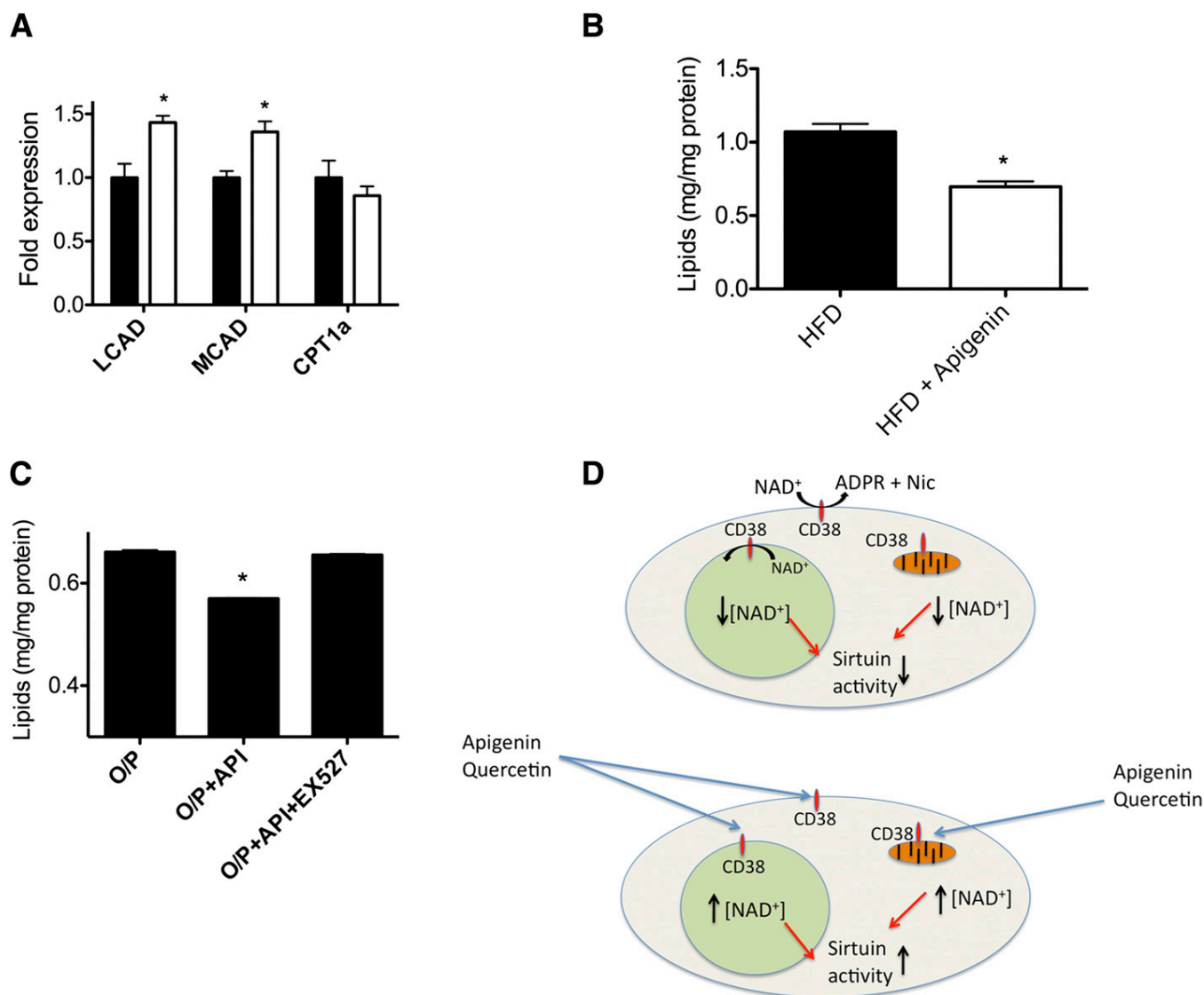


FIG. 8. CD38 inhibition by apigenin promotes fatty acid oxidation in the liver. **A:** mRNA expression of lipid oxidation markers LCAD, MCAD, and CPT1a in the liver measured by RT-PCR in mice treated with apigenin (□) or vehicle (■) (**P* < 0.05, *n* = 6 per group). **B:** Total triglyceride (TG) content in the liver of mice treated with apigenin or vehicle (**P* < 0.05, *n* = 6 per group). HFD, high-fat diet. **C:** Total triglycerides levels in HepG2 cells incubated with 0.5 mmol/L oleate/palmitate (O/P) (2:1 ratio), oleate/palmitate plus 25 μmol/L apigenin (API), or oleate/palmitate plus apigenin plus 10 μmol/L EX527 (**P* < 0.05, *n* = 3). **D:** Working model for apigenin and quercetin effect on CD38. In cells, CD38 maintains low intracellular NAD⁺ levels with a consequent low sirtuin activity. The inhibition of CD38 in different subcellular compartments leads to an increase in NAD⁺ levels, which becomes available for sirtuin activation. We propose that the effect of apigenin will activate nuclear and cytoplasmic and also mitochondrial sirtuins, where CD38 has been shown to be expressed.

ACKNOWLEDGMENTS

This work was supported in part by grants from the American Federation for Aging Research and from the Mayo Foundation; by the Strickland Career Development Award; by the National Institute of Diabetes and Digestive and Kidney Diseases, National Institutes of Health (NIH), grant DK-084055; by Mayo-UOFM Decade of Discovery Grant 63-01; and by Minnesota Obesity Council Grant DK-50456-15. D.A.S. is supported by grants from the NIH/National Institute on Aging, the Juvenile Diabetes Research Foundation, the United Mitochondrial Disease Foundation, and the Glenn Foundation for Medical Research. C.E. is supported by American Heart Association postdoctoral fellowship award 11POST7320060 and A.P.G. by a fellowship from the Portuguese Foundation for Science and Technology (SFRH/BD/44674/2008).

E.N.C. and M.T.B. are inventors in a patent for CD38 and obesity (U.S. patent no. 8143014). E.N.C. and D.A.S. are inventors on a provisional patent for apigenin as a CD38 inhibitor to treat metabolic syndrome. D.A.S. is a consultant for Sirtris, a GlaxoSmithKline company aiming to develop medicines that target sirtuins. No other potential conflicts of interest relevant to this article were reported.

C.E. measured CD38 activity, measured effect of compounds in NAD⁺ levels, evaluated the effect of CD38 and CD38 inhibitors on protein acetylation, performed in vivo experiments, analyzed tissue samples, performed the lipid measurements, wrote the manuscript, designed experiments, discussed and analyzed data, and corrected the manuscript. V.N. measured CD38 activity, evaluated the effect of CD38 and CD38 inhibitors on protein acetylation, performed in vivo experiments, analyzed tissue samples,

performed the longevity studies, designed experiments, discussed and analyzed data, and corrected the manuscript. N.L.P. performed the library screening, performed qPCR, designed experiments, discussed and analyzed data, and corrected the manuscript. V.C. measured CD38 activity and evaluated the effect of CD38 and CD38 inhibitors on protein acetylation. A.P.G. performed qPCR. M.T.B. performed the longevity studies. L.O. analyzed tissue samples. T.A.W. measured CD38 activity. D.A.S. and E.N.C. developed the original idea, designed experiments, discussed and analyzed data, and corrected the manuscript. E.N.C. is the guarantor of this work and, as such, had full access to all the data in the study and takes responsibility for the integrity of the data and the accuracy of the data analysis.

The authors thank Caroline Shamu and the staff at Harvard's Institute of Chemistry and Cell Biology facility, where the small-molecule screen was conducted.

REFERENCES

- Hedley AA, Ogden CL, Johnson CL, Carroll MD, Curtin LR, Flegal KM. Prevalence of overweight and obesity among US children, adolescents, and adults, 1999-2002. *JAMA* 2004;291:2847-2850
- Popkin BM, Adair LS, Ng SW. Global nutrition transition and the pandemic of obesity in developing countries. *Nutr Rev* 2012;70:3-21
- Spiegel AM, Alving BM. Executive summary of the Strategic Plan for National Institutes of Health Obesity Research. *Am J Clin Nutr* 2005;82 (Suppl.):211S-214S
- Eckel RH, Grundy SM, Zimmet PZ. The metabolic syndrome. *Lancet* 2005; 365:1415-1428
- Barbosa MT, Soares SM, Novak CM, et al. The enzyme CD38 (a NAD glycohydrolase, EC 3.2.2.5) is necessary for the development of diet-induced obesity. *FASEB J* 2007;21:3629-3639
- Bai P, Cantó C, Oudart H, et al. PARP-1 inhibition increases mitochondrial metabolism through SIRT1 activation. *Cell Metab* 2011;13:461-468
- Yoshino J, Mills KF, Yoon MJ, Imai S. Nicotinamide mononucleotide, a key NAD(+) intermediate, treats the pathophysiology of diet- and age-induced diabetes in mice. *Cell Metab* 2011;14:528-536
- Haigis MC, Sinclair DA. Mammalian sirtuins: biological insights and disease relevance. *Annu Rev Pathol* 2010;5:253-295
- Chalkiadaki A, Guarente L. Sirtuins mediate mammalian metabolic responses to nutrient availability. *Nat Rev Endocrinol* 2012;8:287-296
- Vaziri H, Dessain SK, Ng Eaton E, et al. hSIR2(SIRT1) functions as an NAD-dependent p53 deacetylase. *Cell* 2001;107:149-159
- Yeung F, Hoberg JE, Ramsey CS, et al. Modulation of NF-kappaB-dependent transcription and cell survival by the SIRT1 deacetylase. *EMBO J* 2004;23:2369-2380
- Rodgers JT, Lerin C, Haas W, Gygi SP, Spiegelman BM, Puigserver P. Nutrient control of glucose homeostasis through a complex of PGC-1alpha and SIRT1. *Nature* 2005;434:113-118
- Imai S, Armstrong CM, Kaeberlein M, Guarente L. Transcriptional silencing and longevity protein Sir2 is an NAD-dependent histone deacetylase. *Nature* 2000;403:795-800
- Pfluger PT, Herranz D, Velasco-Miguel S, Serrano M, Tschöp MH. Sirt1 protects against high-fat diet-induced metabolic damage. *Proc Natl Acad Sci USA* 2008;105:9793-9798
- Escande C, Chini CC, Nin V, et al. Deleted in breast cancer-1 regulates SIRT1 activity and contributes to high-fat diet-induced liver steatosis in mice. *J Clin Invest* 2010;120:545-558
- Baur JA, Pearson KJ, Price NL, et al. Resveratrol improves health and survival of mice on a high-calorie diet. *Nature* 2006;444:337-342
- Aksoy P, White TA, Thompson M, Chini EN. Regulation of intracellular levels of NAD: a novel role for CD38. *Biochem Biophys Res Commun* 2006; 345:1386-1392
- Aksoy P, Escande C, White TA, et al. Regulation of SIRT 1 mediated NAD dependent deacetylation: a novel role for the multifunctional enzyme CD38. *Biochem Biophys Res Commun* 2006;349:353-359
- Kellenberger E, Kuhn I, Schuber F, Muller-Steffner H. Flavonoids as inhibitors of human CD38. *Bioorg Med Chem Lett* 2011;21:3939-3942
- Ross JA, Kasum CM. Dietary flavonoids: bioavailability, metabolic effects, and safety. *Annu Rev Nutr* 2002;22:19-34
- Budhraja A, Gao N, Zhang Z, et al. Apigenin induces apoptosis in human leukemia cells and exhibits anti-leukemic activity in vivo. *Mol Cancer Ther* 2012;11:132-142
- Hwang YP, Oh KN, Yun HJ, Jeong HG. The flavonoids apigenin and luteolin suppress ultraviolet A-induced matrix metalloproteinase-1 expression via MAPKs and AP-1-dependent signaling in HaCaT cells. *J Dermatol Sci* 2011; 61:23-31
- Caltagirone S, Rossi C, Poggi A, et al. Flavonoids apigenin and quercetin inhibit melanoma growth and metastatic potential. *Int J Cancer* 2000;87: 595-600
- Birt DF, Mitchell D, Gold B, Pour P, Pinch HC. Inhibition of ultraviolet light induced skin carcinogenesis in SKH-1 mice by apigenin, a plant flavonoid. *Anticancer Res* 1997;17:85-91
- Zang M, Xu S, Maitland-Toolan KA, et al. Polyphenols stimulate AMP-activated protein kinase, lower lipids, and inhibit accelerated atherosclerosis in diabetic LDL receptor-deficient mice. *Diabetes* 2006;55:2180-2191
- Suou K, Taniguchi F, Tagashira Y, Kiyawa T, Terakawa N, Harada T. Apigenin inhibits tumor necrosis factor α -induced cell proliferation and prostaglandin E2 synthesis by inactivating NF-kB in endometrial stromal cells. *Fertil Steril* 2011;95:1518-1521
- Kang OH, Lee JH, Kwon DY. Apigenin inhibits release of inflammatory mediators by blocking the NF-kB activation pathways in the HMC-1 cells. *Immunopharmacol Immunotoxicol* 2011;33:473-479
- Lee JH, Zhou HY, Cho SY, Kim YS, Lee YS, Jeong CS. Anti-inflammatory mechanisms of apigenin: inhibition of cyclooxygenase-2 expression, adhesion of monocytes to human umbilical vein endothelial cells, and expression of cellular adhesion molecules. *Arch Pharm Res* 2007;30:1318-1327
- Haberland M, Montgomery RL, Olson EN. The many roles of histone deacetylases in development and physiology: implications for disease and therapy. *Nat Rev Genet* 2009;10:32-42
- Howitz KT, Bitterman KJ, Cohen HY, et al. Small molecule activators of sirtuins extend *Saccharomyces cerevisiae* lifespan. *Nature* 2003;425:191-196
- Li Y, Xu S, Giles A, et al. Hepatic overexpression of SIRT1 in mice attenuates endoplasmic reticulum stress and insulin resistance in the liver. *FASEB J* 2011;25:1664-1679
- Rodgers JT, Puigserver P. Fasting-dependent glucose and lipid metabolic response through hepatic sirtuin 1. *Proc Natl Acad Sci USA* 2007;104: 12861-12866
- Milne JC, Lambert PD, Schenk S, et al. Small molecule activators of SIRT1 as therapeutics for the treatment of type 2 diabetes. *Nature* 2007;450:712-716
- Pacholec M, Bleasdale JE, Chrnyk B, et al. SRT1720, SRT2183, SRT1460, and resveratrol are not direct activators of SIRT1. *J Biol Chem* 2010;285: 8340-8351
- Borra MT, Smith BC, Denu JM. Mechanism of human SIRT1 activation by resveratrol. *J Biol Chem* 2005;280:17187-17195
- Price NL, Gomes AP, Ling AJ, et al. SIRT1 is required for AMPK activation and the beneficial effects of resveratrol on mitochondrial function. *Cell Metab* 2012;15:675-690
- Anders CK, Winer EP, Ford JM, et al. Poly(ADP-Ribose) polymerase inhibition: "targeted" therapy for triple-negative breast cancer. *Clin Cancer Res* 2010;16:4702-4710
- Rossi MN, Carbone M, Mostocotto C, et al. Mitochondrial localization of PARP-1 requires interaction with mitofilin and is involved in the maintenance of mitochondrial DNA integrity. *J Biol Chem* 2009;284:31616-31624
- Lapucci A, Pittelli M, Rapizzi E, Felici R, Moroni F, Chiarugi A. Poly(ADP-ribose) polymerase-1 is a nuclear epigenetic regulator of mitochondrial DNA repair and transcription. *Mol Pharmacol* 2011;79:932-940
- Xu F, Gao Z, Zhang J, et al. Lack of SIRT1 (Mammalian Sirtuin 1) activity leads to liver steatosis in the SIRT1^{+/+} mice: a role of lipid mobilization and inflammation. *Endocrinology* 2010;151:2504-2514
- Yamazaki Y, Usui I, Kanatani Y, et al. Treatment with SRT1720, a SIRT1 activator, ameliorates fatty liver with reduced expression of lipogenic enzymes in MSG mice. *Am J Physiol Endocrinol Metab* 2009;297:E1179-E1186
- Yamada M, Mizuguchi M, Otsuka N, Ikeda K, Takahashi H. Ultrastructural localization of CD38 immunoreactivity in rat brain. *Brain Res* 1997;756:52-60
- Liang M, Chini EN, Cheng J, Dousa TP. Synthesis of NAADP and cADPR in mitochondria. *Arch Biochem Biophys* 1999;371:317-325

Altered behavioral and metabolic circadian rhythms in mice with disrupted NAD⁺ oscillation

Saurabh Sahar^{1,3}, Veronica Nin², Maria Thereza Barbosa², Eduardo Nunes Chini² and Paolo Sassone-Corsi^{1,3}

¹ Department of Pharmacology, University of California, Irvine, CA 92697, USA

² Department of Anesthesiology, Mayo Clinic College of Medicine, Rochester, MN 55902, USA

³ Unite 904 of INSERM (Institut National de la Sante et de la Recherche Medicale) University of California, Irvine, CA 92697, USA

Running Title: Effect of altered NAD⁺ on circadian rhythms

Keywords: Circadian Rhythm, Clock, NAD⁺, CD38, Amino acid metabolism

Received: 8/26/11; Accepted: 8/29/11; Published: 8/31/11

Correspondence to Paolo Sassone-Corsi, psc@uci.edu

Copyright: © Sassone-Corsi et al. This is an open-access article distributed under the terms of the Creative Commons Attribution License, which permits unrestricted use, distribution, and reproduction in any medium, provided the original author and source are credited

Abstract: The Intracellular levels of nicotinamide adenine dinucleotide (NAD⁺) are rhythmic and controlled by the circadian clock. However, whether NAD⁺ oscillation in turn contributes to circadian physiology is not fully understood. To address this question we analyzed mice mutated for the NAD⁺ hydrolase CD38. We found that rhythmicity of NAD⁺ was altered in the CD38-deficient mice. The high, chronic levels of NAD⁺ results in several anomalies in circadian behavior and metabolism. CD38-null mice display a shortened period length of locomotor activity and alteration in the rest-activity rhythm. Several clock genes and, interestingly, genes involved in amino acid metabolism were deregulated in CD38-null livers. Metabolomic analysis identified alterations in the circadian levels of several amino acids, specifically tryptophan levels were reduced in the CD38-null mice at a circadian time paralleling with elevated NAD⁺ levels. Thus, CD38 contributes to behavioral and metabolic circadian rhythms and altered NAD⁺ levels influence the circadian clock.

INTRODUCTION

Circadian rhythms occur with a periodicity of about 24 hours and regulate a wide array of metabolic and physiologic functions. A robust circadian clock allows organisms to anticipate environmental changes and to adapt their behavior and physiology to the appropriate time of day. Disturbances in the functionality of this “body clock” have been shown to lead to various diseases, such as sleep disorders, depression, metabolic syndrome and cancer [1,2]. Circadian rhythms are regulated by transcriptional and post-translational feedback loops generated by a set of interplaying clock proteins. The transcription factors CLOCK and BMAL1 operate as the master regulators of the clock machinery. CLOCK:BMAL1 heterodimers bind to promoters of clock controlled genes (CCGs) and

regulate their expression. Some CCGs are special in the sense that they encode other core-clock regulators, such as *Period* and *Cryptochrome* genes, which negatively feedback on the clock machinery [1-3]. Recently, the deacetylase sirtuin 1 (SIRT1) was identified as a modulator of the circadian clock machinery that counterbalances the acetyltransferase activity of CLOCK [4-7]. Moreover, an additional novel transcriptional/enzymatic feedback loop that regulates the circadian clock has recently been uncovered [8,9]. The circadian clock controls the levels of NAD⁺ by regulating the expression of nicotinamide phosphoribosyltransferase (NAMPT), the rate-limiting enzyme in the salvage pathway of NAD⁺ biosynthesis [8,9]. NAD⁺ is also synthesized from the amino acid tryptophan by the *de novo* synthesis pathway. Tryptophan levels have been shown to oscillate in

plasma [10], perhaps contributing to the oscillations in NAD^+ levels. NAD^+ is a cofactor and/or substrate for over 300 enzymes and acts as a cellular energy currency. SIRT1 is one such enzyme whose deacetylase activity is NAD^+ -dependent [11]. In addition, poly(ADP-ribose) polymerase (PARP)-1 and PARP-2 are NAD^+ -consuming enzymes, and their deletion raises NAD^+ levels in mice [12,13]. Moreover, the SIRT1 and PARPs systems have been linked as they possibly use the same NAD^+ cellular pool [14]. Circadian oscillations in NAD^+ levels drive SIRT1 rhythmic activity [4]. SIRT1, in turn, is recruited to the *Nampt* promoter along with CLOCK and BMAL1. Thus, the circadian machinery is regulated by an enzymatic/transcriptional feedback loop, wherein SIRT1 regulates the levels of its own coenzyme [8,9]. Interestingly, PARP-1 activity has also been shown to display circadian oscillation [15]. These findings highlight the intimate connections between the circadian clock and cellular metabolism [16].

[17,18]. CD38 is a membrane protein that has multiple enzymatic activities [19], the major being the hydrolysis of NAD^+ , through which it controls cellular NAD^+ levels [20,21]. CD38 is also present on the inner nuclear membrane and regulates SIRT1 activity through modulation of NAD^+ levels [17,22]. SIRT1 activity is higher in the CD38-KO mice [22]. Interestingly, CD38-KO mice are resistant to high-fat diet-induced obesity, in part through the activation of the SIRT1-PGC1 α axis [23]. Our present study shows that chronically elevated levels of NAD^+ in CD38-null mice lead to modulation of the circadian clock illustrated by altered circadian behavior, clock gene expression and amino acid metabolism.

RESULTS

Altered circadian NAD^+ levels in CD38-null mice. It has been reported that the CD38-KO mice have elevated levels of NAD^+ in most tissues [17,18]. We analyzed the profile of NAD^+ levels throughout the circadian cycle. NAD^+ levels were measured at various zeitgeber times (ZTs) and were found to oscillate in the liver as described [9] (Fig. 1A). The oscillation of NAD^+ was significantly altered in the liver of CD38-KO mice, being much higher than in WT mice at ZT7 and ZT15, with unchanged levels at ZT23 (Fig. 1A). Most remarkably, NAD^+ levels in the CD38-KO mice were about 5 times higher than in WT animals at ZT15. Next, we wanted to determine whether the differences in NAD^+ levels between WT and CD38-KO mice may be due to a change in NADase activity. Indeed, NADase activity in the liver of CD38-KO mice was drastically lower as compared to the WT animals at ZT7 and ZT15 (Fig 1B; ref. 13). Surprisingly, CD38-KO mice display high level of NADase activity (~50% of the WT activity) at ZT23. While the reasons for this could be due to a time-specific increase in the expression/activity of another unrecognized NAD^+ glycohydrolase, this result explains the comparable NAD^+ levels at ZT23.

CD38-KO mice display a shorter period length of locomotor activity. The deregulation of NAD^+ oscillation in the CD38-KO mice prompted us to monitor the circadian behavior of these mice. We analyzed the period length (*tau*) of locomotor activity under constant conditions. After entrainment on a 12 hour Light: 12 hour Dark (LD) cycle for more than 3 weeks, CD38 WT and KO mice were transferred to constant darkness (DD, free running) starting at the time of lights “off”, (ZT 12). This day was defined as day 1. We used passive (pyroelectric) infrared sensors to

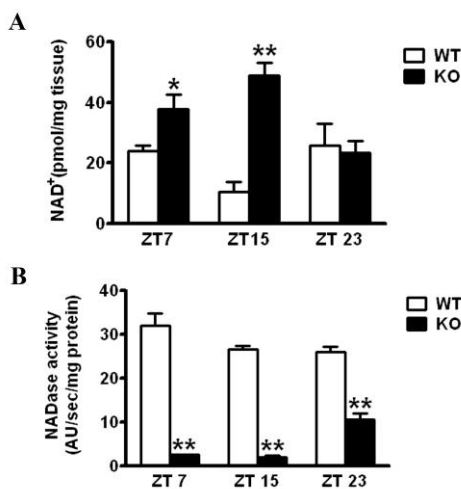


Figure 1. Effect of CD38 on NAD^+ levels. WT and CD38 KO mice entrained in 12 hr Light – 12 hr Dark (LD) cycles were sacrificed at indicated times and their liver was dissected out. **(A)** NAD^+ concentration was measured by a cycling enzymatic assay. *, $p < 0.05$ (WT vs KO ZT7); **, $p < 0.001$ (WT vs KO ZT 15) [n=3 each time point] **(B)** NADase activity was measured by a flurometric assay. **, $p < 0.001$ (WT vs KO for each time point) [n=3 each time point].

Since the clock machinery controls the cyclic levels of NAD^+ , we wondered about the importance of this oscillation with respect to circadian function. We thereby questioned whether an imbalance of NAD^+ levels in animals with an intact clock system would lead to defects in circadian rhythms. To test this hypothesis, we analyzed the circadian behavior and metabolism of CD38-deficient (KO) mice which display very high levels of NAD^+ in tissues such as the brain and liver

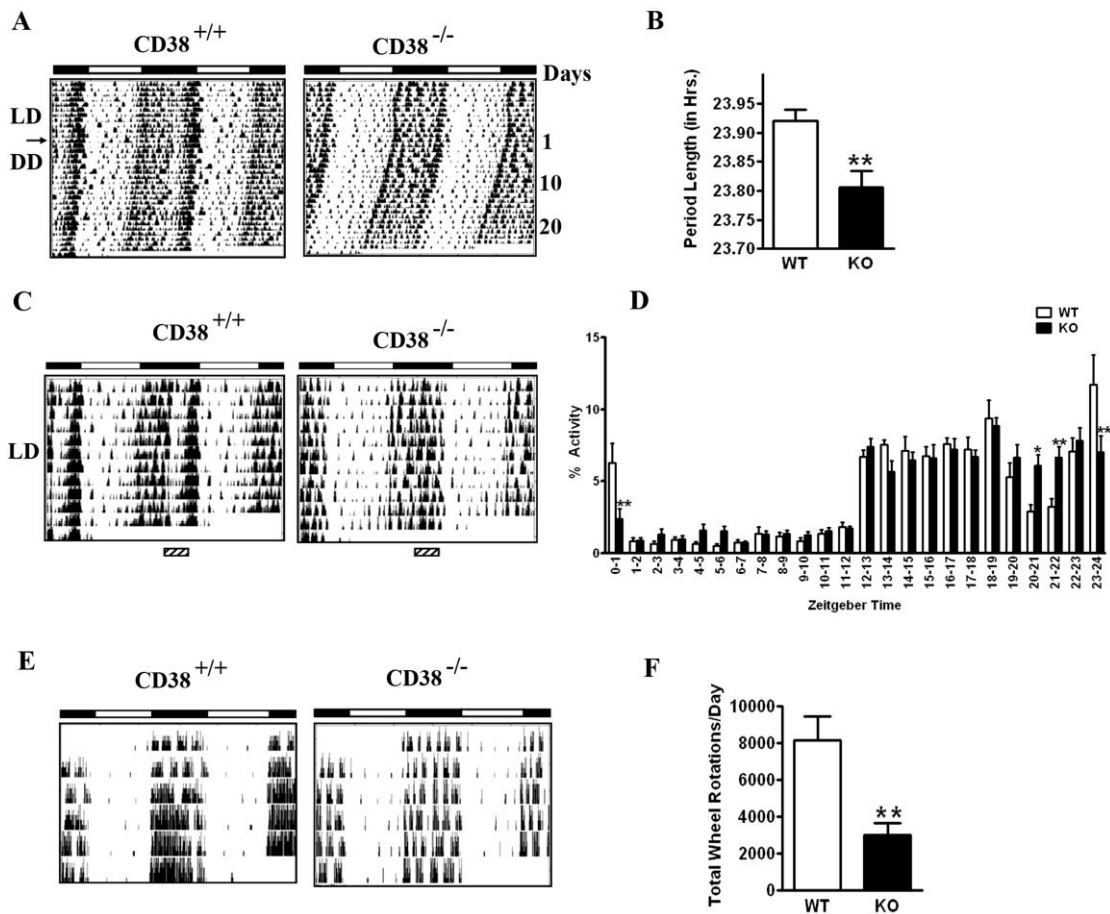


Figure 2. Circadian defects in the behavioral rhythm of CD38-KO mice. (A) Representative activity records (actograms) of Wild type (CD38^{+/+}) and CD38 knockout (CD38^{-/-}) mice are shown in double plotted format. Mice were entrained in 12 hr Light – 12 hr Dark cycles (LD) and then placed in constant darkness (DD) from the light off (ZT12), on day 1. (B) Bar graph representing the period length of WT and CD38-KO mice. Measurement of the free-running period was based on the onset of activity in DD. Data is represented as mean ± S.E. **, p = 0.008, n = 6, 8. (C) Representative actograms of Wild type (CD38^{+/+}) and CD38 knockout (CD38^{-/-}) mice in LD cycle. (D) Bar graph representing % daily locomotor activity in a one-hour period at the indicated ZTs. Data represents mean ± S.E. of 10 days of activity. *, p < 0.05; **, p < 0.01 compared to the corresponding wild type, n = 6, 8. (E) Representative actograms from wheel running activity of Wild type (CD38^{+/+}) and CD38 knockout (CD38^{-/-}) mice in LD cycle. (F) Bar-graph representing total number of wheel rotations per day. Data is represented as mean ± S.E. **, p = 0.008, n = 6, 5.

measure period length (*tau*) [24]. While the WT mice displayed a *tau* of 23.92 hours, the CD38-KO mice displayed a *tau* of 23.80 hours (Fig 2A, B). While this is a relatively small difference in *tau* (about 7 minutes), it is highly significant (P = 0.008, n=6, 8).

To establish whether WT and CD38-KO mice differed in the resetting responses to light, mice entrained to a LD cycle for several weeks were exposed to an 8 hr extension of the light period, followed by constant darkness. A phase delay is expected when mice are exposed to light during this period of night (ZT 12-20). Both WT and CD38-KO mice showed a similar phase angle of ~ 4 hr; however, the CD38-null mice displayed a further shortening of the period length to 23.75 hours,

compared to 23.94 hours displayed by WT mice after the phase extension (Fig S1 A,B). These results indicate that the CD38-deficient animals have normal resetting responses to light, while their *tau* is shorter.

Altered rest/activity rhythms in the CD38-null mice.

While monitoring locomotor activity of the WT and CD38-KO mice, we noticed a marked difference in their rest/activity patterns. The WT mice displayed a significant break from activity during the middle of the night; however, CD38-null mice did not appear to take this break (Fig. 2C, area over the striped bar). Instead, CD38-KO mice appeared to take multiple breaks, randomly spread throughout the day. Quantitation of this difference in activity revealed that while WT mice

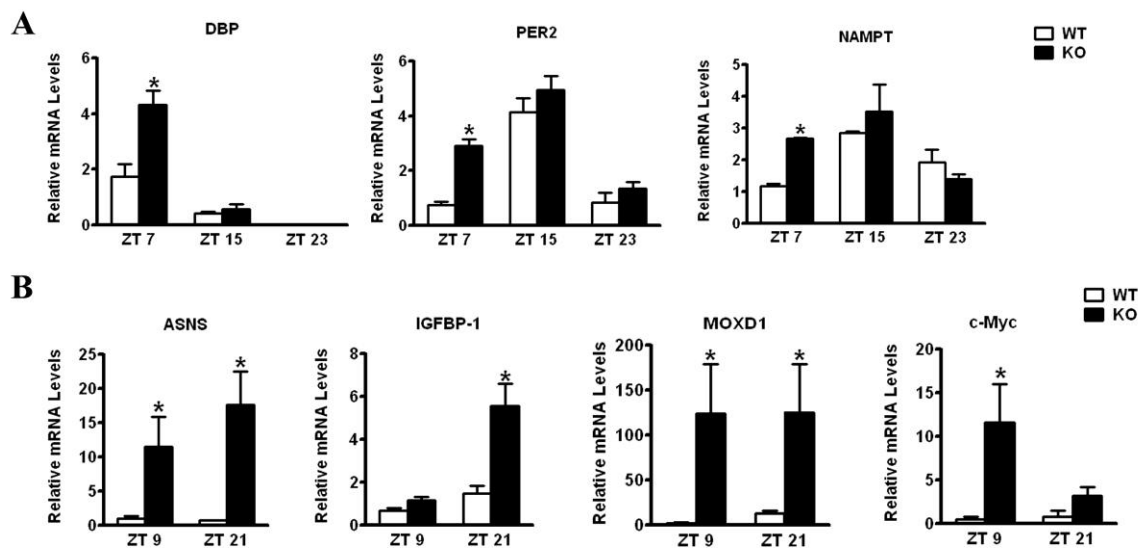


Figure 3. Differential liver gene expression in CD38-null mice. Mice entrained in 12 hr Light – 12 hr Dark cycles were sacrificed at indicated times and their liver was dissected out. **(A)** RNA was prepared at indicated times, reverse transcribed, and real-time PCR was performed using primers for *Dbp*, *Per2*, *Nampt* and 18S rRNA. Data is represented as relative levels of indicated gene normalized to 18S rRNA. **(B)** Same as in (A), except real-time PCR was performed using primers for *Asns*, *Igfbp1*, *Moxd1* and *c-Myc*. Data is represented as relative levels of indicated gene normalized to 18S rRNA. *, $p < 0.05$ compared to the corresponding wild type, $n = 3$ each time point.

decrease their locomotor activity significantly between ZT20 and ZT22, CD38-null mice maintained almost constant levels of activity throughout the night (Fig. 2D). Significant differences in activity levels were also detected at several times during the circadian cycle. The differential activity pattern persists even under free running conditions (compare the actograms in Fig. 2A).

Analysis of the actograms indicated that the total locomotor activity in the CD38-KO mice might be lower than their WT counterparts. To accurately quantitate total locomotor activity, wheel-running activity was monitored. The actograms from the wheel-running analysis demonstrated that the CD38-KO mice have reduced locomotor activity (Fig. 2E). Total locomotor activity is reduced by ~3 fold in the CD38-KO mice, compared to the WT mice (Fig. 2F). The alterations in the rest/activity rhythms observed by the passive infrared sensors were also detected in the wheel-running activity. While WT mice took a break from wheel running only during a small period at late night, the CD38-KO mice took intermittent breaks. These results demonstrate that the rest/activity rhythm is disturbed in the CD38-deficient mice.

Ablation of CD38 results in disturbances in the peripheral clockwork. The behavioral analysis of the

CD38-KO mice indicates that deregulated and elevated levels of NAD^+ alter central clock functions. To address whether peripheral clock function is also affected by deregulated NAD^+ levels, we analyzed the circadian gene expression of representative clock genes from liver. WT and CD38-KO mice were entrained to a 12 hr LD cycle and livers were harvested at various circadian times. As shown in Fig. 3A, the amplitude of circadian gene expression of *Dbp*, *Per2* and *Nampt* is significantly higher in CD38-null than in WT mice, with most divergent levels at ZT7. These results indicate that peripheral clock is also affected by elevated NAD^+ levels.

To establish if circadian metabolic pathways are influenced by deregulation of NAD^+ in the CD38-KO mice, we performed a microarray analysis. Entrained WT and CD38-KO mice were sacrificed at two circadian times (ZT9 and ZT 21), and liver mRNAs were used for microarray analysis. Among the genes that are differentially regulated between WT and CD38-KO mice (Table S1), we validated 4 genes which were upregulated in the mutant mice (Fig. 3B). These genes were *Asparagine Synthetase (Asns)*; *Insulin-like growth factor binding protein 1 (Igfbp1)*; *c-Myc*; and *monooxygenase, DBH-like 1 (Moxd1)*. Among these genes, *c-Myc* and *Igfbp1* have been shown to display a

circadian profile of expression [25,26]. While *Asns* and *Moxdl* were elevated at both ZTs in the CD38-KO mice, *c-Myc* and *Igfbp1* elevation is more pronounced at ZT9 and ZT 21, respectively (Fig. 3B). Interestingly, SIRT1 might be involved in the regulation of *Asns* expression. SIRT1 activity highly correlates with *Asns* expression levels: *Asns* levels are high in CD38-KO mice (where the SIRT1 activity is high); and, conversely, *Asns* expression levels are very low in SIRT1 liver-specific KO mice (Fig. S2A).

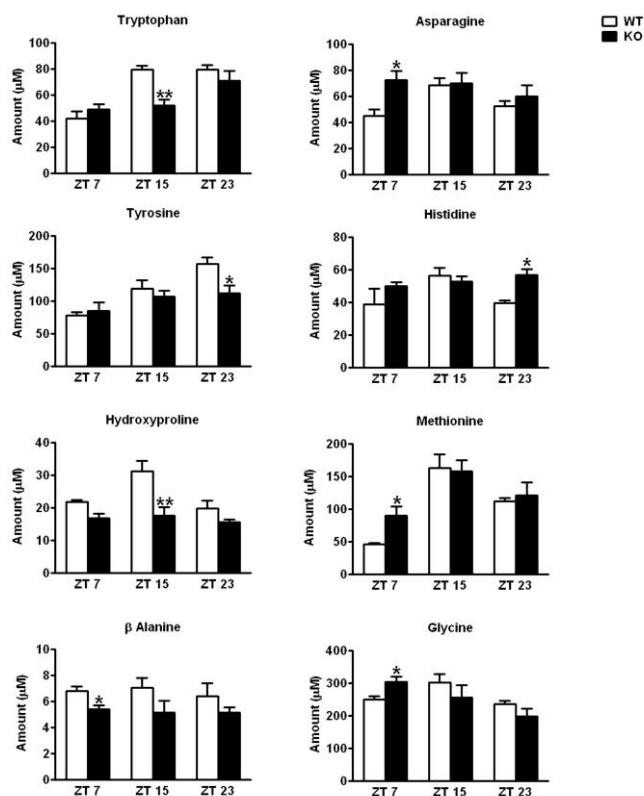


Figure 4. Alterations in the plasma amino acid levels in CD38-KO mice. Mice were entrained in 12 hr Light – 12 hr Dark cycles and blood was drawn at indicated times. Amino acid levels in plasma were determined as described in Materials and Methods. Amino acids that displayed statistically significant differences in abundance between the wild type and the CD38-KO mice are shown here. *, $p < 0.05$; **, $p < 0.01$ compared to the corresponding wild type, $n = 3$ each time point.

The expression of *Asns* and *Igfbp1* is known to be upregulated under conditions of amino acid deprivation [27-29]. We verified that the *Asns* promoter is responsive to amino acid starvation. Indeed, *Asns*-promoter driven luciferase activity was induced over six-fold after amino acid depletion (Fig. S2B). Since most amino acids display a circadian profile in mouse plasma [10], these results prompted us to evaluate

whether the circadian regulation of amino acid metabolism might be dependent on the presence of CD38.

Alterations in the plasma amino acid levels in the CD38-KO mice. We performed a metabolomic study to determine the plasma amino acid levels in WT and CD38-KO mice along the circadian cycle, according to the method described by Lanza *et al.* [30]. Most amino acid levels oscillated in a pattern consistent with that recently described by Minami *et al.* [10]. We observed significant changes in the amino acid levels between the WT and the CD38-KO mice, at different circadian times. Four amino acids (Tryptophan, Hydroxyproline, Tyrosine, and β -Alanine) displayed significantly reduced levels at one or more circadian time in the plasma of CD38-KO mice (Fig. 4). On the other hand, four amino acids (Asparagine, Glycine, Histidine and Methionine) displayed higher levels in the CD38-KO mice (Fig. 4). These results demonstrate that the circadian oscillations in amino acids levels are compromised in the CD38 KO mice, thereby establishing a direct link between specific amino acid metabolic pathways and controlled NAD^+ levels.

DISCUSSION

Our current work has addressed the question whether alterations in NAD^+ rhythmicity *in vivo* could affect the functioning of central and peripheral clocks. For this purpose we explored the circadian behavior of CD38-KO mice which have elevated NAD^+ levels. We observed that oscillations in NAD^+ levels were altered in the liver of CD38-KO mice. Strikingly, at ZT 15 (the trough of NAD^+ levels in WT liver), NAD^+ levels peaked in CD38-KO mice and were ~ 5 times higher than those in the liver of WT mice. Surprisingly, NAD^+ levels were similar between WT and CD38-KO mice at ZT23. This could be due to an increase at this circadian time of $NADase$ activity in CD38-null mice. Although CD38 is the major NAD^+ hydrolase in cells, it is possible that in its absence other NAD^+ hydrolases (such as CD157, a gene duplication product of CD38) could be induced as a compensatory mechanism.

CD38 also plays a role in the synthesis of second messengers cyclic ADP-Ribose (cADPR), ADPR, and nicotinic acid adenine dinucleotide phosphate (NAADP) [19]. CD38 can produce one molecule of cADPR for every 100 molecules of NAD^+ hydrolyzed [21,31], suggesting that the major enzymatic activity of CD38 is the hydrolysis of NAD^+ . CD38 regulates

SIRT1 through a cADPR independent pathway [23]. Acetylation of several SIRT1 targets, such as p53, is reduced in the CD38-KO mice [22,23], and CLOCK-induced BMAL1 acetylation is enhanced by ectopic expression of CD38, possibly through modulation of SIRT1 activity (Fig. S3). In keeping with this observation, several circadian behavioral defects were observed in the CD38-KO mice. Their free-running period length is ~ 7 minutes shorter than the WT animals. Although this difference may appear small, deletion of CLOCK, the master regulator of circadian rhythms, changes the period length by only 20 minutes [32]; and mutants in NPAS2 (a paralog of CLOCK highly expressed in the brain) show only a 12 minute shortening in period length [33]. Interestingly, CD38-null mice displayed an altered pattern of rest/activity rhythm, reminiscent of that reported for NPAS2 mutant mice [33]. WT mice on a C57/BL6 background are known to take a break at late night (ZT 20-22), which generally corresponds to a short nap [33]. Both CD38-null mice and NPAS2 mutant mice remain active at that time. However, differently from NPAS2 mutant mice, CD38-deficient mice appear to keep taking intermittent breaks throughout the day. Moreover, the total locomotor activity of CD38-null mice is also significantly lower. This reduction in locomotor activity could be attributed to increased SIRT1 activity in the CD38-KO mice (17), since transgenic mice overexpressing SIRT1 display a similar reduction in locomotor activity [34]. The altered rest/activity rhythm in the CD38-KO mice does not seem to be caused by defects in the motivation for running. These mice took several breaks from running and kept running at regular intervals. This behavior could potentially be described as a fatigue syndrome. Further studies are required to prove this hypothesis.

The central circadian clock is located in the suprachiasmatic nucleus (SCN) of the hypothalamus, while peripheral clocks are present in most organs [35]. We have shown that ablation of CD38 results in elevated levels of NAD⁺ in the liver, leading to perturbation in clock function. The stringency of circadian oscillation is compromised in the absence of CD38, as demonstrated by the gene expression profiles of *Dbp*, *Per2* and *Nampt*. The deregulation of circadian gene expression extends to several genes involved in amino acid metabolism, which we found to be upregulated in the liver of CD38-deficient mice. These genes were *Asparagine synthetase (Asns)*; *Insulin-like growth factor binding protein 1 (Igfbp1)*; *c-Myc*; and *monooxygenase, DBH-like 1 (Moxd1)*. The liver is a

major organ involved in the amino acid metabolism. Nutritional stresses, such as reduced availability of an amino acid, can initiate a signaling cascade referred to as the amino acid response (AAR) pathway [29]. *Asns* and *Igfbp1* are genes that are known to be upregulated by the AAR pathway. Asparagine synthetase converts amino acids aspartate and glutamine into asparagine and glutamate. Interestingly, SIRT1 activity positively correlates with *Asns* expression levels. SIRT1 has also been shown to induce the expression of *Igfbp1* [36]. Low *Igfbp1* levels are considered to be markers of metabolic syndrome [37] and the *Igfbp1* transgenic mice are protected from diet-induced obesity [38], a trait shared by the CD38-null mice [23]. c-MYC, besides having the well characterized role in cell cycle regulation, also regulates glutaminolysis [39]. MOXD1 is a monooxygenase with a yet unidentified function; however, monooxygenases are known to regulate conversion of one amino acid into another (e.g. phenylalanine hydroxylase, a monooxygenase, converts phenylalanine to tyrosine). It is interesting to speculate that MOXD1 might also function in inter-conversion of amino acids and is upregulated under conditions of deficiency of a subset of amino acids.

A metabolomic analysis confirmed our hypothesis that circadian oscillations in amino acid levels are disrupted in the absence of CD38. Levels of tryptophan, tyrosine, hydroxyproline and β -alanine were found to be reduced in CD38-null mice, whereas asparagine, glycine, histidine and methionine were elevated. Moreover, oscillations in most of these amino acids were dampened in mutant mice. Changes in asparagine and tryptophan levels are of special interest. Since *Asns* levels are higher in CD38-null mice, we predicted that asparagine levels would also be higher. Surprisingly, asparagine levels were high only at ZT7, although *Asns* expression was constitutively higher in mutant mice. This suggests that ASNS activity might be modulated in a circadian manner. As tryptophan is a source for NAD⁺ biosynthesis, it is intriguing that levels of NAD⁺ were very high and levels of tryptophan were significantly reduced at ZT15 in CD38-null mice, alluding to the consumption of tryptophan during NAD⁺ biosynthesis. Finally, it can be concluded that the altered levels of some amino acids might trigger the amino acid response pathway in CD38-KO mice.

An intriguing speculation relates to the notion that amino acids and their metabolites can also function as neurotransmitters or their precursors. Glutamate, aspartate, glycine and γ -amino butyric acid (GABA) are

neurotransmitters. Tryptophan is a precursor for serotonin, whereas tyrosine is a precursor for catecholamines, such as dopamine, epinephrine and norepinephrine. An imbalance in these amino acids can potentially change the concentration of certain neurotransmitters in the brain. Further studies will establish whether changes in these neurotransmitters are responsible for alterations in the rest/activity rhythms and locomotor activity in the CD38-null mice.

In conclusion, our results reveal a role for NAD⁺ homeostasis and SIRT1 activity in circadian regulation of behavioral and metabolic rhythms. Increased NAD⁺ levels and concomitant activation of SIRT1 might lead to reduction in several amino acids, which activates the AAR pathway in CD38-null mice. Our findings underscore the importance of circadian control in amino acid metabolism.

MATERIALS AND METHODS

Animals

Generation of CD38-deficient mice (C57BL/6J.129 CD38^{-/-}, N12 backcross) has been described [40]. Liver-specific *Sirt1*^{-/-} mice have also been described [4]. Mice housed in individual cages were entrained on a L12:D12 (12 h light–12 h dark) cycle for two weeks before analyses. Mice were sacrificed at specified circadian times. All research involving vertebrate animals has been performed under protocol approved by the Institutional Animal Care and Use Committee (IACUC). Animals are monitored on a daily basis by both the lab and University Lab Animal Resources (ULAR) veterinary staff for signs of distress, pain, and/or infection, and are given *ad libitum* access to food and water. Cages were cleaned on a weekly basis and when visibly soiled to maintain a clean environment. All husbandry procedures and welfare policies are conducted according to the Guide for the Care and Use of Laboratory Animals, set forth by the Institute of Laboratory Animal Resources, Commission on Life Sciences, and National Research Council.

NAD⁺ measurements

NAD⁺ was measured as described previously [17]. Briefly, frozen tissue was pulverized with a pestle and mortar in liquid nitrogen, immediately extracted in ice-cold 10% trichloroacetic acid (sigma) and sonicated with 3 pulses of 3 seconds. After a short centrifugation the supernatant was extracted with 2 volumes of a

combination of 1,1,2-trichloro-1,2,2-trifluoroethane : trioctylamine in a 3 to 1 ratio. The samples were vigorously vortexed and 2 phases were allowed to separate at room temperature. The pH of the extracted aqueous layer containing the NAD⁺ was adjusted with 1M Tris pH 8. The NAD⁺ concentration was measured by a cycling enzymatic assay. The samples were diluted in 100 mM NaH₂PO₄, pH 8 and incubated with a solution containing 0.76% ethanol; 4 μM flavine mononucleotide; 40 μg/ml alcohol dehydrogenase; 0.04 U/ml diaphorase; and 8 μM resazurin in buffer 100 mM NaH₂PO₄, pH 8. The fluorescence (excitation 544, emission 590) was monitored over time in a fluorometric plate reader (Spectramax Gemini XPS, Molecular devices). A NAD⁺ standard curve was performed using yeast NAD⁺ (sigma). NAD⁺ concentration was expressed as pmol per mg of tissue.

NADase activity

The NADase activity in liver samples was measured as described previously [17]. Frozen liver samples were homogenized in sucrose 0.25M - Tris 40mM, pH 7.4 buffer supplemented with protease inhibitors (Roche), and centrifuged 10 minutes at 11200 g. 200 μg of homogenate was incubated with 100 μM of 1,N⁶-etheno-adenine dinucleotide (etheno-NAD)(Sigma) and the fluorescence was measured in a fluorometric plate reader (Spectramax Gemini XPS, Molecular devices). The change in fluorescence over time (excitation 300nm, emission 410) was followed and the NADase activity was expressed as the change in the arbitrary units of fluorescence per second per mg of protein.

Analysis of behavioral rhythms

Circadian rhythms in locomotor activity was analyzed as described [24]. Briefly, locomotor activity was detected using running wheels and passive (pyroelectric) infrared sensors (PU-2201; EK Japan). Locomotion data were collected using the VitalView data acquisition system (Mini-Mitter) using a sampling interval of 5 min. Actograms were acquired using ActiView Biological Rhythm Analysis software (Mini-Mitter). Circadian period and phase shift of the activity rhythms were analyzed by Clocklab software (Actimetrics).

Quantitative Real-Time RT-PCR

Each quantitative real-time RT-PCR was performed using the PTC-200 real time detection system (MJ

Research). The PCR primers are available upon request. For a 20 µl PCR, 50 ng of cDNA template was mixed with the primers to final concentrations of 200 nM and 10 µl of iQ SYBR Green Supermix (BIO-RAD), respectively. The reaction was first incubated at 95°C for 3 min, followed by 40 cycles at 95°C for 30 s and 60°C for 1 min.

Luciferase assays

Hepa1c1c7 cells (ATCC, Manassas, VA) were cultured in Minimal Essential Media supplemented with 10% FBS and antibiotics. Cells growing in 24-well plates were transfected with indicated plasmids using BioT transfection reagent (Bioland Scientific LLC, Cerritos, CA) according to manufacturer's recommendations. Plasmid expressing 3.4 kb ASNS-promoter-driven luciferase was a gift from Dr. Pierre Fafournoux [41]. The total amount of DNA applied per well was adjusted by adding an empty vector. Cell extracts were subjected to luminometry-based-luciferase assay (Promega), and luciferase activity was normalized by β-galactosidase activity. All experiments were performed in multiple replicates.

Amino acid analysis

Amino acid concentrations in plasma samples were determined at the Metabolomics facility at Mayo Clinic College of Medicine, Rochester, Minnesota according to the method described by Lanza *et. al.* [30]. Briefly, plasma samples were deproteinized with cold MeOH prior to derivatization using 6-aminoquinoly1-N-hydroxysuccinimidyl carbamate. Amino acid levels were then determined by LC-MS/MS.

Data Analyses

Results are expressed as means ± SE of multiple experiments. Student *t* tests were used to compare 2 groups or ANOVA with the Bonferroni post tests for multiple groups using Prism software (Graph Pad). Statistical significance was detected at the 0.05 level.

ACKNOWLEDGEMENTS

We would like to thank all the members of the Sassone-Corsi and Chini laboratories for reagents and helpful discussions. We also wish to express our gratitude to Dr. Satoru Masubuchi and Dr. Kristin Eckel-Mahan for help with behavioral analysis. This research was supported by grants from the National Institutes of

Health (R01-GM081634), the Institut National de la Sante et de la Recherche Medicale [INSERM-44790] (France), and Sirtris Pharmaceutical Inc. to PSC and National Institutes of Health (DK-084055 from NIDDK), the American Federation for Aging Research, the Mayo Foundation and by the Strickland Career Development Award to ENC.

CONFLICT OF INTEREST STATEMENT

The authors declare no conflicts of interest.

REFERENCES

1. Sahar S, Sassone-Corsi P. Metabolism and cancer: The circadian clock connection. *Nat Rev Cancer* 2009;9:886-896.
2. Takahashi JS, Hong HK, Ko CH, McDearmon EL. The genetics of mammalian circadian order and disorder: Implications for physiology and disease. *Nat Rev Genet* 2008;9:764-775.
3. Gallego M, Virshup DM. Post-translational modifications regulate the ticking of the circadian clock. *Nat Rev Mol. Cell. Biol.* 2007;8:139-148.
4. Nakahata Y, Kaluzova M, Grimaldi B, Sahar S, Hirayama J, Chen D, Guarente LP, Sassone-Corsi P. The nad⁺-dependent deacetylase sirt1 modulates clock-mediated chromatin remodeling and circadian control. *Cell* 2008;134:329-340.
5. Asher G, Gatfield D, Stratmann M, Reinke H, Dibner C, Kreppel F, Mostoslavsky R, Alt FW, Schibler U. Sirt1 regulates circadian clock gene expression through per2 deacetylation. *Cell* 2008;134:317-328.
6. Doi M, Hirayama J, Sassone-Corsi P. Circadian regulator clock is a histone acetyltransferase. *Cell* 2006;125:497-508.
7. Hirayama J, Sahar S, Grimaldi B, Tamaru T, Takamatsu K, Nakahata Y, Sassone-Corsi P. Clock-mediated acetylation of bmal1 controls circadian function. *Nature* 2007;450:1086-1090.
8. Nakahata Y, Sahar S, Astarita G, Kaluzova M, Sassone-Corsi P. Circadian control of the nad⁺ salvage pathway by clock-sirt1. *Science* 2009;324:654-657.
9. Ramsey KM, Yoshino J, Brace CS, Abrassart D, Kobayashi Y, Marcheva B, Hong HK, Chong JL, Buhr ED, Lee C, Takahashi JS, Imai S, Bass J. Circadian clock feedback cycle through namp1-mediated nad⁺ biosynthesis. *Science* 2009;324:651-654.
10. Minami Y, Kasukawa T, Kakazu Y, Iigo M, Sugimoto M, Ikeda S, Yasui A, van der Horst GT, Soga T, Ueda HR. Measurement of internal body time by blood metabolomics. *Proceedings of the National Academy of Sciences of the United States of America* 2009;106:9890-9895.
11. Imai S, Armstrong CM, Kaeberlein M, Guarente L. Transcriptional silencing and longevity protein sir2 is an nad-dependent histone deacetylase. *Nature* 2000;403:795-800.
12. Bai P, Canto C, Oudart H, Brunyanszki A, Cen Y, Thomas C, Yamamoto H, Huber A, Kiss B, Houtkooper RH, Schoonjans K, Schreiber V, Sauve AA, Menissier-de Murcia J, Auwerx J. Parp-1 inhibition increases mitochondrial metabolism through sirt1 activation. *Cell metabolism* 2011;13:461-468.
13. Bai P, Canto C, Brunyanszki A, Huber A, Szanto M, Cen Y, Yamamoto H, Houten SM, Kiss B, Oudart H, Gergely P, Menissier-de Murcia J, Schreiber V, Sauve AA, Auwerx J. Parp-2

regulates sirt1 expression and whole-body energy expenditure. *Cell metabolism* 2011;13:450-460.

14. Kolthur-Seetharam U, Dantzer F, McBurney MW, de Murcia G, Sassone-Corsi P. Control of aif-mediated cell death by the functional interplay of sirt1 and parp-1 in response to DNA damage. *Cell cycle* 2006;5:873-877.

15. Asher G, Reinke H, Altmeyer M, Gutierrez-Arcelus M, Hottiger MO, Schibler U. Poly(adp-ribose) polymerase 1 participates in the phase entrainment of circadian clocks to feeding. *Cell* 2010;142:943-953.

16. Eckel-Mahan K, Sassone-Corsi P. Metabolism control by the circadian clock and vice versa. *Nature structural & molecular biology* 2009;16:462-467.

17. Aksoy P, White TA, Thompson M, Chini EN. Regulation of intracellular levels of nad: A novel role for cd38. *Biochemical and biophysical research communications* 2006;345:1386-1392.

18. Young GS, Choleris E, Lund FE, Kirkland JB. Decreased cadpr and increased nad+ in the cd38-/- mouse. *Biochemical and biophysical research communications* 2006;346:188-192.

19. Malavasi F, Deaglio S, Funaro A, Ferrero E, Horenstein AL, Ortolan E, Vaisitti T, Aydin S. Evolution and function of the adp ribosyl cyclase/cd38 gene family in physiology and pathology. *Physiology reviews* 2008;88:841-886.

20. Hoshino S, Kukimoto I, Kontani K, Inoue S, Kanda Y, Malavasi F, Katada T. Mapping of the catalytic and epitopic sites of human cd38/nad+ glycohydrolase to a functional domain in the carboxyl terminus. *J Immunol* 1997;158:741-747.

21. Chini EN. Cd38 as a regulator of cellular nad: A novel potential pharmacological target for metabolic conditions. *Current pharmaceutical design* 2009;15:57-63.

22. Aksoy P, Escande C, White TA, Thompson M, Soares S, Benech JC, Chini EN. Regulation of sirt 1 mediated nad dependent deacetylation: A novel role for the multifunctional enzyme cd38. *Biochemical and biophysical research communications* 2006;349:353-359.

23. Barbosa MT, Soares SM, Novak CM, Sinclair D, Levine JA, Aksoy P, Chini EN. The enzyme cd38 (a nad glycohydrolase, ec 3.2.2.5) is necessary for the development of diet-induced obesity. *Faseb J* 2007;21:3629-3639.

24. Masubuchi S, Gao T, O'Neill A, Eckel-Mahan K, Newton AC, Sassone-Corsi P. Protein phosphatase phlpp1 controls the light-induced resetting of the circadian clock. *Proceedings of the National Academy of Sciences of the United States of America*;107:1642-1647.

25. Fu L, Pelicano H, Liu J, Huang P, Lee C. The circadian gene period2 plays an important role in tumor suppression and DNA damage response in vivo. *Cell* 2002;111:41-50.

26. Hou TY, Ward SM, Murad JM, Watson NP, Israel MA, Duffield GE. Id2 (inhibitor of DNA binding 2) is a rhythmically expressed transcriptional repressor required for circadian clock output in mouse liver. *The Journal of biological chemistry* 2009;284:31735-31745.

27. Gong SS, Guerrini L, Basilico C. Regulation of asparagine synthetase gene expression by amino acid starvation. *Molecular and cellular biology* 1991;11:6059-6066.

28. Straus DS, Burke EJ, Marten NW. Induction of insulin-like growth factor binding protein-1 gene expression in liver of protein-restricted rats and in rat hepatoma cells limited for a single amino acid. *Endocrinology* 1993;132:1090-1100.

29. Kilberg MS, Pan YX, Chen H, Leung-Pineda V. Nutritional control of gene expression: How mammalian cells respond to amino acid limitation. *Annual review of nutrition* 2005;25:59-85.

30. Lanza IR, Zhang S, Ward LE, Karakelides H, Raftery D, Nair KS. Quantitative metabolomics by h-nmr and lc-ms/ms confirms altered metabolic pathways in diabetes. *PloS one*;5:e10538.

31. Kim H, Jacobson EL, Jacobson MK. Synthesis and degradation of cyclic adp-ribose by nad glycohydrolases. *Science* 1993;261:1330-1333.

32. Debruyne JP, Noton E, Lambert CM, Maywood ES, Weaver DR, Reppert SM. A clock shock: Mouse clock is not required for circadian oscillator function. *Neuron* 2006;50:465-477.

33. Dudley CA, Erbel-Sieler C, Estill SJ, Reick M, Franken P, Pitts S, McKnight SL. Altered patterns of sleep and behavioral adaptability in npas2-deficient mice. *Science* 2003;301:379-383.

34. Banks AS, Kon N, Knight C, Matsumoto M, Gutierrez-Juarez R, Rossetti L, Gu W, Accili D. Sirt1 gain of function increases energy efficiency and prevents diabetes in mice. *Cell metabolism* 2008;8:333-341.

35. Schibler U, Sassone-Corsi P. A web of circadian pacemakers. *Cell* 2002;111:919-922.

36. Gan L, Han Y, Bastianetto S, Dumont Y, Unterman TG, Quirion R. Foxo-dependent and -independent mechanisms mediate sirt1 effects on igfbp-1 gene expression. *Biochemical and biophysical research communications* 2005;337:1092-1096.

37. Ruan W, Lai M: Insulin-like growth factor binding protein. A possible marker for the metabolic syndrome? *Acta diabetologica*;47:5-14.

38. Rajkumar K, Modric T, Murphy LJ. Impaired adipogenesis in insulin-like growth factor binding protein-1 transgenic mice. *The Journal of endocrinology* 1999;162:457-465.

39. Wise DR, DeBerardinis RJ, Mancuso A, Sayed N, Zhang XY, Pfeiffer HK, Nissim I, Daikhin E, Yudkoff M, McMahon SB, Thompson CB. Myc regulates a transcriptional program that stimulates mitochondrial glutaminolysis and leads to glutamine addiction. *Proceedings of the National Academy of Sciences of the United States of America* 2008;105:18782-18787.

40. Cockayne DA, Muchamuel T, Grimaldi JC, Muller-Steffner H, Randall TD, Lund FE, Murray R, Schuber F, Howard MC. Mice deficient for the ecto-nicotinamide adenine dinucleotide glycohydrolase cd38 exhibit altered humoral immune responses. *Blood* 1998;92:1324-1333.

41. Bruhat A, Averous J, Carraro V, Zhong C, Reimold AM, Kilberg MS, Fafournoux P. Differences in the molecular mechanisms involved in the transcriptional activation of the chop and asparagine synthetase genes in response to amino acid deprivation or activation of the unfolded protein response. *The Journal of biological chemistry* 2002;277:48107-48114.

SUPPLEMENTAL DATA

The Supplemental Information is found in Full Text version of this manuscript.

REFERENCIAS

1. Borch-Johnsen, K., *The metabolic syndrome in a global perspective. The public health impact--secondary publication*. Dan Med Bull, 2007. **54**(2): p. 157-9.
2. Hu, F.B., *Globalization of diabetes: the role of diet, lifestyle, and genes*. Diabetes Care, 2011. **34**(6): p. 1249-57.
3. Stevens, G.A., et al., *National, regional, and global trends in adult overweight and obesity prevalences*. Popul Health Metr, 2012. **10**(1): p. 22.
4. WHO. *Global Health Observatory* 2014; Available from: http://www.who.int/gho/ncd/risk_factors/obesity_text/en/.
5. Kelly, T., et al., *Global burden of obesity in 2005 and projections to 2030*. Int J Obes (Lond), 2008. **32**(9): p. 1431-7.
6. WHO. <http://gamapserver.who.int/mapLibrary/Files/Maps/Global Obesity BothSexes 2008.png>. 2011.
7. International-Diabetes-Federation, *Diabetes Atlas*. 6 ed.
8. Byrne , C.W., SH., *The metabolic syndrome*. 2nd ed, ed. C.D.B.a.S.H. Wild. 2011: Wiley-Blackwell.
9. Ravussin, E. and C. Bouchard, *Human genomics and obesity: finding appropriate drug targets*. Eur J Pharmacol, 2000. **410**(2-3): p. 131-145.
10. DeFronzo, R.A., D. Simonson, and E. Ferrannini, *Hepatic and peripheral insulin resistance: a common feature of type 2 (non-insulin-dependent) and type 1 (insulin-dependent) diabetes mellitus*. Diabetologia, 1982. **23**(4): p. 313-9.
11. Biddinger, S.B., et al., *Hepatic insulin resistance is sufficient to produce dyslipidemia and susceptibility to atherosclerosis*. Cell Metab, 2008. **7**(2): p. 125-34.
12. Kahn, B.B. and J.S. Flier, *Obesity and insulin resistance*. J Clin Invest, 2000. **106**(4): p. 473-81.
13. Biddinger, S.B. and C.R. Kahn, *From mice to men: insights into the insulin resistance syndromes*. Annu Rev Physiol, 2006. **68**: p. 123-58.
14. Hotamisligil, G.S., et al., *Increased adipose tissue expression of tumor necrosis factor-alpha in human obesity and insulin resistance*. J Clin Invest, 1995. **95**(5): p. 2409-15.
15. Hotamisligil, G.S., N.S. Shargill, and B.M. Spiegelman, *Adipose expression of tumor necrosis factor-alpha: direct role in obesity-linked insulin resistance*. Science, 1993. **259**(5091): p. 87-91.
16. Hotamisligil, G.S. and B.M. Spiegelman, *Tumor necrosis factor alpha: a key component of the obesity-diabetes link*. Diabetes, 1994. **43**(11): p. 1271-8.
17. Kroder, G., et al., *Tumor necrosis factor-alpha- and hyperglycemia-induced insulin resistance. Evidence for different mechanisms and different effects on insulin signaling*. J Clin Invest, 1996. **97**(6): p. 1471-7.

18. Kanda, H., et al., *MCP-1 contributes to macrophage infiltration into adipose tissue, insulin resistance, and hepatic steatosis in obesity*. J Clin Invest, 2006. **116**(6): p. 1494-505.
19. Xu, H., et al., *Chronic inflammation in fat plays a crucial role in the development of obesity-related insulin resistance*. J Clin Invest, 2003. **112**(12): p. 1821-30.
20. Weisberg, S.P., et al., *Obesity is associated with macrophage accumulation in adipose tissue*. J Clin Invest, 2003. **112**(12): p. 1796-808.
21. Ramkhelawon, B., et al., *Netrin-1 promotes adipose tissue macrophage retention and insulin resistance in obesity*. Nat Med, 2014. **20**(4): p. 377-84.
22. Amano, S.U., et al., *Local proliferation of macrophages contributes to obesity-associated adipose tissue inflammation*. Cell Metab, 2014. **19**(1): p. 162-71.
23. De Taeye, B.M., et al., *Macrophage TNF-alpha contributes to insulin resistance and hepatic steatosis in diet-induced obesity*. Am J Physiol Endocrinol Metab, 2007. **293**(3): p. E713-25.
24. Uysal, K.T., S.M. Wiesbrock, and G.S. Hotamisligil, *Functional analysis of tumor necrosis factor (TNF) receptors in TNF-alpha-mediated insulin resistance in genetic obesity*. Endocrinology, 1998. **139**(12): p. 4832-8.
25. Uysal, K.T., et al., *Protection from obesity-induced insulin resistance in mice lacking TNF-alpha function*. Nature, 1997. **389**(6651): p. 610-4.
26. Samuel, V.T., et al., *Mechanism of hepatic insulin resistance in non-alcoholic fatty liver disease*. J Biol Chem, 2004. **279**(31): p. 32345-53.
27. Marchesini, G., et al., *Association of nonalcoholic fatty liver disease with insulin resistance*. Am J Med, 1999. **107**(5): p. 450-5.
28. Michael, M.D., et al., *Loss of insulin signaling in hepatocytes leads to severe insulin resistance and progressive hepatic dysfunction*. Mol Cell, 2000. **6**(1): p. 87-97.
29. Brown, M.S. and J.L. Goldstein, *Selective versus total insulin resistance: a pathogenic paradox*. Cell Metab, 2008. **7**(2): p. 95-6.
30. Koo, S.H., et al., *PGC-1 promotes insulin resistance in liver through PPAR-alpha-dependent induction of TRB-3*. Nat Med, 2004. **10**(5): p. 530-4.
31. Cai, D., et al., *Local and systemic insulin resistance resulting from hepatic activation of IKK-beta and NF-kappaB*. Nat Med, 2005. **11**(2): p. 183-90.
32. Fabbrini, E., S. Sullivan, and S. Klein, *Obesity and nonalcoholic fatty liver disease: biochemical, metabolic, and clinical implications*. Hepatology, 2010. **51**(2): p. 679-89.
33. Korenblat, K.M., et al., *Liver, muscle, and adipose tissue insulin action is directly related to intrahepatic triglyceride content in obese subjects*. Gastroenterology, 2008. **134**(5): p. 1369-75.
34. Eckel, R.H., *Obesity and heart disease: a statement for healthcare professionals from the Nutrition Committee, American Heart Association*. Circulation, 1997. **96**(9): p. 3248-50.
35. McNeill, A.M., et al., *The metabolic syndrome and 11-year risk of incident cardiovascular disease in the atherosclerosis risk in communities study*. Diabetes Care, 2005. **28**(2): p. 385-90.
36. Flegal, K.M., et al., *Cause-specific excess deaths associated with underweight, overweight, and obesity*. JAMA, 2007. **298**(17): p. 2028-37.
37. Dunaif, A., *Insulin resistance and the polycystic ovary syndrome: mechanism and implications for pathogenesis*. Endocr Rev, 1997. **18**(6): p. 774-800.

38. Dunaif, A., et al., *Profound peripheral insulin resistance, independent of obesity, in polycystic ovary syndrome*. *Diabetes*, 1989. **38**(9): p. 1165-74.
39. Gambineri, A., et al., *Obesity and the polycystic ovary syndrome*. *Int J Obes Relat Metab Disord*, 2002. **26**(7): p. 883-96.
40. Wolin, K.Y., K. Carson, and G.A. Colditz, *Obesity and cancer*. *Oncologist*, 2010. **15**(6): p. 556-65.
41. Kanneganti, T.D. and V.D. Dixit, *Immunological complications of obesity*. *Nat Immunol*, 2012. **13**(8): p. 707-12.
42. Heilbronn, L.K. and E. Ravussin, *Calorie restriction and aging: review of the literature and implications for studies in humans*. *Am J Clin Nutr*, 2003. **78**(3): p. 361-9.
43. Weindruch, R., *The retardation of aging by caloric restriction: studies in rodents and primates*. *Toxicol Pathol*, 1996. **24**(6): p. 742-5.
44. Colman, R.J., et al., *Caloric restriction delays disease onset and mortality in rhesus monkeys*. *Science*, 2009. **325**(5937): p. 201-4.
45. Mattison, J.A., et al., *Calorie restriction in rhesus monkeys*. *Exp Gerontol*, 2003. **38**(1-2): p. 35-46.
46. Roth, G.S., et al., *Biomarkers of caloric restriction may predict longevity in humans*. *Science*, 2002. **297**(5582): p. 811.
47. Everitt, A.V. and D.G. Le Couteur, *Life extension by calorie restriction in humans*. *Ann N Y Acad Sci*, 2007. **1114**: p. 428-33.
48. Wing, R.R., et al., *Caloric restriction per se is a significant factor in improvements in glycemic control and insulin sensitivity during weight loss in obese NIDDM patients*. *Diabetes Care*, 1994. **17**(1): p. 30-6.
49. Ingram, D.K., et al., *Calorie restriction mimetics: an emerging research field*. *Aging Cell*, 2006. **5**(2): p. 97-108.
50. Ingram, D.K., et al., *Development of calorie restriction mimetics as a prolongevity strategy*. *Ann N Y Acad Sci*, 2004. **1019**: p. 412-23.
51. AARP. *On the Verge of Discovery: The Fountain of Youth in Pill Form*. 2013 [cited 2014 13 de mayo]; Available from: <http://blog.aarp.org/2013/03/18/on-the-verge-of-discovery-the-fountain-of-youth-in-pill-form/>.
52. Walters, B. *Resveratrol-Fountain of youth*. 2012 [cited 2014 13 de mayo]; Available from: <https://www.youtube.com/watch?v=f5gPOjDFfzg>.
53. NBCNews. *Big doses of red wine could promote long life*. 2006 [cited 2014 13 de mayo]; Available from: http://www.nbcnews.com/id/15511128/ns/health-health_care/t/big-doses-red-wine-could-promote-long-life/#.U3JKguCczfA.
54. Nogueiras, R., et al., *Sirtuin 1 and sirtuin 3: physiological modulators of metabolism*. *Physiol Rev*, 2012. **92**(3): p. 1479-514.
55. Lin, S.J., P.A. Defossez, and L. Guarente, *Requirement of NAD and SIR2 for life-span extension by calorie restriction in *Saccharomyces cerevisiae**. *Science*, 2000. **289**(5487): p. 2126-8.
56. Imai, S., et al., *Transcriptional silencing and longevity protein Sir2 is an NAD-dependent histone deacetylase*. *Nature*, 2000. **403**(6771): p. 795-800.
57. Bitterman, K.J., et al., *Inhibition of silencing and accelerated aging by nicotinamide, a putative negative regulator of yeast sir2 and human SIRT1*. *J Biol Chem*, 2002. **277**(47): p. 45099-107.

58. Lin, S.J., et al., *Calorie restriction extends Saccharomyces cerevisiae lifespan by increasing respiration*. Nature, 2002. **418**(6895): p. 344-8.
59. Kaerberlein, M., et al., *Sir2-independent life span extension by calorie restriction in yeast*. PLoS Biol, 2004. **2**(9): p. E296.
60. Tsuchiya, M., et al., *Sirtuin-independent effects of nicotinamide on lifespan extension from calorie restriction in yeast*. Aging Cell, 2006. **5**(6): p. 505-14.
61. Lamming, D.W., et al., *HST2 mediates SIR2-independent life-span extension by calorie restriction*. Science, 2005. **309**(5742): p. 1861-4.
62. Smith, D.L., Jr., et al., *Calorie restriction extends the chronological lifespan of Saccharomyces cerevisiae independently of the Sirtuins*. Aging Cell, 2007. **6**(5): p. 649-62.
63. Sanders, B.D., B. Jackson, and R. Marmorstein, *Structural basis for sirtuin function: what we know and what we don't*. Biochim Biophys Acta, 2010. **1804**(8): p. 1604-16.
64. Rogina, B. and S.L. Helfand, *Sir2 mediates longevity in the fly through a pathway related to calorie restriction*. Proc Natl Acad Sci U S A, 2004. **101**(45): p. 15998-6003.
65. Chen, D., et al., *Increase in activity during calorie restriction requires Sirt1*. Science, 2005. **310**(5754): p. 1641.
66. Cohen, H.Y., et al., *Calorie restriction promotes mammalian cell survival by inducing the SIRT1 deacetylase*. Science, 2004. **305**(5682): p. 390-2.
67. Chen, D., et al., *Tissue-specific regulation of SIRT1 by calorie restriction*. Genes Dev, 2008. **22**(13): p. 1753-7.
68. Bordone, L., et al., *SIRT1 transgenic mice show phenotypes resembling calorie restriction*. Aging Cell, 2007. **6**(6): p. 759-67.
69. Banks, A.S., et al., *Sirt1 gain of function increases energy efficiency and prevents diabetes in mice*. Cell Metab, 2008. **8**(4): p. 333-41.
70. Pfluger, P.T., et al., *Sirt1 protects against high-fat diet-induced metabolic damage*. Proc Natl Acad Sci U S A, 2008. **105**(28): p. 9793-8.
71. Burnett, C., et al., *Absence of effects of Sir2 overexpression on lifespan in C. elegans and Drosophila*. Nature, 2011. **477**(7365): p. 482-5.
72. Howitz, K.T., et al., *Small molecule activators of sirtuins extend Saccharomyces cerevisiae lifespan*. Nature, 2003. **425**(6954): p. 191-6.
73. Wood, J.G., et al., *Sirtuin activators mimic caloric restriction and delay ageing in metazoans*. Nature, 2004. **430**(7000): p. 686-9.
74. Baur, J.A., et al., *Resveratrol improves health and survival of mice on a high-calorie diet*. Nature, 2006. **444**(7117): p. 337-42.
75. Lagouge, M., et al., *Resveratrol improves mitochondrial function and protects against metabolic disease by activating SIRT1 and PGC-1alpha*. Cell, 2006. **127**(6): p. 1109-22.
76. Kaerberlein, M., et al., *Substrate-specific activation of sirtuins by resveratrol*. J Biol Chem, 2005. **280**(17): p. 17038-45.
77. Beher, D., et al., *Resveratrol is not a direct activator of SIRT1 enzyme activity*. Chem Biol Drug Des, 2009. **74**(6): p. 619-24.
78. Feng, Y., et al., *A fluorometric assay of SIRT1 deacetylation activity through quantification of nicotinamide adenine dinucleotide*. Anal Biochem, 2009. **395**(2): p. 205-10.

79. Dasgupta, B. and J. Milbrandt, *Resveratrol stimulates AMP kinase activity in neurons*. Proc Natl Acad Sci U S A, 2007. **104**(17): p. 7217-22.
80. Kitada, M., et al., *Resveratrol improves oxidative stress and protects against diabetic nephropathy through normalization of Mn-SOD dysfunction in AMPK/SIRT1-independent pathway*. Diabetes, 2011. **60**(2): p. 634-43.
81. Bass, T.M., et al., *Effects of resveratrol on lifespan in Drosophila melanogaster and Caenorhabditis elegans*. Mech Ageing Dev, 2007. **128**(10): p. 546-52.
82. Feige, J.N., et al., *Specific SIRT1 activation mimics low energy levels and protects against diet-induced metabolic disorders by enhancing fat oxidation*. Cell Metab, 2008. **8**(5): p. 347-58.
83. Milne, J.C., et al., *Small molecule activators of SIRT1 as therapeutics for the treatment of type 2 diabetes*. Nature, 2007. **450**(7170): p. 712-6.
84. Mitchell, S.J., et al., *The SIRT1 activator SRT1720 extends lifespan and improves health of mice fed a standard diet*. Cell Rep, 2014. **6**(5): p. 836-43.
85. Libri, V., et al., *A pilot randomized, placebo controlled, double blind phase I trial of the novel SIRT1 activator SRT2104 in elderly volunteers*. PLoS ONE, 2012. **7**(12): p. e51395.
86. Pacholec, M., et al., *SRT1720, SRT2183, SRT1460, and resveratrol are not direct activators of SIRT1*. J Biol Chem, 2010.
87. Park, S.J., et al., *Resveratrol ameliorates aging-related metabolic phenotypes by inhibiting cAMP phosphodiesterases*. Cell, 2012. **148**(3): p. 421-33.
88. Tennen, R.I., E. Michishita-Kioi, and K.F. Chua, *Finding a target for resveratrol*. Cell, 2012. **148**(3): p. 387-9.
89. Greer, E.L., et al., *An AMPK-FOXO pathway mediates longevity induced by a novel method of dietary restriction in C. elegans*. Curr Biol, 2007. **17**(19): p. 1646-56.
90. Schulz, T.J., et al., *Glucose restriction extends Caenorhabditis elegans life span by inducing mitochondrial respiration and increasing oxidative stress*. Cell Metab, 2007. **6**(4): p. 280-93.
91. Onken, B. and M. Driscoll, *Metformin induces a dietary restriction-like state and the oxidative stress response to extend C. elegans Healthspan via AMPK, LKB1, and SKN-1*. PLoS ONE, 2010. **5**(1): p. e8758.
92. Edwards, A.G., et al., *Life-long caloric restriction elicits pronounced protection of the aged myocardium: a role for AMPK*. Mech Ageing Dev, 2010. **131**(11-12): p. 739-42.
93. Hwang, J.T., et al., *Resveratrol protects ROS-induced cell death by activating AMPK in H9c2 cardiac muscle cells*. Genes Nutr, 2008. **2**(4): p. 323-6.
94. Um, J.H., et al., *AMP-activated protein kinase-deficient mice are resistant to the metabolic effects of resveratrol*. Diabetes, 2010. **59**(3): p. 554-63.
95. Martin-Montalvo, A., et al., *Metformin improves healthspan and lifespan in mice*. Nat Commun, 2013. **4**: p. 2192.
96. Musi, N., et al., *Metformin increases AMP-activated protein kinase activity in skeletal muscle of subjects with type 2 diabetes*. Diabetes, 2002. **51**(7): p. 2074-81.
97. Zhou, G., et al., *Role of AMP-activated protein kinase in mechanism of metformin action*. J Clin Invest, 2001. **108**(8): p. 1167-74.
98. DeFronzo, R.A. and A.M. Goodman, *Efficacy of metformin in patients with non-insulin-dependent diabetes mellitus*. The Multicenter Metformin Study Group. N Engl J Med, 1995. **333**(9): p. 541-9.

99. Stumvoll, M., et al., *Metabolic effects of metformin in non-insulin-dependent diabetes mellitus*. N Engl J Med, 1995. **333**(9): p. 550-4.
100. Bergeron, R., et al., *Effect of 5-aminoimidazole-4-carboxamide-1-beta-D-ribofuranoside infusion on in vivo glucose and lipid metabolism in lean and obese Zucker rats*. Diabetes, 2001. **50**(5): p. 1076-82.
101. Hardie, D.G., S.A. Hawley, and J.W. Scott, *AMP-activated protein kinase--development of the energy sensor concept*. J Physiol, 2006. **574**(Pt 1): p. 7-15.
102. Salt, I.P., et al., *AMP-activated protein kinase is activated by low glucose in cell lines derived from pancreatic beta cells, and may regulate insulin release*. Biochem J, 1998. **335 (Pt 3)**: p. 533-9.
103. Wilson, W.A., S.A. Hawley, and D.G. Hardie, *Glucose repression/derepression in budding yeast: SNF1 protein kinase is activated by phosphorylation under derepressing conditions, and this correlates with a high AMP:ATP ratio*. Curr Biol, 1996. **6**(11): p. 1426-34.
104. Hardie, D.G., *AMPK: a key regulator of energy balance in the single cell and the whole organism*. Int J Obes (Lond), 2008. **32 Suppl 4**: p. S7-12.
105. Agius, L., *Targeting hepatic glucokinase in type 2 diabetes: weighing the benefits and risks*. Diabetes, 2009. **58**(1): p. 18-20.
106. Hardie, D.G., F.A. Ross, and S.A. Hawley, *AMPK: a nutrient and energy sensor that maintains energy homeostasis*. Nat Rev Mol Cell Biol, 2012. **13**(4): p. 251-62.
107. Hawley, S.A., et al., *Complexes between the LKB1 tumor suppressor, STRAD alpha/beta and MO25 alpha/beta are upstream kinases in the AMP-activated protein kinase cascade*. J Biol, 2003. **2**(4): p. 28.
108. Woods, A., et al., *LKB1 is the upstream kinase in the AMP-activated protein kinase cascade*. Curr Biol, 2003. **13**(22): p. 2004-8.
109. Shaw, R.J., et al., *The tumor suppressor LKB1 kinase directly activates AMP-activated kinase and regulates apoptosis in response to energy stress*. Proc Natl Acad Sci U S A, 2004. **101**(10): p. 3329-35.
110. Hurley, R.L., et al., *The Ca²⁺/calmodulin-dependent protein kinase kinases are AMP-activated protein kinase kinases*. J Biol Chem, 2005. **280**(32): p. 29060-6.
111. Hawley, S.A., et al., *Calmodulin-dependent protein kinase kinase-beta is an alternative upstream kinase for AMP-activated protein kinase*. Cell Metab, 2005. **2**(1): p. 9-19.
112. McBride, A., et al., *The glycogen-binding domain on the AMPK beta subunit allows the kinase to act as a glycogen sensor*. Cell Metab, 2009. **9**(1): p. 23-34.
113. Hardie, D.G. and D.R. Alessi, *LKB1 and AMPK and the cancer-metabolism link - ten years after*. BMC Biol, 2013. **11**: p. 36.
114. Brown, G.C., *Control of respiration and ATP synthesis in mammalian mitochondria and cells*. Biochem J, 1992. **284 (Pt 1)**: p. 1-13.
115. Michan, S. and D. Sinclair, *Sirtuins in mammals: insights into their biological function*. Biochem J, 2007. **404**(1): p. 1-13.
116. Carafa, V., A. Nebbioso, and L. Altucci, *Sirtuins and disease: the road ahead*. Front Pharmacol, 2012. **3**: p. 4.
117. Tanno, M., et al., *Nucleocytoplasmic shuttling of the NAD⁺-dependent histone deacetylase SIRT1*. J Biol Chem, 2007. **282**(9): p. 6823-32.
118. Lin, H. <http://lin.chem.cornell.edu/research/>. 2014 [cited 2014 13 de mayo]; Available from: <http://lin.chem.cornell.edu/research/>.

119. Tanner, K.G., et al., *Silent information regulator 2 family of NAD- dependent histone/protein deacetylases generates a unique product, 1-O-acetyl-ADP-ribose*. Proc Natl Acad Sci U S A, 2000. **97**(26): p. 14178-82.
120. Ahuja, N., et al., *Regulation of insulin secretion by SIRT4, a mitochondrial ADP-ribose transferase*. J Biol Chem, 2007. **282**(46): p. 33583-92.
121. Pan, M., et al., *SIRT1 contains N- and C-terminal regions that potentiate deacetylase activity*. J Biol Chem, 2012. **287**(4): p. 2468-76.
122. Kang, H., et al., *Peptide switch is essential for Sirt1 deacetylase activity*. Mol Cell, 2011. **44**(2): p. 203-13.
123. Picard, F., et al., *Sirt1 promotes fat mobilization in white adipocytes by repressing PPAR-gamma*. Nature, 2004. **429**(6993): p. 771-6.
124. Qiang, L., et al., *Brown remodeling of white adipose tissue by SirT1-dependent deacetylation of Ppargamma*. Cell, 2012. **150**(3): p. 620-32.
125. Bordone, L., et al., *Sirt1 regulates insulin secretion by repressing UCP2 in pancreatic beta cells*. PLoS Biol, 2006. **4**(2): p. e31.
126. Lee, J.H., et al., *Overexpression of SIRT1 protects pancreatic beta-cells against cytokine toxicity by suppressing the nuclear factor-kappaB signaling pathway*. Diabetes, 2009. **58**(2): p. 344-51.
127. Vetterli, L., et al., *Resveratrol potentiates glucose-stimulated insulin secretion in INS-1E beta-cells and human islets through a SIRT1-dependent mechanism*. J Biol Chem, 2011. **286**(8): p. 6049-60.
128. Rodgers, J.T., et al., *Nutrient control of glucose homeostasis through a complex of PGC-1alpha and SIRT1*. Nature, 2005. **434**(7029): p. 113-8.
129. Rodgers, J.T. and P. Puigserver, *Fasting-dependent glucose and lipid metabolic response through hepatic sirtuin 1*. Proc Natl Acad Sci U S A, 2007. **104**(31): p. 12861-6.
130. Park, J.M., et al., *Role of resveratrol in FOXO1-mediated gluconeogenic gene expression in the liver*. Biochem Biophys Res Commun, 2010. **403**(3-4): p. 329-34.
131. Inoue, H., et al., *Role of STAT-3 in regulation of hepatic gluconeogenic genes and carbohydrate metabolism in vivo*. Nat Med, 2004. **10**(2): p. 168-74.
132. Nie, Y., et al., *STAT3 inhibition of gluconeogenesis is downregulated by SirT1*. Nat Cell Biol, 2009. **11**(4): p. 492-500.
133. Erion, D.M., et al., *SirT1 knockdown in liver decreases basal hepatic glucose production and increases hepatic insulin responsiveness in diabetic rats*. Proc Natl Acad Sci U S A, 2009. **106**(27): p. 11288-93.
134. Caton, P.W., et al., *Fructose induces gluconeogenesis and lipogenesis through a SIRT1-dependent mechanism*. J Endocrinol, 2011. **208**(3): p. 273-83.
135. Singh, B.K., et al., *FoxO1 deacetylation regulates thyroid hormone-induced transcription of key hepatic gluconeogenic genes*. J Biol Chem, 2013. **288**(42): p. 30365-72.
136. Liu, Y., et al., *A fasting inducible switch modulates gluconeogenesis via activator/coactivator exchange*. Nature, 2008. **456**(7219): p. 269-73.
137. Caton, P.W., et al., *Metformin suppresses hepatic gluconeogenesis through induction of SIRT1 and GCN5*. J Endocrinol, 2010.
138. Li, Y., et al., *Hepatic overexpression of SIRT1 in mice attenuates endoplasmic reticulum stress and insulin resistance in the liver*. Faseb J, 2011. **25**(5): p. 1664-79.

139. Wang, R.H., et al., *Hepatic Sirt1 deficiency in mice impairs mTorc2/Akt signaling and results in hyperglycemia, oxidative damage, and insulin resistance*. J Clin Invest, 2011. **121**(11): p. 4477-90.
140. Yeung, F., et al., *Modulation of NF-kappaB-dependent transcription and cell survival by the SIRT1 deacetylase*. Embo J, 2004. **23**(12): p. 2369-80.
141. Ghosh, H.S., et al., *Sirt1 interacts with transducin-like enhancer of split-1 to inhibit nuclear factor kappaB-mediated transcription*. Biochem J, 2007. **408**(1): p. 105-11.
142. Escande, C., et al., *Deleted in breast cancer-1 regulates SIRT1 activity and contributes to high-fat diet-induced liver steatosis in mice*. J Clin Invest, 2010. **120**(2): p. 545-58.
143. Purushotham, A., et al., *Hepatocyte-specific deletion of SIRT1 alters fatty acid metabolism and results in hepatic steatosis and inflammation*. Cell Metab, 2009. **9**(4): p. 327-38.
144. Gillum, M.P., et al., *Sirt1 regulates adipose tissue inflammation*. Diabetes, 2011. **60**(12): p. 3235-45.
145. Yoshizaki, T., et al., *SIRT1 Inhibits Inflammatory Pathways in Macrophages and Modulates Insulin Sensitivity*. Am J Physiol Endocrinol Metab, 2009.
146. Houtkooper, R.H., E. Pirinen, and J. Auwerx, *Sirtuins as regulators of metabolism and healthspan*. Nat Rev Mol Cell Biol, 2012. **13**(4): p. 225-38.
147. Noriega, L.G., et al., *CREB and ChREBP oppositely regulate SIRT1 expression in response to energy availability*. EMBO Rep, 2011. **12**(10): p. 1069-76.
148. Hayashida, S., et al., *Fasting promotes the expression of SIRT1, an NAD+ -dependent protein deacetylase, via activation of PPARalpha in mice*. Mol Cell Biochem, 2010. **339**(1-2): p. 285-92.
149. Nemoto, S., M.M. Fergusson, and T. Finkel, *Nutrient availability regulates SIRT1 through a forkhead-dependent pathway*. Science, 2004. **306**(5704): p. 2105-8.
150. Xiong, S., et al., *FoxO1 mediates an autofeedback loop regulating SIRT1 expression*. J Biol Chem, 2011. **286**(7): p. 5289-99.
151. Bai, P., et al., *PARP-2 regulates SIRT1 expression and whole-body energy expenditure*. Cell Metab, 2011. **13**(4): p. 450-60.
152. Han, L., et al., *SIRT1 is regulated by a PPAR{gamma}-SIRT1 negative feedback loop associated with senescence*. Nucleic Acids Res, 2010. **38**(21): p. 7458-71.
153. Aksoy, P., et al., *Regulation of intracellular levels of NAD: a novel role for CD38*. Biochem Biophys Res Commun, 2006. **345**(4): p. 1386-92.
154. Aksoy, P., et al., *Regulation of SIRT 1 mediated NAD dependent deacetylation: a novel role for the multifunctional enzyme CD38*. Biochem Biophys Res Commun, 2006. **349**(1): p. 353-9.
155. Barbosa, M.T., et al., *The enzyme CD38 (a NAD glycohydrolase, EC 3.2.2.5) is necessary for the development of diet-induced obesity*. Faseb J, 2007. **21**(13): p. 3629-39.
156. Escande, C., et al., *Flavonoid apigenin is an inhibitor of the NAD+ ase CD38: implications for cellular NAD+ metabolism, protein acetylation, and treatment of metabolic syndrome*. Diabetes, 2013. **62**(4): p. 1084-93.
157. Bai, P., et al., *PARP-1 inhibition increases mitochondrial metabolism through SIRT1 activation*. Cell Metab, 2011. **13**(4): p. 461-8.
158. Imai, S., *The NAD World: a new systemic regulatory network for metabolism and aging--Sirt1, systemic NAD biosynthesis, and their importance*. Cell Biochem Biophys, 2009. **53**(2): p. 65-74.

159. Revollo, J.R., A.A. Grimm, and S. Imai, *The regulation of nicotinamide adenine dinucleotide biosynthesis by Nampt/PBEF/visfatin in mammals*. *Curr Opin Gastroenterol*, 2007. **23**(2): p. 164-70.
160. Zhang, T., et al., *Enzymes in the NAD⁺ Salvage Pathway Regulate SIRT1 Activity at Target Gene Promoters*. *J Biol Chem*, 2009. **284**(30): p. 20408-17.
161. Canto, C., et al., *The NAD⁽⁺⁾ precursor nicotinamide riboside enhances oxidative metabolism and protects against high-fat diet-induced obesity*. *Cell Metab*, 2012. **15**(6): p. 838-47.
162. Yoshino, J., et al., *Nicotinamide mononucleotide, a key NAD⁽⁺⁾ intermediate, treats the pathophysiology of diet- and age-induced diabetes in mice*. *Cell Metab*, 2011. **14**(4): p. 528-36.
163. Canto, C., et al., *AMPK regulates energy expenditure by modulating NAD⁺ metabolism and SIRT1 activity*. *Nature*, 2009. **458**(7241): p. 1056-60.
164. Sahar, S., et al., *Altered behavioral and metabolic circadian rhythms in mice with disrupted NAD⁺ oscillation*. *Aging (Albany NY)*, 2011. **3**(8): p. 794-802.
165. Ramsey, K.M., et al., *Circadian clock feedback cycle through NAMPT-mediated NAD⁺ biosynthesis*. *Science*, 2009. **324**(5927): p. 651-4.
166. Nakahata, Y., et al., *Circadian control of the NAD⁺ salvage pathway by CLOCK-SIRT1*. *Science*, 2009. **324**(5927): p. 654-7.
167. Nakahata, Y., et al., *The NAD⁺-dependent deacetylase SIRT1 modulates CLOCK-mediated chromatin remodeling and circadian control*. *Cell*, 2008. **134**(2): p. 329-40.
168. Belden, W.J. and J.C. Dunlap, *SIRT1 is a circadian deacetylase for core clock components*. *Cell*, 2008. **134**(2): p. 212-4.
169. Kim, J.E., J. Chen, and Z. Lou, *DBC1 is a negative regulator of SIRT1*. *Nature*, 2008. **451**(7178): p. 583-6.
170. Zhao, W., et al., *Negative regulation of the deacetylase SIRT1 by DBC1*. *Nature*, 2008. **451**(7178): p. 587-90.
171. Hamaguchi, M., et al., *DBC2, a candidate for a tumor suppressor gene involved in breast cancer*. *Proc Natl Acad Sci U S A*, 2002. **99**(21): p. 13647-52.
172. Chini, E.N., et al., *Deleted in breast cancer-1 (DBC-1) in the interface between metabolism, ageing and cancer*. *Biosci Rep*, 2013.
173. Sundararajan, R., et al., *Caspase-dependent processing activates the proapoptotic activity of deleted in breast cancer-1 during tumor necrosis factor-alpha-mediated death signaling*. *Oncogene*, 2005. **24**(31): p. 4908-20.
174. Fu, J., et al., *Deleted in breast cancer 1, a novel androgen receptor (AR) coactivator that promotes AR DNA-binding activity*. *J Biol Chem*, 2009. **284**(11): p. 6832-40.
175. Li, Z., et al., *Inhibition of SUV39H1 methyltransferase activity by DBC1*. *J Biol Chem*, 2009. **284**(16): p. 10361-6.
176. Chini, C.C., et al., *HDAC3 is negatively regulated by the nuclear protein DBC1*. *J Biol Chem*, 2010. **285**(52): p. 40830-7.
177. Koyama, S., et al., *Repression of estrogen receptor beta function by putative tumor suppressor DBC1*. *Biochem Biophys Res Commun*, 2010. **392**(3): p. 357-62.
178. Hiraike, H., et al., *Identification of DBC1 as a transcriptional repressor for BRCA1*. *Br J Cancer*, 2010. **102**(6): p. 1061-7.
179. Trauernicht, A.M., et al., *Modulation of estrogen receptor alpha protein level and survival function by DBC-1*. *Mol Endocrinol*, 2007. **21**(7): p. 1526-36.

180. Suter, M.A., et al., *A maternal high-fat diet modulates fetal SIRT1 histone and protein deacetylase activity in nonhuman primates*. *Faseb J*, 2012. **26**(12): p. 5106-14.
181. Zannini, L., et al., *DBC1 phosphorylation by ATM/ATR inhibits SIRT1 deacetylase in response to DNA damage*. *J Mol Cell Biol*, 2012. **4**(5): p. 294-303.
182. Yuan, J., et al., *Regulation of SIRT1 activity by genotoxic stress*. *Genes Dev*, 2012. **26**(8): p. 791-6.
183. Zheng, H., et al., *hMOF acetylation of DBC1/CCAR2 prevents binding and inhibition of SirT1*. *Mol Cell Biol*, 2013. **33**(24): p. 4960-70.
184. Park, S.H., P.t. Riley, and S.M. Frisch, *Regulation of anoikis by deleted in breast cancer-1 (DBC1) through NF-kappaB*. *Apoptosis*, 2013. **18**(8): p. 949-62.
185. Salminen, A., et al., *Krebs cycle dysfunction shapes epigenetic landscape of chromatin: Novel insights into mitochondrial regulation of aging process*. *Cell Signal*, 2014. **26**(7): p. 1598-1603.
186. Nakayasu, E.S., et al., *Multi-omic data integration links deleted in breast cancer 1 (DBC1) degradation to chromatin remodeling in inflammatory response*. *Mol Cell Proteomics*, 2013. **12**(8): p. 2136-47.
187. Yu, E.J., et al., *Reciprocal roles of DBC1 and SIRT1 in regulating estrogen receptor alpha activity and co-activator synergy*. *Nucleic Acids Res*, 2011. **39**(16): p. 6932-43.
188. Chini, C.C., et al., *DBC1 (Deleted in Breast Cancer 1) modulates the stability and function of the nuclear receptor Rev-erbalpha*. *Biochem J*, 2013. **451**(3): p. 453-61.
189. Joshi, P., et al., *A Functional Proteomics Perspective of DBC1 as a Regulator of Transcription*. *J Proteomics Bioinform*, 2013. **Suppl 2**.
190. Nin, V., et al., *Role of deleted in breast cancer 1 (DBC1) protein in SIRT1 deacetylase activation induced by protein kinase A and AMP-activated protein kinase*. *J Biol Chem*, 2012. **287**(28): p. 23489-501.
191. Gelling, R.W., et al., *Lower blood glucose, hyperglucagonemia, and pancreatic alpha cell hyperplasia in glucagon receptor knockout mice*. *Proc Natl Acad Sci U S A*, 2003. **100**(3): p. 1438-43.
192. Taniguchi, C.M., B. Emanuelli, and C.R. Kahn, *Critical nodes in signalling pathways: insights into insulin action*. *Nat Rev Mol Cell Biol*, 2006. **7**(2): p. 85-96.
193. Gerhart-Hines, Z., et al., *The cAMP/PKA Pathway Rapidly Activates SIRT1 to Promote Fatty Acid Oxidation Independently of Changes in NAD(+)*. *Mol Cell*, 2011. **44**(6): p. 851-63.
194. Lee, C.W., et al., *AMPK promotes p53 acetylation via phosphorylation and inactivation of SIRT1 in liver cancer cells*. *Cancer Res*, 2012. **72**(17): p. 4394-404.
195. Haberland, M., R.L. Montgomery, and E.N. Olson, *The many roles of histone deacetylases in development and physiology: implications for disease and therapy*. *Nat Rev Genet*, 2009. **10**(1): p. 32-42.
196. Vaziri, H., et al., *hSIR2(SIRT1) functions as an NAD-dependent p53 deacetylase*. *Cell*, 2001. **107**(2): p. 149-59.
197. Zeng, L., et al., *HDAC3 is crucial in shear- and VEGF-induced stem cell differentiation toward endothelial cells*. *J Cell Biol*, 2006. **174**(7): p. 1059-69.
198. Mihaylova, M.M., et al., *Class Iia histone deacetylases are hormone-activated regulators of FOXO and mammalian glucose homeostasis*. *Cell*, 2011. **145**(4): p. 607-21.

199. Motta, M.C., et al., *Mammalian SIRT1 represses forkhead transcription factors*. Cell, 2004. **116**(4): p. 551-63.
200. Chen, L., et al., *Duration of nuclear NF-kappaB action regulated by reversible acetylation*. Science, 2001. **293**(5535): p. 1653-7.
201. Gregoire, S., et al., *Histone deacetylase 3 interacts with and deacetylates myocyte enhancer factor 2*. Mol Cell Biol, 2007. **27**(4): p. 1280-95.
202. Zhao, X., et al., *Regulation of MEF2 by histone deacetylase 4- and SIRT1 deacetylase-mediated lysine modifications*. Mol Cell Biol, 2005. **25**(19): p. 8456-64.
203. Sun, Z., et al., *Hepatic Hdac3 promotes gluconeogenesis by repressing lipid synthesis and sequestration*. Nat Med, 2012. **18**(6): p. 934-42.
204. Nin, V., et al., *Deleted in breast cancer 1 (DBC1) protein regulates hepatic gluconeogenesis*. J Biol Chem, 2014. **289**(9): p. 5518-27.
205. Chiba, T., et al., *Development of calorie restriction mimetics as therapeutics for obesity, diabetes, inflammatory and neurodegenerative diseases*. Curr Genomics, 2010. **11**(8): p. 562-7.
206. Kaeberlein, M., et al., *Regulation of yeast replicative life span by TOR and Sch9 in response to nutrients*. Science, 2005. **310**(5751): p. 1193-6.
207. Chiba, T., et al., *Development of a bioassay to screen for chemicals mimicking the anti-aging effects of calorie restriction*. Biochem Biophys Res Commun, 2010. **401**(2): p. 213-8.
208. Maherli, N., et al., *Directly reprogrammed fibroblasts show global epigenetic remodeling and widespread tissue contribution*. Cell Stem Cell, 2007. **1**(1): p. 55-70.
209. Fraga, M.F., et al., *Epigenetic differences arise during the lifetime of monozygotic twins*. Proc Natl Acad Sci U S A, 2005. **102**(30): p. 10604-9.
210. Choudhary, C., et al., *Lysine acetylation targets protein complexes and co-regulates major cellular functions*. Science, 2009. **325**(5942): p. 834-40.
211. Smith, K.T. and J.L. Workman, *Introducing the acetylome*. Nat Biotechnol, 2009. **27**(10): p. 917-9.
212. Weinert, B.T., et al., *Proteome-wide mapping of the Drosophila acetylome demonstrates a high degree of conservation of lysine acetylation*. Sci Signal, 2011. **4**(183): p. ra48.
213. Zhao, S., et al., *Regulation of cellular metabolism by protein lysine acetylation*. Science, 2010. **327**(5968): p. 1000-4.